# JOURNAL OF APPLIED PHYSICS

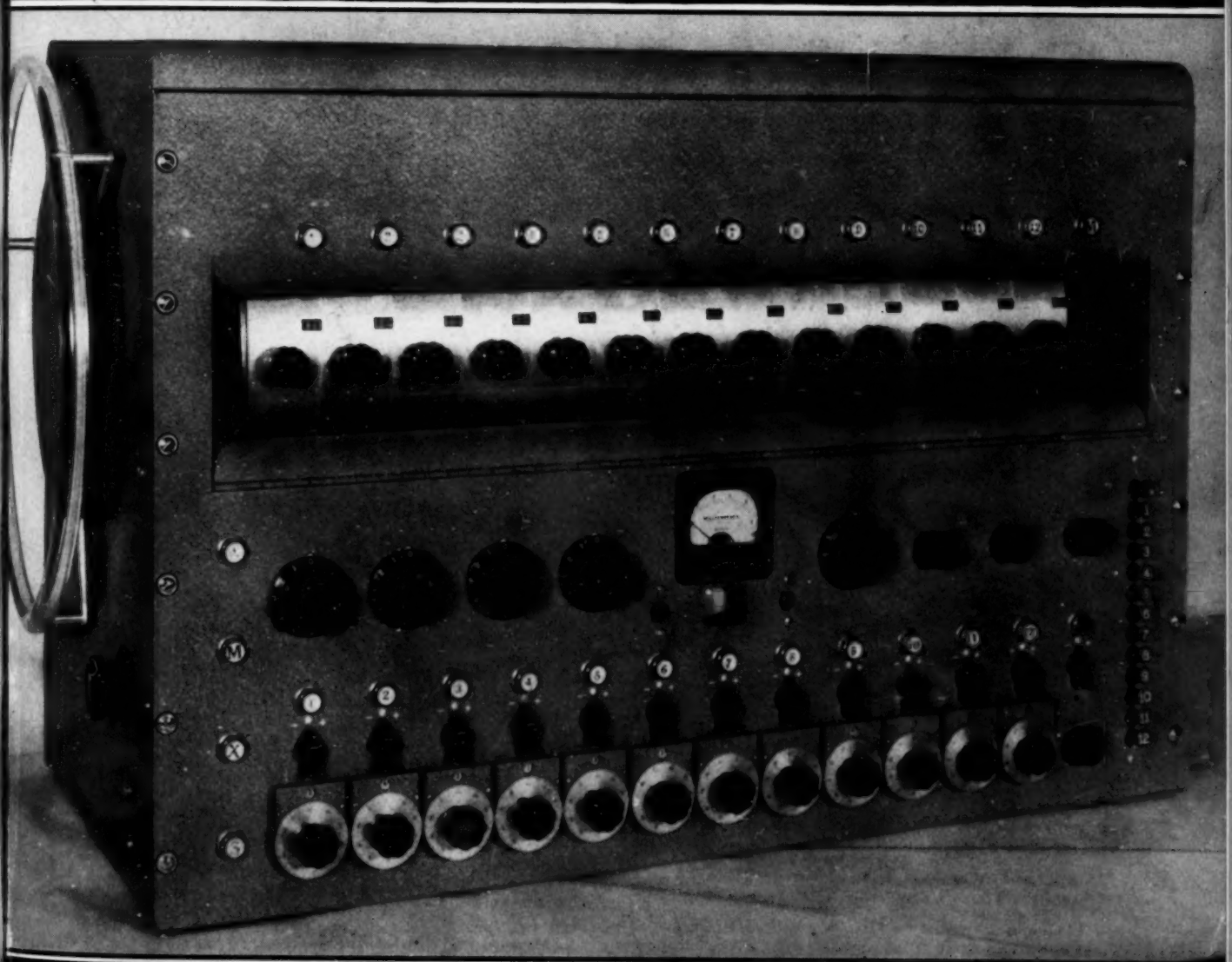

# JOURNAL OF APPLIED PHYSICS

Vol. 17, No. 4 APRIL, 1946


## *In This Issue*


*Page*

*Contributed Original Research*

**New Electrolytic Selenium Photo-Cell**
A. VON HIPPEL, J. H. SCHULMAN, AND E. S. RITTNER 215

**Studies of Plastic Flow of Steel, Especially in Two-Dimensional Compression** P. W. BRIDGMAN 225

**Method of Determining the Size of Droplets Dispersed in a Gas** R. L. STOKER 243

**Accuracy of Lumping in an Electric Circuit Representing Heat Flow in Cylindrical and Spherical Bodies**
VICTOR PASCHKIS AND MICHAEL P. HEISLER 246

**Determination of the Temperature Rise and the Maximum Safe Current through Multiconductor Electric Cables**
HAIG P. ISKENDERIAN AND WILLIAM J. HORVATH 255

**Computer for Solving Linear Simultaneous Equations**
CLIFFORD E. BERRY, DOYLE E. WILCOX, SIBYL M. ROCK, AND H. W. WASHBURN 262

**Thin Cylindrical Antenna: A Comparison of Theories**
DAVID MIDDLETON AND RONOLD KING 273

**Correction of Diffraction Amplitudes for Lorentz and Polarization Factors** M. J. BUERGER AND GILBERT E. KLEIN 285

**Further Improvement in the Resolving Power of the Electron Microscope** JAMES HILLIER 307

**Preparation of Electron Microscope Specimens for Determination of Particle Size Distribution in Aqueous Suspensions**
A. M. CRAVATH, A. E. SMITH, J. R. VINOGRAD, AND J. N. WILSON 309

*In Every Issue*

**Calendar of Meetings** 284
**Here and There** 311
**New Books** 312
**Index to Advertisers** xxx



**BOARD OF EDITORS**

ELMER HUTCHISSON, *Editor*

*Associate Editors*
R. BOWLING BARNES
OTTO BEECK
W. F. BUSSE
S. H. CALDWELL
CLARK GOODMAN
SELIG HECHT
W. JAMES LYONS
PAUL E. SABINE
FREDERICK SEITZ
J. R. TOWNSEND

**Publication of the American Institute of Physics**

**ADMINISTRATIVE STAFF**

HENRY A. BARTON, *Director*

MARGARET S. GRIFFIN *Publications Manager*

THEODORE VORBURGER, *Business Manager*

JOHN T. TATE, *Adviser on Publications*

**GOVERNING BOARD**

PAUL E. KLOPSTEG, *Chairman*

WALLACE WATERFALL, *Secretary*

GEORGE B. PEGRAM, *Treasurer*

R. B. DOW
L. A. DUBRIDGE
W. F. FAIR, JR.
FLOYD A. FIRESTONE
HARVEY FLETCHER
R. C. GIBBS
K. S. GIBSON
W. H. MARKWOOD, JR.
A. H. PFUND
JOHN T. TATE
L. W. TAYLOR
A. G. WORTHING



The JOURNAL OF APPLIED PHYSICS, published monthly at Prince and Lemon Sts., Lancaster, Pa., is devoted to physics in its role as the science basic to other natural sciences and to the arts and industries. Previous to 1937 this publication was known as PHYSICS. The JOURNAL OF APPLIED PHYSICS publishes editorials, news of physicists, and reviews, as well as technical papers of applied physics.

**Manuscripts** should be submitted to Elmer Hutchisson, Editor, Case School of Applied Science, Cleveland 6, Ohio.

**Subscriptions** and orders for back numbers should be addressed to Prince and Lemon Streets, Lancaster, Pa. or to the American Institute of Physics, 57 East 55 Street, New York 22, N. Y.

**Subscription Price**

| | U. S. AND CANADA | ELSEWHERE |
|---|---|---|
| To members of scientific societies | $5.00 | $5.70 |
| To all others | 7.00 | 7.70 |

**Back Number Prices**

Complete set: Vol. 1, July, 1931–Vol. 16, 1945—$101.50
Yearly back number rate: $7.70
Single copies: $0.70 each.

**Changes of address** and proofs should be addressed to the Publications Manager.

**Advertising rates** supplied on request. Orders, advertising copy, and cuts should be sent to the American Institute of Physics.

Entered as second class matter January 22, 1937, at the Post Office at Lancaster, Pennsylvania, under the Act of March 3, 1879
Accepted for mailing at the special rate of postage provided for in the Act of February 28, 1925, authorized May 2, 1932.



Copyright 1946, by the American Institute of Physics.

Journal
of
Applied Physics

Volume 17, Number 4 April, 1946

# A New Electrolytic Selenium Photo-Cell[1]

A. VON HIPPEL, J. H. SCHULMAN, AND E. S. RITTNER
*Laboratory for Insulation Research, Massachusetts Institute of Technology, Cambridge, Massachusetts*

(Received December 20, 1945)

A new electrolytic selenium photo-cell is described and its characteristics given as a function of operating voltage, temperature, external resistance, and time. Data are included indicative of its response to unmodulated, modulated, and monochromatic light; comparison is made with cells of similar type or possessing similar characteristics; and a method of compensating for the dark current of photo-cells is shown.

An electronic circuit is also described which can greatly improve the voltage output of the photo-element. It is generally applicable to photo-conductive and photo-voltaic cells.

## INTRODUCTION

A PROCESS of electroplating metallic selenium has recently been developed in this laboratory.[2] In the course of that research it was found that electrolytic selenium photo-cells of excellent sensitivity and relatively high impedance could be produced. These characteristics made it desirable to investigate in detail the performance of the new photo-elements in order to determine their usefulness in war equipment. The results of this study are presented below.

## DESCRIPTION OF PHOTO-CELL

The electrolytic photo-cell consists of a metal electrode, completely coated with metallic selenium, immersed in an aqueous solution of an electrolyte, preferably selenium dioxide, together with an auxiliary electrode of a noble metal-like platinum, or a second selenium-coated electrode. The particular model of the glass-enclosed cell employed in the major part of our experimental work is illustrated in Fig. 1. On the application of a small external d.c. voltage making the auxiliary electrode the anode, the cell becomes immediately sensitive to light incident upon the selenium cathode. The cell so employed as a photo-conductor exhibits essentially instantaneous and linear response to light. With a selenium dioxide electrolyte and an applied e.m.f. of 2 v the cell possesses a short circuit sensitivity of the order of 1000 $\mu$amp./lumen and a dark current of 0.2–2.0 $\mu$amp. (total cathode area = 2 cm$^2$).

The most important factors controlling the quality of the cell are (1) the composition of the electrolytic solution and (2) the nature of the selenium coating on the cathode. The first may impose a limitation upon the useful life of the photo-cell; the second affects principally the short-circuit current and the voltage sensitivity.

## THE ELECTROLYTE

Photo-sensitivity has been observed in cells containing a large number of different aqueous electrolytic solutions (Table I). In all of these

[1] This research was carried out under contract OEMsr 561 with Division 16, Section 16.4, of the National Defense Research Committee, and finished by June 10, 1943. Publication has been delayed because of the war.

[2] To be published elsewhere.

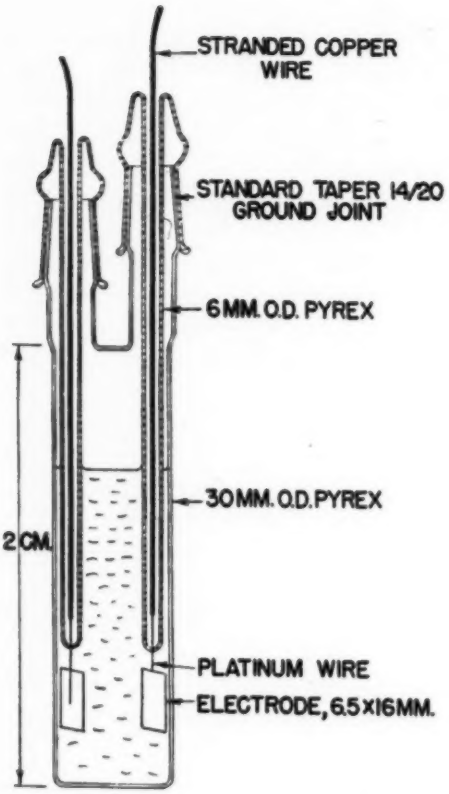


FIG. 1. The electrolytic selenium photo-cell.

cases there appears to be an optimum voltage, below or above which either the sensitivity decreases or the short circuit current output *vs.* illumination deviates from linearity. Employment of these solutions, however, results in the disadvantage that the light sensitive selenium surface is gradually destroyed on illuminating the cell either because of the evolution of $H_2Se$ or of the dissolving of selenium by the locally high concentration of $OH^-$ produced at the cathode in the case of salt electrolytes.

On the other hand, if selenious acid is used as electrolyte, the sensitive cathode is not destroyed, the electrode reactions which occur upon illumination being (1) at the cathode and (2) or (3) at the anode:

(1) $H_2SeO_3+4(-)+4H^+=Se+3H_2O$;

(2) $Se+3H_2O=H_2SeO_3+4H^++4(-)$ (for a Se anode);

(3) $\frac{1}{2}H_2O=H^++\frac{1}{4}O_2+(-)$ (for an inert anode).

For this reason our detailed investigation of the properties of the photo-cell was confined to cells containing selenious acid solutions.

The selenium dioxide employed was of the best grade commercially available, and its state of high purity was verified by spectroscopic analysis. The major impurity was Te, present in a concentration of 14 parts per million. All other metals found in the sample were present in concentration less than 2 parts per million. Despite this fact samples of selenium dioxide obtained from different companies and even different batches from the same manufacturer gave rise to cells of widely varying quality. Cells made with unsatisfactory samples of $SeO_2$, for example, displayed abnormally high dark currents, or low sensitivities, or non-linearity and sluggishness of response. These differences in behavior would seem to be attributable to traces of impurities, undetectable spectroscopically, in the various lots of $SeO_2$ employed, as no correlation could be drawn between the spectroscopic analyses and the results obtained with varying $SeO_2$ lots. Moreover, attempts to purify unsuitable samples have failed to improve the characteristics of cells made from them, yielding no clue as to the nature of these presumed impurities. It was therefore necessary to select for further studies a single lot of selenium dioxide which gave rise to cells of desirable characteristics.[3] Even with cells made from the same satisfactory solution and with electrodes plated simultaneously in the same plating bath, statistical fluctuations in cell characteristics were observed. Hence all data given below, except where noted, are representative of the average behavior of a minimum of five cells.

TABLE I. Photo-sensitivity as function of electrolyte.

| Composition of solution | Short-circuit sensitivity, μamp./lumen | Dark current, μamp. | Optimum operating voltage (for Se anode) |
|---|---|---|---|
| 0.1*M* HCl | 510 | 0.1 | 1.0 |
| 0.1*M* $H_3PO_4$ | 610 | 0.2 | 1.0 |
| 0.1*M* $H_2SO_4$ | 620 | 0.6 | 1.0 |
| 9.0*M* $H_2SO_4$ | 680 | 2. | 1.0 |
| 0.3*M* $H_2SO_3$ | 540 | 4. | 0.55 |
| 0.1*M* HAc | 500 | 2. | 0.9 |
| 8.7*M* HAc | 500 | 2.5 | 1.0 |
| 0.1*M* $Na_2SO_4$ | 630 | 0.5 | 1.0 |
| 0.1*M* $MgSO_4$ | 800 | 0.3 | 1.0 |

[3] This $SeO_2$ lot was obtained from the American Smelting & Refining Company.

The concentration of the selenious acid may be varied within wide limits without materially affecting the cell's characteristics. Survey experiments showed that these limits extend from at least 4 to 60 weight percent $SeO_2$. Since the eutectic of the system $SeO_2-H_2O$ lies at 57 weight percent $SeO_2$ and $-23°$, this composition seems preferable if the cell is ever to be subjected to low temperatures. Most of the data were obtained on cells whose electrolyte concentrations were close to the eutectic composition.

## THE CATHODE

Although there are several techniques available for coating a metal with metallic selenium, we have confined our attention to the electroplating method as being the simplest and the most satisfactory for our purposes.

Metal electrodes can be electroplated with metallic selenium from a number of plating baths of which two were used in the present work: (1) the "standard" plating bath developed in this laboratory and (2) selenious acid solution (i.e., the cell solution itself) at elevated temperatures, 100°. With the first of these baths, metallic selenium may be plated to large thicknesses with high current efficiency, remarkable speed, and at low voltage. The second operates with low current efficiency owing to hydrogen evolution at the cathode. Strong polarization occurs, voltages of the order of 30 volts being required to pass currents of the order of 30 μamp. after plating has proceeded for only a few minutes. This latter bath is thus unsuited for the production of thick plates.

The plates obtained from the two baths differ in appearance to the unaided eye and under the microscope. Bath (1) gives plates of about 4 percent average reflectivity, the Se crystals presenting the aspect of a grass-like growth with the *C*-axis oriented preferentially normal to the surface of the electrode. Bath (2) gives a much finer grained plate of about 25 percent average reflectivity with no sign of crystal orientation. Plates from bath (1) are easily wetted by water or $SeO_2$ solution, those from bath (2) shed liquid. Corresponding to the above-mentioned reflectivities, the former plates are very black in appearance, the latter a light gray.

When Pt electrodes plated in bath (1) are formed into cells (2 v applied), the initially high values of photo-sensitivity and dark current decrease rapidly with time.[4] An equilibrium dark current of 0.2–2.0 μamp. is attained within ten minutes to two days while a steady sensitivity of about 1000 μamp./lumen is reached within a few days. This sensitivity is maintained over long periods of time, whether the cell is kept on voltage in the dark or stored on voltage under intense light.

With Pt electrodes plated in bath (2) for 5–10 minutes the situation is similar except for the fact that the equilibrium sensitivities are of the order of 500 μamp./lumen and are attained only after one to two weeks. By exposing such cells to strong illumination for several hours the original grey color of the cathode is altered to a deep black, of about 4 percent reflectivity. Microscopic examination of the cathode reveals that an orientated structure similar to that produced in bath (1) has been formed. The change in character of the cathode is accompanied by an increase in sensitivity to 1000 μamp./lumen, and this sensitivity is thereafter maintained.

Other metals, besides Pt, which have been found suitable for use as bases for the Se cathode include Fe, Ni, Mo, and stainless steel. Cathodes plated in bath (1) on these metals gave cells with initially low sensitivities which rose rapidly to their equilibrium values within 1–2 days. With Fe and Ni the final sensitivities were 800–900 μamp./lumen; with Mo and stainless steel the final sensitivities were 1000 μamp./lumen.

All data given below refer to a total cathode area of 2 $cm^2$ whenever the dark current is concerned but to a light sensitive area of 1 $cm^2$. The back side of the cathode, which is not illuminated, can be coated, if desired, with an inert insulating layer such as polystyrene to reduce the dark current.

## THE ANODE

The anode of the photo-cell may consist of any inert metal or it may be a duplicate of the

[4] The change in characteristics with time is so rapid initially that no attempt was made to measure photo-sensitivity until ten minutes after the application of voltage. The sensitivity of different cells at this stage varied between 1200 and 2400 μamp/lumen.

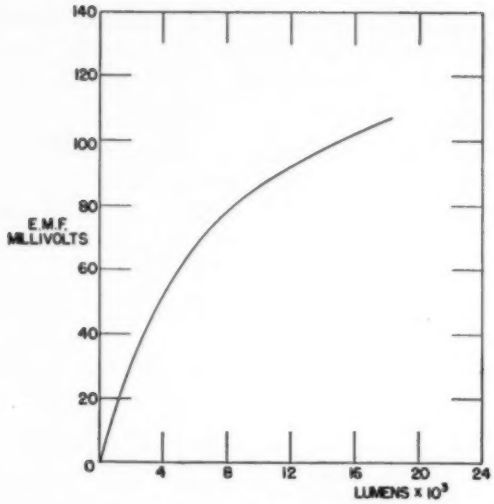


FIG. 2. Open circuit e.m.f. *vs.* illumination. (Illuminated electrode more positive.)

cathode. With an inert metal anode, oxygen is evolved; with a Se-plated anode, selenium dissolves forming selenious acid—the reverse of the cathode reaction. If the cell is to be hermetically sealed, the evolution of gas is undesirable; hence, Se-plated anodes are to be preferred. In this case, however, the selenium on the anode must be of sufficient thickness to last for the lifetime of the cell. For this reason plating of the anode is necessarily done in bath (1) from which thicknesses sufficient for several years of operation may easily be plated. The further possibility exists in cells supplied with Se-plated anodes and cathodes of reversing the polarity at intervals, in which case the cell might be expected to have an indefinitely long lifetime.

Cells with selenium anodes possess slightly higher sensitivities and dark currents at a given applied voltage than cells with platinum anodes, probably owing to the higher back e.m.f. of the cell in the latter instance.

Se electrodes made on a Pt, Mo, or stainless steel base are suitable for anodes; those made on a Ni or Fe base are apparently too porous for such use, the solution becoming contaminated with oxidation products of Fe or Ni which destroy the photo-cell.

## OPERATING VOLTAGE

The cell can be stored on open circuit without deterioration. The magnitude of the open circuit potential generated, when one of two selenium electrodes in selenious acid solution is illuminated, varies greatly with individual electrodes, but the general shape of the cell e.m.f. *vs.* illumination curve is indicated in Fig. 2. Without applied potential the photo-current observed on illuminating a short-circuited cell quickly decays. This is likewise true of cells operated with applied potentials of less than about 0.5 volt, although the magnitude of the photo-current first observed increases with applied voltage. With further progressive increase of operating voltage the short-circuit sensitivity can be measured and typical data obtained on one cell with a Se-anode are shown in Fig. 3. It can be seen that a minimum potential between 0.55 and 1.0 volt must be applied to obtain linear photo-response. The maximum operating voltage that can be employed without visible hydrogen evolution at the cathode is about 4 volts.

The equilibrium values of the white light sensitivity attained with cells operated at different voltages are shown in Table II for both gray and black cathodes (platinum anodes used in all cases). The data show that there is little gain in sensitivity with increasing voltage above 2 volts

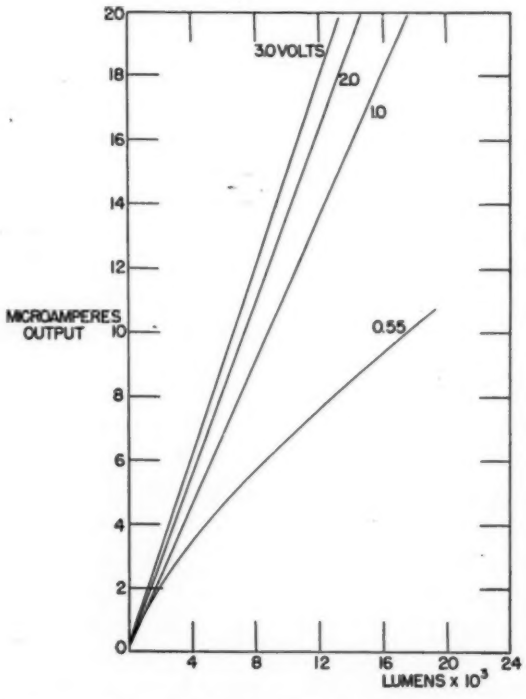


FIG. 3. Short-circuit sensitivity *vs.* operating voltage.

when black cathodes are employed. On the other hand, the dark current and the noise level (to be discussed below) increase rapidly with the applied voltage. Hence operation of the cell at an applied voltage of 2 v represents a good compromise. Unless otherwise stated, all data reported below refer to this operating voltage.

### TEMPERATURE

A lower limit upon the temperature to which the photo-cell can be exposed is imposed by the freezing of the solution. As mentioned previously, this limit is $-23°$ for a 57 weight percent solution of $SeO_2$ in water. No intrinsic upper temperature limit seems to exist below the boiling point of the solution, unless one is imposed by the particular cell housing employed. However, the dark current increases steeply with temperature (Fig. 4), while the light response, expressed as $I_{\text{light}} - I_{\text{dark}}$, remains constant within 10 percent over the temperature interval given. On replotting the data of Fig. 4 in the form log $I_d$ *vs.* $1/T°\text{K}$, a straight line is obtained (Fig. 4a), the slope of which indicates an activation energy of about 0.38 electron volt for the conduction process. The variation of back e.m.f. with temperature may account for the slight deviation from the straight line at lower temperatures.

TABLE II.

| Applied voltage | Sensitivity, μamp./lumen Gray cathodes | Black cathodes |
|---|---|---|
| 2.0 | 450±100 | 1000±100 |
| 3.0 | 800±100 | 1100±100 |
| 4.0 | 1250±100 | 1350±100 |

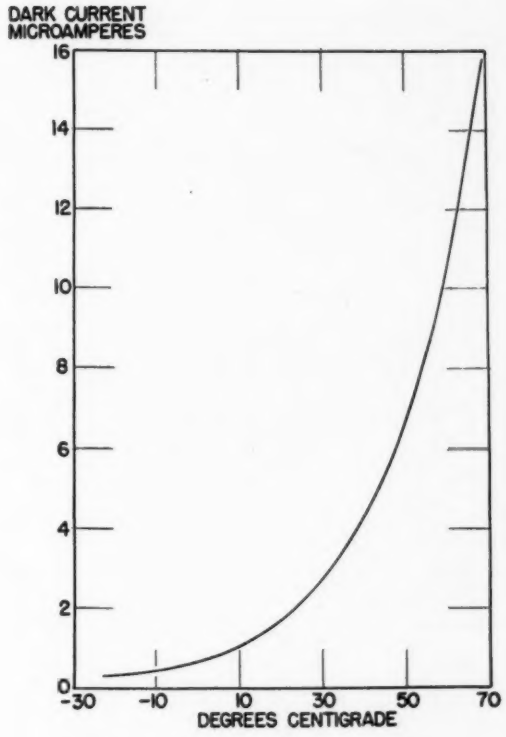


FIG. 4. Dark current *vs.* temperature.

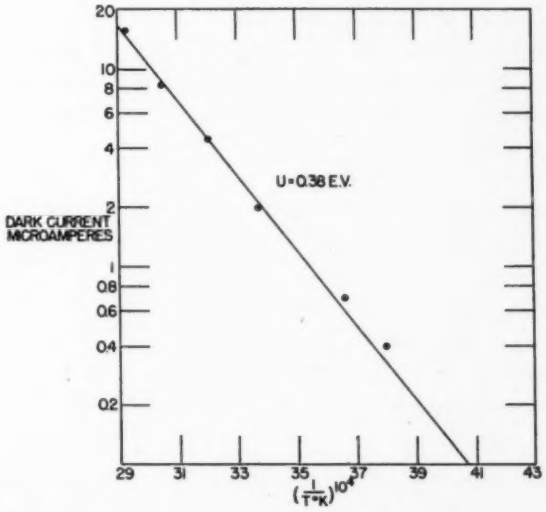


FIG. 4a. Temperature dependence of dark current.

### COMPENSATION OF DARK CURRENT AND NOISE LEVEL

In order to employ the photo-cell with feeble illumination where the corresponding photo-current might be considerably smaller than the dark current, it is necessary to compensate for the latter. This can be readily accomplished by employing the cell as one arm of a Wheatstone bridge as illustrated in Fig. 5. If $R_1$ is made high compared to the sum of the resistances of the measuring instrument, $R_G$, and $R_3$, and if the voltage across the cell is adjusted to be 2 volts, then the current output of the cell will be identical with that shown in Fig. 7, where $R_{\text{external}} = R_G + R_3$. The bridge circuit might also be employed to compensate automatically for the temperature dependence of the dark current by replacing $R_1$ by another photo-cell having a temperature dependence of dark current identical with that of the original cell. Another possibility

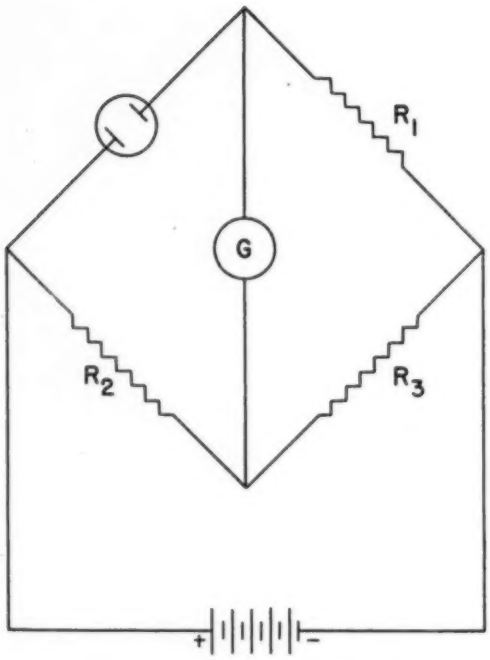


FIG. 5. Dark current compensation.

would be to employ a single cell with a common anode and two cathodes, replacing $R_2$ by the resistance between the anode and the added cathode. However, this scheme has the disadvantage that if $R_3$ is to be kept low, then $R_1$ must be made low in order to balance the bridge, resulting in the shunting of the meter and $R_3$ when off-balance current flows.

It was found that fluctuations of the order of $10^{-8}$ to $10^{-9}$ ampere exist in the dark current.

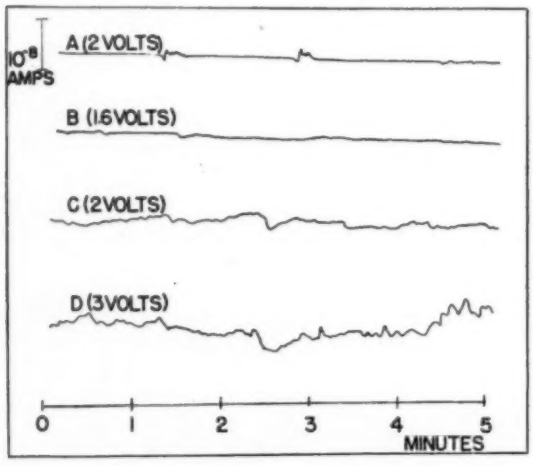


FIG. 6. Dark current fluctuations. $A$ = cell No. 1. $B$, $C$, $D$ = cell No. 2.

Figure 6 gives typical photographic records of the deflections of a sensitive galvanometer used as a null-instrument in the bridge with two different cells operated at different voltages. It is evident that some cells may have very few disturbances and others many, and that the frequency and magnitude of the "noise" increases with voltage, the signal equivalent of the noise being $1\times10^{-5}$ $-1\times10^{-6}$ lumen of unmodulated light.

## LIGHT RESPONSE

### Unmodulated Light

The current output of the photo-cell with a Se-plated anode as a function of unmodulated illumination with various values of resistance in

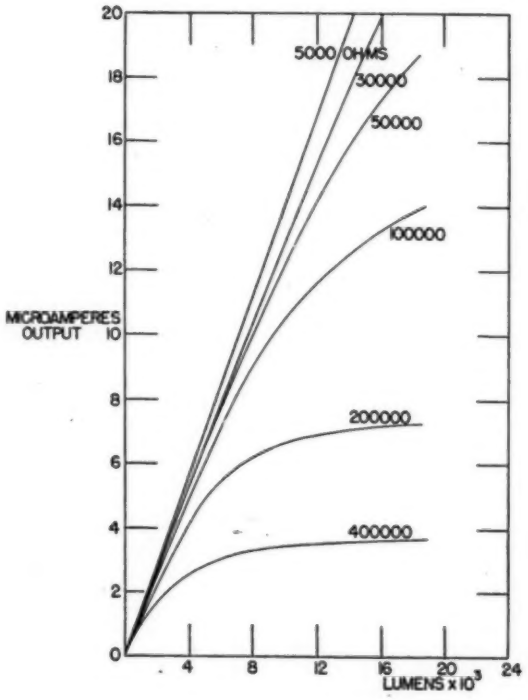


FIG. 7. Effect of illumination and external resistance on current output.

the external circuit and with 2 volts always maintained across the cell in the dark is shown in Fig. 7. The decrease in output and departure from linearity that occur with large values of resistance result from the fact that the cell acts as a photo-conductor with external driving voltage. With increasing current this driving potential is reduced by the voltage drop across the external resistance, thus decreasing the cell's

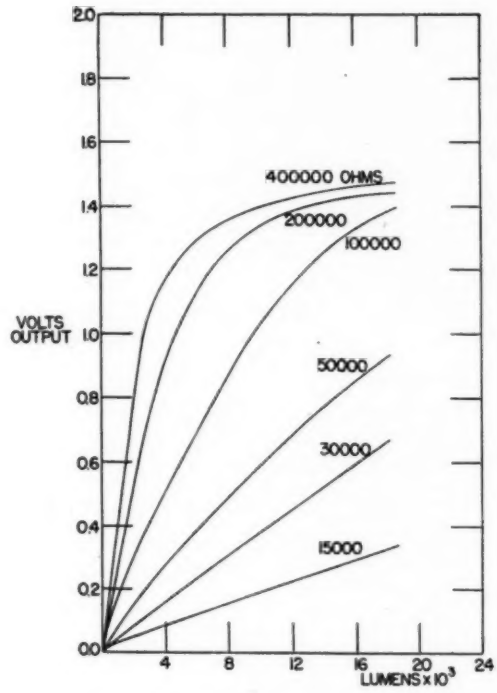


FIG. 8. Effect of illumination and external resistance on voltage output (2 volts applied).

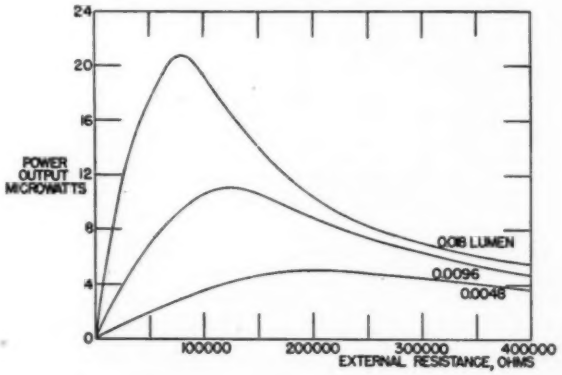


FIG. 9. Power output *vs.* external resistance and illumination.

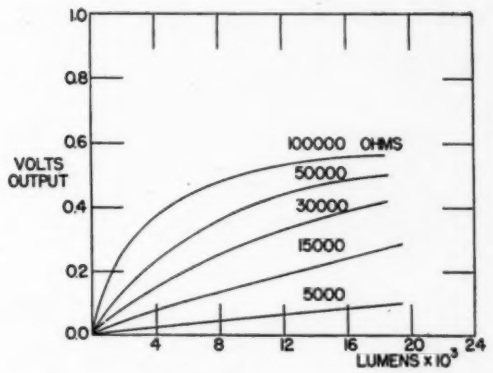


FIG. 10. Effect of illumination and external resistance on voltage output (1 volt applied).

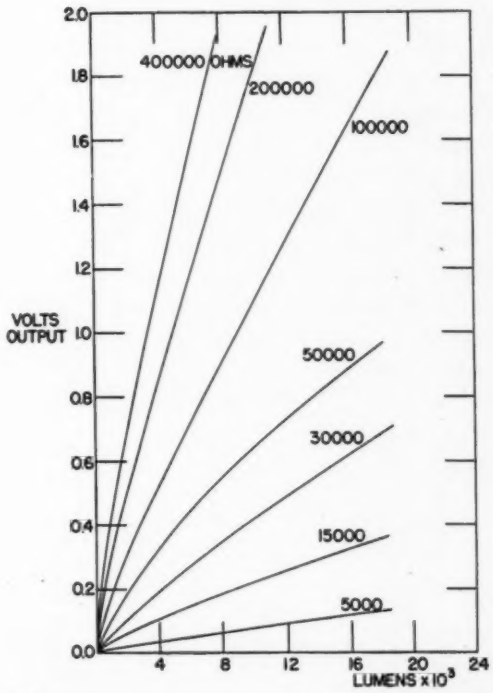


FIG. 11. Effect of illumination and external resistance on voltage output (3 volts applied).

sensitivity. Figure 8 represents the same data, recalculated in terms of the voltage output available across the external resistance, while Fig. 9 gives the power output as a function of external resistance for various values of illumination.

Marked deviation from linearity does not occur until the voltage across the cell falls below a minimum value of the order of 0.6 volt. Consequently, the higher the voltage applied across the cell plus load, the higher will be the voltage available across the external resistance before attaining "saturation" (Figs. 8, 10, 11).

If the voltage across the cell is kept substantially constant by means of a feedback circuit such as that illustrated in Fig. 12, linearity of response results over a wide range of light intensities and external resistances (Figs. 13, 14). The elements included in the broken line in Fig. 12 are part of a bridge network that can be added to compensate for the dark current. The circuit, with minor modification, is generally

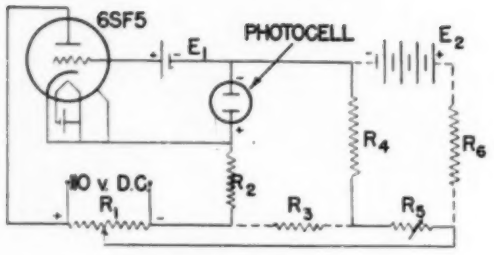


FIG. 12. Feedback circuit.

$E_1 = 1.5$ v $R_1 = 1500\ \omega$ $R_3 = 10000\ \omega$ $R_5 = 500\ \omega$
$E_2 = 22.5$ v $R_2 = 100000\ \omega$ $R_4 =$ Load resistance $R_6 = 10$ megs.

applicable to photo-conductive and photo-voltaic cells.[5]

### Modulated Light

Measurements on the frequency response of the electrolytic photo-element were made using white light, sine-wave modulated, of 150$\mu$ lumens peak value. The circuit consisted of a cell, 2-volt battery and 30,000-ohm resistor in series, the resistance serving to feed the signal into an amplifier coupled to a General Radio Sound Analyzer. Typical data on cells that were several days old, but which had already reached equilibrium sensitivities to unmodulated light, are given in Table III.

A completely fresh cell compared at 80 cycles/second under similar conditions gives a signal output about three times as great and a noise level of about 1$\mu$ volt. An aging phenomenon occurs, however, as cells that have been stored on voltage for some months have a signal output only about one-tenth the value given in Table III at 80 cycles/second and a noise level of about 0.4$\mu$ volt, while the steady light sensitivity is not affected.

Additional data on several cells have been obtained by W. L. Hole at the University of Michigan with square wave modulation of 46$\mu$ lumens peak. For freshly prepared cells response to a 30 cycle/second signal was about one-sixth of that for the unmodulated signal (series resistance = 25,000 ohms), and the noise voltage amounted to about 5$\mu$ volts. Relative response to different frequencies of signal modulation are shown in Table IV.

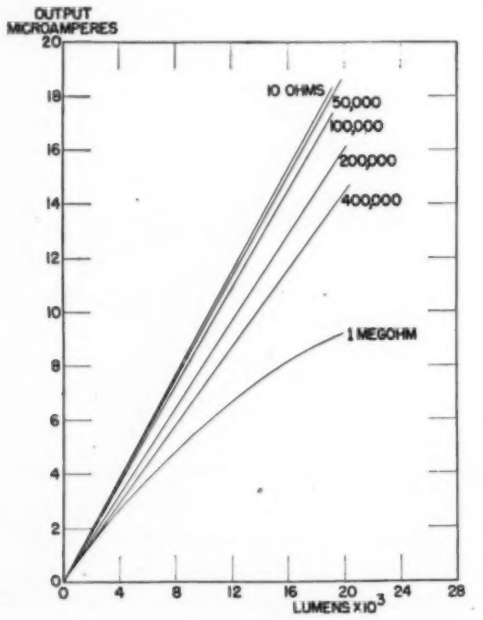


FIG. 13. Effect of illumination and external resistance on current output using feedback circuit.

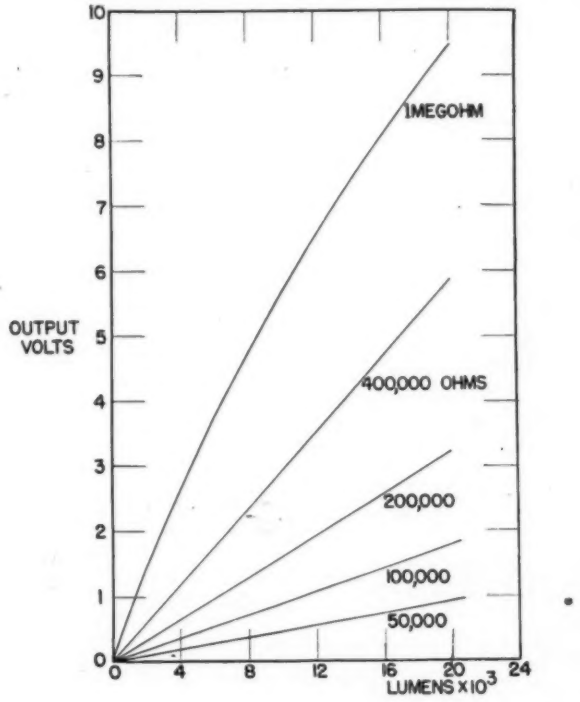


FIG. 14. Effect of illumination and external resistance on voltage output using feedback circuit.

In addition it was ascertained that if the voltage across the cell is maintained at 2 volts, its response to weak, modulated signals becomes independent of strong unmodulated, background illumination. This can be automatically accomplished by the feedback circuit already described.

[5] A discussion will be given elsewhere.

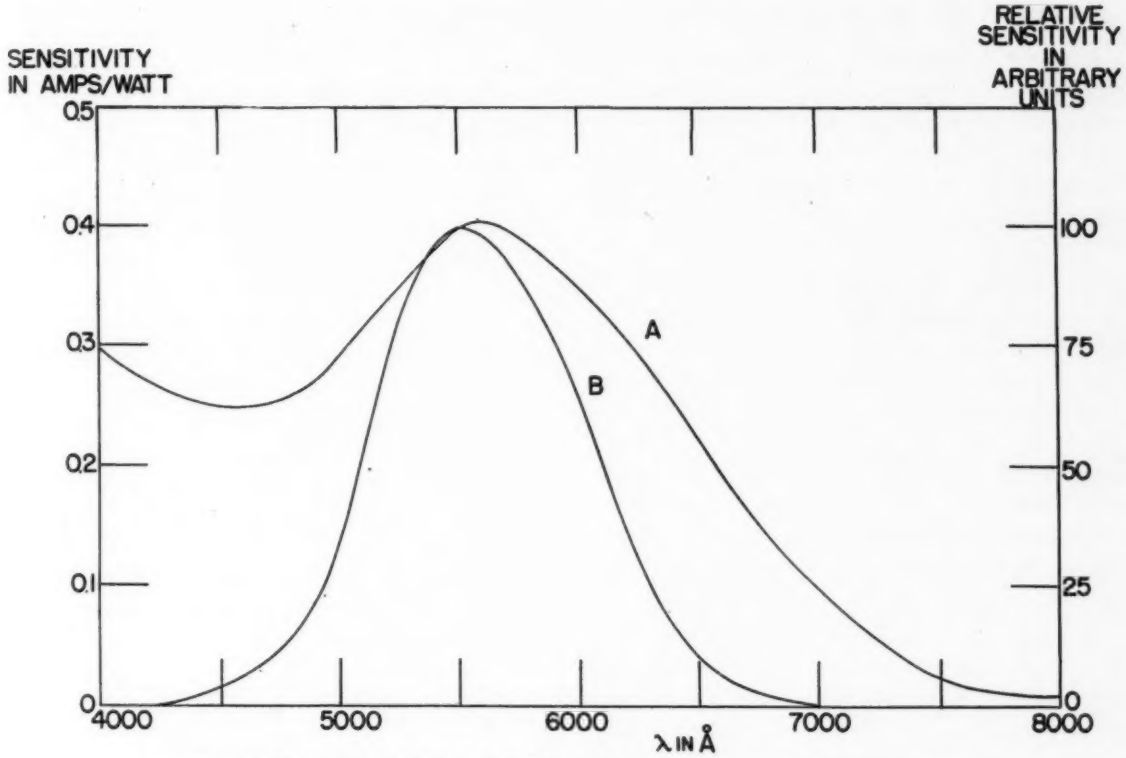


FIG. 15. Spectral sensitivity of *A*—Electrolytic selenium cell, *B*—Average eye.

### Spectral Response

Constant energy spectral sensitivity data for the photo-cell (Fig. 15) were obtained by means of a double monochromator. An electronic regulator, which kept the light output obtained from the monochromator at constant energy by controlling the light input, permitted the automatic recording of the spectral response characteristic. It is of interest to note that the maximum in this characteristic corresponds to a quantum yield of about 0.9 electron per incident quantum.

## LIFE STUDIES

Extensive studies on the life of the photo-element have been made with the following variations: platinum *vs.* selenium anodes; platinum, molybdenum, and stainless steel bases for the selenium; constant illumination and storage in the dark. At the time when the experiments were discontinued, cells containing platinum-base cathodes and either platinum or selenium on platinum anodes had maintained their original equilibrium sensitivity within about 15 percent for a period of six months. The same held true for one such cell with a platinum anode that had been stored in the dark for three months and then constantly illuminated with a 150-watt lamp at 1-foot distance for three months. Cells with molybdenum-base cathodes and platinum anodes and stainless steel-base cathodes and anodes had maintained their high sensitivities during the test period of three months.

TABLE III. Frequency response of electrolytic selenium photo-element.

| Frequency | Signal output | Noise level |
|---|---|---|
| sec.$^{-1}$ | $\mu$ volts | |
| 0 (equivalent unmodulated signal) | 2800 | |
| 80 | 36 | ~0.5$\mu$ volt |
| 200 | 19.5 | |
| 370 | 7.2 | |
| 535 | 5.8 | |

TABLE IV.

| Frequency, sec.$^{-1}$ | 30 | 90 | 330 |
|---|---|---|---|
| Relative response, % | 100 | 36 | 10 |

## COMPARISON WITH OTHER WORK

A number of investigators[6–9] have dealt with electrolytic selenium photo-cells and have observed on illumination of the sensitive selenium surface the development of an e.m.f. as well as the appearance of a short circuit current that quickly decayed. Reinganum[10] has further observed that the cell's sensitivity could be increased and appreciable currents drawn from it if the selenium surface were made the cathode with respect to the other electrode by means of an external battery. An optimum operating voltage was observed using electrolytes of $H_2SO_3$ and HCl in agreement with our data of Table I. A cell almost identical with that of Reinganum was later described by Reiff.[11] Still more recently, a photo-voltaic cell, which we believe to be essentially similar to that of Reinganum, was described by Fink and Alpern.[12] This latter cell made use of a lead anode whose electrochemical counter potential with respect to the solution employed happened to be of the right sign and order of magnitude so that an external battery was not required. The current sensitivity of the cell was of the order of 150 μamp./lumen.[13]

Our cell differs from the earlier electrolytic selenium cells chiefly in that directly electrodeposited metallic selenium gives rise to a higher sensitivity and that the selenious acid permits a higher lifetime as well as hermetical sealing of the cell when a selenium-coated anode is employed. Its characteristics rival most closely those of present commercial selenium "barrier layer" type cells. Its main advantages over the latter type are higher sensitivity, the possibility of making the active surface in practically any shape, and perhaps ease of manufacture. The need for an external voltage supply, the resulting dark current and higher noise level, and the temperature limit imposed by the freezing of the electrolyte are its main disadvantages.

## DISCUSSION

The resistance of a selenium electrode cannot be greater than the order of 100 ohms judging from the over-all conductance of the plating bath. However, the apparent resistance of the electrode in the photo-cell is of the order of a megohm, even if liberal allowance is made for the polarization e.m.f. of the element. The conclusion seems inescapable that a high resistant layer is formed at the cathode by the passage of current. Considering the electrolytes of Table I, the only likely electrode reaction at the cathode is the discharge of hydrogen ions. Hence, the layer may consist of an interstitial solid solution of hydrogen in selenium.

The gradual stripping of the cathode in cells containing acid electrolytes would result from the reaction

$$2H+Se=H_2Se,$$

and similarly the plating of selenium at the cathode in selenious acid solution by hydrogen ion discharge would be the consequence of the reaction

$$H_2SeO_3+4H=Se+3H_2O$$

or

$$H_2SeO_3+2H_2Se=3Se+3H_2O.$$

The rapid decrease in dark current with time after the initial application of voltage is indicative of the building up of the high resistant layer. The large photo-sensitivity observed initially probably represents a lowering of the volume resistivity of the selenium deposit under the influence of light. After the layer of high resistance has been established, the volume resistivity of the selenium is negligible in comparison, and photo-currents observed at that stage probably represent a primary photo-effect.[14]

From a macroscopic viewpoint the presence of a thin layer of high resistance should give rise to an appreciable capacitance. The response of the photo-element to modulated signals can be explained on this basis.

[6] R. Sabine, Phil. Mag. **5**, 401 (1878); Nature **17**, 512 (1878).

[7] G. M. Minchin, Phil. Mag. **31**, 207 (1891); Lúmière éléctrique **48**, 543 (1893); Electrician **26**, 361 (1891).

[8] C. Ries, *Das electrische Verhalten des kristallinischen Selens gegen Wärme and Licht*, Dissertation, Munich (1902).

[9] A. A. C. Swinton, Phys. Soc. Proc. **27**, 186 (1915).

[10] M. Reinganum, Deutsch. Phys. Ges. Ber. **4**, 590 (1906); Physik. Zeits. **7**, 786 (1906); Physik. Zeits. **8**, 293 (1907).

[11] H. J. Reiff, Electrician **60**, 467 (1908).

[12] C. G. Fink and D. K. Alpern, Trans. Am. Elec. Soc. **62**, 369 (1932).

[13] Using an electroplated selenium cathode, we have obtained a current sensitivity in this type of cell as high as 600 μamp./lumen.

[14] The quantum yield for a cell operated at 2 v is quite close to unity at 4000 and 5600A and may slightly exceed 1 at higher voltages. However, primary photo-currents corresponding to yields of 2 electrons per quantum have been observed for the *F'*-bands in the alkali halides and a similar situation may prevail here.

# Studies of Plastic Flow of Steel, Especially in Two-Dimensional Compression

P. W. BRIDGMAN
*The Physics Laboratories, Harvard University, Cambridge, Massachusetts*
(Received November 21, 1945)

The experimental methods are described by which rectangular blocks are subjected to two-dimensional compressional stresses and at the same time flow is maintained two-dimensional with deviations of less than one percent. Within this range of flow a rather wide range of stress conditions is possible, so that the equations of plastic flow can be examined over a correspondingly wide range of conditions. It is found that two-dimensional flow is much more sensitive than three-dimensional flow to shearing instabilities initiated at the edges where there are singularities in the mathematical solution. By proper lubrication it is, however, possible to produce approximately homogeneous deformations in two-dimensional compression at least up to shortenings to two-thirds the initial length. It is found that the transverse stress $X_x$ required to maintain two-dimensional flow is consistently higher than the theoretical value $\frac{1}{2}Z_z$; for some materials the excess above the theoretical value may rise to as much as 20 percent. This excess tends to be less in the early stages of flow, and does not tend to increase beyond strains of 10 percent. The failure of $X_x$ to be equal to $\frac{1}{2}Z_z$ indicates a failure of the fundamental condition of isotropy of flow; this failure may be demonstrated in other ways. The time rate of primary flow is studied at various points on the strain-hardening curve. The rate of flow rises rapidly as the stress increases above the limiting strain-hardening curve. The rate of increase of the rate of flow for a given displacement from the limiting curve is much greater in the early stages of flow. It is this which makes possible the calculation of the rate of propagation of a plastic disturbance from the parameters of the static strain-hardening curve. Beyond the early stages of flow new time effects begin to appear. The flow loses its smoothness and becomes more and more inclined to be jerky. At high strains, flow may not start at once when the load is increased, but there may be an initiation period during which flow is built up. The application of the results to the generalized strain-hardening curve is discussed. In view of the failure of isotropy, strictly speaking, a generalized strain-hardening curve does not exist. Within the strain limits of this paper it is found that both the maximum shearing stress criterion and the "significant" stress-strain criterion apply with errors of the order of 10 percent, the maximum shearing stress criterion being on the whole perhaps somewhat better.

## INTRODUCTION

THE stress conditions under which plastic flow has been studied up to the present have been usually restricted because of the experimental inconvenience of applying stresses which are arbitrarily variable in different directions. The most common method of realizing more than one arbitrary component of stress has been by the simultaneous application of longitudinal tension and internal hydrostatic pressure to thin tubes. By this method it is possible, within certain limits, to apply two arbitrary components of tensile stress. The plastic flow which can be produced in this way is limited to comparatively small values by the incidence of tensile fracture. Much larger strains could be realized without fracture under compressive stresses, but few, if any, such experiments appear to have been made, although it would seem that it would not be especially difficult to expose a tube to external pressure with simultaneous longitudinal compression or tension. It would, however, probably be necessary to use tubes of appreciable thickness in order to avoid buckling under the external pressure, and in this case the strains would not be homogeneous and the interpretation of the results would be complicated.

In the following, experiments are described in which rectangular blocks are exposed to arbitrarily variable compressive forces on two of the three pairs of faces, the remaining pair of faces being free from force. The stresses and the strains are homogeneous, and the mathematical interpretation of the results is especially simple, the experimental test block playing the role of the mathematical element of volume of the fundamental equations. The compressive forces are applied by hard platens pressing against the faces. Obvious geometrical limitations arising from mutual interference of the platens impose rather definite restrictions on the strains. There are doubtless various ways of meeting the geometrical conditions. In the following the strain as well as the stress was kept two-dimensional, on the gross average. Since two-dimensional stress in general produces three-dimensional flow, restriction of the strain approximately to two dimensions might appear to

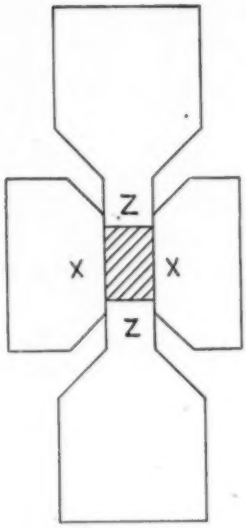


FIG. 1. Section through the platens for simultaneous compression in two directions at right angles. The specimen is shown shaded. The $Z$ blocks and the $X$ blocks are pushed together by two independent hydraulic presses.

seriously limit the part of the two-dimensional stress domain open to exploration. However, small deviations from a rigid two dimensionality in the strain were instrumentally feasible, which gave sufficient flexibility to permit a very considerable variation in the stresses, so that a very appreciable part of the total region of plastic flow under two arbitrary compressive stress components could be explored in spite of the geometrical restrictions.

### THE APPARATUS AND METHOD

The direction of larger compressive stress will be denoted by $z$, that of minor compressive stress by $x$, and the direction of no stress by $y$. The corresponding stresses will be written as $Z_z$, $X_z$, and $Y_y(=0)$. The $Z_z$ stress is applied by a pair of opposing rectangular blocks, of indefinite length in the $y$ direction and with a width in the $x$ direction approximately equal to the $x$ dimension of the specimen. The $X_z$ stress is applied by two hard blocks of indefinite extent in both the $z$ and the $y$ direction; the distance between these two blocks in the $x$ direction must be kept not far from the initial width of the test block. The arrangement is indicated in Fig. 1. If the distance between the $x$ blocks becomes less than the initial $x$ dimension of the $z$ blocks, these will be pinched and the measured stresses will be in error. On the other hand, if the distance becomes too great, the test block will flow plastically into the narrow channel between $z$ and $x$ blocks, destroying the homogeneity of both stress and strain. In the following experiments the initial $x$ dimension of the test block was made 0.502 inch and of the $z$ block 0.500 inch. During the experiment the distance of separation of the $x$ blocks was kept between 0.501 and 0.504 inch; within these limits there was neither pinching nor appreciable plastic flow into the crevasse at the edge, which was only 0.002 inch wide at the most. The $x$ component of force must be maintained in such adjustment as to keep the $x$ dimension in these limits; a rather wide latitude proved possible in meeting these conditions.

The $z$ blocks and the $x$ blocks were pushed together by two independent hydraulic presses. The press driving the $z$ blocks was a standard press that has been used in much of my other work; it has a 3.5-inch plunger, a free space of 10 inches between the rods, and is driven by a hand pump with capacity of 15,000 p.s.i. The $x$ blocks were pushed together with a specially constructed press with 2.5-inch plunger. This press was machined from a single piece of steel 4 inches in diameter and was compact enough to be mounted transversely in the 10-inch free space between the tie rods of the 3.5-inch press. Pressure was furnished by a second hand pump. This press was freely suspended from a point in the vertical line with its center of gravity, so that the whole press floated and could follow the motion of the specimen as it was plastically deformed, without exerting any extraneous force on it. The maximum displacement of the $x$ press was 0.002 inch in the $x$ direction and 0.125 inch in the $z$ direction. Pressure was led into it through copper tubing of 0.25-inch outside diameter and 0.062-inch inside diameter; the tube was made long enough to exert no appreciable constraint.

Two different methods of applying the loads were employed. In the first, the pistons were advanced by pumping until approximately the desired increment of strain was reached. Pumping was then stopped and time allowed to elapse until a steady state was approximately attained. This steady state was reached by a simultaneous further slight automatic change of both strain

and pressure. Since the flow in the $z$ direction was, in general, many-fold greater than that in the $x$ direction, most of the manipulations were connected with the $z$ press. A fraction of a stroke on the pump of the $x$ press at the beginning of the stop usually was sufficient, the pressure of the $x$ press then automatically taking care of itself. The steady-state pressures were read on calibrated Bourdon gauges in the lines of the two presses. In the second method of applying load, measurements were made at controlled intervals of total load. This was accomplished by interposing in the lines leading to the presses two dead weight free piston gauges. Pressure was adjusted by setting the appropriate weight on the pan of the dead weight gauge, and pumping until the piston floated. Since the motion in the $x$ direction was so slight, automatic rise or fall of the free piston of the $x$ gauge was sufficient to maintain the load constant within the limits of $x$ deformation. The motion in the $z$ direction was sufficiently large, however, to demand frequent pumping to keep the $z$ free piston floating. For the more rapid rates of flow in the $z$ direction the sluggishness of response of the free piston gauge was great enough so that the load would have fluctuated within undesirably wide limits even if the piston were kept always floating by rapid pumping. Especial measures had to be taken to meet this condition. In the first place, the piston of the free piston gauge was made much looser than is convenient for normal operation. The most important modification, however, was to provide volume flexibility in the line to the $z$ press by attaching a reservoir of 750-$cm^3$ capacity containing compressed nitrogen, obtained initially from a storage flask carrying 1500 p.s.i. Up to pressures on the 3.5-inch piston of 1500 p.s.i., pressure was obtained from the compressed storage flask by admitting the requisite amount of gas through a valve. Above 1500 p.s.i., the storage flask was cut off and pressure obtained by the hand pump. The maximum pressure on the 3.5-inch plunger was of the order of 7,000 p.s.i. A simple calculation showed that even under the most rapid plastic flow of these experiments inertia effects in the moving parts of the presses are inappreciable.

The running dimensions of the test block in the $z$ and $x$ directions during the course of the experiment were measured by measuring the distance of separation of the $z$ and the $x$ blocks. This was done with Ames dial gauges, mounted on yokes attached to slender rods straddling the specimen and passing through appropriate holes drilled in the blocks. Since the motion in the $z$ direction was large, reaching a maximum of 0.25 inch, it was sufficient to measure the $z$ displacement with an ordinary guage, graduated to 0.001 inch, with 1-inch total stroke. The $x$ displacements, being much smaller, were measured with a jewelled gauge graduated to 0.0001 inch with total stroke of 0.2 inch. Any lagging of the gauge readings due to friction was eliminated by introducing into the whole system a very slight amount of mechanical vibration by pressing an electric razor against an appropriate member of the apparatus. Consistent differential readings of the $x$ dimensions could be made to 0.00001 inch or even better if the pointer of the dial happened to be exactly on a division.

Under stress, the dimensions of the test block differ from the dimensions indicated by the Ames gauges by the elastic distortion of the $z$ and the $x$ blocks. A special study was made of the elastic distortion by stressing hardened test blocks of various dimensions. Any correction of this sort was found to be unimportant. The method finally adopted for dealing with it was to obtain the elastic distortion at the maximum stress by comparing the Ames gauge readings with the micrometer dimensions of the test block after removing from the apparatus, and to distribute the maximum correction over the intermediate stresses in proportion to the load.

The $x$ blocks were made of tool steel, hardened to Rockwell C 67. In general the stress which the $x$ blocks have to carry is one-half that of the $z$ blocks. The $z$ blocks were also at first made of the same tool steel as the $x$ blocks. Their performance was later somewhat improved by setting in carboloy inserts. Carboloy can be highly polished so as to minimize the friction; furthermore, carboloy, being only one-third as deformable as steel, does not permit the test specimen to imbed itself to the same extent, so that the effective friction is reduced as the test specimen extends itself plastically along the platen, pushing its advancing edge up the incline of the depression in the platen.

One of the objects of the experiments was to study the rates of flow for various combinations of stress. The "flow" understood here is the "primary" flow which occurs immediately after application of an increment of load and does not include such long range phenomena as elastic after-effects and creep. Of course, there is no sharp dividing line between these various effects; the time intervals involved in these measurements were not greater than the order of fifteen minutes. At first observations were made with manual recording and an ordinary watch, but these proved inadequate, and the final study of the rates of flow was made with photographic recording. The two Ames dial gauges were mounted side by side in the field of an Eastman Cine Special, for 16-mm film, so arranged that single frames could be exposed, either by hand operation for moderate rates of flow, or for more rapid rates by motor control, permitting up to a maximum of four exposures per second. The full opening, $f$: 1.9, was used, as well as maximum film speed, corresponding to 64 frames per second for normal operation, and one-quarter shutter opening. Illumination was by two suitably mounted 500-watt floodlights. It was necessary to use a film of high contrast, in which the exposure latitude was accordingly small; the film used was Eastman positive. I am much indebted to Mr. Paul Donaldson for skillful development of the film and advice with regard to photographic details. The time was provided by a synchronous Telechron motor connected so as to give one revolution per second, the hand sweeping over a dial graduated to 1/100's. The total number of revolutions (i.e., seconds) was counted by a conventional Veeder counter mounted so that it was also in the field of the camera. The current weights on the free piston gauges were also recorded photographically, suitable labels being placed manually in the field when the weights were changed. An additional check on the $z$ load was obtained by also recording the stretch of the tie rods of the $z$ press; this stretch gives the actual load on the specimen without the component due to friction of the ram. The stretch of the tie rods was measured with an Ames 0.0001-jewelled gauge, connected to the tie rods through a lever giving fivefold multiplication, so that changes of length of 0.000002 inch could be established. This corresponds to a $Z_z$ stress on the test specimen of about 2 kg/cm². With the tie rod gauge it was possible to establish that there was perceptible sluggishness in the response of the stress to changes of load on the free piston gauge, in spite of the amelioration by the use of the gas reservoir. This sluggishness, however, was confined to the initial stages immediately after change of load when the rate of flow was high, and was therefore not a matter of importance. On the conclusion of a run, the specimen was removed and several photographs taken of it on the same film, as a matter of record. The film was then developed, transferred to a couple of spools which permitted it to be conveniently examined under a microscope, and the desired data read off from the film and recorded. The photographic record was sharp enough so that times could be read to a fraction of a hundredth of a second, and the Ames gauges to a tenth of their smallest divisions.

## THEORETICAL BACKGROUND

The experimental procedure was guided by the accepted equations of plasticity; investigation of the validity of these equations was one of the principal objects of this work. We shall write these equations in the form for flow:

$$\frac{\dot{\epsilon}_x}{X_x-\frac{1}{2}(Y_y+Z_z)}=\frac{\dot{\epsilon}_y}{Y_y-\frac{1}{2}(Z_z+X_x)}=\frac{\dot{\epsilon}_z}{Z_z-\frac{1}{2}(X_x+Y_y)}.$$

In these equations the $x$, $y$, and $z$ axes are assumed to be the principal axes both of stress and of strain. This demands that the axes do not rotate in space during the straining process; this condition is obviously satisfied in the present experiments. The strains are the "natural" strains, that is, $\epsilon_x=\log_e(l/l_0)_x$. The usual sign convention will be followed; a tensile stress will be taken as positive and a strain of extension positive. Under the conditions of our experiments, $Y_y$ vanishes identically, so that the equations can be specialized as follows:

$$\frac{\dot{\epsilon}_x}{X_x-\frac{1}{2}Z_z}=\frac{\dot{\epsilon}_z}{Z_z-\frac{1}{2}X_x}.$$

Furthermore, $Z_z$ is always larger numerically than $X_x$. If we put $X_x=\alpha Z_z$, $\alpha$ will vary between zero and unity. Under these conditions $\dot{\epsilon}_z$ always has the sign of $Z_z$. The flow along the $x$ axis

vanishes for $\alpha=\frac{1}{2}$, has the same sign as $\dot{\epsilon}_z$ for $\alpha$ greater than 0.5, and the opposite sign if $\alpha$ is less than 0.5. The ratio of the two velocities expressed in terms of $\alpha$ is: $\dot{\epsilon}_x/\dot{\epsilon}_z=(2\alpha-1)/(2-\alpha)$.

In the following experiments the conditions are investigated under which there is no flow in the $x$ direction, and also, when there is such flow, whether the velocity of flow in the $x$ direciton bears the theoretical ratio to velocity in the $z$ direction in terms of $\alpha$. These questions are to be investigated at various points on the strain hardening curve; it is conceivable that one relation might hold in the initial stages of flow and another in the later stages when there has been appreciable strain hardening. The basic physical postulate back of the above expressions for flow is the postulate of isotropy. One of the objects of the following experiments may therefore be phrased: to find to what extent the basic assumption of isotropy is satisfied.

It is obvious that if $\alpha$ varies arbitrarily during the straining process the flow equations cannot be simply integrated, and we may *not* write the conventional expression

$$\frac{\epsilon_x}{\epsilon_z}=\frac{X_x-\frac{1}{2}Z_z}{Z_z-\frac{1}{2}X_x}.$$

In these experiments $\alpha$ did vary during the straining process, so that the simple integrated form is not admissible. In general, it is obvious that no integrated form of the equations, in which the history of the variation of $\alpha$ or something equivalent to it does not appear, can be better than an approximation. The mere existence of an integrated form of the flow equations obviously imposes restrictions. It is customary to suppose that not only are the restrictions met, so that the history of $\alpha$ does not enter the final equations for strains, but that there is such a simple connection between strains and stresses of different types that if the relation between strain and stress is known for one type of stress it may be inferred for other types of stress. Various suggestions have been made as to the nature of the generalized relation. One of the most recent, and also one of apparently wide applicability, is that the "significant" stress, $\bar{S}$, is a universal function of "significant" strain, $\bar{\epsilon}$, for all types of plastic flow. The significant stress and strain are defined as follows:

$$\bar{S}=\{\tfrac{1}{2}[(X_x-Y_y)^2+(Y_y-Z_z)^2+(Z_z-X_x)^2]\}^{\frac{1}{2}}$$
$$=Z_z(1-\alpha+\alpha^2)^{\frac{1}{2}},\ (\text{if } Y_y=0,\ X_x=\alpha Z_z)$$
$$\bar{\epsilon}=[\tfrac{2}{3}(\epsilon_x^2+\epsilon_y^2+\epsilon_z^2)]^{\frac{1}{2}}=\epsilon_z(4/3)^{\frac{1}{2}},$$
$$(\text{if } \epsilon_x=0,\ \epsilon_y=-\epsilon_z).$$

The curve which gives $\bar{S}$ as a function of $\bar{\epsilon}$ may be described as the generalized strain-hardening curve. One of the objects of the following experiments was to determine the generalized strain-hardening curve under the present conditions (i.e., strain approximately two-dimensional, with two-dimensional stress), and to find whether significant stress is indeed a universal function of significant strain by comparing with the plastic flow obtained under other conditions of stress, in particular under simple compressive stress ($X_x=Y_y=0$).

Returning now to the rate of flow, we have so far considered only relative rates of flow in different directions. There is also the more fundamental matter of absolute rate of flow. To consider this question the flow equation must be expanded into the form:

$$\frac{\dot{\epsilon}_x}{X_x-\frac{1}{2}Z_z}=\frac{\dot{\epsilon}_z}{Z_z-\frac{1}{2}X_x}=\varphi.$$

A complete investigation of the phenomena demands that we find of what arguments $\varphi$ is a function, and what is the value of the function for various values of its arguments. It is obvious physically that for points in the stress-strain plane below the strain-hardening curve $\varphi$ must vanish identically, there being no plastic flow here, and that $\varphi$ must be everywhere positive in a region above the stress-strain curve. The mere existence of a strain-hardening curve would seem to suggest that $\varphi$ gets larger very rapidly as the distance from the strain-hardening curve increases. Too great displacement from the strain-hardening curve would lead into the domain of fracture. $\varphi$ must then, at the very least, be a function of stress and strain. It is such a function that for every value of stress, within limits, there is some strain which makes $\varphi$ vanish; in general, the larger the stress, the larger the corresponding strain. In addition to being a function of stress and strain, $\varphi$ may also well be a function of history. If it is not a function of history, as

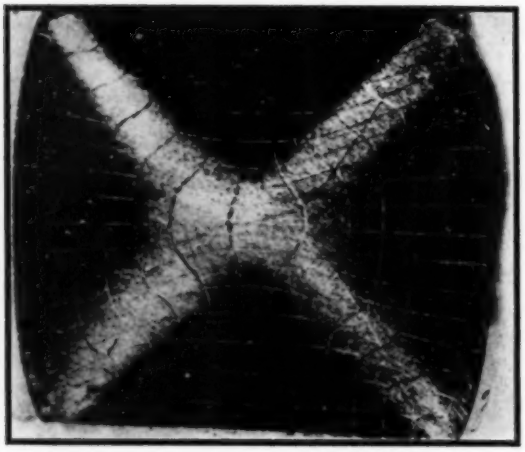

FIG. 2. Typical deformation with high friction.

perhaps we may assume provisionally as a first approximation, then $\varphi=0$ is the equation of the strain-hardening curve. Considerations of symmetry demand that under these conditions the stresses and strains enter through their invariants, or $\varphi$ have the form $\varphi\{\text{stress invariant} - f(\text{strain invariant})\}$. Comparison with the definitions for significant stress and strain shows that this is equivalent to $\varphi\{\bar{S}-f(\bar{\epsilon})\}$.

It was one of the purposes of the following experiments to get some indications as to the form of $\varphi$ and to find to what extent the above simple assumptions about its nature are justified.

In actually carrying out the measurements the conditions are by no means as simple as in the ideal mathematical discussion above. The chief disturbing factor is terminal friction on the $z$ faces. It is well known that in a simple compression test, with free lateral expansion, the specimen has a tendency to barrel out because of the frictional constraint on the ends. If friction is reduced by proper lubrication, barrelling disappears and the strain becomes homogeneous. Under our conditions, compression with one component of lateral flow prevented, the effects of terminal friction proved to be much larger, and were also much more difficult to eliminate. The nature of the distortion can be made visible by scratching on the $X$ surfaces of the virgin specimen a rectangular grid, together with a couple of diagonals to make the distortion at the corners more manifest. Figure 2 is a photograph of the $x$ face of a compressed specimen in which the lubrication of the $z$ face was not adequate. Part of the original $y$ face has rolled up onto the $z$ face, the edge still being, however, a more or less sharp right angle. This would suggest that there must be some sort of mathematical singularity at the edge. In fact, a moment's consideration shows that in a compressed specimen flowing over the platen with friction there must be a mathematical singularity at the edge. For in the $z$ face, because of friction, there is at the edge a non-vanishing tangential stress $Y_z$, whereas in the $y$ face at the edge the tangential stress component $Z_y$ vanishes identically merely because the surface is free. Here is a contradiction, because the conditions of mathematical equilibrium demand that everywhere $Y_z=Z_y$. An exact mathematical characterization of the details of the singularity demanded to avoid this contradiction would depend in any particular case on the elastic deformation of the platen, and would doubtless be difficult to obtain. The general nature of the singularity, however, is probably the same whatever the details, and may be obtained from any particular solution. There is one particular solution in the literature due to Nadai.[1] Another particular solution, involving only very simple mathematical functions, has been found by Westergaard, but has not yet been published. Both of these solutions agree that the singularity at the edge involves a shearing stress which is a maximum on the plane approximately bisecting the edge angle. In the present work there was frequently observed a region of maximum shearing distortion in a 45° zone; it is plainly evident in Fig. 2. Slip in this zone gets started with great ease and propagates itself so as to amount to an essential instability. This instability may be favored by the geometry of the specimen. This sort of slip starts most easily if the $x$ face is a square ($z$ and $y$ dimension equal). If the initial dimensions of the block are in the proportion of 3:2, 45° slip is not inclined to start at first, but as the distortion proceeds and the ratio of the sides passes through 1:1, diagonal slip is very likely to start. In fact, if the ratio of the $y$ dimension to the $z$ dimension is integral, a shearing pattern on 45° lines is very apt to develop; Fig. 3 suggests such

[1] A. Nadai, Zeits. f. Physik **30**, 115 (1924).

patterns that have been observed for the 2:1 and the 3:1 ratio.

These regions of concentrated shear may be suppressed by suitable lubrication; the requirements are much more difficult to meet than they are for ordinary simple compression. This seems natural, for we are here concerned with slip on a single set of planes, whereas in simple compression, cross slip on two interfering systems of planes is involved, with greater destruction of the microscopic structure. In the description of the detailed experiments the details of the lubrication will be described, and also the investigations to find what error is introduced by the inhomogeneities that actually occur.

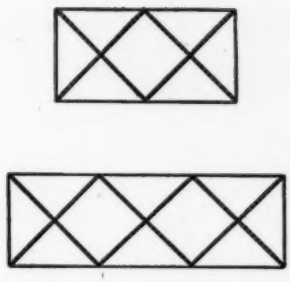

FIG. 3. Schematic diagram showing the regions of maximum shearing distortion of blocks compressed with friction on the bearings faces, with an integral ratio of height to breadth.

## THE MEASUREMENTS

Three types of measurements were made: those in which an approximately steady state was reached, those in which the velocity of flow was measured under constant load, and those in which the rate of flow was maintained constant and the stress determined as a function of strain.

### 1. Approximately Steady-State Measurements

These measurements embrace a determination of the strain-hardening curve, and a determination of the ratio of $X_z$ to $Z_z$ (that is, of $\alpha$) for vanishing flow in the $x$ direction. This type of measurement was made first, and involved considerable preliminary work, the nature of which will be indicated.

The original program called for a series of measurements corresponding to those already made in simple compression; in these experiments the height of the block was reduced to $\frac{2}{3}$ its initial height in a single stage of compression, the block was then remachined back to its original proportions, and the process repeated seven or eight times until the total reduction was some twenty-fold. It was soon obvious that there would be great difficulties in carrying through an analogous program for two-dimensional compression because of the much greater tendency to distortion during compression. Even a single stage of compression with a reduction of height to $\frac{2}{3}$ demanded much more perfect lubrication. A number of experiments were made to find the best lubrication. The method used successfully for simple compression was the same as that used for the lubrication of the external conical surfaces of my high pressure containers, namely, two thicknesses of 0.002-inch lead foil smeared on all sides with a thin paste of colloidal graphite, glycerine, and water. The distortion with this lubrication proved undesirably large under present conditions. Other simple lubricants were tried: Scotch tape, stearic acid, lead oleate, gold leaf, either alone or in various combinations with the lead foil, but were not satisfactory. A thin layer of soft solder applied with a soldering iron was not bad, but was not used for fear of annealing effects from the heat of the iron. Experience with the coat of solder was useful, however, in indicating that a plastic film tightly attached to the steel is desirable. If the film has not some sort of attachment it will be entirely squeezed out; this was the trouble with the lead. Various schemes were tried on the idea of a guard ring, that is, a separate layer of the same material in contact with the platens, the idea being that the deformation due to friction would be confined to the guard layer, leaving the central portion homogeneously strained. Any arrangement analogous to a guard ring proved, however, extraordinarily sensitive; it would either flow completely away from the central block or else embed itself in it, and the scheme was abandoned. The method finally adopted was to copperplate the $z$ faces with a film of copper about 0.001 inch thick, and then put on top of the copper the sandwich of lead foil and graphite paste described above. Some difficulty was found in making the copperplating sufficiently adherent; the final technique was to start the plating in a cyanide bath and finish in an acid sulphate bath. The $x$

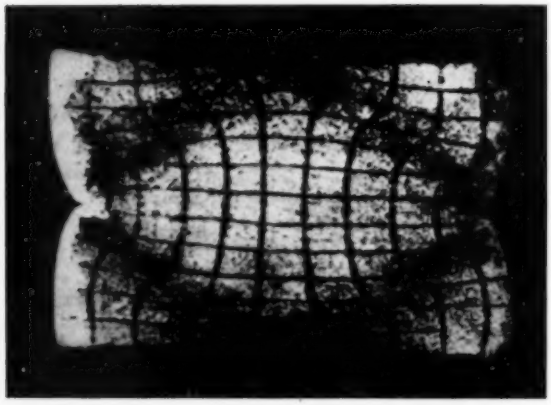

FIG. 4. Typical distortion of a block compressed for the second time after refiguring.

faces are not as sensitive to friction effects as are the $z$ faces; for the $x$ faces the simple lead foil sandwich was adequate.

After the first compression, the equator was always bulged slightly, even with the best lubrication. Under the best conditions the strain at the equator might be two or three percent greater than at the ends. If now the compressed specimen is machined back to the original proportions and subjected to a second compression, the equator at the beginning of the second compression will be more strain hardened, so that the ends will start to flow first. It might be thought that this condition would be self-correcting, since an excess flow at the ends would harden them and the flow would be thrown back to the equator. Actually, however, initial excess flow at the ends is followed by the development of shearing instability and the block folds into a crease based on the equator, as shown by Fig. 4. It might appear that this sort of thing could be avoided by making the end friction somewhat greater on the second application, but this proved too sensitive to manage, the second compression being almost certain to develop an instability like that of either Fig. 2 or Fig. 4, if the initial stage of compression was pushed as far as a shortening to $\frac{2}{3}$. It therefore proved infeasible to carry through the original program of pushing the strains to large values by the device of multiple compressions with refigurings. If, however, the strain of the individual stages is kept to something of the order of 10 percent, multiple compressions with refiguring can be carried out, and runs were made on two different steels with six stages of compression with a total shortening to one-half.

The extra labor of making six stages in order to reach a strain of 0.7 (shortening to one-half) is not justified, however, because in a single stage strains up to 0.4 (shortening to two-thirds) can be reached with no appreciable error from lack of homogeneity of flow, although the inhomogeneity may be too great to permit a second stage of compression. The question of the character of the inhomogeneities and the error that might be introduced by them was examined with some care. The nature of the plastic flow was studied with the help of a network of squares scratched on the $x$ faces, as already indicated. After compression the squares are deformed, and a measurement of the deformed squares under a micrometer microscope gives the local deformations. If the end friction is too great, the sort of plastic flow indicated in Fig. 2 is produced. The $y$ face rolls up onto the $z$ face at the edge, the angle at the new edge remaining comparatively sharp. The edges are, therefore, a region of infinite strain. From the edges a shearing cross is developed diagonally across the $x$ faces; this shearing cross is marked by surface roughening of the steel, plainly visible in the photograph, and by great angular distortion of the squares. Based on the $z$ faces are two triangular prismatic wedges which are pushed almost bodily into the remaining material. In this wedge the squares preserve nearly their original dimensions. At the center of the $x$ face, where the shearing diagonals cross, the square is deformed to a rectangle, without angular rotation.

If the deformation were homogeneous, the initial height being $h_0$ and the final height $h$, it is easy to see that a square would be deformed to a rectangle, the ratio of whose sides is $(h/h_0)^2$. (For the height of the square is reduced in the ratio $h/h_0$, and the width is increased in the ratio $h_0/h$.) The deviation of the ratio of the sides of the deformed square from $(h/h_0)^2$ may be taken as a measure of the failure of the deformation to be homogeneous. With good lubrication this ratio was found to have its theoretical value within experimental error. Thus, a block of soft Cr V steel compressed to

approximately two-thirds its initial height gave a ratio for the sides of the deformed square at the center of the $x$ face of 2.23 against an $(h_0/h)^2$ of 2.28, and another block of the same steel under approximately the same compression gave 2.32 and 2.33, respectively. On the other hand a specimen in which there was a well-developed shearing cross and marked rolling at the edges gave for the ratio at the center of the $x$ face 5.01 and at the base of the prismatic wedge 1.70, against an $(h_0/h)^2$ of 2.19.

Another method of measuring the failure of homogeneity, simpler and not so detailed, but adequate for most purposes, is merely to determine the ratio of the $y$ dimension at the equator of the $x$ face after compression to the average of the $y$ dimension at the two ends of the $x$ face. For good specimens this differs from unity by only a few percent.

In determining the strain-hardening curves it is the average stresses and the average strains which are determined, and it might be suspected that these averages would be relatively insensitive to local deviations from homogeneity. It turned out as a matter of fact that the averages were so insensitive that one could practically disregard any inhomogeneities within the limits of compression mentioned. Thus, in one experiment with a soft Cr V steel, the lubrication on the $z$ face was intentionally omitted so as to develop the maximum inhomogeneity. The compressed specimen had a strongly developed shearing cross, and the rolling at the edges was so great that 16 percent of the final $z$ face had originally been part of the $y$ face. The strain-hardening curve for this specimen lay only 5 percent below the average of the curves for several other specimens, the deformation of which was essentially homogeneous. It was a general result that, if anything, the average stress for non-homogeneous distortion is less than for homogeneous distortion.

The general method of determining the strain-hardening curve with approximately zero velocity of flow in the $x$ direction was as follows. The hand pumps were direct connected to the presses, without the intermediary of a free piston gauge, and the pressures were read from the corresponding Bourdon gauges. The dead spaces in the presses and connections were minimized so that a maximum pressure increment would be produced by a given increment of strain. A preliminary run was made to determine the approximate values of the $x$ pressure required for zero $x$ flow corresponding to various $z$ pressures and strains. Two observers took part in the final run; the function of one was to observe the $x$ pressure gauge and of the other to perform the pumping and observe the $z$ gauge. Both presses were first brought to pressures slightly below the initial plastic yield point. The $x$ press was then raised somewhat, and the $z$ pump then operated slowly. On passing the yield point the $x$ pressure started to drop slowly, since it had been intentionally set too high, at the same time the $x$ dimension decreasing. As the $z$ pressure continued to rise with continued flow in the $z$ direction, the drop of $x$ pressure slowed down, ceased, and then reversed. Constant $x$ pressure means zero velocity of $x$ flow. The instant the $x$ observer detected a reversal, the $z$ pumping was stopped and the various readings recorded, thus obtaining the data necessary for a calculation of a point on the strain-hardening curve and for the simultaneous values of $X_z$ and $Z_z$ which make $\dot{\epsilon}_z$ vanish. The $x$ pressure was then raised so as to be slightly "too high," and the process repeated. After familiarity had been acquired, it was possible by cautious procedure to obtain from 5 to 10 points on the strain-hardening curve in a total range of $z$ strain of 0.4. This "familiarity" involved so choosing the increments of $x$ pressure that the total flow in the $x$ direction never passed the limits of 0.002 inch. No rigid time schedule was adhered to; the pumping was "slow," which meant that from 5 to 10 minutes was used in giving an increment of strain of 0.05. The $x$ Bourdon pressure gauge was graduated to 10 kg/cm$^2$; it was constructed by the Société Genvoise in the early 1900's, and had a very good multiplying mechanism, which gave readings with no perceptible back lash. It was possible to establish the point of reversal within 1 kg/cm$^2$ or better. From the known dimensions of the dead space in the $x$ press and the compressibility of the transmitting oil it is possible to calculate that a pressure increment of 1 kg/cm$^2$ should correspond to a distortion of the specimen of approximately 0.000003 inch. That is, the pressure gauge should provide a sensitivity

in the detection of changes of the $x$ dimension several times as great as that of the Ames 0.0001-inch gauge; this indeed proved to be the case.

The effects of friction were very small. The pistons of the presses were packed with the minimum amount of packing, and special tests showed that friction was not more than 2 or 3 percent under unfavorable conditions. Under the conditions of the experiment, the stress $Z_z$ is smaller than that calculated with no allowance for friction because the $z$ piston is advancing, overcoming both friction and the stress $Z_z$, whereas the stress $X_x$ is greater than that calculated with no allowance for friction, because the stress $X_x$ is advancing the $x$ piston against friction and against the pressure of the $x$ gauge. The calculations in the following were made with no allowance for friction. The corrected $Z_z$ and $X_x$ would be brought nearer together by a correction for friction; the maximum such effect is somewhere of the order of 5 percent.

The strain-hardening curves under conditions of zero $x$ flow, with the simultaneous values of $X_x$ were determined for the following materials: annealed "Solar" tool steel (typical composition: C 0.50, Mn 0.40, Si 1.00, Mo 0.50), eight different blocks cut in various orientations from a bar of 2-inch round stock; annealed Cr V steel (typical composition: C 0.40, Mn 0.25, Si 0.20, V 0.22), one series on 6 blocks of various orientations and with various methods of lubrication, one series of six compressings with refiguring on the same block, and another series on another block for four compressings with refigurings; a stainless steel of unknown composition, six compressions with refiguring on a single block; a 1045 steel provided by the Watertown Arsenal in the following heat treatments: austempered at 650°, 600°, 550°, 500°, and 450°, quenched and tempered at 650°, 550°, and 450°. Runs were made on one specimen of each of these heat treatments. or in a couple of cases on two or three. The initial dimensions of the specimens were: $z$, 0.750″; $y$, 0.500″; $x$, 0.502″. The compressions, except for the multiple compressions with refiguring, were pushed to a reduction of height of two-thirds.

In addition to the data for two-dimensional flow, the strain-hardening curves in simple compression ($X_x = Y_y = 0$, $\epsilon_x = \epsilon_y = -\frac{1}{2}\epsilon_z$) were also determined, either by special experiment or else taken from previous data.

The results are shown graphically in Figs. 5–13.

An examination of the curves shows that universally $X_x$ is greater by up to 20 percent than its theoretical value, $\frac{1}{2}Z_z$. The discrepancy is greatest for the specimens austempered to the highest temperatures. Correction for friction would accentuate the discrepancy. In the initial stages of plastic flow $X_x$ tends to be equal to $\frac{1}{2}Z_z$; the discrepancy reaches its maximum in the neighborhood of a strain of 0.1, and beyond this there does not seem to be usually any marked tendency for the discrepancy to become accentuated.

The result signifies, among other things, that the material is no longer isotropic after plastic flow in compression has taken place. In order to obtain some idea of the degree of failure of isotropy two other sorts of experiment were made. In the first of these, circular cylinders were cut from the compressed blocks with the axis of the cylinder along the original $x$ direction, and then subjected to simple compression. If the material were isotropic, the section should remain circular on the second compression. Isotropy would hardly be expected, however, because one of the transverse dimensions is in the direction of previous maximum extension, whereas the transverse dimension at right angles to it is the direction of previous maximum shortening. Since the new lateral deformation is an extension, it would be expected that the strain hardening to the new deformation would be a maximum in the direction of previous extension. This would mean that the cross section of the circular cylinder would become elliptical, with the minor axis along the previous $y$ direction. The experiment was tried with the stainless steel and annealed Cr V. With the latter, the distortion was in the expected direction, the minor axis of the ellipse being the former $y$ direction. The maximum transverse strain in this particular experiment was 0.095 and the minimum 0.072. There was, therefore, a failure of isotropy by 32 percent ($0.095/0.072 = 1.32$), produced by an initial two-dimensional straining of 0.7 (the specimen was cut from the sample subjected to multiple com-

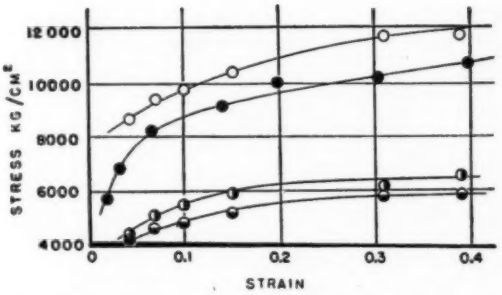


FIG. 5. Stress-strain relations for 1045 steel, austempered at 650°C. Reading from the top down, the first, third, and fourth curves relate to the block compressed, by suitable manipulation of $X_z$, so that flow in the $x$ direction vanishes. The first curve plots $Z_z$, the third $X_x$, and the fourth $\frac{1}{2}Z_z$, which by elementary theory should be equal to $X_x$. The second curve is for another block with no lateral support.

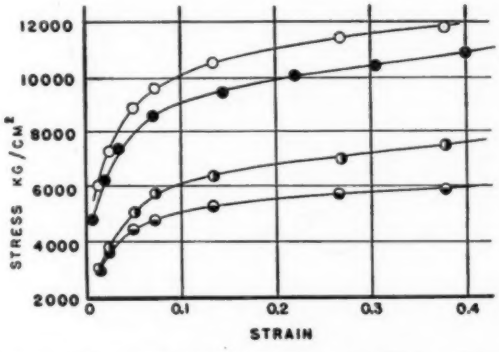


FIG. 6. Stress-strain relation for soft 1045 steel, austempered at 600°C. Reading from the top down, the first, third, and fourth curves relate to the block compressed, by suitable manipulation of $X_z$, so that flow in the $x$ direction vanishes. The first curve plots $Z_z$, the third $X_x$, and the fourth $\frac{1}{2}Z_z$, which by elementary theory should be equal to $X_x$. The second curve is for another block with no lateral support.

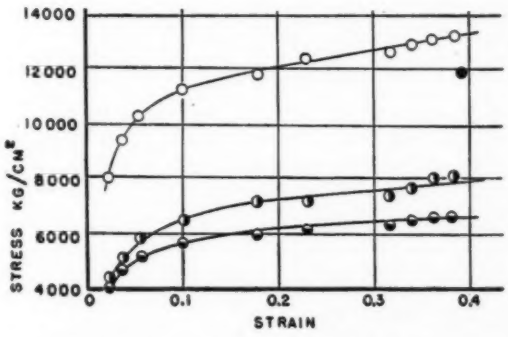


FIG. 7. Stress-strain relations for 1045 steel, austempered at 550°C. Reading from the top down, the first curve shows $Z_z$, the second $X_x$, and the third $\frac{1}{2}Z_z$ for a block compressed in such a way that flow in the $x$ direction vanishes. This block was compressed in two stages; the points for strains greater than 0.2 are for the second stage, after the stress had been released, the block refigured, and again exposed to stress. The solid black disk shows a single point for another block compressed without lateral support.

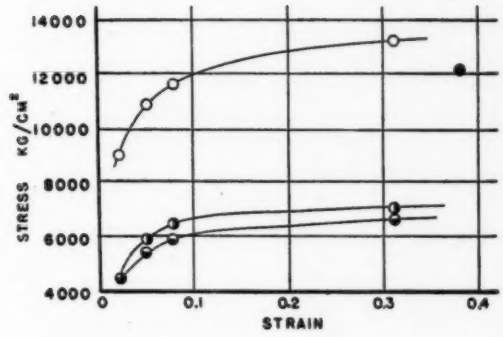


FIG. 8. Stress-strain relations for 1045 steel, austempered at 500°C. Reading from the top down, the first curve shows $Z_z$, the second $X_x$, and the third $\frac{1}{2}Z_z$ for a block compressed in such a way that the flow in the $x$ direction vanishes. The solid black disk shows a single reading for another block compressed without lateral support.

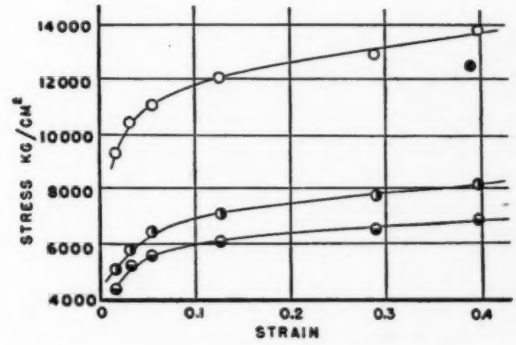


FIG. 9. Stress-strain relations for 1045 steel, austempered at 450°C. Reading from the top down, the first curve shows $Z_z$, the second $X_x$, and the third $\frac{1}{2}Z_z$ for a block compressed in such a way that flow in the $x$ direction vanishes. The solid black disk shows a single reading for another block compressed without lateral support.

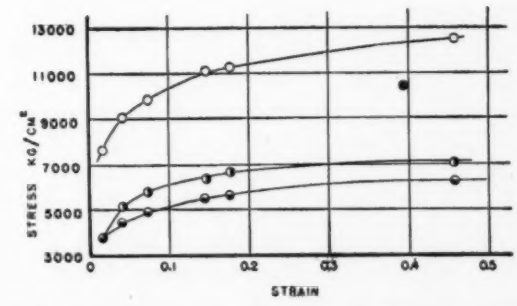


FIG. 10. Stress-strain relations for 1045 steel, quenched and drawn back to 650°C. Reading from the top down, the first curve shows $Z_z$, the second $X_x$, and the third $\frac{1}{2}Z_z$ for a block compressed in such a way that flow in the $x$ direction vanishes. The solid black disk shows a single reading for another block compressed without lateral support.

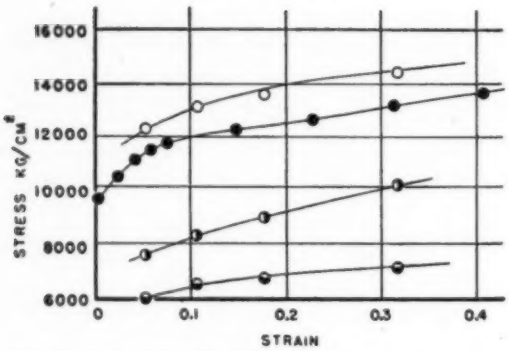


FIG. 11. Stress-strain relations for 1045 steel, quenched and drawn back to 550°C. Reading from the top down, the first, third, and fourth curves relate to the block compressed, with suitable manipulation of $X_z$, so that flow in the $x$ direction vanishes. The first curve plots $Z_z$, the third $X_z$, and the fourth $\frac{1}{2}Z_z$. The second curve is for another block with no lateral support.

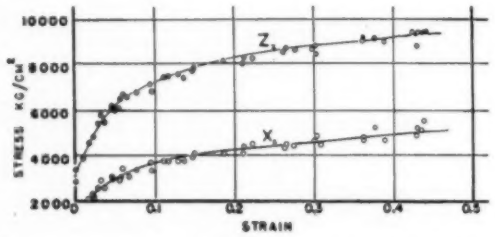


FIG. 12. Stress-strain relations for six different blocks of Cr V steel, $X_z$ being so manipulated that flow in the $x$ direction vanishes.

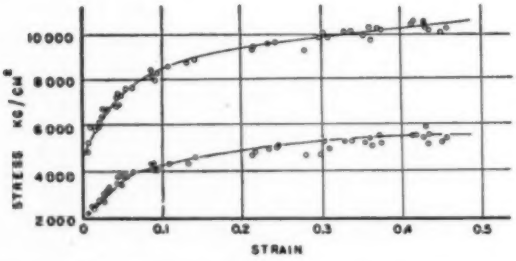


FIG. 13. Stress-strain relations for eight different blocks of "Solar" steel, $X_z$ being so manipulated that flow in the $x$ direction vanishes.

pression and refiguring). With the stainless steel, on the other hand, the expected relations were exactly reversed, the major axis of the ellipse being along the previous $y$ direction. In this case the maximum and minimum transverse strains were 0.0675 and 0.0535, denoting a failure of isotropy in the unexpected direction of 26 percent ($0.0675/0.0535=1.26$). In other respects, also, the behavior of stainless steel in strain hardening is unlike that of the other steels investigated here; in particular, the relation between stress

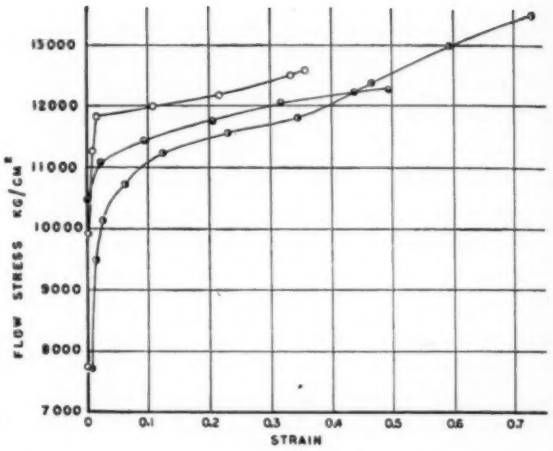


FIG. 14. Stress-strain relations in tension for small specimens of "Solar" steel cut in different orientations from a block previously strained in compression. Reading from the top down, the length of the first specimen is along the previous $x$ direction (direction of previous zero strain), that of the second is along the previous $y$ direction (direction of previous extension), and that of the third along the previous $z$ direction (direction of previous compression). Fracture occurred at the final points of all curves.

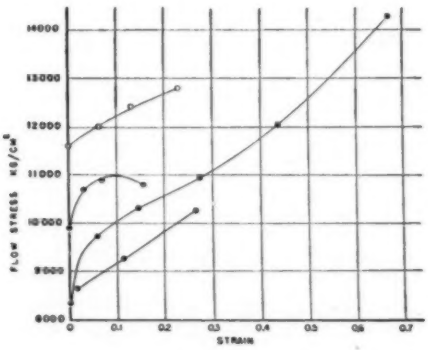


FIG. 15. Stress-strain relations in tension for small specimens of an annealed 1035 steel. The lower curve is for a virgin specimen. The three other curves are for specimens cut in various orientations from a block previously strained in compression. The top curve is for the specimen cut with its length in the previous $y$ direction (direction of previous extension strain), the second curve for the previous $x$ direction (direction of previous zero strain), and the third for the previous $z$ direction (direction of previous compressive strain). Fracture occurred at the final points of all curves.

and strain shows much less curvature than for the other steels.

In the second test for failure of isotropy, small tension samples were cut from the compressed blocks in three different orientations, and stretched to fracture. The results are shown in Figs. 14 and 15. Again there is very marked failure of isotropy. The strain hardening for tension is least in the $z$ direction, that is, in the

direction of previous compression. Furthermore, the strain to fracture in tension is greatest in the $z$ direction. Both of these features seem natural, and suggest that there is a small reversible component in plastic flow. The strain hardening in the other two directions is relatively different for the two steels; the full situation is obviously complex.

In addition to the experiments with steel, a single run was made with a block of commercial annealed copper. In the initial stages of plastic flow simultaneous values of $Z_z$ and $X_z$ were 2,780 and 1,520 kg/cm², respectively; at the end of the test when $\epsilon_z$ had reached a value of 0.404, the corresponding values were 3,860 and 2,110. Again, as with steel $X_z$ is somewhat more than one-half $Z_z$, indicating a failure of the perfect isotropy assumed in the equations. A marked difference between the behavior of steel and copper was that the steady state was reached more quickly with copper after pumping stopped.

### 2. The Velocity of Flow

The use of photographic recording in measuring the velocity of flow has already been described. The velocity measurements were made at constant load; this demanded the use of the free piston gauges, as already indicated. With constant pressure on the $x$ press, the stress $X_z$ is rigorously constant, because the area of the $x$ face does not change during flow. The $z$ face does, however, increase in area as flow progresses, so that constant $z$ load does not ensure constant $Z_z$. The dependence of $Z_z$ on $\epsilon_z$ at constant $z$ load may be calculated as follows. We have:

$$Z_z = \text{load/section}, \quad \text{section} \times z = \text{vol.}$$

Hence

$$Z_z = (\text{load/vol.})z,$$

$$(dZ_z/dz)_{\text{load}} = \text{load/vol.} = Z_z/z,$$

$$\epsilon_z = \log\,(z/z_0),$$

$$dz = z d\epsilon_z,$$

and

$$(dZ_z/d\epsilon_z)_{\text{load}} = Z_z.$$

The usual procedure was to keep the $x$ load constant at some selected value, and determine the flow for successive increments in the $z$ load.

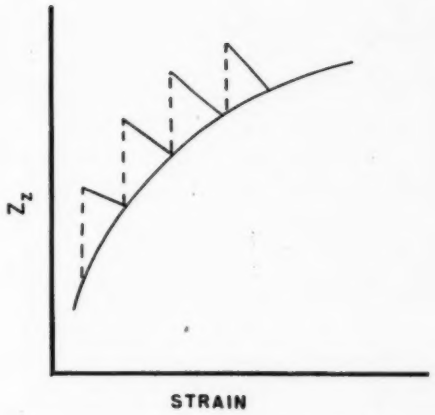


FIG. 16. Shows the general connection between stress and strain in determinations of rate of flow off the strain-hardening curve.

Each increment of $z$ load was suddenly applied, by suddenly opening a valve to the gas reservoir in which the requisite pressure had been previously established. The initial stages of flow were comparatively rapid, and the camera exposures were made rapidly, at intervals of a second or less. The first exposure was made a fraction of a second after the application of load, as soon as it was safe to assume that inertia effects had vanished. As the flow slowed down, exposures were made at roughly equal increments of strain. Exposures were continued until the rate of flow in the $z$ direction had dropped to something of the order of 0.0005 inch per minute. This procedure gives the velocity of flow at different points on the inclined parts of the sawtooth pattern indicated in Fig. 16. The slopes of the inclined part are given by $dZ_z/d\epsilon_z = -Z_z$ ($\epsilon_z$ drawn positive in the diagram). Successive increments of $z$ load were made in this way at constant $x$ load until the total deformation in the $x$ direction had reached its permissible limit; the $x$ load was now increased sufficiently to reverse the direction of $x$ flow, and the step-wise increase of the $z$ load was resumed. This was continued until the total shortening was about 33 percent. The total number of $z$ steps varied from 10 to 25, average somewhere around 15, with a total number of photographic exposures of several hundred. Not all the exposures were usually used in taking the record off the film.

The flow phenomena of the following materials were studied: an annealed 1035 steel, five

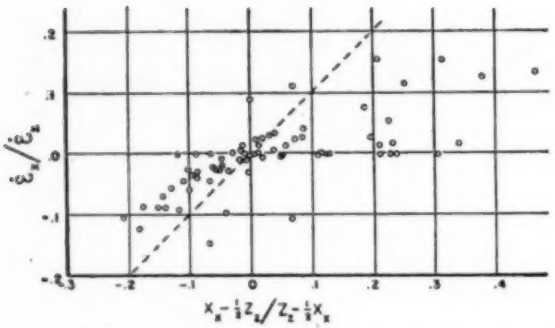


FIG. 17. Plot of all the observed ratios of rate of flow in the $x$ direction to that in the $z$ direction against the ratio of the "effective driving stresses" in these two directions. According to the elementary theory the points should lie on the dotted 45° line.

specimens in two-dimensional compression and one in simple compression; annealed "Omega" tool steel, typical composition C 0.55, Mn 0.80, Si 2.30, V 0.25, Mo 0.50, P 0.015, S. 0.025, four set-ups with two-dimensional compression and one with simple compression; stainless steel, one specimen in two-dimensional and one in simple compression; five heat treatments of the 1045 steel from the Watertown Arsenal, one specimen each in two-dimensional and in simple compression.

The photographic record gives the strains and the times. The rates of flow were calculated from the record by dividing increments of strain by increments of time. These rates were then plotted in one way or another depending on the point at issue. The photographic record contains the material for determining the strain-hardening curve from the limiting readings when the steady state was approximately reached. The strain-hardening curves were calculated from the photographic data and compared with those obtained by the first method of procedure. The agreement by the two methods was within experimental error; it is not worth while reproducing the details.

Although principal interest in the measurements was in the $z$ rates of flow, the photographic record also contains the material for a calculation of the $x$ rate of flow, but with less accuracy than for the $z$ rate. This permits a calculation of $\dot{\epsilon}_x/\dot{\epsilon}_z$. Since the corresponding values of $X_x$ and $Z_z$ are known, we have the material for a comparison of the actual value of $\dot{\epsilon}_x/\dot{\epsilon}_z$ with its theoretical value in terms of the stresses, or in terms of $\alpha$. In Fig. 17, $\dot{\epsilon}_x/\dot{\epsilon}_z$ is plotted as a function of $R$ $[\equiv(X_x-\frac{1}{2}Z_z)/(Z_z-\frac{1}{2}X_x)]$ for all the samples of steel for which $\dot{\epsilon}_x$ could be determined with any accuracy. The wide scatter of the points is understandable in view of the very small $x$ strains. The conventional equations of plasticity demand that these points all lie on the 45° line. In spite of the scatter of the points, it is obvious that the 45° line definitely does not represent the results. So far as they can be represented by a line, the line has a considerably smaller slope, and furthermore passes somewhat below the origin instead of through it. This agrees with the results of the first part, namely $\dot{\epsilon}_x$ vanishes for a value of $\alpha$ somewhat greater than 0.5. No correlation could be found between the deviations of the points from a line and any other obvious single factor, such as grade of steel, location on the strain-hardening curve, or absolute value of the flow velocity. Only one point was found for which the *sign* of $\dot{\epsilon}_x/\dot{\epsilon}_z$ was definitely "wrong" in terms of the stresses. This particular point is hard to explain by experimental error, the increments of both $\epsilon_x$ and $\epsilon_z$ being too large to allow any chance for an error of sign. It may well be that the points actually should be scattered, and that the ratio $\dot{\epsilon}_x/\dot{\epsilon}_z$ depends on some combination of parameters more complicated than any that were obvious.

Much numerical material was collected for the velocity of primary flow, $\dot{\epsilon}_z$, and many curves were drawn. The maximum observed rate was $5\times10^{-3}$ sec.$^{-1}$; the minimum was $0.00\times10^{-5}$. The material is too extensive and complicated to

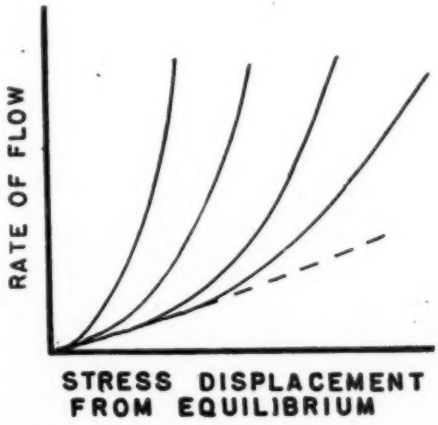


FIG. 18. Shows the progressive change in the character of the flow curves for increasing degrees of strain hardening.

attempt to reproduce in detail. There are, however, certain outstanding approximate generalizations. As seemed natural, the velocity of flow was found to increase rapidly with increasing distance from the limiting strain-hardening curve. To a rough first approximation the increase is exponential, that is, at points not too near the origin the logarithm of the rate is approximately linear in terms of the displacement from the strain-hardening curve. This displacement may be taken in terms either of stress or of strain. The rate at which the rate increases on moving away from the strain-hardening curve is itself a strong function of location on the strain-hardening curve, being much greater in the early stages of deformation, that is, for small strains. The qualitative nature of the effect is suggested in Fig. 18, the successive curves being drawn for the successive steps indicated in Fig. 16.

The abruptness of the rise of the rate in the early stages of plastic flow is suggested by the following example. The maximum strain rate measured in these experiments, $5\times10^{-3}$ sec.$^{-1}$, was for Omega steel at a total strain of 0.04, where the equilibrium stress is 8600 kg/cm$^2$. This rate was produced by a stress displacement from the equilibrium curve of 130 kg/cm$^2$ or 1.5 percent. The rate just mentioned was the average over a time interval of 0.4 sec.; the initial rate must have been much higher.

The curves of Fig. 18 have a linear envelope, which approaches the origin with a finite slope. If the displacement from the strain-hardening curve is measured in terms of normal distance, instead of along the stress axis, the drawing apart of the curves becomes even more marked than in the figure. The general order of magnitude of the drawing apart of the rate curves may be suggested by a single example. For the 1045 steel, austempered at 650°, the rate of flow was $1.0\times10^{-3}$ sec.$^{-1}$ for a displacement from the strain-hardening curve of 13 kg/cm$^2$ in the early stages where the equilibrium stress was 5,800 kg/cm$^2$, whereas in the later stages, where the equilibrium stress was 11,000 kg/cm$^2$, a displacement from the strain-hardening curve of 470 kg/cm$^2$, or 36 times as much, was necessary to reach the same rate of flow. The slope of the linear envelope shown in Fig. 18 depends markedly on the grade of steel, being less for the harder steels.

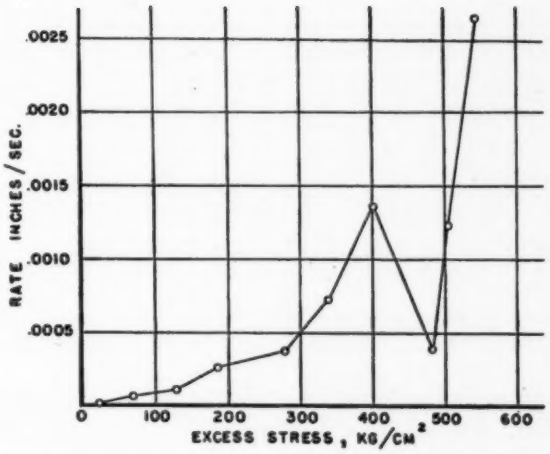


FIG. 19. Example, for soft "Omega" steel of regeneration of rate of flow, after drop from a high initial value.

As an example, this slope was $2.7\times10^{-6}$ cm$^2$ sec.$^{-1}$ kg$^{-1}$ for the stainless steel, and $7\times10^{-7}$ cm$^2$ sec.$^{-1}$ kg$^{-1}$ for the 1045 steel tempered at 450°.

No material difference could be found between the character of the rate curves for two-dimensional and simple compression. The very rapid increase in the rate of flow for slight displacements from the strain-hardening curve in the early stages of flow explains the possibility of approximately calculating the velocity of propagation of the plastic front from the statically determined stress-strain curve. The loss in the abruptness of the flow phenomena at higher strains, shown by the drawing apart of the curves in Fig. 18, would suggest that in a wire which had been previously severely strained the velocity of propagation could not be calculated from the stress-strain curve with as close a degree of approximation as for the virgin wire.

The actual rate curves, as a general rule, have the smooth idealized configuration shown in Fig. 18 over their entire extent only for the early stages of the strain-hardening curves, that is, only for small strains. For larger strains the smooth-rate curves are often interrupted by episodes with an abnormally high rate. This holds for both simple and two-dimensional compression. Figure 19 shows an example. The location of the episodes may be anywhere on the curve and would seem to be a probability affair. One is practically certain to find several of these episodes, if one waits long enough, in the region close to the strain-hardening curve

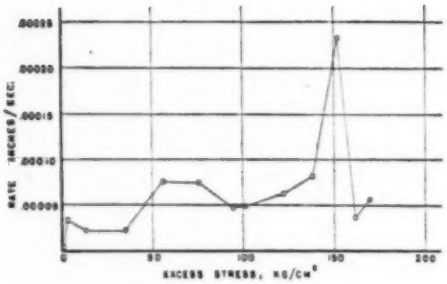


FIG. 20. Example, for soft "Omega" steel, of attainment of a relatively high rate of flow after a slow beginning.

where the rate on the average is approaching zero. It was not at all uncommon for the strain to hang at a steady value, constant within 0.00001 inch for one or two minutes, and then within 2 or 3 seconds increase by 0.001 inch.

This flow in jumps is not contained in the conventional equations of plasticity, but is obviously a matter of considerable importance in its suggestions as to the mechanism of plastic flow. There would seem to be little doubt that it is a real phenomenon and not an artifact. One might be inclined, at first, to think it an effect of friction. But it cannot be friction of the $x$ face, because the jumps are shown equally in simple compression where the $x$ face is free. Neither can it be friction on the piston of the press, because the effect occurs only when the *specimen* has received comparatively large strains. Similar effects are found in other circumstances. One is reminded of deep-seated earthquakes. The continued internal fractures with self-healing which I have found when shearing is combined with high hydrostatic pressure are doubtless somewhat similar.[2]

It would be interesting and important to establish whether a jump in the $z$ flow is accompanied by a jump in the $x$ flow. The answer to this question could not be certainly found from the data, the absolute value of the $x$ flow usually being too small. In two or three instances, however, there were slight jumps in the $x$ flow accompanying those in the $z$ flow. The only conclusion that is justified is that there is no present evidence against supposing that jumps in the two flows occur together, or in the theoretical ratio.

[2] P. W. Bridgman, J. App. Phys. **8**, 328 (1937); Proc. Am. Acad. **71**, 387 (1937).

In addition to the flow in jumps there is another phenomenon sometimes found at the larger strains. On increasing the load suddenly at constant strain, flow is very likely not to begin at once, but the flow hangs and requires time to build up to its maximum rate. This is not an inertia effect, for it is found only in the later stages of flow, and the time intervals are too long. This effect was found only in the 1035 and Omega steels. An example is shown in Fig. 20. I have previously found a similar effect in tension. Tension specimens, pulled under hydrostatic pressure to an elongation far beyond the elongation at fracture under normal conditions, and then repulled at atmospheric pressure, may show a similar initial hanging of the flow. The mere existence of the effect shows that strictly the velocity of flow cannot be a function of stress and strain only, but must involve the history to some extent. The same conclusion, of course, could have been drawn from the existence of jumps in the flow.

For the more rapid rates of flow, the rate is not sensitive to $X_z$; under the conditions of these experiments the regular sequence of curves indicated in Fig. 18 was usually not affected by a discontinuous change in $X_z$. At the smaller rates, where the effect to be expected from a change of $X_z$ is more nearly of the same magnitude as the rate itself, the effect of changing $X_z$ is more easily exhibited, and in particular the paradoxical effect already suggested, namely that an increase of $X_z$ at constant $Z_z$ may increase the rate of $z$ flow. Figure 21 shows for the 1035 steel the effect of an increase of $X_z$ in

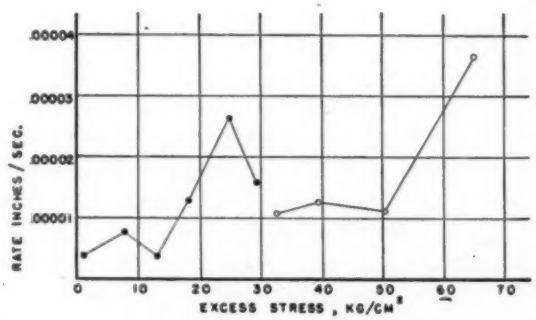


FIG. 21. Example, for 1035 steel, of the increase in flow velocity along $z$ which may be brought about by an increase in $X_z$. At excess stresses greater than 30 the value of $X_z$ was 4420 kg/cm²; below 30 it was increased to 5600. $Z_z$ was approximately constant at 8100.

increasing $\dot{\epsilon}_z$. This increase of rate is contained in the equations of plasticity, as a consequence of an increase of the function $\varphi$ due to an increase in the stress invariant part of the argument. Not all increases of $X_x$ bring about an increase of $\varphi$, but obviously any increase of $X_x$ from a value greater than $\frac{1}{2}Z_z$ to a value still greater than $\frac{1}{2}Z_z$ will result in such an increase; these are the conditions prevailing in Fig. 21.

### 3. Measurements with Constant Rate of Flow

Since the results of these measurements were mostly negative, they may be dismissed with a brief description. A constant rate of flow was maintained independent of the load by pumping liquid into the press at a constant rate. The primary source of motion was a "gerotor" gear pump, which is essentially an arrangement for injecting a constant amount of liquid per revolution. The useful range of the pump is only a few hundred pounds per square inch, at higher pressure the leak back through the gearing becoming serious. It was necessary, therefore, to interpose intermediate stages between the gerotor pump and the press deforming the specimen. The gerotor pump was arranged to drive an 8-inch piston, which drove a 1-inch piston, which in turn drove the 3.5-inch piston of the press. With this arrangement the pressures were kept within the necessary limits. The gerotor pump was driven through variable speed pulleys and gears by a motor of such large capacity that its speed was practically unaffected by variations of pressure in the range. The data were recorded photographically as before. The running load was taken from the stretch of the tie rods of the press.

Only simple compression was studied. Three different steels were examined, the 1045 steel tempered at 650°, 550°, and 450°. Each steel was examined at three rates of strain: 0.00212, 0.00080, and 0.000157 inches per second, that is, a range of 13.5-fold. Within this range the existence of an effect could be detected in the expected direction; the stress-strain curve for the highest speed lay higher than for the lowest speed by something of the order of 4 percent at the highest strains. The accuracy was not sufficient, however, to permit any more detailed study. The sensitivity of the readings would have permitted this, but the results were made irregular by a comparatively large correction for the thermal expansion of the tie rods during the run by the heating of the flood lamps. It did not seem worth while to make the complicated modifications that would have been necessary to eliminate this source of disturbance, since the speed effect has been the subject of studies by other observers over a much greater range of speed and a wider range of conditions. One comment is perhaps worth making: It would be expected from the results in Part 2 that the effect of speed on the stress-strain curve would be more marked at large strains than at small ones.

## THE GENERALIZED STRAIN-HARDENING CURVE

The problem of deducing the strain-hardening curve for one type of deformation from measurements on another type of deformation has been much discussed and is one on which the present measurements have some bearing. The two types of deformation with which we are concerned are simple compression and two-dimensional compression. Three possibilities in the way of generalizing the strain-hardening curve will be considered.

1. The maximum stress is a universal function of the maximum strain. The maximum stress is $Z_z$ and the maximum strain $\epsilon_z$ for both simple and two-dimensional compression. If this function is the correct one, then $Z_z$ plotted against $\epsilon_z$ should give coincident curves for simple and two-dimensional compression.

2. The maximum shearing stress is a universal function of the maximum shearing strain. For simple compression:

$$X_x = Y_y = 0, \quad \epsilon_x = \epsilon_y = -\tfrac{1}{2}\epsilon_z,$$

$$\left.\begin{aligned}\text{Maximum shearing stress} &= \tfrac{1}{2}Z_z \\ \text{Maximum shearing strain} &= \tfrac{3}{4}\epsilon_z\end{aligned}\right\}.$$

For two-dimensional compression:

$$Y_y = 0; \quad |X_x| < |Z_z|, \quad X_x \text{ and } Z_z \text{ of same sign.}$$
$$\epsilon_x = 0; \quad \epsilon_y = -\epsilon_z.$$

$$\left.\begin{aligned}\text{Maximum shearing stress} &= \tfrac{1}{2}Z_z \\ \text{Maximum shearing strain} &= \epsilon_z\end{aligned}\right\}.$$

If this is the correct function, $Z_z$ plotted against $\frac{3}{4}\epsilon_z$ for simple compression should give the same curve as $Z_z$ plotted against $\epsilon_z$ for two-dimensional compression.

**3.** The "significant stress," $\bar{S}$ is a universal function of the "significant strain," $\bar{\epsilon}$. The definitions are as follows:

$$\bar{S}=\{\tfrac{1}{2}[(X_x-Y_y)^2+(Y_y-Z_z)^2+(Z_z-X_x)^2]\}^{\frac{1}{2}},$$

$$\bar{\epsilon}=[\tfrac{2}{3}(\epsilon_x^2+\epsilon_y^2+\epsilon_z^2)].$$

For simple compression:

$$\bar{S}=Z_z, \quad \bar{\epsilon}=\epsilon_z.$$

For two-dimensional compression:

$$\bar{S}=Z_z(1-\alpha+\alpha^2)^{\frac{1}{2}}, \quad \text{where} \quad X_x=\alpha Z_z.$$

$$\bar{\epsilon}=\epsilon_z(4/3)^{\frac{1}{2}}=1.155\epsilon_z.$$

If this is the correct function, $Z_z$ plotted against $\epsilon_z$ for simple compression should give the same curve as $Z_z(1-\alpha+\alpha^2)^{\frac{1}{2}}$ plotted against $1.155\ \epsilon_z$ for two-dimensional compression.

Under present experimental conditions there is one qualitative difference between the various criteria. If either of the first two is correct, $Z_z$ plotted against $\epsilon_z$ for two-dimensional compression should give a curve passing smoothly without jump over any points where $X_x$ may be changed discontinuously. If, however, the third criterion is correct, there should be a jump in the $Z_z$ *versus* $\epsilon_z$ curves provided there is a jump in $\bar{S}$ on changing $X_x$, for $\bar{S}$ *versus* $\bar{\epsilon}$ is smooth. The larger the jump in $\bar{S}$, the more critical should be the test. Now $\bar{S}$ as a function of $X_x$ or of $\alpha$ has a flat minimum in the neighborhood of $\alpha=\frac{1}{2}$, so that any jumps of $X_x$ which keep it in the general neighborhood of $\frac{1}{2}$ will not afford a sensitive test. It is for this reason that all the quasi-static measurements described under the heading on page 231 are not well adapted to bring out the distinction that we are seeking. The curves specially determined for rate of flow by photographic recording in some cases embraced changes of $X_x$ in a more favorable domain, and it is the limiting curves given by these measurements that were used in comparing the three criteria. It has already been mentioned that the limiting strain-hardening curves determined in this way were the same as those obtained by the first method.

As it turned out, the cases in which there were favorably situated jumps in $X_x$ did not permit a decision between the various criteria. In one instance, that of Omega tool steel, at a point where there was a jump in $\alpha$ from 0.45 to 0.72, there was a greater jump in the curve of $\bar{S}$ *vs.* $\bar{\epsilon}$ than in the curve of $Z_z$ *vs.* $\epsilon_z$, the former jumping up by 5 percent and the latter jumping in the same direction by only 2 percent. The 1045 steel, tempered at 650°, gave two opportunities for comparison. There was one jump of $\alpha$ from 0.38 to 0.68; at this point there was no discontinuity in the $\bar{S}$ curve, whereas $Z_z$ jumped down by 3 percent. At a somewhat greater strain for the same material there was a jump down in $\alpha$ from 0.64 to 0.50. The $\bar{S}$ curve now jumped down by 2 percent, whereas the $Z_z$ curve was sensibly continuous. Various points of discontinuity in $\alpha$ for other steels did not permit a decision between a jump or an abrupt change in direction of the curves, the experimental points not being sufficiently closely spaced. On the whole it appeared that the tendency to a break of some sort was greater on the $\bar{S}$ curves than on the $Z_z$ curves.

The data would appear, therefore, not to permit a clean-cut decision on the basis of the breaks in the curves, and the decision must be sought from a comparison of the whole general course of the curves.

In making this comparison it is to be kept in mind that $\bar{S}$ and $\bar{\epsilon}$ are identically equal to $Z_z$ and $\epsilon_z$, respectively, for simple compression. In anticipation, neither of the criteria are met within the limits of error of the measurements, and it becomes a question of choosing the one which is the best approximation. As regards the criterion that $Z_z$ is a universal function of $\epsilon_z$, the $Z_z$ curve for two-dimensional compression consistently lies above that for simple compression for all the steels except the 1035 steel. For strains above 0.1 the order of magnitude of the excess is 10 percent. For the 1035 steel the curves cross at a strain of 0.07, and at a strain of 0.15 the curve for simple compression has risen to 10 percent above the curve for two-dimensional compression. For all steels the curve of $\bar{S}$ for two-dimensional compression lies below that for simple compression. The discrepancy between the curves may be either greater or less than for the $Z_z$ curves, but on the whole is inclined to be rather less, so that on the whole the $\bar{S}$ criterion is to be preferred to

the $Z_s$ criterion. With regard to the maximum shearing stress criterion, the curve for maximum shearing stress for two-dimensional compression consistently lies above that for simple compression, except for the 1035 steel. The discrepancies are again of the general order of 10 percent, but detailed comparison would show that for the present selection of steels the maximum shearing stress criterion is on the whole the best by a narrow margin. For the stainless steel, either the significant stress or the maximum shearing stress criterion holds with much less error than for the other steels. In fact, the general behavior of the stainless steel is different from that of the others; its strain-hardening curve, for example, is sensibly linear up to a strain of 0.5.

All of the above remarks apply in the region of strains of moderate magnitude, say above 0.02. In the initial stages of flow, with the single exception of the 1035 steel, the stress for two-dimensional flow is less than for the three-dimensional flow of simple compression. It is natural to associate this with an initial slip on a single set of slip planes in two-dimensional flow as contrasted with cross slip on systems of interfering planes in simple compression.

I am much indebted to Mr. Charles Chase for the skillful construction of the apparatus and assistance with the manipulations.

## A Method of Determining the Size of Droplets Dispersed in a Gas

R. L. Stoker
*Western Precipitation Corporation, Los Angeles, California*
(Received November 20, 1945)

A method applicable to determining droplet sizes in the interior of an already existing atmosphere of fog or mist is developed and described. The method makes use of the fact that if droplets strike a suitably coated surface without wetting the surface, a track of the contact area is formed. A criterion is derived and experimentally evaluated for relating the droplet diameter and the track diameter. An apparatus for utilizing this method is briefly described.

IF a liquid droplet strikes a plane surface without wetting the surface, the droplet will undergo a deformation and momentarily, at least, will have a finite area of contact with the surface. If the surface had been previously coated with, for example, a thin layer of soot, the area of contact of the droplet would be indicated by a disturbance in the soot film which would be clearly visible under a microscope. The carbon particles of the soot have the advantage of being very small and are not easily wetted.

In order to utilize the above, it is necessary to have the relationship between the size of the soot disturbance and the size of the droplet producing the disturbance. As the basis of an analysis for determining this relationship the assumption is made that the only significant forces brought into play during the impact are the inertia forces and the forces due to the surface tension of the droplet. Thus, by this assumption, it is implied that such forces as those due to viscosity, gravity, and compressibility are of negligible importance. Therefore, since

$$F_I \text{ varies as } \rho d^2 v^2,$$

and

$$F_\sigma \text{ varies as } \sigma d,$$

it follows that

$$F_I/F_\sigma \text{ varies as } \rho d v^2/\sigma.$$

Hence, if only the above assumed forces are important in producing deformation of the droplet during its impact with the soot-coated surface, then the last expression, which is known as Weber's number, is a criterion of dynamical similarity for the phenomenon. Consequently, all dimensionless ratios of quantities related to the phenomenon are some function of the above Weber's number. Thus, the ratio of the track diameter to the droplet diameter can be indicated mathematically by

$$\frac{d'}{d} = \varphi(\rho d v^2/\sigma).$$

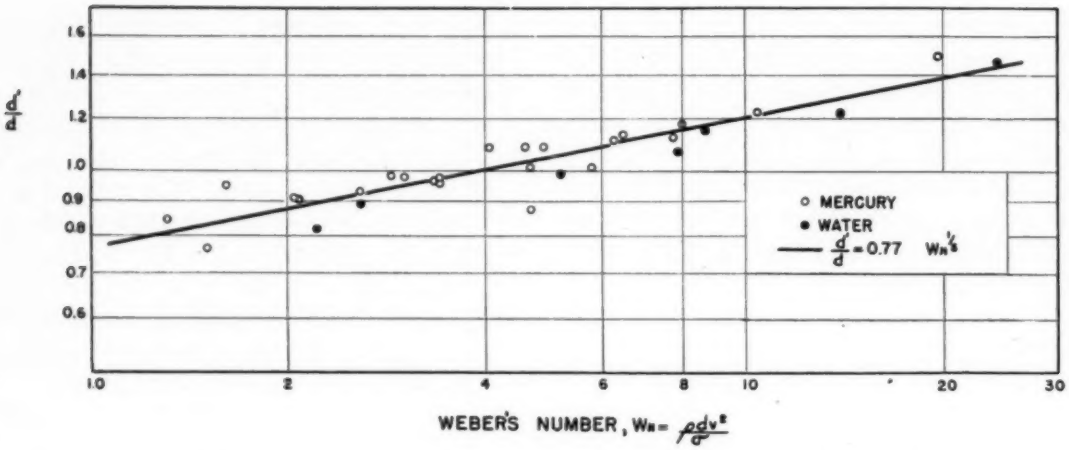


FIG. 1. Experimental relationship between Weber's number and the ratio of track diameter to droplet diameter.

This functional relationship of the diameter ratio and Weber's number was determined experimentally by allowing droplets of mercury and water of known diameters to fall from various measured heights onto a soot-coated glass surface and observing the tracks under a microscope. The velocity at impact was taken as the free fall velocity. The error in the value of Weber's number due to this choice, which neglected air resistance, did not exceed 3 percent in any test and the data are plotted without this correction.

The diameter of the mercury droplets varied from 280 to 800 microns, and were measured at rest under a microscope. For these diameters the shape of the mercury droplets, while at rest on a flat glass surface, differed imperceptibly from spheres and thus this apparent diameter was taken as the diameter under free fall. The measured mercury droplets were swept off the glass surface and fell a known distance to the soot-coated plate below.

The diameter of the water droplets was computed from the weight of a known number of drops formed by a very fine tipped eye-dropper. Water droplets of about 1500 microns in diameter were obtained. In the weighing of a small number (usually ten) of these droplets it was necessary to make a slight correction for evaporation loss. The height of fall of water droplets was taken as the distance of the droplet center above the soot-coated glass just prior to leaving the eye-dropper. This fall distance was varied between one-half and two inches, and was also the range used with the mercury droplets.

The following graph of the ratio of the track diameter to the droplet diameter *versus* Weber's number was plotted from data which were obtained in the above manner (Fig. 1). All experimental points that were determined are included on the plot. Although reasonable experimental care was taken, no claim to less than $\pm 2$ percent error in the plotted results is justified. Never-

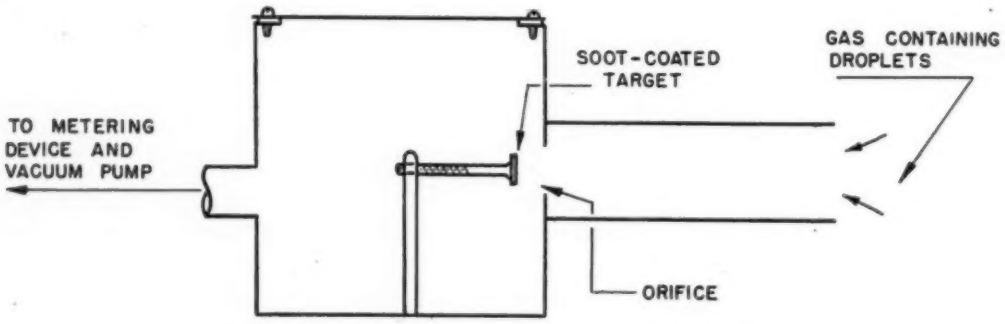


FIG. 2. Schematic sketch of sampling device for obtaining droplet tracks.

theless, it appears that the plotted points define a relationship between the diameter ratio and Weber's number that can be expressed by

$$\frac{d'}{d}=0.77\left(\frac{\rho d v^2}{\sigma}\right)^{1/5}.$$

It is apparent from the graph that if Weber's number is about four, the track diameter is equal to the droplet diameter. This would exist, for example, if a water droplet, 5 microns in diameter, struck the coated plate with a velocity of approximately 25 feet per second.

## APPLICATION

To apply the above it is more convenient to have the droplet diameter expressed in terms of a Weber's number based on the track diameter. Thus, from the above equation, it can be shown that

$$d=1.25\frac{d'}{(\rho d' v^2/\sigma)^{1/6}}.$$

It is interesting to note that owing to the small fractional exponent in the last equation, the error in the value of the droplet diameter will not exceed one-sixth the error in the measured value of Weber's number.

If the liquid forming the droplets is a pure compound, its density and surface tension will probably be known or can be determined without undue difficulty. If, however, the droplets are not derived from a pure compound, the surface tension and density will depend upon the amount of evaporation that has occurred since their formation. The latter complicates evaluating Weber's number, but in an actual case one is usually able to estimate these variables within reasonable limits and thereby retain fair accuracy for the droplet diameter, since the error in droplet size is much less than the error in Weber's number as was noted above.

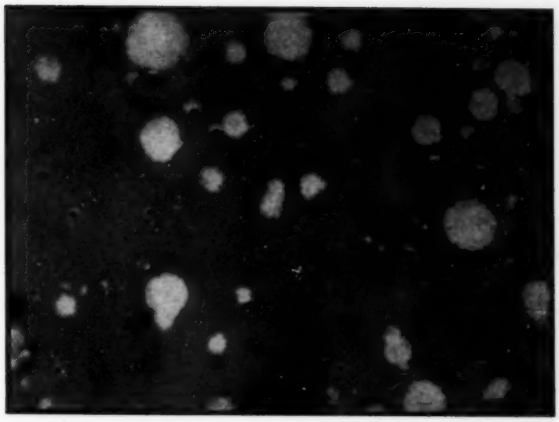

FIG. 3. Photomicrograph (200×) of water droplet tracks on a soot-coated glass target.

The velocity at impact can be determined and controlled by means of a sampling device as indicated in the schematic sketch in Fig. 2. The gas containing the droplets is drawn through a short length of straight pipe and then through an orifice, so that the central portion of the jet impinges against a soot-coated target plate. By metering the gas flow in the suction line and knowing the orifice diameter, the impact velocity can be calculated.

The included photomicrograph, which is an enlargement of 200 diameters, shows water droplet tracks on a portion of a $\frac{1}{4}''\times\frac{1}{4}''$ soot-coated glass target (Fig. 3). The impingement velocity was approximately 25 feet per second, and the droplet temperature was 60°F.

## NOMENCLATURE

$F_I$ = Inertia force.
$F_\sigma$ = Surface tension force.
$\rho$ = Density of droplet.
$d$ = Diameter of droplet.
$d'$ = Track diameter of droplet.
$v$ = Impingement velocity of droplet.
$\sigma$ = Surface tension of droplet.
$W_N$ = Weber's number.

# The Accuracy of Lumping in an Electric Circuit Representing Heat Flow in Cylindrical and Spherical Bodies†

VICTOR PASCHKIS* AND MICHAEL P. HEISLER**
*Columbia University, New York, New York*

(Received November 29, 1945)

In using lumped resistance-capacitance circuits for studying heat conduction problems the influence of number and size of lumps is important. Several methods of lumping are conceivable for representation of cylindrical or spherical bodies and results of comparative tests show that equal geometrical size of lumps is most accurate. In the various lumps resistance and capacitance have to be in certain definite relationships, which are established in the paper. The influence of number of lumps is also investigated.

FOR the solution of heat flow problems in solids, the electric analogy method has been used increasingly in recent years.[1] The method consists in building a resistance-capacitance circuit representing the bodies subjected to heat flow, impressing on this circuit appropriate boundary conditions, and transforming the measured electrical effects into their thermal counterparts. The application of the electric analogy method is greatly facilitated by the use of a versatile arrangement of resistors, capacitors, switches, and equipment which permits the rapid setting-up of various circuits. One such arrangement is known as the heat and mass flow analyzer.[2] It consists, briefly, of 15 equal capacitor banks, each bank comprising 6 trays with a total per bank of 41 capacitors of various sizes, between 0.1 and 20 microfarads (total capacitance per bank, 160 microfarads); and of a resistor network comprising a total of 115 sections. Each section has four resistor decades of $10^2$, $10^3$, $10^4$, and $10^5$ ohms, respectively. Recording electronic voltmeters allow measurement of 4 voltage-time curves simultaneously. A milliampere-minutemeter automatically integrates the current-time curve (equivalent to measuring the total heat flow, not merely the rate of heat flow).

Solutions found on the heat and mass flow analyzer were compared repeatedly with mathematical solutions and direct thermal measurements and found to check closely.[3] However, there are inaccuracies inherent in the approximation by lumping. In a previous paper,[4] the inaccuracy caused by lumping was studied for one particular case: namely, for a circuit representing a slab or large wall of finite thickness but having no end effects, that is, a wall having heat flow in one direction only.

The present paper deals with circuits representing long cylinders and spheres. In such circuits the resistance per unit length increases from the surface towards the center, and the capacitance per unit length decreases.

Because of their importance it is particularly desirable to know how the number of lumps and the way of subdividing the total capacitance and resistance of the circuit influence the results. In a general way the following laws for the radial heat flow in cylinder and sphere can be stated.

*Cylinder:* The resistance of a cylindrical shell per unit length (in radial direction) is proportional to the logarithm of the ratio of the radii

† This investigation has been made possible through a grant from the Engineering Foundation and has been carried out under the auspices of the A.S.M.E. Committee on Research through the agency of the A.S.M.E. Heat Transfer Division, Subcommittee on Heated and Cooled Enclosures. The authors are indebted to the above organization for its sponsorship and support. Publication assisted by the Ernest Kempton Adams Fund for Physical Research of Columbia University.

* Victor Paschkis is Research Associate in Mechanical Engineering, Columbia University. He is in charge of the technical and scientific work carried out in the Heat and Mass Flow Analyzer Laboratory.

** Michael P. Heisler is Laboratory Assistant in the same laboratory.

[1] V. Paschkis and H. D. Baker, "Method for determining unsteady-state heat transfer by means of an electrical analogy," Trans. A.S.M.E. **64**, 105–112 (1942).

[2] V. Paschkis, "Electrical analogy method for the investigation of transient heat flow problems," Industrial Heating **9**, 1162–1170 (1942).

[3] M. Avrami and V. Paschkis, "Application of an electrical model to the study of two-dimensional heat flow," Trans. A.I.C.E. **38**, 631–652 (June 25, 1942). V. Paschkis, "Establishment of cooling curves of welds by means of electric analogy," Welding Research Council of The Engineering Foundation, **8**, 462$_s$–483$_s$ (October, 1943).

[4] V. Paschkis and M. P. Heisler, "Accuracy of measurements in lumped *R-C* cable circuits as used in the study of transient heat flow," Elec. Eng. **63**, 165 (1944).

limiting the shell; the capacitance is proportional to the cross-sectional area of the shell.

*Sphere:* The resistance of a spherical shell is proportional to the difference of the inverse of the inside and outside radii; the capacitance is proportional to the difference of the third powers of the radii limiting the shell.

It must be kept in mind that the capacitance mentioned here is the thermal capacitance, which is proportional to the volume of the body. The electric capacitance is a function of the surface of the body. However, in representing a section of a body, the electric capacitance used to represent its thermal capacitance is proportional to the volume of the lump in the same way as the thermal capacitance.

Obviously the shell at the center has infinite resistance, and part of the work refers to methods of overcoming this difficulty. This characteristic makes it impossible to conceive of a steady-state flow radially through a solid cylinder or sphere, and therefore the influence of capacitor leakage as studied in part of the previous paper[4] could not be similarly analyzed for the present case.

## I. PROBLEMS IN COMMON BETWEEN CYLINDERS AND SPHERES

In working with lumped circuits, a body having evenly distributed electrical or thermal properties—capacitance and resistance—is replaced by a body divided into sections or lumps in which capacitance is concentrated at the center of each lump and resistance along the axis of each lump. This sectionalized body is represented by the electric network of the heat and mass flow analyzer, and determining the influence of the method of lumping on the accuracy of the experimental results was the object of the present investigations.

In slabs there are only two problems to be considered in lumping, the number of lumps and the influence of lumps of unequal thickness. The use of uneven lumps makes it possible to concentrate limited experimental equipment on that part of the circuit which is considered to be the most important (e.g., near the surface, etc.). In each lump, however, the capacitance is always located in the center of the lump. In so arranging the capacitance, the following conditions are fulfilled:

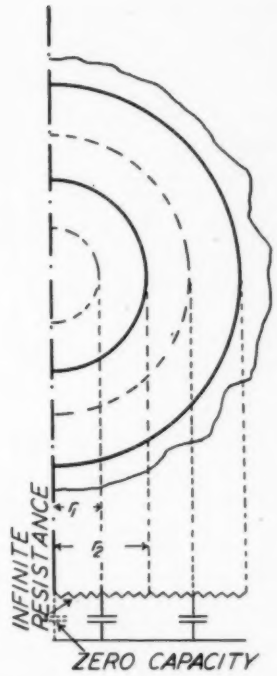


FIG. 1. Explanation of signs for lumping cylinders.

1. Resistance and capacitance both are symmetric in reference to the center.
2. The product of resistance×capacitance on one side of the center is equal to the product of resistance ×capacitance on the other side.

In cylinders and spheres two additional difficulties arise: First, if the entire radius be divided, either equally or unequally, into a number of lumps, at what points in the lumps should the capacitors be placed? (See Fig. 1.) In Fig. 1, the capacitors are shown in the geometric center of the lump ($r_1 = r_2/2$). However, at least three other positions are defensible: placing the capacitor so that the capacitance on one side of the lump is equal to the capacitance on the other side; placing the capacitor so that the resistances on either side of the capacitor are equal; or putting the capacitor so that the values of the products of resistance×capacitance are the same for either side of the lump. Second, whatever way of lumping is selected, the first section next to the center offers additional problems. The center of the body has no capacitance, and the resistor connecting the center with the first capacitor is infinitely large, independent of the position of the condenser in the lump. This position, then, determines the resistance of the outside part of

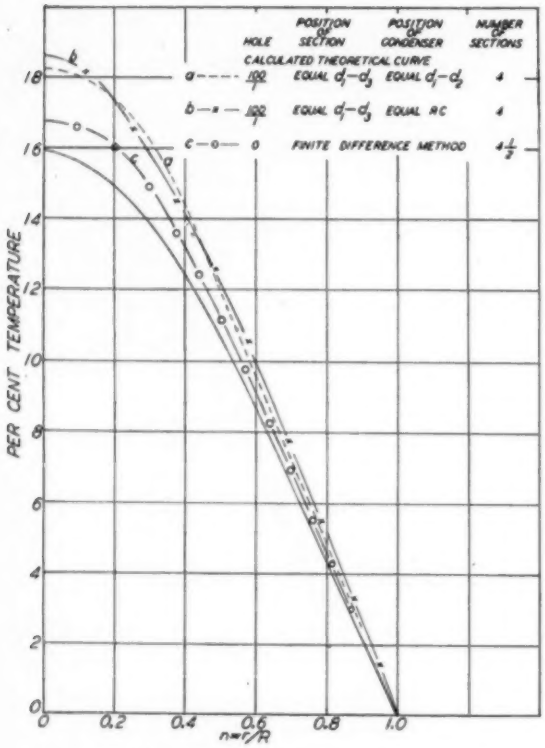
HOLE
POSITION OF SECTION
POSITION OF CONDENSER
NUMBER OF SECTIONS
CALCULATED THEORETICAL CURVE
a ---- 1/2 EQUAL $d_1-d_3$ EQUAL $d_1-d_2$ 4
b —x— 1/2 EQUAL $d_1-d_3$ EQUAL RC 4
c —o— 0 FINITE DIFFERENCE METHOD 4 1/2
PER CENT TEMPERATURE
n=t/R

FIG. 2. Cylinder. Comparison of theoretical results (solid line) with experimental results (curves $a$, $b$, $c$), for $at/r^2=0.4$ and four sections. "Equal $d_1-d_3$" indicates that the sections have equal thickness. "Equal $d_1-d_2$" indicates that the condensers are in the geometric center of each lump. "Equal $RC$" indicates that the products of resistance ×capacitance on either side of the condenser in each section are equal.

the lump ($r_1$ to $r_2$—Fig. 1) and a minor change in position of capacitor $C_1$ has a very large influence on this resistance.

One way of overcoming the latter difficulty is to replace the solid cylinder or sphere by a hollow cylinder or sphere having a very small center hole. As soon as a center hole is provided, the resistance from this hole to the innermost condenser becomes finite.

Experiments in which hollow cylinders were substituted for solid ones have revealed various shortcomings in this method. The use of such hypothetical hollow bodies can be avoided, however, by a method of lumping based on finite difference equations. The mathematical basis for this procedure, as related to cylinders, was first published by Jackson and co-workers.[5] The basis for lumping of cylinders by the finite difference method is explained in Appendix I. This method also proved helpful in a similar development for the sphere. The basis for the lumping of spheres is explained in Appendix II. However, the method of lumping and problems of accuracy are numerically different for cylinder and sphere and will therefore be treated separately.

In heating or cooling a body from its surface, the resistance to heat transfer between the surrounding and the surface enters the picture. It has been explained previously[4] that the severest test for an approximate solution is found in assuming that the surface of the uniformly heated body is subjected to a sudden change of temperature. Therefore, the experiments were carried out for this condition.

All tests have been carried out so that voltage-time curves obtained with differently lumped circuits were compared with theoretically obtained curves.

## II. CYLINDER

In working with the cylinder, the feasibility of assuming a hollow cylinder was first analyzed.

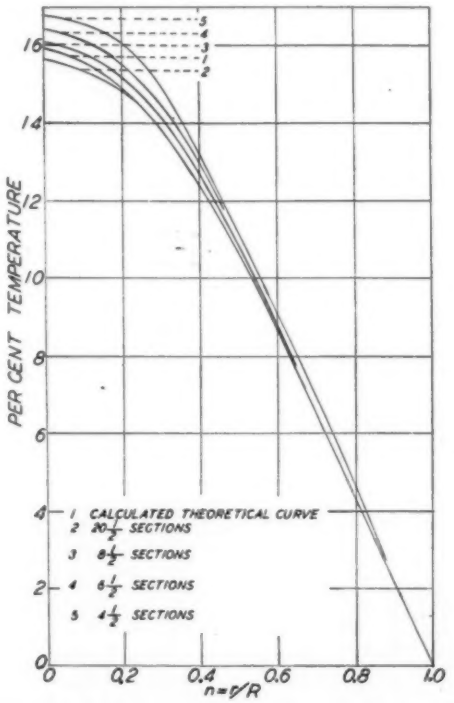


FIG. 3. Cylinder. Comparison of theoretical results (line 1) with experimental results (curves 2–5). Finite difference method; $at/r^2=0.4$; influence of number of sections.

[5] R. Jackson, R. J. Sarjant, J. B. Wagstaff, N. R. Eyres, D. R. Hartree, and J. Ingham, "Variable Heat Flow in Steel," paper No. 15 (1944), Iron and Steel Institute, London, England.

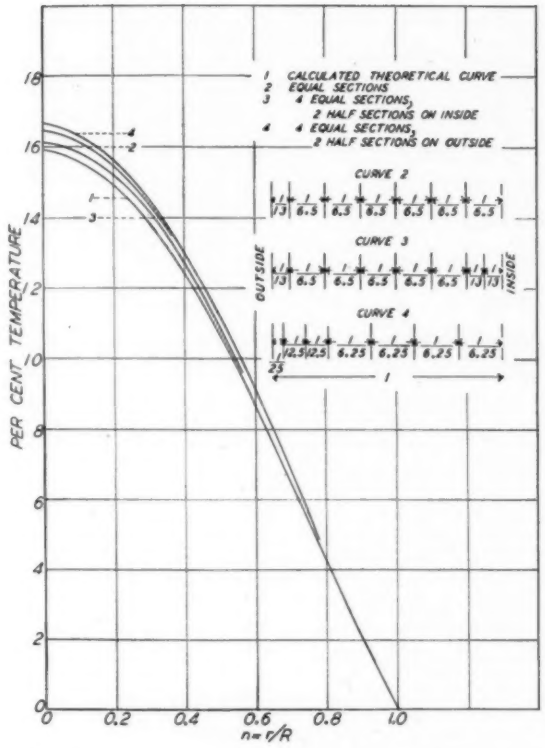


FIG. 4. Comparison of theoretical results (line 1) with experimental results (curves 2–4); $at/r^2=0.4$; finite difference method; $6\frac{1}{2}$ sections; equal and unequal lumping.

In order to verify experimental results it was, of course, necessary to have the theoretical curve. The curves published in McAdams' book on heat transmission (Gurney-Lurie charts) are not very accurate; therefore curves were calculated for $at/r^2=0.2$, 0.4, and 0.6 ($a$ = thermal diffusivity, $t$ = time, $r$ = radial distance). Each of these three curves gives temperatures, expressed in dimensionless units, plotted against relative position "$n$" in the cylinder. The calculation for the point at the axis of the cylinder was checked against tables published by Schultz and Olsen,[6] and all points were compared with the values of T. F. Russell.[7]

The greatest number of these investigations was carried out for $at/r^2=0.4$. Figs. 2–4 refer to this dimensionless time. Figure 2 compares different positions of the capacitors for one small assumed hole; the hole was 0.01 times the outside diameter. Therefore, the material neglected because of the hole is only $10^{-4}$ times the entire material of the cylinder. The lumps were selected geometrically, that is, the distance from the outside diameter to the assumed hole diameter was divided into four equal parts. In each part, the capacitor was placed first at the geometric center of the lump and then at a point such that the products of resistance times capacitance on either side of the capacitor were equal. The results are shown by curves $a$ and $b$. In addition, a third test was run; the lumping in this case was based on finite difference equations; the results are shown by curve $c$. It is in the nature of this method that there is never a full number of lumps. Therefore, the two curves for the hollow cylinder with four lumps compare with the curve for $4\frac{1}{2}$ lumps for the finite difference method. From Fig. 2 it can be seen that near the center the differences are quite appreciable and reach values more than 15 percent above the calculated values in the most unfavorable case. The two ways of positioning the condenser have no marked influence on the accuracy, but the method of finite differences is considerably better and is accurate to within $5\frac{1}{2}$ percent at the center. Toward the outside all curves more nearly coin-

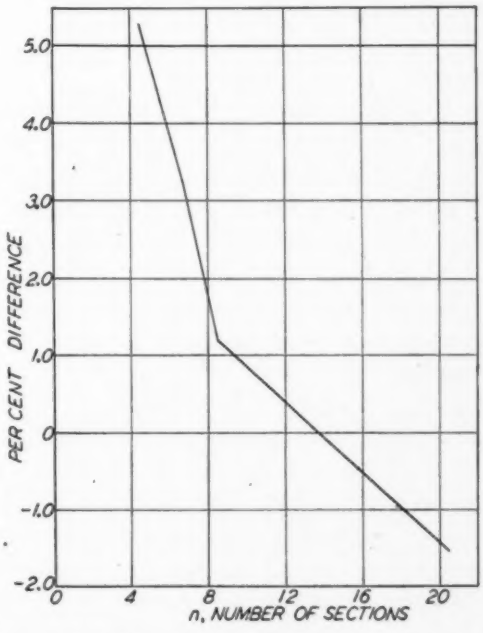


FIG. 5. Cylinder. Percent difference of temperature at center between theoretical curve and experimental curves; $at/r^2=0.4$; finite difference method.

[6] F. C. W. Olsen and O. T. Schultz, Ind. Eng. Chem. **34**, 874 (1942).

[7] T. F. Russell, "Some Mathematical Considerations on the Heating and Cooling of Steel," special paper No. 14 (1936), Iron and Steel Institute, London, England.

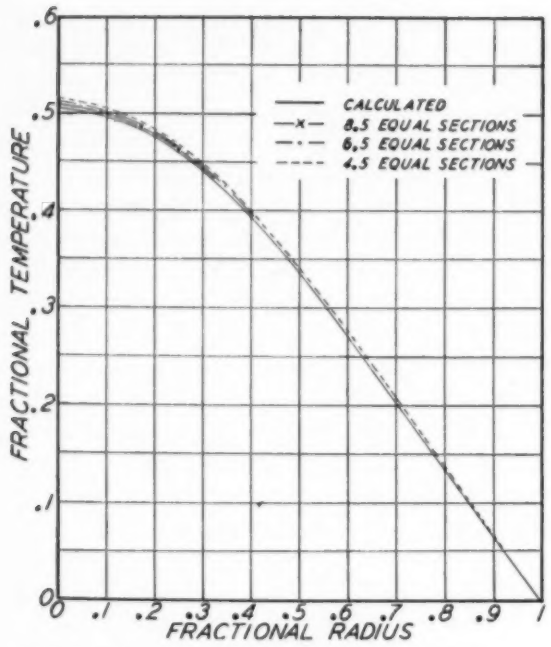


FIG. 6. Cylinder. Finite difference method. Temperature distribution curves with various numbers of sections compared with theoretical curve; $at/r^2=0.2$.

cide. However, on a percentage basis the error seems to be almost constant and independent of the distance from the center.

Having found the finite difference method to be satisfactory even with relatively few lumps, all further work was concentrated on this method.

Figure 3 shows the influence of the number of lumps. It is apparent that with $8\frac{1}{2}$ lumps the results are extremely good and will be in error in the order of magnitude of only 1 or $1\frac{1}{2}$ percent. An increase of number of lumps beyond $8\frac{1}{2}$ does not seem to have much influence very close to the center; with $20\frac{1}{2}$ lumps the error becomes negative but of the same order of magnitude as with $8\frac{1}{2}$ lumps. However, at a radius of approximately two-tenths of the outside radius the error with $20\frac{1}{2}$ lumps becomes zero. The influence of the number of lumps on the error is also shown in Fig. 5, where the difference in dimensionless temperature units, expressed as a percentage of the theoretical value, is plotted *versus* the number of sections.

In many instances it is desirable to have uneven sizes of lumps in order to concentrate available equipment at important points. Figure 4 refers to such uneven lumping conditions. The actual lumping is shown in the sketch on the side. The total number of sections was always $6\frac{1}{2}$. In one case the sections were of equal size (curve 2); in the other instances four larger sections were used together with two sections each one-half of the size of the large sections. In the tests of curve 3 the small sections were on the inside, and in the test of curve 4 they were on the outside. The differences between the three curves are so small as to be considered almost within measuring accuracy. It appears, though, that the small sections on the inside improve the accuracy somewhat; this is not surprising, because it is there that the resistance ratios differ most from the logarithmic theoretical values. In Figs. 6 and 7, the influence of lumping for dimensionless times other than 0.4 were investigated.

Figure 6 shows the curves for $at/r^2=0.2$, and it can be seen that the discrepancies between any of the three curves and the theoretical curve are very small indeed. All curves refer to the finite difference method and are distinguished by the number of sections used ($4\frac{1}{2}$, $6\frac{1}{2}$, and $8\frac{1}{2}$ sections). Figure 7 refers to $at/r^2=0.6$ and compares the theoretical curve with the curve for finite differences, using $4\frac{1}{2}$ sections. The error is again in the order of magnitude of 5 percent at the center, the same as had been found for $at/r^2=0.4$.

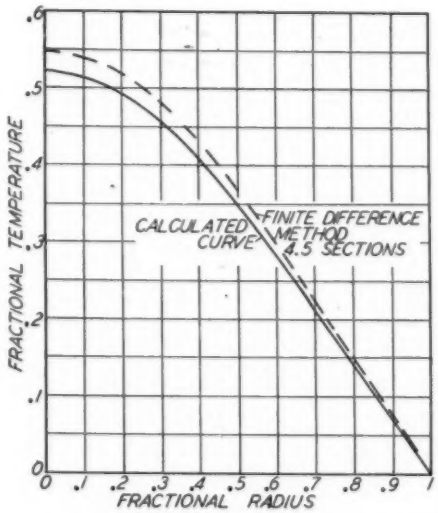


FIG. 7. Cylinder. Finite difference method. Temperature distribution curve for 4.5 sections compared with theoretical curve; $at/r^2=0.6$.

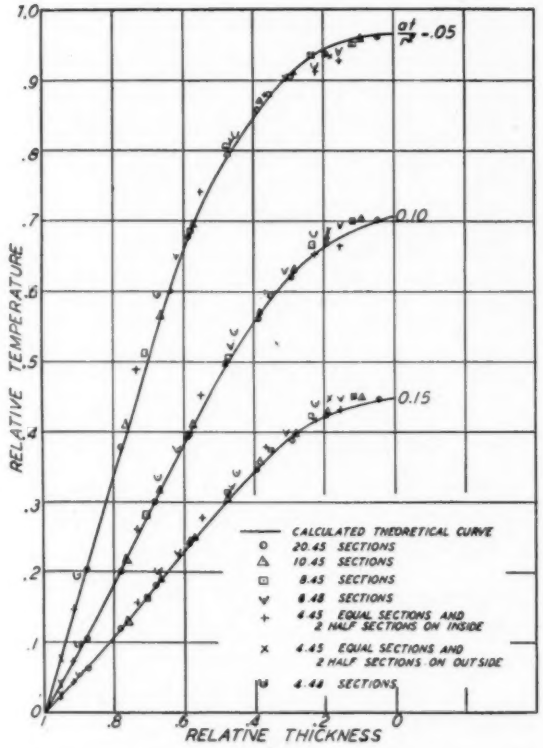


FIG. 8. Spheres. Temperature distribution curves. Relative thickness zero at center; relative thickness 1 at surface. Theoretical curves (full lines) are compared with experimental results by finite difference methods and various numbers of sections as explained in legend.

In conclusion it can be said that for cylinders the finite difference method yields satisfactory results, if 8.5 lumps and more are used.

### III. SPHERES

An investigation (Appendix II) shows that for spheres the finite difference method, based on equally sized lumps, still leads to the concept of a hollow sphere—a hole in the center. The capacity in the center turns out to be zero, and the resistance from the center to the next capacitance becomes infinite. If, therefore, the temperatures near the center are of interest, it is necessary to use many lumps. With 10.45 lumps (the fraction 45/100 is explained in the appendix), the point at $0.45/10.45=0.041\times$diameter is the one closest to the center. Temperatures closer to the center may be found by extrapolating from the point $0.041\times$diameter and the next point farther out, that is, point $0.041+1/10.45=0.137\times$diameter. If such extrapolation is not sufficient, more lumps may be necessary. For example, with 20.45 lumps, temperatures at $0.45/20.45=0.021\times$diameter can be measured directly.

In Fig. 8, results obtained with various numbers of lumps are compared with the theoretical curves; relative thickness is plotted as abscissa and relative temperatures as ordinate. Three theoretical curves are shown, one each for $t/RC(=at/r^2)$ equal to 0.05, 0.10, and 0.15. The results obtained with various methods of lumping are shown grouped about each curve.

With 8.45 lumps, the greatest observed discrepancy is 0.012 of the total ordinate scale of one. In cooling ($t/RC=0.15$) this causes an error of $0.012/0.43=2.8$ percent near the center. Other times and other positions are better. Close to the center there is an error even with 10.45 sections; but with 20.45 sections no dis-

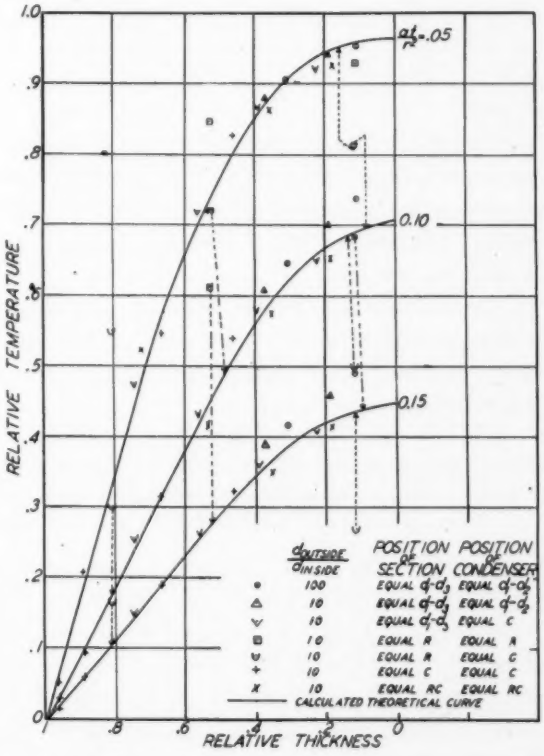


FIG. 9. Spheres. Temperature distribution curves. Relative thickness 1 at surface. Theoretical curves (full lines) are compared with experimental results following different methods as explained by legend. $d_{outside}$ is the outside diameter of the sphere; $d_{inside}$, the diameter of the hole in the center. "Equal $d_1-d_2$" indicates that the sections have equal thickness. "Equal $C$" indicates that the capacitances on either side of the condenser are equal. "Equal $R$" indicates that the resistances on either side of the condenser are equal.

crepancy, even close to the center, can be detected.

The influence of non-uniform lumping was next examined. If a limited number of lumps is to be used and results are desired particularly in one region, then it may appear useful to make the lumps unequal in size. Thus, two cases were investigated, and in each a total of 7 condensers (6.45 sections) was used. Instead of making each section 1/6.45 of the diameter, the size of each large section was made 1/5.45 of the diameter. One of the large sections was then divided into two smaller sections. In one experiment these smaller sections were located near the center, and in another experiment, near the surface. At early times ($t/RC=0.05$) the splitting of the section near the center does not seem to give very good results, but with increasing time conditions become better. Subdividing on the outside (near the surface) gives excellent results there, but the results near the center are not much better than those obtained with the 4.45 sections.

In Fig. 9, results for lumping based on equal capacitance, equal resistance, etc., are compared with theoretical curves. In no case are results as close as those obtained by the finite difference method.

In conclusion it can be said that also for spheres the finite difference method yields satisfactory results; at least 6.45, preferably 8.45 sections are recommended.

## APPENDIX I. FINITE DIFFERENCE METHOD FOR DETERMINING RESISTANCES AND CAPACITANCES IN EVENLY LUMPED CYLINDERS

Figure 10 is a vertical section through a cylinder or sphere and shows (in the lower part of the figure) the wiring diagram of the equivalent circuit. In this case 6 condensers are shown, which would make $m+1=5$. In the figure $R$ stands for resistance, $C$ for capacitance, and $V$ for the potential at any one instant.

The conductance $S=1/R$, time is denoted by $t$. By applying Kirchhoff's law to point $m$ for $m\neq 0$, it follows that

$$(V_{m+1}-V_m)\cdot S_{m+1} = (V_m-V_{m-1})\cdot S_m + C_m\cdot dV_m/dt. \quad (1)$$

For the center the equation becomes

$$S_1(V_1-V_0)=C_0 dV_0/dt. \quad (2)$$

Now, by way of approximation (using a concept originally introduced by Binder and E. Schmidt and applied to cylinders by R. Jackson and co-authors,[5] and apparently independently by Perry and Berggren[8]), the following statements can be made, referring to a cylindrical shell other than at the center. (See Fig. 11.)

The temperature increase $(Q-S)$ at radius $m\Delta r$ can be calculated from:

$$\frac{\partial V_m}{\partial t}=\frac{1}{\rho c 2m(\Delta r)^2}[(2m+1)V_{m+1}-4mV_m + (2m-1)V_{m-1}]=\frac{\Delta V_m}{\Delta t}, \quad (3)$$

where $\rho c$ is the volumetric specific heat.

Now, for the center of the cylinder slightly other conditions prevail, because for $m=0$ the line $P-Q-U$ (Fig. 11) changes direction at $Q$.

For the center (3) becomes:

$$\frac{\Delta V_0}{\Delta t}=\frac{4}{\rho c(\Delta r)^2}(V_1-V_0). \quad (4)$$

Equations (1) and (3) are equivalent, if

$$\frac{S_{m+1}}{2m+1}=\frac{S_m+S_{m+1}}{4m}=\frac{S_m}{2m-1}=\frac{C_m}{2m(\Delta r)^2\rho c}. \quad (5)$$

From (5) it follows that the resistors in the various sections must be in the ratio

$$R_m/R_{m+1}=(2m+1)/(2m-1). \quad (6)$$

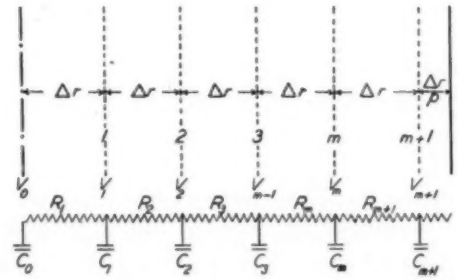


FIG. 10. Explanation of symbols. For finite difference method; cylinders and spheres.

[8] R. L. Perry, and W. P. Berggren, "Transient heat conduction in hollow cylinders after sudden change of inner-surface temperature," *University of California Publications in Engineering* (University of California Press, Berkeley, California, 1944), Vol. 5, No. 3, pp. 59–88.

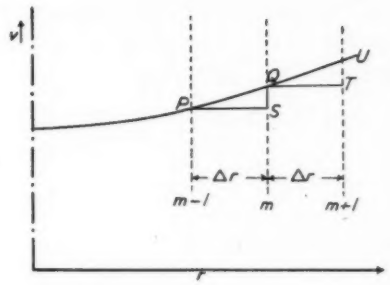


FIG. 11. Method of averaging temperatures in finite difference method.

In the thermal system the diffusivity

$$a\left(\frac{\text{thermal conductivity}}{\text{specific heat}\times\text{density}}\right)$$

takes the place of $1/\rho c$.

If now the thermal times are indicated by $T$, and the electric times by $t$, then the time ratio is given by

$$t/T=C_1R_1a/2(\Delta r)^2. \tag{7}$$

## APPENDIX II. FINITE DIFFERENCE METHOD FOR DETERMINING RESISTANCES AND CAPACITANCES IN EVENLY LUMPED SPHERES

The procedure for spheres follows closely the one used for cylinders. The approximations expressed by Eqs. (1) and (2) hold for spheres as well as cylinders. For spheres Eq. (3) should be replaced by Eq. (8)

$$\frac{\Delta V_m}{\Delta t}=\frac{1}{\rho cm(\Delta r)^2}$$
$$\times[(m+1)V_{m+1}-2mV_m+(m-1)V_{m-1}]. \tag{8}$$

This equation is found by transforming the basic equation

$$\frac{\partial V}{\partial t}=\frac{1}{\rho c}\left(\frac{\partial^2 V}{\partial r^2}+\frac{2}{r}\frac{\partial V}{\partial r}\right). \tag{9}$$

The rate of change is approximately

$$\frac{\Delta^2 V}{\Delta r^2}=\left(\frac{UT}{\Delta r}-\frac{QS}{\Delta r}\right)\frac{1}{\Delta r}$$
$$=\frac{(V_{m+1}-V_m)-(V_m-V_{m-1})}{(\Delta r)^2}$$
$$=\frac{V_{m+1}-2V_m+V_{m-1}}{(\Delta r)^2}. \tag{10}$$

The approximate value of $\partial V_m/\partial r$ can be found by replacing the curve $PU$ by a straight line; then:

$$\Delta V_m=(V_{m+1}-V_{m-1})/2. \tag{11}$$

Finally $r=m\Delta r$. By combining these equations with Eq. (9), Eq. (8) may be obtained. Equations (1) and (8) are equivalent, if

$$\frac{S_{m+1}}{m+1}=\frac{S_m+S_{m+1}}{2m}=\frac{S_m}{m-1}=\frac{C_m}{\rho cm(\Delta r)^2}. \tag{13}$$

From (13) it follows that the resistors in the various sections must be in the ratio

$$R_m/R_{m-1}=(m+1)/(m-1). \tag{13a}$$

It can be readily seen that, for $m=1$,

$$R_m/R_{m+1}=\infty.$$

Hence the inside resistance becomes infinite, and as will be seen later, $C_0$ becomes 0. Therefore it is convenient to call $R_2=1$. Then

$$R_2:R_3:R_4:R_5:\cdots=1:\tfrac{1}{3}:\tfrac{1}{6}:\tfrac{1}{10}\cdots.$$

It can be readily seen that the series is formed by fractions, the numerators of which always equal one. The denominators increase by adding 2, 3, 4, 5, etc.; the first denominator is 1, the next $3=1+2$, then $6=3+3$, then $10=6+4$, then $15=10+5$, etc. The resistance of a spherical shell is proportional to $(1/d_i)-(1/d_a)$, where $d_i$ and $d_a$ are the inside and outside diameters, respectively. The ratio of resistance of the second to that of the third shell is

$$\frac{1/\Delta r-1/2\Delta r}{1/2\Delta r-1/3\Delta r}=\frac{\frac{1}{2}}{\frac{1}{2}-\frac{1}{3}}=\frac{3}{1},$$

which is exactly the ratio found from Eq. (13a).

From Eq. (13), it follows that the capacitors other than the one in the center must be in the ratio:

$$C_1:C_2:C_3:C_4:\cdots=1:4:9:16:\cdots.$$

Actually the capacitors should be proportional to the volumes of the shells, and should be located at the center of the shell. The question arises where the end of each section is. If the capacitor is to be at the mean radius, then the sectioning would be at $0.5r$; $1.5r$; $2.5r$; etc.

The volume of each shell is proportional to the

TABLE I.

| 1 | 2 | 3 | 4 | 5 | 6 | 7 |
|---|---|---|---|---|---|---|
| Section No. | Radius $m\Delta r$ | $(m\Delta r)^3$ | Difference $(m\Delta r)^3$ | Volume ratio | Volume ratio from Eq. (14) | Comparison of volume ratios Col. 5/ Col. 6 |
| 1 | .5 | 0.125 | | | | |
| | | | 3.25 | | | |
| 2 | 1.5 | 3.375 | | 1 | 1 | 1 |
| | | | 12.25 | | | |
| 3 | 2.5 | 15.625 | | 3.77 | 4 | 0.942 |
| | | | 27.25 | | | |
| 4 | 3.5 | 42.875 | | 8.39 | 9 | 0.933 |
| : | : | : | : | : | : | : |
| : | : | : | : | : | : | : |
| 11 | 10.5 | 1157.625 | | | | |
| | | | 363.25 | 111.8 | 121 | 0.923 |
| 12 | 11.5 | 1520.875 | | | | |

difference of the third powers of the outside and inside radius. Table I shows for some sections the radius, the third power of the radius, the difference of the third powers, the ratio based on these differences, the ratio as found from Eq. (13) and a comparison between the two ratios.

Because the comparison of the volume ratios (Col. 6) does not appear to be very good, the capacitor was put on a radius other than the mean value. The results with the radii at 0.45, 1.45, 2.45, etc., appear to be better, as may be seen from Table II. In order to determine the value of the center capacitor, $C_0$, equations similar to (4) must be found. By writing Eqs. (10)–(12) for the center the expression (8a) replacing Eq. (4) is found.

$$\frac{\Delta V_0}{\Delta t}=\frac{6}{\rho c(\Delta r)^2}(V_1-V_0). \tag{8a}$$

TABLE II.

| 1 | 2 | 3 | 4 | 5 | 6 | 7 |
|---|---|---|---|---|---|---|
| Section No. | Radius $m\Delta r$ | $(m\Delta r)^3$ | Difference $(m\Delta r)^3$ | Volume ratio | Volume ratio from Eq. (14) | Comparison of volume ratios Col. 5/ Col. 6 |
| 1 | .45 | .091 | | | | |
| | | | 2.958 | 1 | 1 | |
| 2 | 1.45 | 3.049 | | | | |
| | | | 11.657 | 3.94 | 4 | 0.985 |
| 3 | 2.45 | 14.706 | | | | |
| | | | 26.357 | 8.91 | 9 | 0.992 |
| 4 | 3.45 | 41.063 | | | | |
| • | • | • | | | | |
| • | • | • | | | | |
| 11 | 10.45 | 1141.17 | | | | |
| | | | 359.95 | 121.6 | 121 | 1.003 |
| 12 | 11.45 | 1501.12 | | | | |

In order to determine the value of the center capacitor combine Eq. (2) with (8a):

$$C_0=\rho c(\Delta r)^2/6R_1. \tag{14}$$

As stated above the resistance $R_1=\infty$; hence $C_0=0$.

# Determination of the Temperature Rise and the Maximum Safe Current through Multiconductor Electric Cables*

HAIG P. ISKENDERIAN
*Federal Telephone and Radio Corporation, New York, New York*

AND

WILLIAM J. HORVATH
*Navy Department, Washington, D. C.*

(Received November 29, 1945)

A general method of calculating the temperature rise in multiconductor rubber insulated electric cables based upon the thermal constants of the cable has been derived. The predictions of the theory have been verified experimentally for a number of cables and values of the thermal resistivity constants have been obtained as a function of size and composition of the cable. The results are used to predict the maximum safe current for different size cables to limit the temperature rise at the center to 25°C above an ambient temperature of 50°C.

## INTRODUCTION

IN the design of cable installations it is necessary to know the maximum current which can be sent through a given cable without raising its temperature to a value which would injure the insulation. In general the maximum temperature which the insulation will endure under continuous operation is known, and the problem becomes one of calculating the temperature rise in the cable as a function of the current running through it. Previous work on this subject[1] has been confined to cables containing one, two, or three conductors. The present investigation develops the complete theory for a cable consisting of any number of rubber covered electric wires, all carrying the same current.

Application of the theory depends on accurate knowledge of the radial and surface thermal resistivities. These have been obtained with considerable precision by measuring the temperature drops in experimental cables. The rubber insulation used in these cables is known to withstand continuous operation at 75°C. The maximum safe currents have therefore been calculated for a temperature rise at the center of the cable of 25°C over a 50°C ambient.

* This work was done in the Spring of 1941 while the authors were employed by the Bureau of Ordnance, Navy Department.

[1] Report by S. J. Rosch, published by the N.E.M.A. (January, 1938).

## I. THEORY

The theoretical expressions are derived first for a cable made up of an infinite number of conductors distributed uniformly in a cylindrical insulating medium. In order to apply these expressions to actual cables it is necessary to take into account the variation of the thermal constants of the cable with the size and number of wires. Empirical relations for these constants have been established experimentally. The excellent agreement between theory and experiment is adequate justification for this method of procedure.

The temperature as a function of time may be obtained by writing the fundamental heat relationship for an element of cylindrical shell of unit length and radii $x$ and $x+\Delta x$:

Heat generated = Heat dissipated + Heat stored.

$$I^2R_{cu}N_{x,x+\Delta x}dt=-\left\{\frac{2\pi x}{\rho}\left(\frac{dT}{dx}\right)_x-\frac{2\pi(x+\Delta x)}{\rho}\left(\frac{dT}{dx}\right)_{x+\Delta x}\right\}dt+2\pi x\Delta xS_0d_0dT, \quad (1)$$

where

$I$ = current in amperes through each wire,
$R_{cu}$ = resistance in ohms per cm of each conductor,
$N_{x,x+\Delta x}$ = number of conductors in a shell of radii $x$ and $x+\Delta x$,
$= \frac{2\pi x\Delta x}{\pi r^2}n$
($r$ is the radius of the cable in cm; $n$ is the number of conductors in the cable),

$S_0$ = average specific heat of cable in watt sec./°C,
$d_0$ = average density of cable,
$T$ = temperature rise in °C, and
$\rho$ = radial thermal resistivity of the cable in °C/watt/cm.

Substituting for $N_{x,x+\Delta x}$ and noting that the second term in (1) is the differential of $(2\pi x/\rho)\cdot(dT/dx)$, we obtain:

$$\frac{dT}{dt}=a+\frac{b}{x}\frac{d}{dx}\left(x\frac{dT}{dx}\right), \tag{2}$$

where,

$$a=\frac{I^2R_{cu}n}{\pi r^2S_0d_0} \quad \text{and} \quad b=\frac{1}{\rho S_0d_0}. \tag{3}$$

*For the steady state* $dT/dt=0$ and (2) becomes by successive integrations:

$$T_x=T_c-\frac{ax^2}{4b}, \tag{4}$$

where $T_x$ = the temperature rise at equilibrium, at a distance $x$ from the center of the cable, and $T_c$ = the temperature rise at equilibrium at the center of the cable.

*The general solution of* (2) must satisfy the following initial and boundary conditions:

$$\left.\begin{matrix} t=0 \\ T=0 \end{matrix}\right\} \text{ (I) and } T_s=-\frac{B}{\rho}\frac{dT}{dx}\Big]_{x=r}, \text{ (II)}$$

where $B$ is the thermal surface resistivity in °C/watt/cm².

The solution may be expressed in the following form:

$$T(x,t)=f(t)u(x)+T_c-\frac{ax^2}{4b}, \tag{5}$$

where $f(t)$ is a function of time only and $u(x)$ is a function of radial distance only.

By substituting (5) in (2) and by separating variables we obtain:

$$\left.\begin{matrix} f(t)=C_0\exp(-\alpha^2bt) \\ \text{and} \\ \dfrac{d^2u}{dx^2}+\dfrac{1}{x}\dfrac{du}{dx}+\alpha^2u=0 \end{matrix}\right\}, \tag{6}$$

where $C_0$ and $\alpha$ are constants.

The second equation in (6) is Bessel's equation. Thus our solution (5) becomes:

$$T(x,t)=\sum_i A_iJ_0(\alpha_ix)\exp(-\alpha_i^2bt)+T_c-\frac{ax^2}{4b}. \tag{7}$$

The constants are obtained by making use of the boundary condition (II) and Eq. (7):

$$\sum_i A_iJ_0(\alpha_ir)\exp(-\alpha_i^2bt)+T_c-\frac{ar^2}{4b}$$
$$=\frac{B}{\rho}\left\{\sum_i A_i\alpha_iJ_1(\alpha_ir)\exp(-\alpha_i^2bt)+\frac{ar}{2b}\right\}.$$

Separating the variables this expression reduces to

$$J_0(\alpha_ir)-\frac{B}{\rho}\alpha_iJ_1(\alpha_ir)=0 \tag{8}$$

and

$$T_c=\frac{ar^2}{4b}+\frac{B}{\rho}\frac{ar}{2b}=I^2R_{cu}n\left(\frac{\rho}{4\pi}+\frac{B}{\pi D}\right), \tag{9}$$

where $\alpha_i$ are the roots of Eq. (8).

The relation (9) gives the maximum temperature rise at the center of the cable. It may be written in the form of two equations:

$$T_r=I^2R_{cu}n\frac{\rho}{4\pi}, \tag{10}$$

$$T_s=I^2R_{cu}n\frac{B}{\pi D}, \tag{11}$$

where $T_r$ = temperature rise in the cable from $x=r$ to $x=0$ and $T_s$ = temperature rise at the surface of the cable.

From (10) to (11) the constants $\rho$ and $B$ may be found in terms of the radial and surface temperature rises, the power loss, and the diameter of the cable. Or, conversely, knowing $\rho$, $B$, $D$, and $I^2R_{cu}n$ of a cable, the maximum temperature rise, $T_c$, may be computed.

To evaluate the coefficients, $A_i$, use is made of the initial condition (I) and Eq. (7):

$$A_1J_0(\alpha_1x)+A_2J_0(\alpha_2x)+\cdots, \text{ etc.}=-T_c+\frac{ax^2}{4b},$$

which yields by virtue of the orthogonality

properties of the Bessel functions:

$$A_i=\frac{2\alpha_i^2}{\left[\left(r\frac{\rho}{B}\right)^2+\alpha_i^2r^2\right][J_0(\alpha_i r)]^2}\times\int_0^r x\left(-T_c+\frac{ax^2}{4b}\right)J_0(\alpha_i x)dx; \quad (12)$$

carrying out the integration and substituting for $a$ and $b$, we find for $A_i$:

$$A_i=\frac{2\alpha_i^2}{r^2\left[\alpha^2+\left(\frac{\rho}{B}\right)^2\right][J_0(\alpha_i r)]^2}\left\{\frac{I^2R_{cu}n\rho}{2\pi\alpha_i^2}J_0(\alpha_i r)+\left[\frac{I^2R_{cu}n\rho}{4\pi\alpha_i^2}\left(\alpha_i r-\frac{4}{\alpha_i r}\right)-\frac{T_c r}{\alpha_i}\right]J_1(\alpha_i r)\right\}. \quad (13)$$

Having determined the constants $A_i$ and $\alpha_i$ of Eq. (7), we now have the complete solution for the temperature of the cable as a function of time and radial distance.

The time variation of temperature at the center of the cable is of special interest. For this case Eq. (7) reduces to:

$$T(0,t)=A_1\exp(-\alpha_1^2bt)+A_2\exp(-\alpha_2^2bt)+\cdots,\text{ etc.}+T_c. \quad (14)$$

It will be shown in Part III that the coefficients, $A_i$, converge very rapidly and therefore the above expression reduces to the form:

$$T(0,t)\simeq T_c[1-\exp(-\alpha_1^2bt)]. \quad (15)$$

A comparison between Eq. (15) and the experimental curves is made in Part III.

## II. EXPERIMENTAL PROCEDURE

After considerable experimentation with thermocouple methods, it was found that the measurement of the change of resistance of the copper conductors gave much more reproducible results and consequently all measurements were made by this method.

If the resistance is measured at some known temperature $T_0$ and again at some other temperature $T_1$, then we may use the relationship

$$R_{T_1}=R_{T_0}[1+\beta(T_1-T_0)]$$

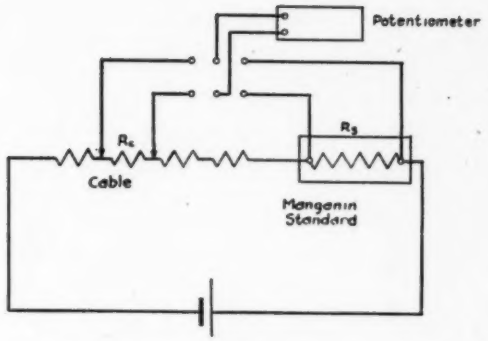


FIG. 1.

to obtain the temperature difference $T_1-T_0$

$$T_1-T_0=\frac{1}{\beta}\left[\frac{R_{T_1}}{R_{T_0}}-1\right], \quad (16)$$

where $R_{T_0}$ is the resistance at a known temperature, $T_0$, $R_{T_1}$ is the resistance at any other temperature, $T_1$, and $\beta$ is the temperature coefficient of resistivity of copper $=1/(234.5+T_0)$.

The circuit used for the measurements is shown schematically in Fig. 1. A standard manganin resistor, $R_s$, is placed in series with the cable so that all resistance measurements could be referred to this standard. Let $R_{c,T_0}$ be the resistance of one of the wires in the cable at the initial temperature $T_0$. The ratio $R_{c,T_1}/R_{c,T_0}$ in Eq. (16) may be obtained by voltage measurements as follows:

From Ohm's law,

$$V_{c,T_0}=I_{T_0}R_{c,T_0}$$

and

$$V_{s,T_0}=I_{T_0}R_{s,T_0};$$

hence,

$$R_{c,T_0}=\frac{V_{c,T_0}}{V_{s,T_0}}R_{s,T_0}, \quad (17)$$

where $V$, $I$, and $R$ have their usual meanings, the subscript, $T_0$, referring to the values of these quantities when the cable is at $T_0$ degrees centigrade, and the subscripts, $c$ and $s$, to the cable and manganin resistance, respectively.

Similarly

$$R_{c,T_1}=\frac{V_{c,T_1}}{V_{s,T_1}}R_{s,T_1}. \quad (18)$$

Since the temperature coefficient of manganin is negligibly small,

$$R_{s,T_0}=R_{s,T_1};$$

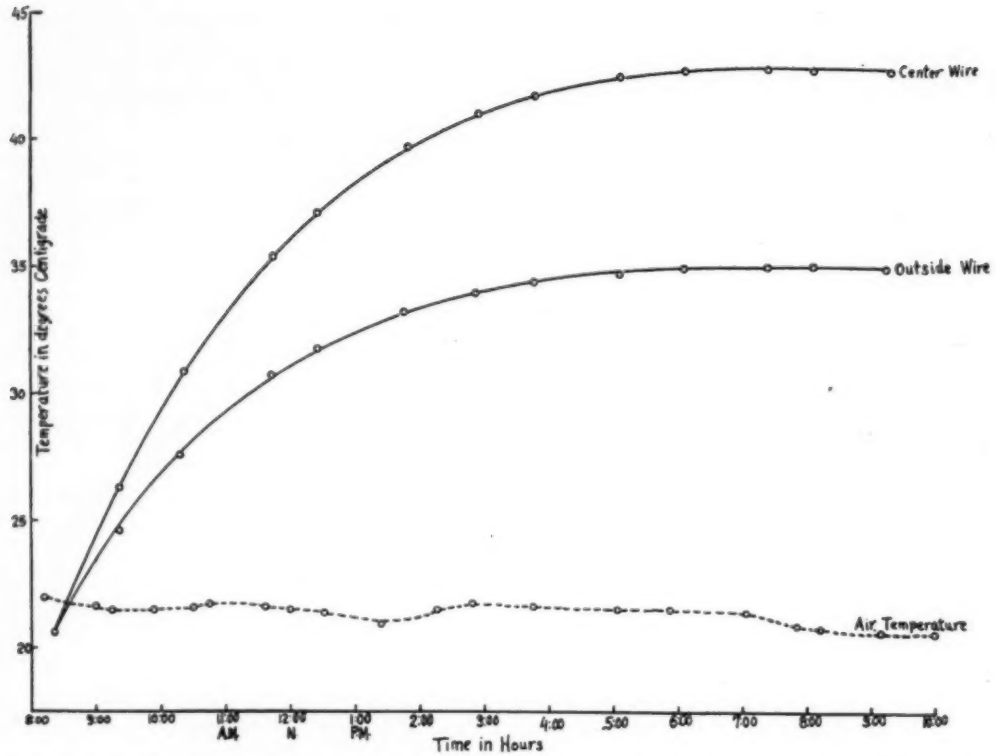


FIG. 2. Experimental variation of cable temperature in a cable having 61 conductors of No. 3 wire when a current of 27 amperes flows continuously through it.

dividing (18) by (17) and substituting the result in (16) yields:

$$T_1 - T_0 = \frac{1}{\beta}\left[\frac{V_c, r_1}{V_s, r_1}\frac{V_s, r_0}{V_c, r_0} - 1\right]. \qquad (19)$$

The expression (19) gives the temperature rise in terms of measurable quantities. The voltage drops across $R_c$ and $R_s$ were measured by means of a Rubicon type "B" potentiometer.

TABLE I. Experimental data on cables.

| No. of wires in cables | AWG No. | No. of layers in cables | Dimensions of cables Length (cm) | Diameter (cm) | Current in amp. | Total power in watts | $T_c$ temp. rise at center in °C | Radial temp. rise in °C |
|---|---|---|---|---|---|---|---|---|
| 19 | 1 | 2 | 375 | 7.24 | 57 | 104 | 20.5 | 4.0 |
| 37 | 1 | 3 | 416 | 10.04 | 45 | 135 | 21.0 | 5.7 |
| 61 | 1 | 4 | 415 | 14.06 | 37 | 162 | 21.8 | 8.1 |
| 19 | 3 | 2 | 412 | 6.48 | 42 | 100.7 | 19.5 | 4.3 |
| 37 | 3 | 3 | 417 | 8.80 | 33 | 120 | 20.9 | 6.1 |
| 61 | 3 | 4 | 415 | 11.20 | 27 | 134 | 21.4 | 7.7 |
| 91 | 3 | 5 | 420 | 13.12 | 24 | 160 | 23.5 | 9.5 |
| 19 | 6 | 2 | 414 | 6.06 | 27 | 82.0 | 17.0 | 4.1 |
| 37 | 6 | 3 | 420 | 8.12 | 22 | 107.5 | 20.0 | 6.0 |
| 61 | 6 | 4 | 416 | 9.52 | 18 | 115.3 | 20.9 | 7.3 |
| 19 | 9 | 2 | 424 | 4.44 | 17 | 77.0 | 18.1 | 4.1 |
| 37 | 9 | 3 | 421 | 5.90 | 14 | 85.5 | 18.7 | 5.2 |
| 61 | 9 | 4 | 420 | 7.78 | 12 | 97.0 | 19.6 | 6.5 |
| 37 | 15 | 3 | 425 | 4.14 | 5.8 | 58.2 | 14.9 | 3.6 |
| 61 | 15 | 4 | 422 | 5.20 | 5 | 71.5 | 16.6 | 4.8 |
| 61 | 18 | 4 | 425 | 4.80 | 4 | 96.8 | 25.3 | 6.6 |

The cables used in the experiment are listed in Table I. All were made up out of standard rubber covered wire which had a safe operating limit of 75°C. The cables were assembled in such a way that a given wire remained in the same layer throughout the length of the cable. A canvas sleeve was sewn over the assembled cable and this was painted with a coating of preservative paint. Subsequent measurements showed that the painting had no measurable effect on the results of the experiments.

All the wires in the cable were put in series so that the current flowed back and forth through the length of the sample. Each sample was approximately 14 feet long, the ends being enclosed in two wooden boxes packed with insulating material. With this arrangement, thermocouples showed no appreciable temperature gradient along the length of the cable. This was essential since the resistance method yields an average value of the temperature in any one layer and not just the temperature at one point.

Since it would not be practical, especially in the larger cables, to measure the voltage drop across every wire, only four wires in each layer were selected for these measurements. The leads from these wires were run to two selector switches, $S_1$ and $S_2$, and thence to two double pole-double throw switches, $S_3$ and $S_4$, leading to the potentiometer. $S_3$ served as a reversing switch, and $S_4$ connected the potentiometer either to the manganin resistor or to one of the wires in the cable.

The current was furnished by a d.c. motor generator set with four storage batteries "floating" across the output. Since the fluctuations in voltage across the cable were large (about $\frac{1}{2}$ percent) a switch, $S_5$, was installed which disconnected the generator from the cable, leaving only the batteries to furnish the current during measurements. This switch was thrown about 10 minutes before every reading to allow the batteries to come to equilibrium. With this arrangement there was no difficulty in reading the voltage drops to within .01 millivolt.

A complete run on a cable consisted of the following:

1. The voltage drops $V_c,T_0$ and $V_s,T_0$ were measured with reduced currents to prevent any heating during the measurement. $T_0$ was measured by means of several Fe-Con. thermocouples imbedded in the cable. The "cold" junction of these couples was kept in air but its temperature could be read to 0.1°C.

2. Readings were taken of $V_c,T_1$ and $V_s,T_1$ at hourly intervals using only the center wire and one of the outer wires. With the aid of these readings the approach to equilibrium could be studied.

3. When equilibrium had been reached, the voltage drops across the other wires were measured and the temperatures were calculated by means of (19).

The ambient temperature was read at half-hour intervals on several mercury thermometers located 3 or 4 feet from the cable. The air temperature as measured in different parts of the room agreed to within two-tenths of a degree, indicating a relatively draft-free condition.

The over-all accuracy of the method was estimated to be between 0.2°–0.3°C.

## III. RESULTS OF MEASUREMENTS

Measurements were made on the sixteen cables listed in Table I. The currents which were used were chosen rather arbitrarily to give a temperature rise of 20°–25°C at the center of the cable. Several runs were usually made on each cable and curves were plotted showing the variation of temperature with time as well as the radial temperature distribution at equilibrium. Typical curves are shown in Figs. 2 and 3. From such curves as in Fig. 3 it is possible to obtain the surface temperature rise, $T_s$, and the radial temperature rise, $T_R$. These have been listed for the test cables in Table I.

From the measured values of the temperature rise and the power input, the values of the radial thermal resistivity, $\rho$, and the surface thermal resistivity, $B$ may be calculated according to Eqs. (10) and (11). The resultant values for $\rho$ are plotted in Figs. 4 and 5 which show the variation of $\rho$ with size of wire and number of layers. Figure 6 shows the variation of $B$ with the diameter $D$ of the cable. The general shape

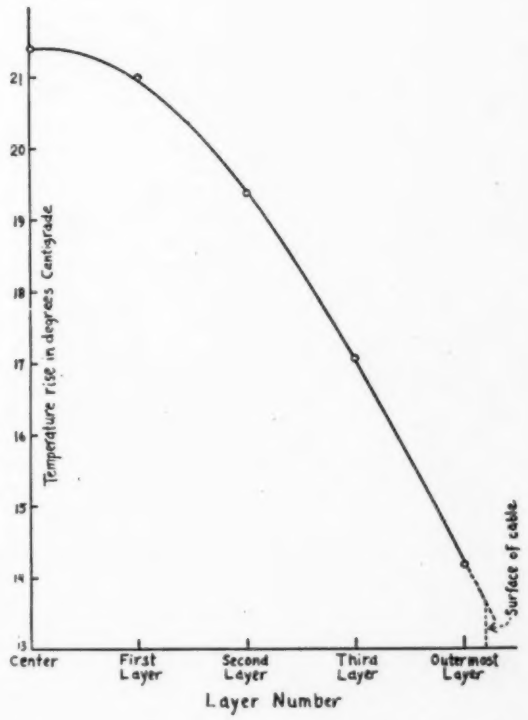


FIG. 3. Temperature rise in each layer of the cable having 61 turns of No. 3 wire (diameter 11.2 cm).

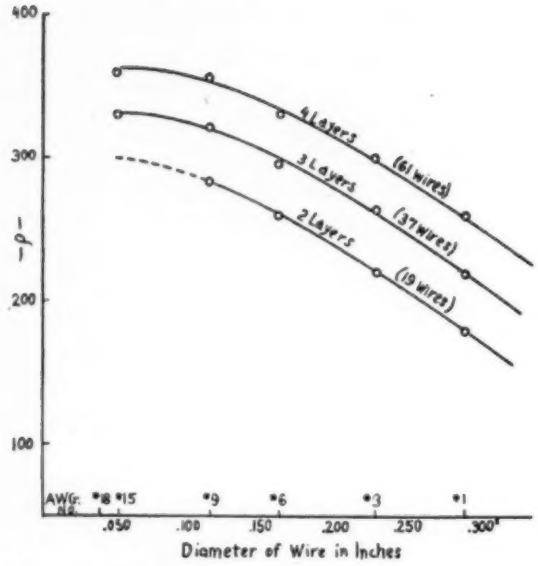


FIG. 4. Value of thermal resistivity, $\rho$, in degrees centigrade per watt per centimeter, for wire cables.

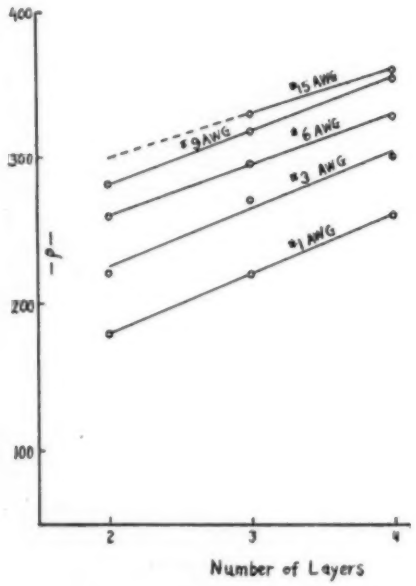


FIG. 5. Values of thermal resistivity, $\rho$, in degrees centigrade per watt per centimeter, for wire cables.

of this last curve is quite similar to the one obtained by S. J. Rosch.[1]

By interpolation of these curves, the constants for all other cables may be obtained and the maximum safe current computed from:

$$I=\left\{\frac{25}{R_{cu}n[\rho/4\pi+B/\pi D]}\right\}^{\frac{1}{2}}. \qquad (20)$$

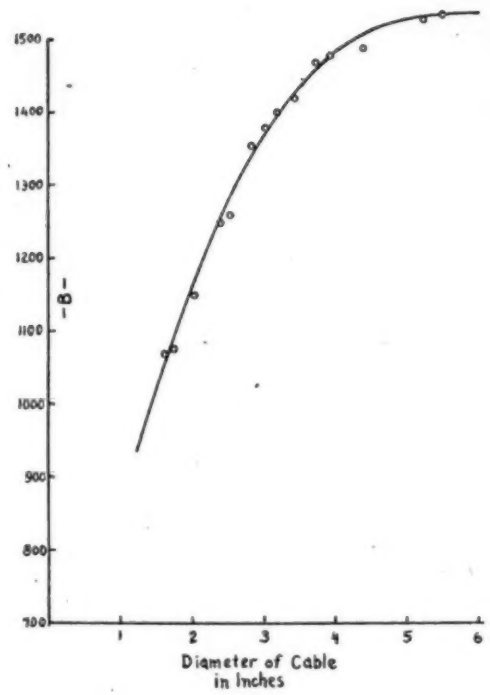


FIG. 6. Values of thermal surface resistivity, $B$, in degrees centigrade per watt per square centimeter, for wire cables.

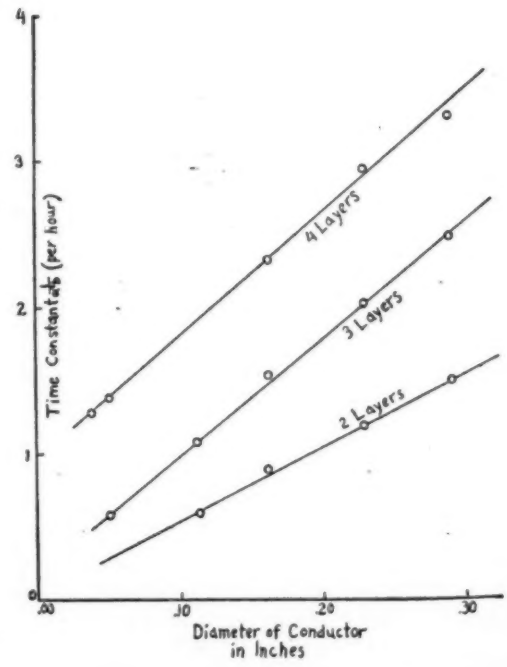


FIG. 7. "Time constant" of cable *vs.* size of conductor.

TABLE II. Average temperature in cables. For a rise of 25°C in cable and an ambient temperature of 50°C.

| Number of layers | 2 | 3 | 4 | 5 |
|---|---|---|---|---|
| Average temperature (°C) | 71.7 | 70.7 | 69.8 | 68.8 |

This current will give a 25°C rise in temperature at the center of the cable. Since we wished to allow for an ambient of 50°C, the resistance of the cable per cm $R_{cu}n$ had to be calculated for the average temperature of the copper which would exist at that ambient with the maximum current flowing. These average temperatures were found to be independent of the wire size and depended only on the number of layers. The values are listed in Table II. The currents were calculated from Eq. (20) using resistances from standard tables at the average temperature shown in Table II. The results of these calculations are given in Table III for cables with 19, 37, and 61 wires, corresponding to 3, 4, and 5 layers. Intermediate values may be obtained satisfactorily by interpolation.

In order to compare the theoretical expression (14) with the actual time variation of the temperature at the center of the cable, the coefficients $A_1$, $A_2$, and $A_3$ were calculated for several cables. They were found to converge very rapidly, and in the worst case (91 conductors of No. 3 wire) $A_1$ differed from $T_c$ by only 4 percent. The expression (15) may therefore be used to get the temperature-time relation at the center of the cable:

$$T(0, t) = T_c[1 - \exp(-\alpha_1^2 bt)], \qquad (21)$$

where $\alpha_1 = f((B/\rho), r)$ is a root of (8) and the value of $b$ is given by $b = 1/\rho S_0 d_0$. $S_0 d_0$ has been calculated from handbook values for the specific heats and densities of rubber, copper, and air by using the expression

TABLE III. Maximum safe currents for cables. For a rise of 25°C in cable and an ambient temperature of 50°C.

| No. of wires in cables | AWG No. | Amperes I | Diameter of cable (inches) | No. of wires in cables | AWG No. | Amperes I | Diameter of cable (inches) |
|---|---|---|---|---|---|---|---|
| 19 | 0 | 70.8 | 3.16 | 19 | 6 | 30.9 | 2.38 |
| 37 | 0 | 54.4 | 4.43 | 37 | 6 | 23.4 | 3.20 |
| 61 | 0 | 44.6 | 5.70 | 61 | 6 | 18.7 | 3.75 |
| 19 | 1 | 60.0 | 2.85 | 19 | 7 | 27.0 | 2.02 |
| 37 | 1 | 46.7 | 3.95 | 37 | 7 | 20.4 | 2.83 |
| 61 | 1 | 38.0 | 5.54 | 61 | 7 | 16.6 | 3.64 |
| 19 | 2 | 52.9 | 2.66 | 19 | 8 | 23.0 | 1.73 |
| 37 | 2 | 40.2 | 3.72 | 37 | 8 | 17.5 | 2.42 |
| 61 | 2 | 32.5 | 4.79 | 61 | 8 | 14.2 | 3.11 |
| 19 | 3 | 45.0 | 2.55 | 19 | 9 | 19.1 | 1.75 |
| 37 | 3 | 34.2 | 3.46 | 37 | 9 | 15.3 | 2.32 |
| 61 | 3 | 27.8 | 4.41 | 61 | 9 | 12.9 | 3.06 |
| 91 | 3 | 23.7 | 5.17 | | | | |
| | | | | 19 | 12 | 14.1 | 1.47 |
| 19 | 4 | 40.2 | 2.36 | 37 | 12 | 10.6 | 2.05 |
| 37 | 4 | 30.4 | 3.30 | 61 | 12 | 8.6 | 2.64 |
| 61 | 4 | 24.8 | 4.25 | | | | |
| | | | | 37 | 15 | 7.1 | 1.63 |
| 19 | 5 | 35.2 | 2.23 | 61 | 15 | 6.4 | 2.05 |
| 37 | 5 | 26.6 | 3.12 | | | | |
| 61 | 5 | 21.6 | 4.02 | 61 | 18 | 3.8 | 1.89 |

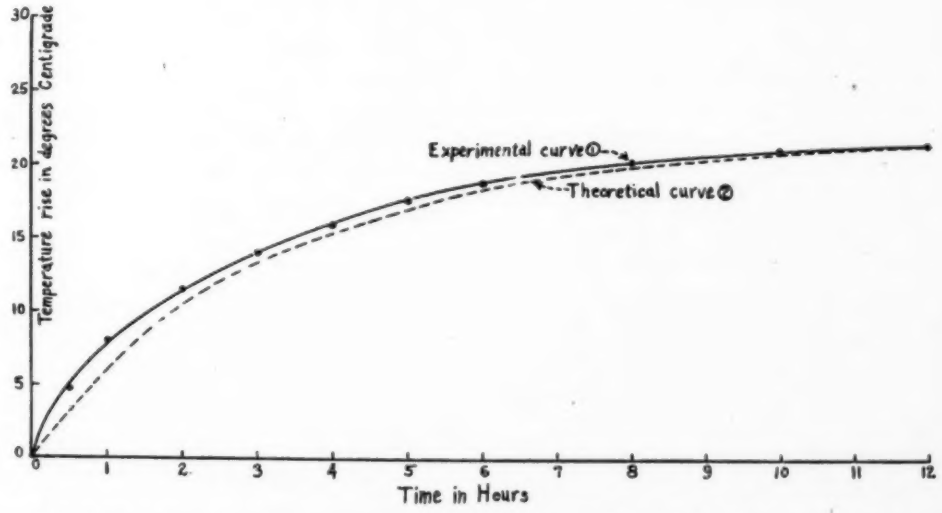


FIG. 8. Variation of temperature with time at the center of a cable having 61 conductors. ①——— Experimental curve; ②– – – Theoretical curve.

$$S_0 d_0 = \frac{1}{A}[(aSd)_{\text{copper}} + (aSd)_{\text{rubber}} + (aSd)_{\text{air in cable}}],$$

$A$ = cross-section area of cable,
$S$ = specific heat in watt sec./deg. C,
$d$ = density in g/cm³, and
$a$ = cross-section area of constituents in cm².

Values of $\alpha_1^2 b$ have been obtained for all the cables tested. The reciprocal of $\alpha_1^2 b$, the time constant, is plotted in Fig. 7 as a function of the diameter of the conductor.

In Fig. 8 the experimental temperature-time curve for one of the larger cables is compared with the theoretical curve of Eq. (15). The agreement between the two is quite good and indicates that Eq. (15) may be used with considerable confidence to represent the temperature-time relationship at the center of a multiconductor cable.


### ACKNOWLEDGMENT

The authors wish to express their thanks to Dr. George I. Welch for many helpful discussions of the problem and to Mr. George Bigelow for assistance with the experimental techniques.


## A Computer for Solving Linear Simultaneous Equations


CLIFFORD E. BERRY, DOYLE E. WILCOX, SIBYL M. ROCK, AND H. W. WASHBURN
*Consolidated Engineering Corporation, Pasadena, California*



(Received November 16, 1945)



The mathematical principles of the classical iterative method of solving linear simultaneous equations are discussed. Basic electrical circuits for setting up an analog of the mathematical relations are given, and a commercial model of a 12-equation computer is briefly described. The results of solving a number of problems on the computer are given to illustrate its accuracy and speed of operation. It is found that solving sets of 12 equations requires only 1/4 to 1/7 the time required by conventional methods.


DURING the war a large number of mass spectrometers and infra-red spectrophotometers were installed in petroleum refineries and research institutions. In the application of each of these instruments to analytical work there is the frequent necessity of solving linear simultaneous algebraic equations, particularly in analysis of complex hydrocarbon mixtures. Often mixtures requiring the solution of eight or ten simultaneous equations for their analysis are encountered, and occasional mixtures may involve as many as twelve equations. As is well known, the labor involved in solving sets of this size is considerable, with the result that the present limitation on speed of analysis is often not the obtaining of the data, but rather its computation. It was this problem primarily which prompted the authors to develop the computer described in this paper.

A second factor influencing the development of a computer was the frequency with which simultaneous equations are encountered in engineering, in physics, and in mathematics; for example, such equations occur in the study of electrical circuits, structures, aircraft flutter analysis, and statistics. Few computing devices have been available which rapidly yield solutions of engineering accuracy. The computer to be described will fill a need for such a device in many fields.

The present computer, in common with most previously proposed computers,[1-4] is of the analog type; i.e., certain physical quantities in the computer are used to represent, or are analogous to, the numbers involved. In the present computer the physical quantities involved are not voltage, current, or mechanical displacement, but are merely the *ratios* among certain resistances. This feature, together with a simple method of obtaining the summation of a number of quantities, contributes greatly to the simplicity and to the high inherent accuracy of the computer.

### BASIC MATHEMATICAL PRINCIPLES

Before describing the details of the computer it is necessary to describe the mathematical method

upon which it is based. This method is known as the "Gauss-Seidel method" or the "Classical Iterative method."[5] In it, an arbitrary solution, or an approximate solution if it is known, is used to compute a second approximation to the solution, which is then used to compute a third, and so forth until a negligible difference exists between successive approximations. These operations, although laborious by conventional methods, are extremely rapid in the present computer, as each step consists merely of adjusting a circuit to a null, with the instrument itself remembering the previous approximation as long as necessary.

For three equations the method is as follows: Let the set of equations be defined by

$$a_{11}x_1+a_{12}x_2+a_{13}x_3=m_1, \quad (1)$$

$$a_{21}x_1+a_{22}x_2+a_{23}x_3=m_2, \quad (2)$$

$$a_{31}x_1+a_{32}x_2+a_{33}x_3=m_3. \quad (3)$$

In the following, a superscript on $x$ (e.g., $x^{(p)}$) indicates the value existing at the end of the $p$th iteration.

*First cycle*:

*a*. The first equation is solved for $x_1^{(0)}$, using the trial values $x_2^{(0)}$ and $x_3^{(0)}$ which are arbitrary.

$$a_{11}x_1^{(1)}+a_{12}x_2^{(0)}+a_{13}x_3^{(0)}=m_1,$$
$$x_1^{(1)}=(1/a_{11})(m_1-a_{12}x_2^{(0)}-a_{13}x_3^{(0)}). \quad (4)$$

*b*. The second equation is solved for $x_2^{(1)}$, using $x_1^{(1)}$ and $x_3^{(0)}$.

$$a_{21}x_1^{(1)}+a_{22}x_2^{(1)}+a_{23}x_3^{(0)}=m_2,$$
$$x_2^{(1)}=(1/a_{22})(m_2-a_{21}x_1^{(1)}-a_{23}x_3^{(0)}). \quad (5)$$

*c*. The third equation is solved for $x_3^{(1)}$, using $x_1^{(1)}$ and $x_2^{(1)}$.

$$a_{31}x_1^{(1)}+a_{32}x_2^{(1)}+a_{33}x_3^{(1)}=m_3,$$
$$x_3^{(1)}=(1/a_{33})(m_3-a_{31}x_1^{(1)}-a_{32}x_2^{(1)}). \quad (6)$$

*Second cycle:*

$$a'. \quad a_{11}x_1^{(2)\prime}+a_{12}x_2^{(1)}+a_{13}x_3^{(1)}=m_1. \quad (7)$$

$$b'. \quad a_{21}x_1^{(2)}+a_{22}x_2^{(2)\prime}+a_{23}x_3^{(1)}=m_2. \quad (8)$$

$$c'. \quad a_{31}x_1^{(2)}+a_{32}x_2^{(2)}+a_{33}x_3^{(2)\prime}=m_3. \quad (9)$$

The primed term is the one solved for in each equation. This procedure is repeated until the variables remain the same on two successive cycles. On the electric computer, this means that a null is obtained on switching to any equation.

For the general case, the method can be expressed concisely in matrix notation as $A_1X^{(p)}+A_2X^{(p-1)}=M_1$, where

$$A=\text{square matrix of the coefficients}=\begin{vmatrix} a_{11} & \cdots & a_{1n} \\ \cdot & & \cdot \\ \cdot & & \cdot \\ \cdot & & \cdot \\ a_{n1} & \cdots & a_{nn} \end{vmatrix},$$

$$A_1=A \text{ with all elements above the principal diagonal equal to zero}=\begin{vmatrix} a_{11} & \cdot\cdot 0 & 0 \\ \cdot & & \\ \cdot & \cdot\cdot a_{ii} & 0 \\ \cdot & & \\ a_{n1} & \cdots & a_{nn} \end{vmatrix},$$

$$A_2=A \text{ with the principal diagonal and all elements below it equal to zero}=\begin{vmatrix} 0 & a_{12} & \cdots & a_{1n} \\ 0 & 0 & & \cdot \\ \cdot & & & \cdot \\ \cdot & & & a_{n-1,n} \\ 0 & \cdots & & 0 \end{vmatrix},$$

$$X=\text{column matrix of the unknowns}=\begin{vmatrix} x_1 \\ \cdot \\ \cdot \\ \cdot \\ x_n \end{vmatrix}, \qquad M=\text{column matrix of the constant terms}=\begin{vmatrix} m_1 \\ \cdot \\ \cdot \\ m_n \end{vmatrix}.$$

### Convergence of the Method

Whether or not the iterative method converges depends upon the coefficients $a_{ij}$, and upon the order in which the equations and variables are placed before solution is begun. A necessary and sufficient condition for convergence of the method has been developed,[5-8] but unfortunately it requires a large amount of computation to apply the criterion. More readily computed criteria may be deduced, but these are merely sufficiency criteria, and give no conclusive information.

It is, therefore, fortunate that in a great many practical problems a satisfactory order of arrangement resulting in convergence is obvious upon inspection. The simple empirical rules used in obtaining this order are:

1. An attempt is made to put the equations in such order that
   - *a*. coefficients on the diagonal are large, and
   - *b*. those off the diagonal—particularly the post-diagonal coefficients—are small.

When these rules can be applied, the problem usually converges in a few cycles.

2. In case rule (1) cannot be applied, a major coefficient in each equation is put on the diagonal. Then the order is adjusted until the product of each pair of diagonal elements is greater in absolute value than the product of the other two elements in the second-order determinant having those diagonal elements as the principal diagonal; i.e.,

$$|a_{ii}a_{jj}| > |a_{ij}a_{ji}|. \tag{10}$$

In this case, also, the smaller off-diagonal terms are placed in post-diagonal positions if possible.

Once a satisfactory order for a given set of coefficients is determined, that order can be used for all problems involving those coefficients, since the conditions for convergence (but not the *rate* of convergence) depend upon coefficients $a_{ij}$ only and not on constant terms $m_i$.

### *K*-Method of Accelerating Solution

For cases in which convergence is slow and/or the optimum order is not immediately apparent, a direct method, called a *K*-method, has been developed. In this method it is only necessary to go through the process once to obtain the final answer; that is, there are no successive approximations to be made. Although the details are too involved to give here, briefly the method is as follows:* The first two equations in the first two variables are solved, then the first three equations in the first three variables, etc., until all equations in $n$ variables have been solved. The coefficients of the successive sets of equations are those which each time include one more element of the principal diagonal of the matrix:

$$\begin{array}{cccccc|c}
a_{11} & a_{12} & a_{13} & a_{14} & \cdots & a_{1n} & \\
a_{21} & a_{22} & a_{23} & a_{24} & \cdots & a_{2n} & \\
a_{31} & a_{32} & a_{33} & a_{34} & \cdots & a_{3n} & \\
a_{41} & a_{42} & a_{43} & a_{44} & \cdots & a_{4n} & \\
\cdot & \cdot & \cdot & \cdot & \cdot & \cdot & \cdot \\
a_{n1} & a_{n2} & a_{n3} & a_{n4} & \cdots & a_{nn} & \cdot \quad \cdot
\end{array}$$

The method of accomplishing the successive solutions directly, without recourse to a trial and error procedure, is to balance each equation not to a null, but to a previously computed portion, $k_i$, of the unbalance observed when switching to that equation. The purpose of solving successively more equations 2, 3, $\cdots$ to $n$, as outlined above is to obtain $k$'s which are functions of the $a$'s and are independent of the $m$'s.

The process requires precomputation of the $k$'s but these can be readily calculated on the computer itself. There are $n(n-1)/2$ $k$'s to be computed for $n$ equations. Since these are functions of the $a$'s only, time can sometimes be saved by utilizing this method when a number of solutions are to be made from the same coefficients but with different constant terms.

### BASIC CIRCUITS

From Eqs. (4) through (9) it is evident that the two basic mathematical operations to be performed are multiplications of pairs of numbers, and additions or subtractions of the quantities which result.

Figure 1 shows the method for adding voltages which is used in the computer. In this, $n$ equal impedances are connected to a common point $O'$ at one end, and the other end of each is connected to one of the voltages to be added. The other side

* It is hoped to publish the full details of this method at an early date.

of each voltage source is connected to another common point $O$, which may for convenience be ground. Then, applying Kirchoff's laws to the circuit, the open circuit voltage between $O'$ and $O$ is easily found to be

$$E_{0c}=(1/n)(E_1+E_2+E_3+\cdots+E_n). \quad (11)$$

In other words, $E_{0c}$ is proportional to the sum of the various source voltages. This is a general result, applying both to direct and alternating voltages, but it will be considered here only with regard to alternating voltages of the same phase and frequency, since the use of alternating current is found to have a number of practical advantages.

In order that an addition circuit of this type yield an accurate sum, two conditions must be satisfied: ($a$) the $n$ impedances comprising the

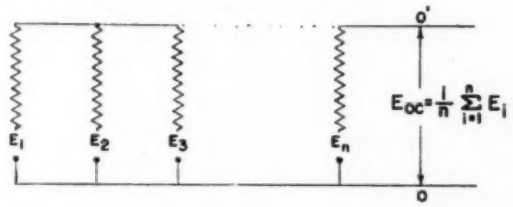


FIG. 1. Diagram of a circuit for obtaining a voltage proportional to the sum of a number of voltages.

circuit must be accurately equal in impedance, and ($b$), the internal impedances of the voltage sources must be negligibly small compared with the coupling impedances. Both of these conditions can be met satisfactorily in practice.

Figure 2 shows the circuit of a multiplying device, utilizing a pair of adjustable voltage dividers, or potentiometers, one supplying the other. If a voltage $E_i$ is connected across the first potentiometer and its slider is set to the fraction $a$ of the total resistance (taking into account the loading effect of the second potentiometer), then the voltage applied to the second potentiometer is $aE_i$. If the slider of the second potentiometer is set at the fraction $x$ of the total resistance, then the output voltage is $E_0=axE_i$. It should be noted that the second potentiometer, which may be called the $x$-potentiometer, is linear, whereas the $a$-potentiometer is non-linear because of its load. This feature is not particularly disadvantageous, because in the interest of the greatest possible accuracy it is desirable to set values on potentiometers not with reference to a calibrated

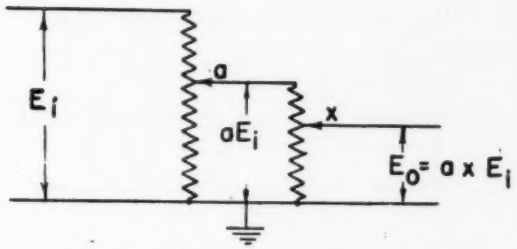


FIG. 2. Diagram of a circuit for obtaining a voltage proportional to the product of two numbers.

scale on the potentiometer itself, but rather with respect to a decade-type standard potentiometer.

In order to accomplish such comparative measurements, a simple Wheatstone bridge circuit is sufficient. Figure 3 shows a measuring circuit, in which the potentiometer to be set and an accurate decade potentiometer are connected in parallel to a common source. A null indicator of some sort is connected between their taps. It is plain that any fraction set on the decade can be transferred to the $a$-potentiometer by adjusting the $a$-potentiometer to a null, and that the loading effect of the $x$-potentiometer is thus automatically taken into account.

With these simple circuits as a basis it is easy to build an analogous circuit representing one equation of the type of (1). Figure 4 shows a combined multiplication-addition circuit which represents

$$a_{i1}x_1+a_{i2}x_2+a_{i3}x_3+\cdots+a_{in}x_n=m_i. \quad (12)$$

One half of a center-tapped transformer supplies a set of $a$-potentiometers in parallel, and between the tap and ground of each of these potentiometers is connected an $x$-potentiometer. Across the other half of the transformer is connected a single potentiometer which represents the $m_i$ term. Recalling now the operation of a multiplying circuit, it is seen that the voltage between the arm of each $x$-potentiometer and ground has the

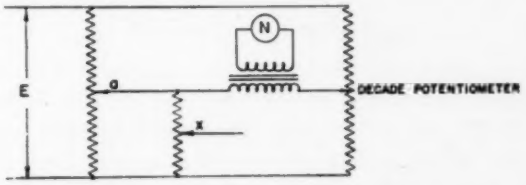


FIG. 3. Diagram of a circuit for setting a ratio on a loaded potentiometer by using a standard decade potentiometer.

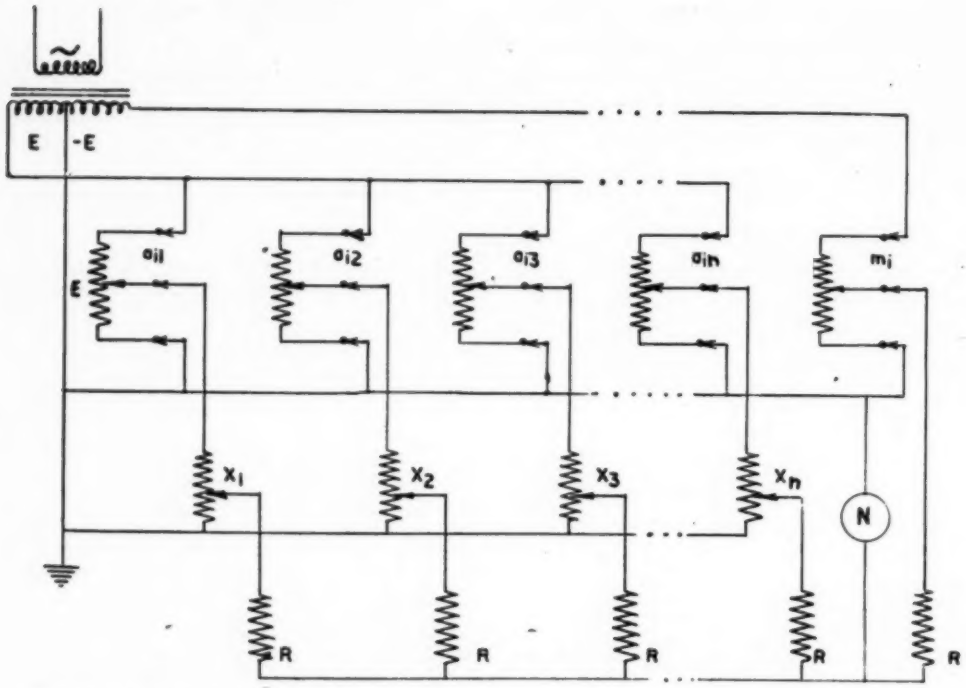


FIG. 4. Diagram of a circuit which is the analog of an equation of the type $\Sigma_j a_{ij}x_j = m_i$.

value

$$V_{ax} = a_{ij}x_iE, \tag{13}$$

and the voltage between the arm of the $m$-potentiometer and ground is simply

$$V_m = -m_iE, \tag{14}$$

where the minus sign must be used because this voltage is opposite in phase to that in Eq. (9). If the arms of the $x$- and $m$-potentiometers are regarded as voltage sources for a circuit of the type shown in Fig. 1, it is only necessary to connect them to a common point through equal high impedances in order to obtain a voltage proportional to the sum. This is accomplished in Fig. 4 by means of the resistors $R$. Thus the voltage between the junction point and ground in Fig. 4 is given by

$$V_n = [1/(n+1)](a_{i1}x_1 + a_{i2}x_2 + a_{i3}x_3 + \cdots + a_{in}x_n - m_i)(E). \tag{15}$$

Now, any adjustment of the $x$-potentiometers which results in a value of zero for $V_n$ transforms Eq. (15) into Eq. (12), since the factors $E$ and $1/(n+1)$ drop out. In other words, any set of $x$-potentiometer settings which causes $V_n$ to be zero represents a solution for the particular equation in question.

The method of extending the circuit of Fig. 4 to sets of equations having any number of unknowns is obvious, since it is merely necessary to provide as many $a$- and $x$-potentiometers, each in combination with its associated addition resistor, as unknowns. Likewise, there must be provided as many rows of $a$- and $m$-potentiometers as there are equations, together with means for switching each row as a group (representing the coefficients and constant term of one equation) into the voltage source and the $x$-circuits as indicated in Fig. 4. For simplicity, only one set of $a$-potentiometers has been shown in Fig. 4.

The circuit shown in Fig. 4 is modified in the commercial computer in that two sets of addition resistors are used to permit positive and negative values to be handled; at the same time this eliminates the need for a center-tapped input transformer. The chief advantage of eliminating the transformer is that high accuracy is more easily obtained without the necessity of maintaining great precision of the center tap under varying load conditions on the two halves of the transformer. Figure 5 is a photograph of a commercial 12-equation computer designed according to the preceding theory.

The operation of a computer based on such a circuit is extremely simple. The coefficients and constant terms are first set in by use of a comparison bridge, as shown in Fig. 3. Then, with the $a$-potentiometers and $m$-potentiometer for the first equation switched into the circuit, the first $x$-potentiometer is adjusted to give a null; the second set of $a$'s and their associated $m$ are switched into the circuit and the second $x$-potentiometer adjusted to satisfy the second equation, and so on. This sequence is repeated until all equations are found to be in balance. The $x$-potentiometers then read the values of the unknowns directly.

## ACCURACY

The question of accuracy is of prime importance in determining the usefulness of any such computer as that described. In engineering applications one of the most useful criteria of accuracy is that the errors introduced by the computations (depending upon the problem) be either small compared with the errors inherent in the initial data, or at least be of the same magnitude as these errors. The initial data are normally the coefficients and constant terms of the equations. It has been found possible to design a computer based on the foregoing circuits such that, in using data accurate to between two and three significant figures, the errors in the $x$ values obtained on the computer are about *one order of magnitude less* than the errors inherent in the data. In using three to four place data the accuracy of the computer is of the same order of magnitude as the accuracy inherent in the data.

A complete discussion of the subject of accuracy in the solution of linear simultaneous algebraic equations is beyond the scope of this

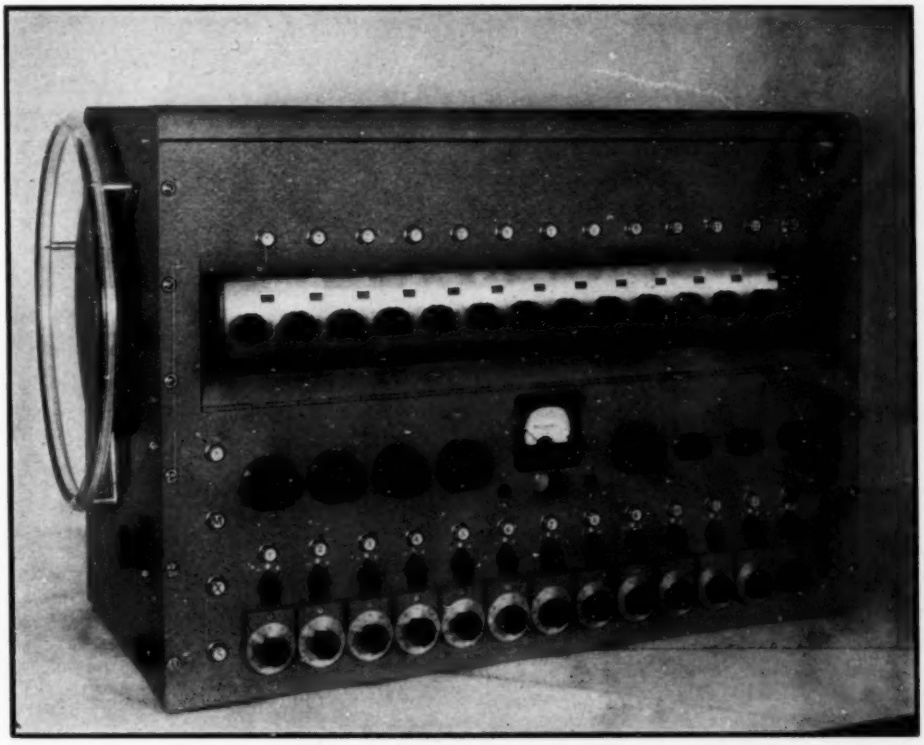

FIG. 5. Front view of a commercial 12-equation computer. The $a$- and $m$-potentiometers are carried on a switching turret operated by the large handwheel. The $m$'s and the $a$'s representing one equation appear in the horizontal window and are automatically switched into the circuit when turned to this position. The bottom row of dials represents the $x$ values. The knobs above the $x$ dials control plus-minus switches, each corresponding to the $x$ dial below it. The vertical row of push-buttons at the right is for presetting positive and negative $m$'s. In the center of the panel is a small cathode-ray tube null indicator, and to the left of this are the four dials of the decade potentiometer. The length of the panel is 32 inches.

TABLE I. Accuracy and time of electric computer solution of twelve simultaneous algebraic equations. The first 12 rows and columns are the coefficients of the equations to be solved; each column representing the coefficients of one variable, each row the coefficients of one equation. The $m$ column contains the constant terms; the $m_{cc}$ column the results of substituting the electric computer answers in each equation.

| Equation No. | $x_1$ | $x_2$ | $x_3$ | $x_4$ | $x_5$ | $x_6$ | $x_7$ | $x_8$ | $x_9$ | $x_{10}$ | $x_{11}$ | $x_{12}$ | $m$ | $m_{cc}$ | $\Delta m = m_{cc} - m$ |
|---|---|---|---|---|---|---|---|---|---|---|---|---|---|---|---|
| (1) | 1.0000 | .1359 | .1070 | .0256 | .0065 | .0091 | .0469 | .0239 | .0046 | .0101 | .0072 | .0086 | .1127 | .1122 | −.0005 |
| (2) | .0278 | 1.0000 | .1944 | .1659 | .1779 | .0585 | .2129 | .1100 | .0248 | .0025 | .0328 | .0323 | .1484 | .1480 | −.0004 |
| (3) | .0020 | .1573 | 1.0000 | .0111 | .1853 | .1161 | .2273 | .1472 | .0921 | .1010 | .0687 | .0029 | .1748 | .1745 | −.0003 |
| (4) | .0015 | .1920 | .0318 | 1.0000 | .7289 | .0030 | .0445 | .0088 | .0362 | .0029 | .0423 | .0036 | .1988 | .1984 | −.0004 |
| (5) | .0050 | .0346 | .0391 | .0822 | 1.0000 | .0199 | .0521 | .0123 | .0089 | .0328 | .0718 | .0042 | .1236 | .1232 | −.0004 |
| (6) | .0216 | .1759 | .0429 | .0254 | .1242 | 1.0000 | .1642 | .0094 | .0034 | .0154 | .0062 | .0062 | .0873 | .0873 | 0 |
| (7) | .0139 | .1379 | .0230 | .0209 | .0562 | .2318 | 1.0000 | .0176 | .0028 | .0056 | .0044 | .0103 | .0668 | .0668 | 0 |
| (8) | .1834 | .2222 | .2103 | .0739 | .1938 | .3345 | .2938 | 1.0000 | .0424 | .0102 | .0053 | .0204 | .2598 | .2598 | 0 |
| (9) | .0724 | .0632 | .0943 | .1028 | .0072 | .0029 | .0423 | .4978 | 1.0000 | .0018 | .0028 | .0183 | .1791 | .1791 | 0 |
| (10) | .0474 | .1947 | .0610 | .0725 | .1880 | .0608 | .0222 | .1024 | .0621 | 1.0000 | .0032 | .0216 | .0832 | .0831 | −.0001 |
| (11) | .0683 | .0457 | .0241 | .0759 | .0139 | .0173 | .0034 | .1521 | .0583 | .4523 | 1.0000 | .0347 | .1302 | .1300 | −.0002 |
| (12) | .1124 | .0320 | .0238 | .0970 | .0908 | .0104 | .0085 | .0383 | .0326 | .0364 | .0121 | 1.0000 | .2111 | .2110 | −.0001 |
| | | | | | | | | | | | | | Value of determinant | | =.76978 |
| Correct $x$'s | .0820 | .0535 | .1145 | .1050 | .0970 | .0480 | .0320 | .1500 | .0680 | .0090 | .0725 | .1685 | *Times* | | |
| | | | | | | | | | | | | | To set matrix (Prorated over 10 solutions) | | 3.6 min. |
| | | | | | | | | | | | | | To set $m$'s | | 3.0 min. |
| Electric computer $x$'s | .0816 | .0532 | .1143 | .1050 | .0966 | .0481 | .0320 | .1502 | .0680 | .0090 | .0723 | .1685 | To balance | | 2.0 min. |
| | | | | | | | | | | | | | To read $x$'s | | 3.0 min. |
| | | | | | | | | | | | | | Total average time per solution | | 11.6 min. |
| $\Delta x$ | −.0004 | −.0003 | −.0002 | 0 | −.0004 | .0001 | 0 | .0002 | 0 | 0 | −.0002 | 0 | Time by conventional calculator method | | 80 min. |

paper. In general, however, each new set of coefficients must be separately investigated.[5,6,9] Some of the unknowns in a single problem may be accurately determined, while others may be very sensitive to small variations in either $a$'s or $m$'s. In routine calculation on a conventional calculator such as the Marchant, Friden, or Monroe, it is often necessary to carry a large number of decimal places[5,9] during the solution of simultaneous equations to obtain three or four figure accuracy in the answers, assuming the coefficients subject to no error. If coefficients are accurate to only four decimal places the unknowns may be accurate to only two or three decimal places, *regardless of how many places* are carried in intermediate steps. Generally, if upon substitution of the values of the unknowns back in the original equations, the resulting constant terms differ from the actual constant terms used by amounts comparable to the possible uncertainties in those constant terms, then the errors in the unknowns are those inherent in the data and no improvement can be made by any method of computation.

The design of the commercial computer shown in Fig. 5 is such that numbers from 0.0000 to 0.1000 can be set to about ±0.0001, and numbers from 0.1000 to 1.0000 can be set to one part in a thousand (or better) of the value being set. The values of the $x$'s can be read with the same accuracy; however, the absolute accuracy of the $x$'s, as pointed out before, depends in large measure upon the particular set of equations in question.

There is a close connection between the inherent accuracy of solution and the nearness to singularity of the set of equations. When coefficients of two equations or of two variables in a set of $n$ equations are proportional, the system has a zero determinant and is said to be singular. Two of the variables or relations are then dependent, and a unique solution for the $n$ variables cannot be obtained. If the coefficients in two rows or two columns of the determinant are nearly proportional the system is nearly singular, and some of the $x$ values will be very sensitive to changes in certain of the $a$'s and $m$'s. In this case more cycles of iteration will be required in the solution and the system may be said to have poor "leverage." The size of the determinant will usually be an index of this characteristic when the $a$'s are positive. For example, consider two sets of equations:

| A | B |
|---|---|
| $1.00x_1+0.10x_2=0.50,$ | $1.00x_1+0.90x_2=0.50,$ |
| $0.10x_1+1.00x_2=0.50,$ | $0.90x_1+1.00x_2=0.50,$ |
| Determinant = 0.99; | Determinant = 0.19. |

The leverage of system A is better than that of system B.

TABLE II. Accuracy and time of electric computer solution of equations used to analyze a $C_2$ through $C_5$ paraffin-olefin mixture from mass spectrometer data.

| Mass | Pentenes | *Iso*-pentane | *N*-pentane | Propane | Ethane | *N*-butane | *Iso*-butane | Ethylene | Propene | Butene-1 | *Iso*-butene | Butene-2 | $m$ | $m_{ec}$ | $\Delta m$ |
|---|---|---|---|---|---|---|---|---|---|---|---|---|---|---|---|
| 70 | 1.0000 | .0021 | .0032 | 0 | 0 | 0 | 0 | 0 | 0 | 0 | 0 | 0 | .0090 | .0088 | −.0002 |
| 57 | .0017 | 1.0000 | .3595 | 0 | 0 | .0580 | .0912 | 0 | 0 | .0374 | .0440 | .0444 | .0476 | .0476 | 0 |
| 72 | 0 | .4727 | 1.0000 | 0 | 0 | 0 | 0 | 0 | 0 | 0 | 0 | 0 | .0098 | .0096 | −.0002 |
| 44 | 0 | .1033 | .1619 | 1.0000 | 0 | .1437 | .1774 | 0 | .0072 | .0020 | .0006 | .0017 | .1524 | .1524 | 0 |
| 30 | .0355 | .0316 | .0274 | .0810 | 1.0000 | .0422 | .0067 | .0051 | 0 | .0233 | .0233 | .0281 | .0408 | .0408 | 0 |
| 58 | 0 | .1412 | .0500 | 0 | 0 | 1.0000 | .2966 | 0 | 0 | .0027 | .0016 | .0026 | .1394 | .1394 | 0 |
| 43 | .0134 | .5920 | .9255 | .1507 | 0 | .8076 | 1.0000 | 0 | .0127 | .0008 | .0013 | .0009 | .3122 | .3123 | .0001 |
| 26 | .1446 | .0702 | .0903 | .1917 | .5226 | .1498 | .0667 | 1.0000 | .1770 | .1089 | .2135 | .2365 | .1758 | .1756 | −.0002 |
| 42 | .7143 | .9620 | 1.0000 | .0708 | 0 | .1836 | .6274 | 0 | .6566 | .0415 | .0440 | .0369 | .3590 | .3587 | −.0003 |
| 41 | .4143 | .6010 | .5525 | .1198 | 0 | .3299 | .5466 | 0 | .6763 | 1.0000 | .9845 | .9007 | .6218 | .6215 | −.0003 |
| 56 | .1027 | .3069 | .0618 | 0 | 0 | .0168 | .0101 | 0 | 0 | .8214 | .9774 | 1.0000 | .2889 | .2890 | .0001 |
| 55 | 1.0000 | .0337 | .0301 | 0 | 0 | .0090 | .0051 | 0 | 0 | .1403 | .1275 | .1594 | .0541 | .0539 | −.0002 |
| | | | | | | | | | | | | | Value of determinant | | =.00306 |
| | | | | | | | | | | | | | *Times* | | |
| $x$ | .0090 | .0080 | .0060 | .0980 | .0200 | .0700 | .2270 | .0150 | .2510 | .0680 | .0950 | .1330 | To set matrix (prorated over 10 solutions) | | 3.6 min. |
| $x_{ec}$ | .0088 | .0080 | .0058 | .0980 | .0200 | .0700 | .2273 | .0148 | .2507 | .0672 | .0956 | .1332 | To set $m$'s | | 3.0 min. |
| | | | | | | | | | | | | | To balance | | 9.0 min. |
| | | | | | | | | | | | | | To read $x$'s | | 3.0 min. |
| | | | | | | | | | | | | | Total average time per solution | | 18.6 min. |
| $\Delta x$ | −.0002 | 0 | −.0002 | 0 | 0 | 0 | .0003 | −.0002 | −.0003 | −.0008 | .0006 | .0002 | Time by conventional calculator method | | 80 min. |

In the examples which follow, the value of the determinant is given as an approximate index of the leverage of each system. Usually, the larger determinants are associated with better leverage and hence with better accuracy and a shorter time for solution.

It is interesting to note that the computer can be used to compute reciprocal matrices or inverses, using the method described by Fisher.[10] The Fisher method involves solving $n$ sets of $n$ equations each to obtain the $n$ columns of the inverse. Here again the intrinsic "leverage" is a substantial factor in determining accuracy. Where greater accuracy is desired in the inverse, the matrix obtained on the electric computer can be used as an initial approximation. Then iterative methods employing either a calculating machine or combining the calculating machine and electric computer can be used to improve the accuracy.

In order to explore the possibilities of the computer alone without auxiliary computation a large number of problems have been solved on a 12-equation model. The results shown in Tables I–IV illustrate the accuracy which has been obtained in solving various typical problems. In Tables I–III, the coefficients, $a_{ij}$, and the constant terms, $m_i$, are tabulated. The three rows beneath this matrix show, respectively, the answers obtained on an 8-bank calculator, the electric computer answers, and the difference between the two, $\Delta x$. Two additional columns are

TABLE III. Accuracy and time of electric computer solution of equations involving both positive and negative coefficients and constant terms.

| Equation No. | $x_1$ | $x_2$ | $x_3$ | $x_4$ | $x_5$ | $x_6$ | $x_7$ | $x_8$ | $m$ | $m_{ec}$ | $\Delta m$ |
|---|---|---|---|---|---|---|---|---|---|---|---|
| (1) | 1.0000 | −.0811 | .0414 | .0018 | .0090 | 0 | 0 | −.0476 | .0925 | .0925 | 0 |
| (2) | −.1290 | 1.0000 | .5280 | −.4650 | .4170 | .2910 | 0 | .0342 | −.1654 | −.1654 | 0 |
| (3) | 0 | −.2980 | 1.0000 | 0 | 0 | 0 | 0 | 0 | .0927 | .0927 | 0 |
| (4) | .0106 | .0207 | −.0312 | 1.0000 | .7100 | −.6650 | 0 | .0012 | .0777 | .0779 | .0002 |
| (5) | .0035 | .0270 | .0082 | .8850 | 1.0000 | −.6400 | 0 | .0004 | .0884 | .0885 | .0001 |
| (6) | .0700 | −.0631 | .0854 | .9650 | −.8850 | 1.0000 | .4530 | .0227 | .0741 | .0738 | −.0003 |
| (7) | −.0870 | .2170 | .3350 | −.0958 | .1005 | .0784 | 1.0000 | −.0532 | .1505 | .1505 | 0 |
| (8) | .2380 | .3630 | −.8390 | .0050 | .0044 | .0021 | .0440 | 1.0000 | .3041 | .3041 | 0 |
| | | | | | | | | | Value of determinant | | =.59314 |
| | | | | | | | | | *Times* | | |
| $x$ | .0930 | −.1870 | .0370 | .0258 | .0518 | −.0282 | .2060 | .3715 | To set matrix (prorated over 10 solutions) | | 1.6 min. |
| $x_{ec}$ | .0930 | −.1869 | .0370 | .0258 | .0516 | −.0286 | .2060 | .3715 | To set $m$'s | | 2.0 min. |
| | | | | | | | | | To balance | | 8.0 min. |
| | | | | | | | | | To read $x$'s | | 2.0 min. |
| $\Delta x$ | 0 | .0001 | 0 | 0 | −.0002 | .0004 | 0 | 0 | Total average time per solution | | 13.6 min. |

TABLE IV. Accuracy and time for solution of equations in spectrometric analysis of typical hydrocarbon mixtures. The components are different for the different columns, ranging from preponderantly butanes and butenes to all pentanes and hexanes.

| Infra-red $C_4$ | | $C_5$, $C_6$ | $C_3-C_5$ | $C_2-C_5$ | $C_4-C_6$ | $C_5''-C_5''$, CP | $C_4''$, $C_5''$ |
|---|---|---|---|---|---|---|---|
| | 0 | 0 | .0002 | 0 | −.0001 | .0032 | −.0003 |
| | .0002 | −.0005 | 0 | −.0001 | 0 | −.0042 | −.0057 |
| | −.0003 | .0003 | .0003 | .0001 | 0 | .0002 | −.0056 |
| | .0001 | .0002 | .0019 | −.0005 | .0002 | −.0005 | −.0058 |
| | .0001 | −.0003 | −.0020 | .0002 | .0001 | 0 | .0179 |
| | .0004 | −.0003 | .0001 | .0007 | .0010 | .0013 | −.0005 |
| | .0001 | −.0005 | −.0001 | −.0010 | −.0003 | .0033 | −.0001 |
| | .0002 | .0002 | 0 | −.0003 | −.0009 | −.0039 | .0003 |
| Max. error | .0004 | .0005 | .0020 | .0010 | .0010 | .0042 | .0179 |
| Mean error | .0002 | .0003 | .0006 | .0004 | .0003 | .0021 | .0045 |
| Value of determinant | .78908 | .05931 | .02891 | .02221 | .00590 | .00080 | .00020 |
| Time to balance (min.) | 4 | 8 | 8 | 10 | 11 | 13 | 20 |
| Time to balance using $k$-method (after computation of $k$'s) | | | | 10 min. | | | |

given. The $m_{ec}$ column is the result of substituting the electric computer answers into the original equations, using an 8-bank calculator. The $\Delta m$ column shows the difference $(m-m_{ec})$ between these values and the actual constant term column used.

Table I illustrates a typical 12-equation system with large diagonal terms and a fairly large determinant. This set required only 5 cycles (2 minutes) to converge. The accuracy, as would be expected, is good, all errors in $x$'s being 0.0004 or less, compared with a total of 1.0000 for the sum of all the $x$'s.

Table II shows a mass spectrometer analysis for a 12-component hydrocarbon mixture including all paraffins from ethane through *iso*-pentane and a number of olefins through $C_5$. Coefficients in the last three columns are nearly proportional, so that errors in the last three variables are larger than in the others. Even so, the errors in these variables are in the fourth decimal place. The largest error is only 0.08 mole percent.

The fact that the $m$'s check to 0.0003 or better indicates that the electric computer errors are equivalent to errors of this magnitude in the original data. Thus again the $x$ errors are of the same order of magnitude as those which would be expected in a physical problem if the $m$ data were subject to error in the fourth place.

A problem similar to those encountered in aircraft structural analysis, involving some negative constant terms and some negative $a$'s, is given in Table III. Positive or negative $m$'s can be set, and positive or negative $x$'s read. Means of pre-setting positive and negative $a$'s can be built into the computer if desired, but with the present computer a change of sign in an $a_{ij}$ value is accomplished by changing the sign of its associated $x$ on switching to a new equation. Otherwise the method of balancing is the same as in the case of positive coefficients.

Table IV summarizes the results of solving seven different sets of eight equations each. In each of these problems a hydrocarbon mixture is analyzed, the first from infra-red data and the remaining 6 from mass spectrometer data. Hence all $a$'s are positive. The error in each component, the maximum error, the average error, and the time for solution are shown. The value of the determinant is given as a general leverage index. As would be anticipated from the fact that different variables are widely different in their response to changes in the coefficients, accuracies in the values of some unknowns are much higher than in others. However, the time of solution and the average error decrease fairly systematically as the determinant increases, as would be expected.

The computer is not, of course, limited to solving sets of 12 equations. Any number up to 12 may also be handled.

## SPEED

The speed of operation of a computer chiefly determines its advantages over conventional

methods of calculation. In the computer described a large saving of time is effected, which becomes more and more apparent as the number of equations to be solved increases. For example, a reasonably expert calculator would require nearly 5 hours (assuming no errors) to solve by conventional machine methods the set of 12 equations given in Table I, as compared with 44 minutes for the first solution on the electric computer. In other words, only 1/7 as much time would be required when using the computer.

In Tables I–III, times of solution are given in which the time for setting the coefficients has been prorated over ten different solutions. The reason for this is that in many applications (e.g., hydrocarbon mixture analysis) a number of mixtures involving the same components are solved successively. Hence the same coefficients are used a number of times with different constant terms. To obtain a realistic picture of the times involved some such weighting is therefore necessary. The comparable average figure for solving 10 sets of 12 equations each involving the same coefficients on a calculator is about 80 minutes per set. The computer times are only $\frac{1}{4}$ to 1/7 the times required by a calculator.

The times given in Table IV are only those required for balancing and are nearly proportional to the number of iterative cycles. It is interesting to note the relation illustrated here between the value of the determinant and the time for balancing; as the determinant increases the time decreases.

One of the primary factors contributing to the speed of the computer is the fact that each of the coefficients is handled only once—when it is originally set on its corresponding potentiometer. This is in contrast to conventional methods in which the operator has to set many more than $n^2+n$ numbers on the keyboard and also has to write down intermediate results. Eliminating these intermediate steps eliminates also one of the most common sources of error in conventional methods of solution.

In addition a relatively unskilled operator usually finds it simpler to adjust dials to obtain a null than to operate a calculating machine, so that facility can be acquired in a very short time. If the wrong dial is turned during the balancing operation, the iterative method compensates for the mistake. Although a few extra cycles may be necessary in this case, the final answer is still correct. So long as the $a$'s and $m$'s are initially set correctly, nulls on all equations indicate that the correct solution has been obtained, regardless of the intermediate steps taken. Thus not only the probability of errors, but also their adverse consequences are reduced to a minimum.

Further time saving results from the fact that each operation is brief. To set each coefficient, $a_{ij}$, and each constant term, $m_i$, requires about $\frac{1}{4}$ minute. The time to balance the equations by successive iterative cycles varies with the intrinsic leverage of the equations and also with the order of equations and unknowns which is chosen for balancing. One cycle for nine equations requires about one minute. The time to read each unknown is less than $\frac{1}{4}$ minute.

In using the $K$-method the time required to solve a given set of equations depends only upon the number of equations, since the method is direct rather than iterative.

To compute $K$'s for eight equations takes about 38 minutes, after which use of the $K$'s in the solution requires about 10 minutes. This figure can be compared with the times shown in Table IV for balancing by the iterative method. The $K$-method is particularly useful in those cases in which convergence is slow and where the order in which variables and equations should be placed is not immediately evident. Usually, if the set of equations can be arranged to converge fairly rapidly, the iterative method is more rapid than the $K$-method.

## CONCLUSION

The computer described may be applied in almost any field in which simultaneous linear equations must be solved. The fact that it can be used on either symmetric or non-symmetric matrices extends its application to many engineering fields. For instance, some problems arising in aircraft structural design have been solved.

In the field of statistics, it is believed that it will prove highly useful not only in solving equations, but also in providing an initial approximation to reciprocal matrices.

It is now being used with eminent success in

the field of hydrocarbon analysis with the mass spectrometer and infra-red spectrophotometer. Here, its accuracy is more than adequate, and its speed is far greater (in many cases by a factor of 5 or more) than that of conventional methods.

The authors wish to acknowledge the fine work of Mr. J. C. Pemberton, who engineered the commercial model of the computer, and of Miss Dorothy Comaford, who accumulated the data given in the tables. The authors also wish to thank Consolidated Engineering Corporation for permission to publish this material.

## BIBLIOGRAPHY

(1) C. H. Ward, U. S. Patent 1,893,009, Jan. 3, 1944.
(2) R. R. M. Mallock, "Electrical calculating machine," Proc. Roy. Soc. London **140**, 457–482 (1933).
(3) O. Wilbur, "The mechanical solution of simultaneous equations," J. Frank. Inst. **222**, 715–724 (1936).
(4) T. D. Morgan and F. W. Crawford, "Time saving computing instruments designed for spectroscopic analysis," Oil Gas J., pp. 100–105 (August 26, 1944).
(5) H. Hotelling, "Some new methods of matrix calculation," Ann. Math. Stat. **14**, 1–34 (1943).
(6) F. E. Satterthwaite, "Error control in matrix calculation," Ann. Math. Stat. **15**, No. 4, 373–387 (1944).
(7) R. von Mises and Hilda Pollaczek-Geiringer, "Zusammenfassende Berichte. Praktische Verfahren der Gleichungsauflosung," Zeits. f. angew. Math. Mechanik **9**, 58–77, 152–164 (1929).
(8) C. E. Berry, "A criterion of convergence for the classical iterative method of solving linear simultaneous equations," Ann. Math. Stat. **16**, 398–400 (1945).
(9) L. A. Tuckerman, "On mathematically significant figures in the solution of simultaneous linear equations," Ann. Math. Stat. **12**, 307 (1941).
(10) R. A. Fisher, *Statistical Methods for Research Workers* (Oliver and Boyd, Ltd., London, 1938), seventh edition.

Other pertinent references not mentioned in the text are:

A. C. Aitken, "Evaluation of determinants, formation of their adjugates, and practical solution of simultaneous linear equations," Proc. Edin. Math. Soc. [2] **3**, 207 (1932–33).
A. C. Aitken, "Studies in practical mathematics," Proc. Roy. Soc. Edin. **57**, 269 (1937).
A. T. Lonseth, "Systems of linear Eq. with coeff. subject to error," Ann. Math. Stat. **13**, 332–337 (1942).
R. A. Frazer, W. J. Duncan, and A. R. Collar, *Elementary Matrices and Some Applications to Dynamics and Differential Equations* (Cambridge University Press, London, 1938).

# The Thin Cylindrical Antenna: A Comparison of Theories

DAVID MIDDLETON AND RONOLD KING
*Cruft Laboratory and the Research Laboratory of Physics, Harvard University, Cambridge 38, Massachusetts*
(Received November 17, 1945)

The solutions of Hallén's integral equation for the cylindrical antenna given by Hallén, Bouwkamp, Gray, King and Middleton are compared. Comparison is also made with the transmission-line theory of Schelkunoff and with experiment.

## I. INTRODUCTION

BECAUSE of its great practical importance the antenna has been the subject of much analysis and discussion. In particular, considerable effort has been devoted to the thin, cylindrical antenna, and much has been written in the attempt to bring theory and experiment into closer agreement, and to give reliable theoretical results for such important and difficult-to-measure quantities as the input impedance and the distribution of current. Summaries are given by Brillouin[1] and by R. King and D. D. King.[2]

To determine the input impedance one must first establish the distribution of current. This is rigorously a three-dimensional problem, but in the case of thin antennas, where the thickness is a negligible fraction of a wave-length, a one-dimensional analysis suffices. A powerful approach has been suggested by Hallén,[3] who obtains an integral equation involving the current as a solution of the one-dimensional wave equation for the vector potential. Recently King and Blake[4] and King and Harrison,[5] using Hallén's method, have given detailed computations for the input impedance and current distribution. Since agreement with the limited available experimental data was not particularly good, a more careful study of the experimental problem,[2,6] and a more critical examination of theory[1,2,7] was begun. Hallén's integral-equation method appears to be physically sound for thin antennas. The difficulties lie in the method of solution and in the assumptions made in going from the actual physical problem to the simplified one of the analysis.[2] A modified form of solution has been suggested by Gray,[8] to bring the theoretical values of impedance more in line with the limited existing experimental ones, and with the theoretical values obtained by S. A. Schelkunoff,[9] who employs a different approach to the problem. More recently, the authors have achieved a solution[10] which, it is believed, is superior to previous attempts.

It is the purpose, then, of this paper to compare the theories developed by (1) Hallén-Bouwkamp,[11] (2) Gray,[8] and (3) King-Middleton,[10] and to discuss the various solutions from theoretical and experimental points of view.[2,12] A brief outline of the principal analyses follows.

## II. ANALYSIS

The fundamental integral equation for the current, obtained originally by Hallén and containing the vector potential $A_z$, is

$$\int_{-h}^{h} I_{z'}\frac{\exp(-j\beta R_1)}{R_1}dz' = \frac{-4\pi j}{R_c}\left[C_1\cos\beta z+\tfrac{1}{2}V_0^e\sin\beta|z| - z^i\int_0^z I(s)\sin\beta(z-s)ds\right]=\frac{4\pi A_z}{\text{II}}, \quad (1)$$

with

$$R_1=((z-z')^2+a^2)^{\frac{1}{2}}, \quad \beta=2\pi/\lambda=\frac{2\pi f}{c}, \quad (2)$$

[1] L. Brillouin, Elect. Comm. **21**, No. 4, **22**, No. 1.
[2] R. King and D. D. King, J. App. Phys. **16**, 445 (1945).
[3] E. Hallén, Nova Acta, Roy. Soc. Uppsala **11**, 1 (1938); see also C. W. Oseen, Arkiv. f. Mat. Astr. Fysik **9**, No. 12, No. 30 (1913).
[4] R. King and F. G. Blake, Proc. I.R.E. **30**, 335 (1942).
[5] R. King and C. W. Harrison, Jr., Proc. I.R.E. **31**, 548 (1943).
[6] D. D. King, J. App. Phys. **16**, 435 (1945).
[7] R. King and C. W. Harrison, Jr., J. App. Phys. **15**, 170 (1944).
[8] M. C. Gray, J. App. Phys. **15**, 61 (1944).
[9] S. A. Schelkunoff, Proc. I.R.E. **29**, 493 (1941); J. App. Phys. **15**, 54 (1944).
[10] R. King and D. Middleton, Quart. App. Math. **3**, 302 (1946).
[11] C. J. Bouwkamp, Physica **9**, 609 (1942).
[12] G. H. Brown and O. M. Woodward, Proc. I.R.E. **33**, 257 (1945).

and where $V_0^e$, $R_c$ and $z^i$ are, respectively, the applied potential difference maintained by a "slice" generator[2] at $z=0$, a characteristic resistance $R_c=120\pi=376.7$ ohms, and the internal impedance per unit length of the antenna. For good conductors $z^i$ is sufficiently small so that the term involving $z^i$ may be dropped in (1) with negligible error.[4] $C_1$ is a constant of integration determined from the boundary condition that requires the current to be zero at the ends $z=\pm h$. II is $4\pi\cdot10^{-7}$ henry/m, and $a$ is the radius of the antenna. The general $m$th order solution for the currents in (1) may then be obtained in the form of a series[3-5, 7, 8, 10, 11]

$$(I_z)_m=\frac{j2\pi V_0^e}{R_c\Psi}\left\{\frac{\sin\beta(h-|z|)+\sum_{n=1}^{m}M_n(z)/\Psi^n}{\cos\beta h+\sum_{n=1}^{m}F_n(h)/\Psi^n}\right\},$$
$$-h\leq z\leq h,\quad h^2\gg a^2, \tag{3}$$

where $\Psi$ is an appropriately chosen expansion parameter, defined by

$$\Psi\equiv|\Psi(z_0)|, \tag{4}$$

with $z_0$ a suitably selected point on the antenna. The function $\Psi(z)$ may be obtained from

$$\Psi(z)=\int_{-h}^{h}g(z,z')\frac{\exp(-j\beta R_1)}{R_1}dz'\equiv\Psi+\gamma(z), \tag{5}$$

and $\gamma(z)$ is defined by

$$\gamma(z)\equiv\Psi[\exp(j\theta_\psi)-1]. \tag{6}$$

Here $g(z,z')$ is a quantity whose character depends on the assumptions made for the distribution of current along the antenna. If $\Psi(z)$ is predominantly real, $\gamma(z)$ is a small complex correction function except at values of $z$ where $I_z$ is small or zero. It is to be noted that $\gamma(z)$ is infinite at $z=\pm h$ but that $I_z\gamma(z)$ is small and finite there. It is also possible that $\Psi(z)$ be entirely real; (see Eq. (17) following). Under these circumstances one may still write (5), but (6) no longer applies; $\gamma(z)$ may then be considered as a small, *real* correction factor, except at points where $I_z$ approaches zero.

By definition $M_n(z)$ is the coefficient of $\Psi^{-n}$ in

$$\sum_{n=0}^{m}F_{nz}/\Psi^n\cdot\sum_{n=0}^{m}G_n(h)/\Psi^n-\sum_{n=0}^{m}G_{nz}/\Psi^n\cdot\sum_{n=0}^{m}F_n(h)/\Psi^n, \tag{7}$$

where in particular

$$M_1(z)\equiv M_1^{\mathrm{I}}(z)+jM_1^{\mathrm{II}}(z)$$
$$=F_1(z)\sin\beta h-F_1(h)\sin\beta|z|+G_1(h)\cos\beta z-G_1(z)\cos\beta h, \tag{8}$$

$$M_2(z)\equiv M_2^{\mathrm{I}}(z)+jM_2^{\mathrm{II}}(z)$$
$$=F_2(z)\sin\beta h-F_2(h)\sin\beta|z|+G_1(h)F_1(z)-G_1(z)F_1(h)+G_2(h)\cos\beta z-G_2(z)\cos\beta h. \tag{9}$$

The $F$- and $G$-functions satisfy the following:

$$F_n(z)=F_{n-1,z}\int_{-h}^{h}g(z,z')\frac{\exp(-j\beta R_1)}{R_1}dz'-\int_{-h}^{h}F_{n-1,z'}\frac{\exp(-j\beta R_1)}{R_1}dz'-F_{n-1,z}\gamma(z), \tag{10}$$

with similar expressions for $G_n(z)$ obtained on replacing $F$ by $G$ in (10) above. The quantities $F_{nz}$, $G_{nz}$ are defined, respectively, as $F_{nz}\equiv F_n(z)-F_n(h)$, $G_{nz}\equiv G_n(z)-G_n(h)$, from which it is clear that $F_{nh}=G_{nh}=0$. When $n=0$ one has

$$F_0(z)=\cos\beta z,\quad G_0(z)=\sin\beta|z| \tag{11}$$

for all expansions. The input impedance follows at once from the definition

$$(Z_0)_m\equiv V_0^e/I_z(0)_m=(R_0)_m+j(X_0)_m. \tag{12}$$

### (a) Hallén[3]-Bouwkamp[11] solution

The relative distribution function for the current is taken to be

$$g(z,z')_H=\exp(j\beta R_1), \tag{13}$$

on the assumption that the vector potential $A_z$, in (1), may be evaluated approximately by considering the current at all points to be $I_z$ and neglecting the effects of retardation. The contributions from all points $z'\neq z$ contribute little, so that $A_z$ depends primarily on the current at or near $z$. For this distribution (5) becomes

$$\Psi(z)_H=\sinh^{-1}\left(\frac{h-z}{a}\right)+\sinh^{-1}\left(\frac{h+z}{a}\right), \tag{14}$$

and in particular with $h^2 \gg a^2$

$$\Psi(0)_H = 2 \log \frac{2h}{a} \equiv \Omega. \tag{15}$$

Here the expansion parameter is chosen to be

$$\Psi = \Psi(0)_H = \Omega, \quad z_0 = 0, \tag{16}$$

from (4); $\gamma(z)_H$, a small real quantity, significant only within a few radii $a$ of the ends $z = \pm h$, is

$$\gamma(z)_H = \log \left(1 - \frac{z^2}{h^2}\right) + \delta(z), \tag{17}$$

where

$$\delta(z) = \log \left[\frac{1}{4}\left\{1 + \left(1 + \frac{a^2}{(h+z)^2}\right)^{\frac{1}{2}}\right\} \times \left\{1 + \left(1 + \left(\frac{a}{h-z}\right)^2\right)^{\frac{1}{2}}\right\}\right]. \tag{18}$$

(The subscript $H$ is used throughout this paper to refer to the Hallén-Bouwkamp solution.) Eq. (3) results for the $m$th order current distribution, with $\Psi$ replaced by $\Omega$ and the subscripts $H$ written on $M_n(z)$ and $F_n(h)$. Fairly extensive tables of these functions are available[4, 10, 11] for $n = 1$, $n = 2$, where

$$F_n(h) \equiv \alpha_n \equiv \alpha_n{}^{\mathrm{I}} + j\alpha_n{}^{\mathrm{II}},$$

and

$$M_n(0)^{\mathrm{I}} + jM_n(0)^{\mathrm{II}} \equiv \beta_n = \beta_n{}^{\mathrm{I}} + j\beta_n{}^{\mathrm{II}}, \tag{19}$$

and where general relations for $F_n(z)_H$ are given by

$$F_n(z)_H = (F_{n-1,z})_H \Omega - \int_{-h}^{h} (F_{n-1,z'})_H \frac{\exp(-j\beta R_1)}{R_1} dz', \tag{20}$$

with similar expressions for $G_n(z)_H$, obtained as before by replacing $F$ by $G$ in (20).

The input impedance is at once seen to be

$$(Z_0)_{mH} = \frac{-j\Omega R_c}{2\pi} \left\{ \frac{\cos \beta h + \sum_{n=1}^{m} \alpha_n/\Omega^n}{\sin \beta h + \sum_{n=1}^{m} \beta_n/\Omega^n} \right\}. \tag{21}$$

Hallén's work included the zeroth and first approximations, ($n = 0$, 1), while Bouwkamp extended the solution through the second-order terms ($n = 0$, 1, 2). Curves for the first- and second-order impedances computed from (21) are shown in Figs. 1–4 for $\Omega = 10$, 20.

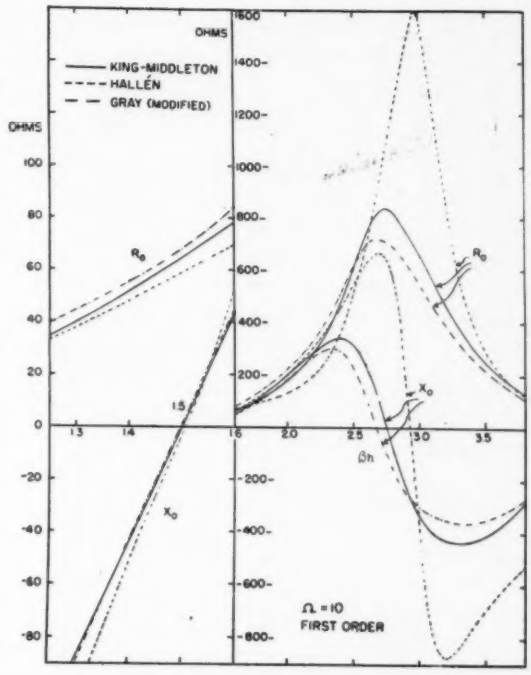


FIG. 1. First-order impedances $Z_0 = R_0 + jX_0$ of cylindrical antenna with $\Omega = 2 \ln 2h/a = 10$.

We give now, in somewhat greater detail as the results are new, a solution based on a distribution function suggested by, but differing in important respects from one introduced by, Gray.[8]

### (b) Modified Gray Solution

In this case $g$ is chosen to be

$$g(z, z')_G = \exp(j\beta R_1) \cos \beta R_1, \tag{22}$$

so that $\Psi(z)_G$ becomes, with the help of (5),

$$\Psi(z)_G = \Psi(z)_H - \mathrm{Cin}\, \beta(h+z) - \mathrm{Cin}\, \beta(h-z), \tag{23}$$

where, as usual,

$$\mathrm{Cin}\, x \equiv \int_0^x \frac{1 - \cos q}{q} dq, \quad \mathrm{Si}\, x \equiv \int_0^x \frac{\sin q}{q} dq. \tag{24}$$

(These and associated functions are considered in detail in the appendix of reference 10.) Instead of setting $z = 0$ as does Hallén, we follow Gray for the moment and use the *average* value of $\Psi(z)_G$ as expansion parameter, *viz.*

$$\Psi_G = \langle \Psi(z)_G \rangle_{\mathrm{Av}} = \frac{1}{2h} \int_{-h}^{h} \Psi(z)_G dz, \tag{25}$$

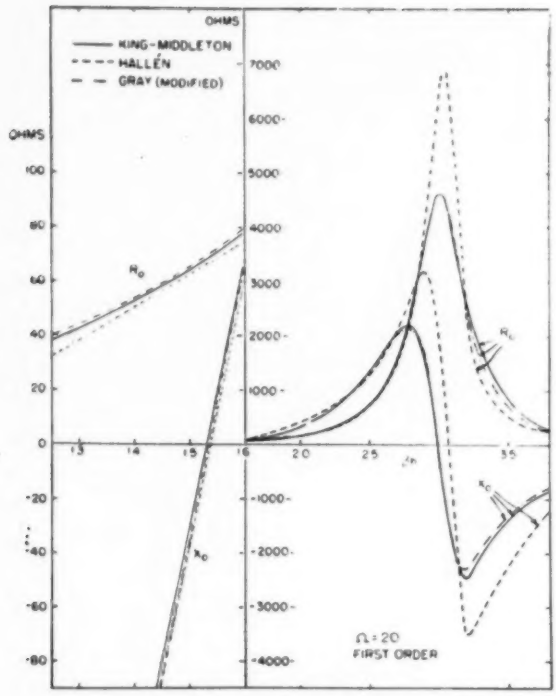


FIG. 2. First-order impedances; $\Omega = 20$.

which integrates to give

$$\Psi_G \equiv \bar{\Omega}_G = \Omega - 2K, \tag{26}$$

where

$$K \equiv \text{Cin } 2\beta h + \frac{\sin 2\beta h}{2\beta h} - \log 2; \quad \gamma(z)_G = 0. \tag{27}$$

Curves showing $\bar{\Omega}_G$ as a function of $\beta h$, with $\Omega$ as parameter, are given in Fig. 5. As in the Hallén solution the value of the current at $z = \pm h$ is subtracted from the fundamental integral Eq. (1), in order that the complete integral solution may vanish for *all* values of $\beta h$ at $z = \pm h$. (See the paragraph following Eq. (18), reference 10.) When this is done, (10) and (22) give the general result

$$F_n(z)_G = (F_{n-1,z})_G \bar{\Omega}_G - \int_{-h}^{h} (F_{n-1,z'})_G \frac{\exp(-j\beta R_1)}{R_1} dz', \tag{28}$$

analogous to (20). Since $F_0(z)_H = F_0(z)_G$, etc., (28) yields at once

$$\begin{aligned} F_1(z)_G &= F_1(z)_H - 2K(F_{0z})_H; \\ F_1(h)_G &= F_1(h)_H; \\ (F_{1z})_G &= (F_{1z})_H - 2K(F_{0z})_H, \end{aligned} \tag{29}$$

and from (29) in (28) there follows for $n = 2$

$$\begin{aligned} (F_{2z})_G &= (F_{2z})_H + 2(-2K)(F_{1z})_H \\ &\quad + (-2K)^2(F_{0z})_H; \end{aligned} \tag{30}$$

$$F_2(h)_G = F_2(h)_H + (-2K)F_1(h)_H.$$

This process may be repeated to give

$$\begin{pmatrix} F_{nz} \\ G_{nz} \end{pmatrix}_G = \sum_{i=0}^{n} \frac{n!}{(n-i)!i!} (\bar{\Omega}_G - \Omega)^i \begin{pmatrix} (F_{n-i,z}) \\ (G_{n-i,z}) \end{pmatrix}_H, \quad n \geq 0, \tag{31}$$

and

$$\begin{pmatrix} F_n(h) \\ G_n(h) \end{pmatrix}_G = \sum_{i=0}^{n-1} \frac{(n-1)!}{(n-1-i)!i!} (\bar{\Omega}_G - \Omega)^i \times \begin{pmatrix} F_{n-i}(h) \\ G_{n-i}(h) \end{pmatrix}_H, \quad n \geq 0, \tag{32}$$

since $-2K = \bar{\Omega}_G - \Omega$, cf. Eq. (26). The functions $M_n(z)_G$ formed from $F$ and $G$ in the manner of (7)–(9) become, in terms of the corresponding Hallén quantities $M_n(z)_H$,

$$M_n(z)_G = \sum_{i=0}^{n} \frac{n!}{(n-i)!i!} (\bar{\Omega}_G - \Omega)^i M_{n-i}(z)_H, \quad n \geqq 0, \tag{33}$$

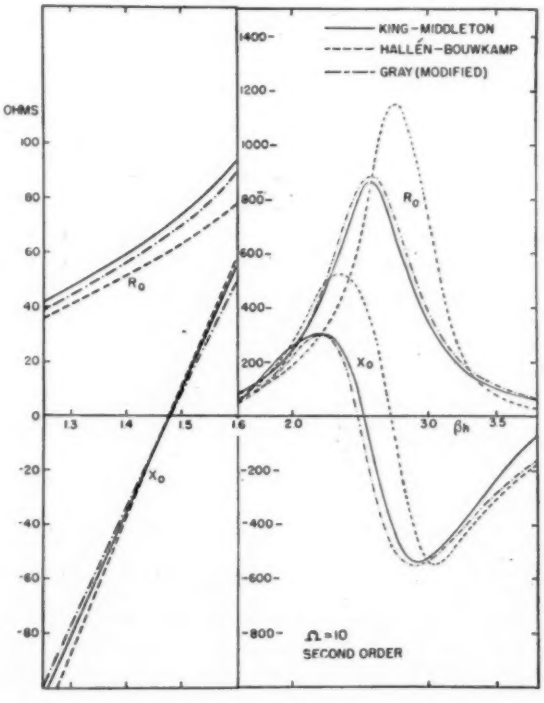


FIG. 3. Second-order impedances; $\Omega = 10$.

where it is understood that

$$M_0(z)_G = M_0(z)_H \equiv \sin\beta(h-|z|). \quad (34)$$

The $m$th order current is obtained in the form (3) after a suitable rearrangement of terms. It becomes finally

$$(I_z)_{mG} = \frac{j2\pi V_0^e}{R_c\bar{\Omega}_G}\left\{\frac{(D_{1,G})_m \sin\beta(h-|z|)+\sum_{n=1}^{m}(D_{n+1,G})_m M_n(z)_H/\bar{\Omega}_G{}^n}{\cos\beta h+\sum_{n=1}^{m}(D_{n,G})_{m-1}F_n(h)_H/\bar{\Omega}_G{}^n}\right\}, \quad (35)$$

where with $y\equiv 1-\Omega/\bar{\Omega}_G$, a table similar to (75), reference 10, may be constructed (see Table I). For a finite number of terms, $m<\infty$, all terms in Table I belonging to a given order $m$ of solution must be retained, and no others. Thus, if an $m$th-order solution is evaluated, only terms contributed by $M_n(z)_G$, $F_n(h)_G$, where $n=0, 1, \cdots, m$ are used. Hence for a first-order theory ($m=1$)

$$(D_{1G})_0=1, \quad (D_{1G})_1=1+\left(1-\frac{\Omega}{\bar{\Omega}_G}\right), \quad (D_{2G})_1=1 \quad (36)$$

only are needed in (35), and for a second-order expansion ($m=2$) only

$$(D_{1G})_2=1+(1-\Omega/\bar{\Omega}_G)+(1-\Omega/\bar{\Omega}_G)^2; \quad (D_{2G})_2=1+2(1-\Omega/\bar{\Omega}_G); \quad (D_{3G})_2=1 \quad (37)$$

are required. Curves of the quantities in (36) and (37) are shown in Fig. 6. When an infinite number of terms ($m\to\infty$) are summed, one observes that

$$(D_{n,G})_{m\to\infty}=\frac{1}{(n-1)!}\frac{d^{n-1}}{dy^{n-1}}\left(\frac{1}{1-y}\right)=\frac{1}{(1-y)^n}=(\bar{\Omega}_G/\Omega)^n, \quad y<1,\ n\geq 1. \quad (38)$$

Then, with the factors $(D_{n,G})_\infty$, (35) becomes identical with the Hallén-Bouwkamp solution for the current and impedance. It is further evident that if the radius $a$ of the antenna becomes vanishingly small, $\bar{\Omega}_G$ approaches $\Omega$ for all values of $\beta h$, so that (35) also approaches the Hallén-Bouwkamp result. The impedance is readily obtained from (12) and (35). It is plotted in Figs. 1–4 for first and second orders. A comparison of the above with Sections V and VI of reference (10) shows that the modified Gray and King-Middleton solutions are formally identical; however, $\bar{\Omega}_G$ and $\Psi_{\text{King-Mid}}$ are in general numerically distinct because of the different assumptions anent the distribution function $g(z, z')$.

### (c) Unmodified Gray Solution[8]

The expansion for the current in this case is obtained with the same value of $g(z, z')$ as for the modified development, cf. Eq. (22), and yields the same expansion parameter $\bar{\Omega}_G$, Eq. (26). However, the generalized formulas for $(F_n)_g$ and $(G_n)_g$ are

$$F_n(z)_g = F_{n-1}(z)_g\int_{-h}^{h} g(z,z')_G\frac{\exp(-j\beta R_1)}{R_1}dz' - \int_{-h}^{h}F_{n-1}(z')_g\frac{\exp(-j\beta R_1)}{R_1}dz', \quad (39)$$

with similar expressions for $G_n(z)_g$. Here the subscript $g$ denotes the unmodified Gray solution. Note that terms involving $F_n(h)_g$ and $G_n(h)_g$ are missing. This occurs because the expression for the current at $z=\pm h$ has not been subtracted from both sides of the fundamental integral Eq. (1) to insure the vanishing of the current at the ends of the antenna for *all* values of $\beta h$. For example, when $\beta h=\pi/2$, the arbitrary constant $C_1$ does not appear in (1) in its present form when $z=\pm h$, and it is not then possible to determine

TABLE I.

| Order $m=$ | 0 | 1 | 2 | 3 | 4 | ⋯ |
|---|---|---|---|---|---|---|
| $(D_{1G})_m$ | 1 | $+y$ | $+y^2$ | $+y^3$ | $+y^4$ | $+\cdots$ |
| $(D_{2G})_m$ | | 1 | $+2y$ | $+3y^2$ | $+4y^3$ | $+\cdots$ |
| $(D_{3G})_m$ | | | 1 | $+3y$ | $+6y^2$ | $+\cdots$ |
| $(D_{4G})_m$ | | | | 1 | $+4y$ | $+\cdots$ |
| ⋮ | | | | | | |
| $(D_{nG})_m$ | | | | | | |

$C_1$ to satisfy the boundary conditions at the ends. As before, it is convenient for purposes of comparison and computation to express the unmodified Gray functions in terms of the (extensively) tabulated Hallén quantities. The results are given in the Appendix.

The $m$th order current distribution becomes, in the present instance

$$(I_z)_{mg}=\frac{j2\pi V_0^e}{R_c\Psi_g(z)}\left\{\frac{\sin\beta(h-|z|)+\sum_{n=1}^{m}M_n(z)_g/\bar{\Omega}_G{}^n}{\cos\beta h+\sum_{n=1}^{m}F_n(h)_g/\bar{\Omega}_G{}^n}\right\}, \tag{40}$$

where from (5) and (22)

$$\Psi(z)_g=\int_{-h}^{h}\frac{\cos\beta R_1}{R_1}dz'=\Psi(z)_H-\text{Cin}\,\beta(h+z)-\text{Cin}\,\beta(h-z).. \tag{41}$$

Although taking $\langle\Psi(z)_g\rangle_{Av}=\bar{\Omega}_G$ as the expansion parameter, Gray *does not replace* $\Psi(z)_g$ *in* (40) *by its average value*. From (12) the $m$th order impedance is seen to be

$$(Z_0)_{mg}=-j60(\Omega-2\,\text{Cin}\,\beta h)\left\{\frac{\cos\beta h+\sum_{n=1}^{m}F_n(h)_g/\bar{\Omega}_G{}^n}{\sin\beta h+\sum_{n=1}^{m}M_n(0)_g/\bar{\Omega}_G{}^n}\right\}, \tag{42}$$

since $R_c/2\pi=60$ ohms. For a first-order solution (42) gives

$$(Z_0)_{1g}=-j60(\Omega-2\,\text{Cin}\,\beta h)\left\{\frac{\cos\beta h+F_1(h)_g/\bar{\Omega}_G}{\sin\beta h+M_1(0)_g/\bar{\Omega}_G}\right\}, \tag{43}$$

while Gray chooses for her solution a combination of first- and second-order terms, to wit,

$$(Z_0)_{3g/2}=-j60(\Omega-2\,\text{Cin}\,\beta h)\left\{\frac{\cos\beta h+F_1(h)_g/\bar{\Omega}_G}{\sin\beta h+M_1(0)_g/\bar{\Omega}_G+[G_1(h)_gF_1(0)_g-F_1(h)_gG_1(0)_g]/\bar{\Omega}_G{}^2}\right\}. \tag{44}$$

This we call the three-halves order solution, inasmuch as the terms in $F_2(h)$, $G_2(h)$, $F_2(0)$, $G_2(0)$ are missing. Curves illustrating (43) and (44) for $\Omega=10$, $\Omega=20$ are shown in Figs. 7 and 8.

### (d) King-Middleton Solution[10]

Here the relative distribution function $g(z,z')_K$ is

$$g(z,z')_K=I_{z'}/I_z$$
$$=\sin\beta(h-|z'|)/\sin\beta(h-|z|), \tag{45}$$

representing the ratio of the *approximate current distributions*, which to the zeroth order are sinusoidal, and to the first order are nearly so.[5,10] The expansion parameter becomes

$$\Psi\equiv\psi=|\Psi(0)_K|=|\psi(0)|/\sin\beta h,\quad \beta h\leq\pi/2$$
$$=|\Psi(h-\lambda/4)_K|=|\psi(h-\lambda/4)|,\quad \beta h\geq\pi/2. \tag{46}$$

The quantity $\psi$ is plotted in Fig. 5 together with $\bar{\Omega}_G$. The point $z=z_0$ of Eq. (4) is thus seen to be zero when $\beta h\leq\pi/2$ and $h-\lambda/4$ for $\beta h\geq\pi/2$. The imaginary part of $\Psi(z)_K$ is always sufficiently small compared with the real part that it may be neglected, except near $z=\pm h$, with the result that $\gamma(z)_K\doteq 0$. A detailed account of the derivation of $\psi$ is given in Section IV, reference 10.

A useful formula for small arguments is

$$\Psi(0)_K=\Omega-2-j\beta h, \tag{47a}$$
$$\psi=|\Psi(0)_K|=\Omega-2+\tfrac{1}{2}\beta h/(\Omega-2) \tag{47b}$$

The function 60 $(\Omega-2)$ is the characteristic impedance used by Schelkunoff.[9] It is seen to be a good approximation for *short* antennas.

As mentioned in (b) the results of the King-Middelton solution are formally identical with those of the modified Gray solution, Eqs. (31)–(38), provided $y=1-\Omega/\bar{\Omega}_G$ is replaced by $x=1-\Omega/\psi$, and $(D_n)_m$ is altered accordingly. The actual results are noticeably different, as can be seen from Figs. 1–4, since $\psi$ and $\bar{\Omega}_G$ are derived using different assumptions.

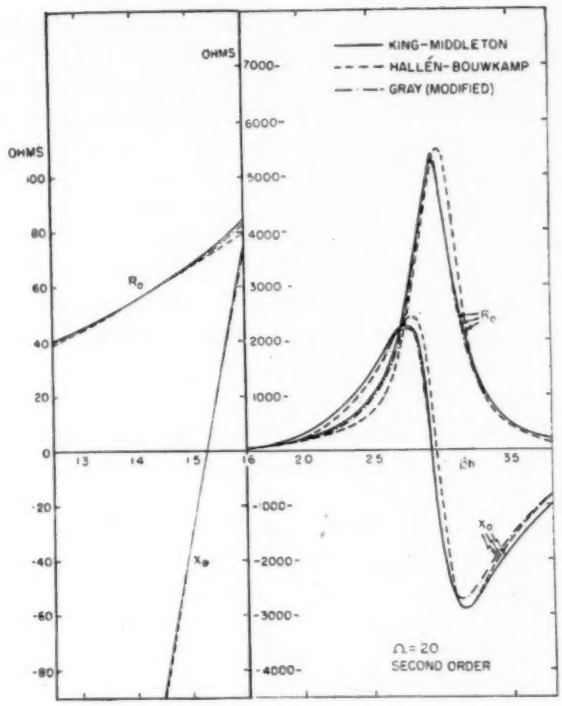


FIG. 4. Second-order impedances; $\Omega = 20$.

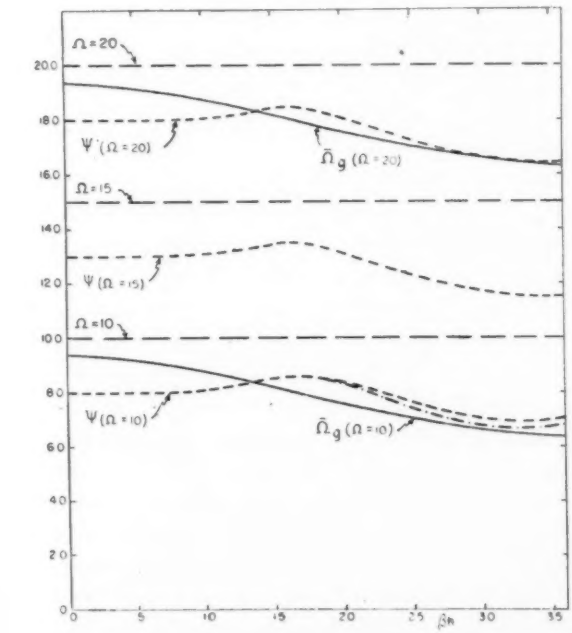


FIG. 5. $\bar{\Omega}_G$ and $\psi$ as functions of $\beta h$.

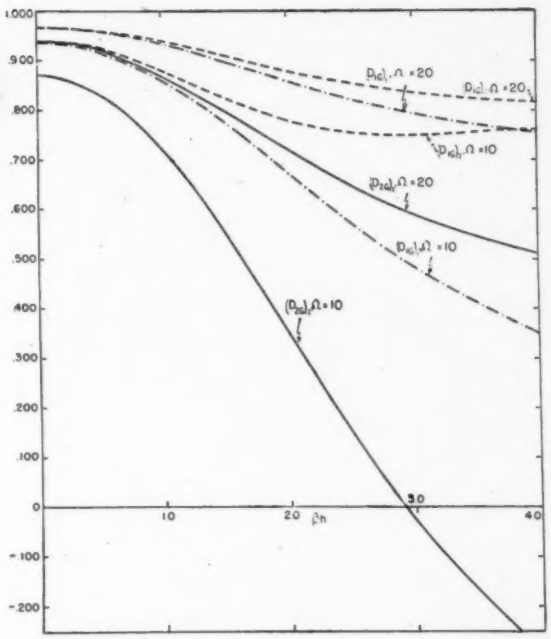


FIG. 6. The functions $D_{1G}$ and $D_{2G}$ defined in Table I.

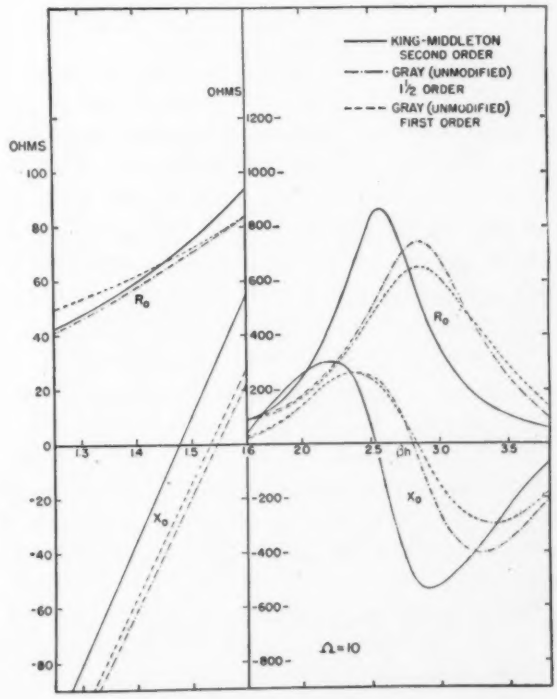


FIG. 7. Impedances according to Gray, $\Omega = 10$.

## III. COMPARISON OF THEORIES AND EXPERIMENT

The broad analytical comparison of the theories of Hallén and Bouwkamp, of Gray, unmodified and modified, and of King and Middleton, reveals that they all solve the identical *mathematical* problem. In all cases the antenna analyzed is the "theoretical antenna"

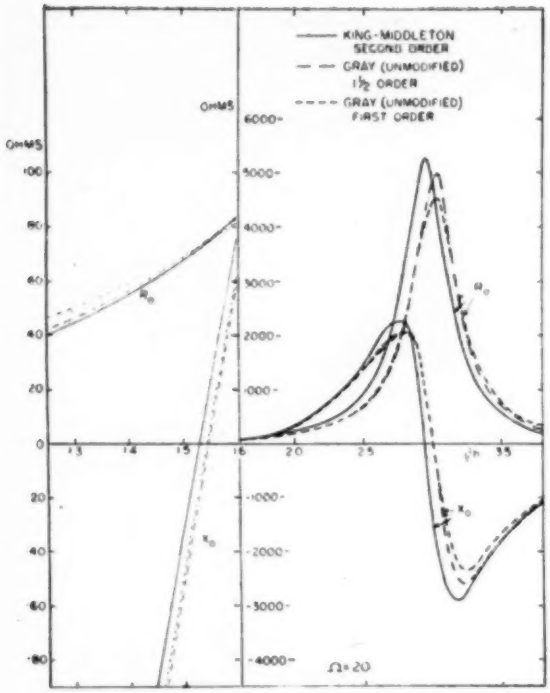


FIG. 8. Impedances according to Gray, $\Omega = 20$.

with its physically unavailable "slice generator," as discussed in an earlier paper.[2] All of the analyses are one-dimensional, all concern themselves with the same integral equation originally set up by Hallén, all follow essentially the same method of expansion in a series. They differ fundamentally only in the choice of function selected to describe approximately the distribution of current under the sign of integration and in the resulting parameter of expansion. All theories give the same results for infinitely thin antennas ($\Omega = \infty$), and all except the unmodified Gray reduce to the same form if an infinite number of terms is used. The unmodified Gray solution differs in this one respect as a result of a peculiar inconsistency in the use of the expansion parameter.

From the practical point of view that theory is most satisfactory which converges most rapidly, other things being equal. In particular it should converge sufficiently rapidly so that at least a second-order solution is a good approximation. Because of the intricacy of the series it has thus far not been possible to determine the rapidity of convergence by direct tests. There remains, however, the obvious fact that the better the original approximation for the current under the sign of integration the more rapid must be the convergence. On this basis the King-Middleton theory is unique in that *it alone actually approximates the distribution of current* in expanding the integral. In effect, the Hallén-Bouwkamp analysis assumes a current of uniform amplitude along the entire antenna equal to that at the point of calculation. It also neglects retardation. The modified and unmodified Gray theories assume a distribution given by $\cos \beta R$ with $R$ measured from the point of calculation. Retardation is also neglected. Neither of these assumptions is even remotely related to the *actual* distribution. The King-Middleton theory, on the other hand, uses in the integrand the actual zeroth order distribution of current common to all theories and also takes retardation into account. The Hallén-Bouwkamp theory is the simplest and the crudest because the expansion parameter $\Omega$ turns out to be independent of $\beta h$. The Gray formulation, while it represents the current no better than does the Hallén form, leads to an expansion parameter that is a function of $\beta h$ as well as of $h/a$ and thereby achieves a better approximation. Finally, the King-Middleton theory, by fitting the current quite accurately, obtains a still better expansion parameter that is actually an excellent approximation of a quantity proportional to the magnitude of the ratio of vector potential to current along the antenna. This ratio has only a very small imaginary part and is sensibly constant over the entire length of the antenna except near and at the ends, where it becomes infinite. Of the three solutions, the King-Middleton form is without question the most refined and it should, therefore, be in better agreement with the results of properly arranged experiments.

Before considering a comparison of theory with experiment, a few remarks must be made regarding the *unmodified* Gray solution. This was presumably originally intended to bring Hallén's theory into better agreement with the theory of Schelkunoff. In view of this purpose, Miss Gray did not take full advantage of the superiority of her parameter of expansion over that of Hallén. In particular, while introducing an *average value* of the expansion parameter in all integrals, she retained the value *at the origin*

as a principal common factor in the expression for the impedance. Thus the unmodified Gray solution actually uses *two* parameters, whereas the modified Gray form uses consistently the average value throughout. As a further but much less important difference, in the modified Gray form, the solution at $z=h$ is subtracted from that at $z=0$. This was not done by Miss Gray. Superficially, this subtraction appears to be an important and necessary step since without it the constant of integration disappears from the solution whenever $\beta h=\frac{1}{2}(2n+1)\pi$, $n=0, 1, 2\cdots$. Actually, in the expanded form, the constant of integration occurs in higher order terms, so that its evaluation is nevertheless possible. A final and seemingly quite unjustified step in the original Gray solution is the addition of only a part of the second-order term to the first-order solution *without any investigation of the relative magnitudes of the two parts*. The term so retained (in the words of Miss Gray) "is not negligible numerically compared with the preceding [first-order] term and it seems advisable to make the current as nearly zero as possible at the ends of the antenna." Actually there is no reason whatever to suppose that the omitted part of the second-order term is negligible or even smaller than the part retained. Indeed, it might possibly be the negative of the part retained. The argument that part of the term must be kept "to make the current as nearly zero as possible at the ends of the antenna" is peculiarly inapplicable because the current as given by Miss Gray's own formula (Eq. (11), reference 8) *is always zero* at the ends with or without the term.

In order to facilitate intercomparison of the several theories, curves showing anti-resonant and resonant resistances, anti-resonant and resonant shifts in $\beta h$, respectively, from $\pi$ and $\pi/2$, and resistances and reactances at $h=\lambda/4$, are given in Figs. 9–13 for both first- and second-order solutions. In the unmodified Gray theory no complete second-order solution is available. Instead the solution of Miss Gray involving only half of the second-order solution is given and marked $1\frac{1}{2}$ order. Its significance is questionable until the complete second order is determined.

First- and second-order solutions differ from each other not only in magnitude of resistance and reactance but also in the magnitude of the shift to shorter lengths of the entire impedance curves. As a result, a simple and clear-cut comparison of convergence by determining the difference between first and second order values is meaningful only for the magnitudes of the resistances at anti-resonance. From Fig. 9 it is clear that first- and second-order solutions agree quite closely in the King-Middleton theory, almost as well in the *modified* Gray theory, and rather poorly in the Hallén-Bouwkamp solution. This is as predicted above from a consideration of the refinements of the several theories. At $\Omega=15$, for example, the difference between first- and second-order anti-resonant resistances is approximately 6 percent for the King-Middleton theory, 9 percent for the modified Gray theory, and 24 percent for the Hallén-Bouwkamp theory when referred to the second-order values. The difference between first and $1\frac{1}{2}$-order solutions in the unmodified Gray theory of course reveals nothing about convergence.

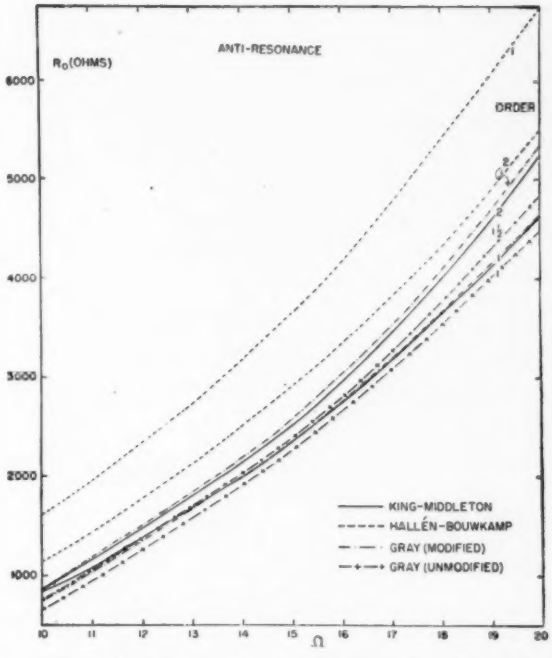


FIG. 9. Anti-resonant resistances as a function of Ω.

As pointed out in discussing the correlation of experiment with theory,[2] there is no physically available equivalent of the idealized slice generator actually assumed or implied in all of the theoretical analyses outlined above. If a continuous conductor is loosely and symmetrically coupled to a loop at the end of a two-wire line,

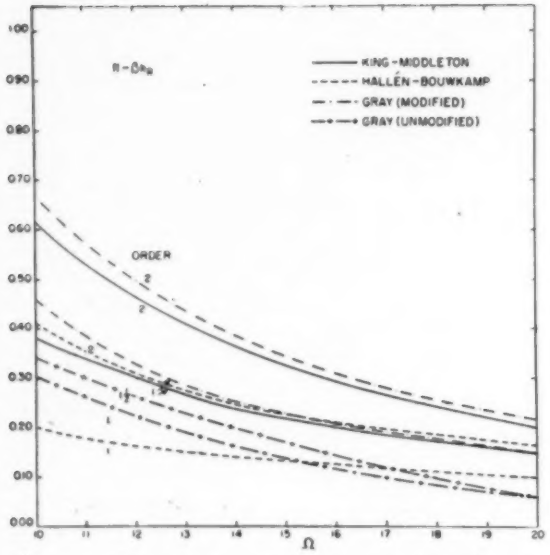


FIG. 10. Difference in radians between the anti-resonant length $\pi$ of an infinitely thin antenna ($\Omega = \infty$) and the anti-resonant lengths of antennas in the range of $\Omega$ from 10 to 20.

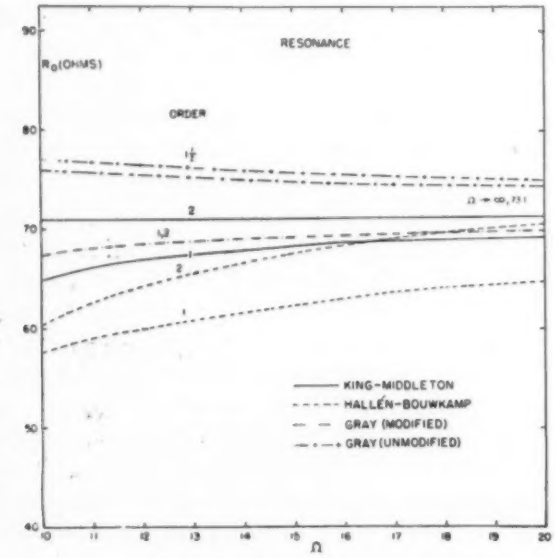


FIG. 11. Resonant resistances as a function of $\Omega$.

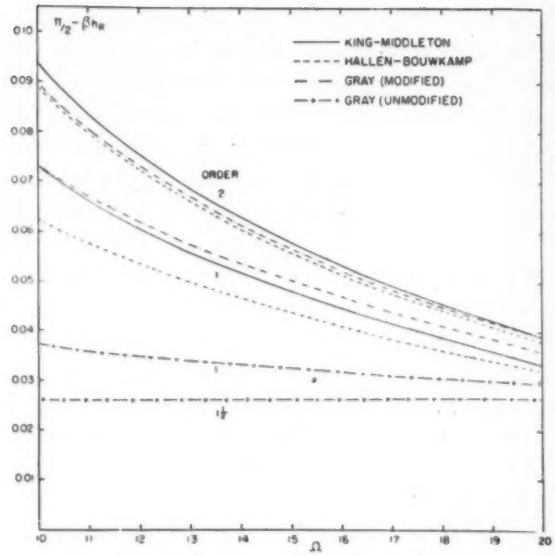


FIG. 12. Difference in radians between the resonant length $\pi/2$ of an infinitely thin antenna ($\Omega = \infty$) and the resonant lengths of antennas in the range of $\Omega$ from 10 to 20.

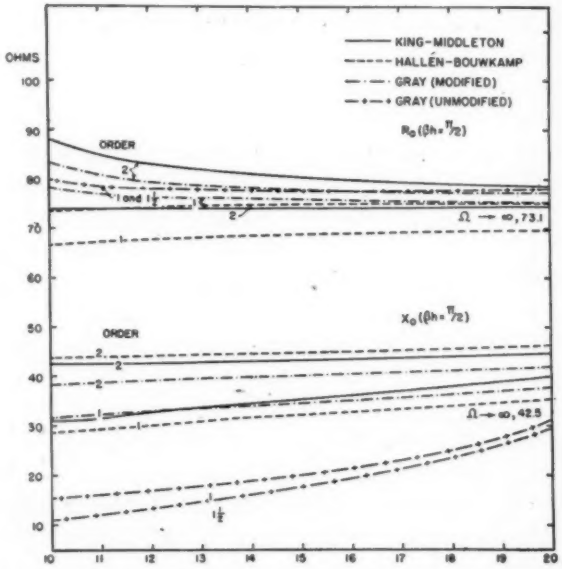


FIG. 13. Resistances and reactances of the half-wave dipole, $\beta h = \pi/2$, as a function of $\Omega$.

the e.m.f. induced in the wire is exactly equivalent to a "slice" generator at the center of the conductor. Similarly, the lumped e.m.f. in the equivalent series circuit of a receiving antenna is in effect that of a "slice" generator. In the case of direct drive probably the nearest physical equivalent of such a generator is a base-driven, cylindrical antenna with hemispherical ends erected vertically over a highly conducting metal plane of sufficient size, the antenna being the extension of the inner conductor of a coaxial line of very small cross section.

Very careful measurements have been made by D. D. King on a coaxial arrangement at a frequency of about 750 megahertz. These are described in complete detail in a doctoral dissertation and will be submitted for publication shortly. A cross section of the experimental results for an antenna with $h/a = 75$ or $\Omega = 10$ is

given in Table II in the form of a list of the primary critical values. The corresponding values for the several theories discussed above are also shown, together with the percentage departure from the experimental values.

In addition, corresponding critical values are given for Schelkunoff's transmission-line theory.[9] The data in this case were estimated from Figs. 23–26 of reference 9. Unfortunately the ratio $|X|_{\min}/|X|_{\max}$ was not actually available in this case since $|X|_{\min}$ does not appear on the curves and extrapolation is difficult. However, the relation $|X|_{\min}+|X|_{\max}\doteq R_{\max}$ is generally a good approximation in all of the theories, so that this relation was used to determine an approximate value of $|X|_{\min}$. Evidently it may be considerably in error, and no great weight should be attached to it until confirmed.

Examination of Table II shows clearly that by and large the King-Middleton second-order theory agrees best with the experimental values, the modified Gray results are next best, the Hallén-Bouwkamp values are poorest. The unmodified Gray and the Schelkunoff values agree quite satisfactorily with this experimental data for resistance at anti-resonance, but show very wide departures for other critical values. On the other hand, the King-Middleton second-order theory agrees very much better with the experimental data for anti-resonant resistance supplied by Schelkunoff than does his own theory. This is shown in Fig. 14 where Schelkunoff's theoretical curve (broken line), his experimental points (small circles), and the King-Middleton curve (unbroken line) are shown together as a function of Ω. In view of the great dependence of the impedance on the driving conditions, as shown for example in the work of Brown and Woodward,[12] and the impossibility of experimentally reproducing as a practical driving device the theoretical slice generator, care must be exercised not to overemphasize the significance of the close agreement. It is, nevertheless, safe and gratifying to conclude that the analytically elegant integral-equation method of Hallén leads to a highly refined and satisfactory theory of the thin cylindrical antenna.

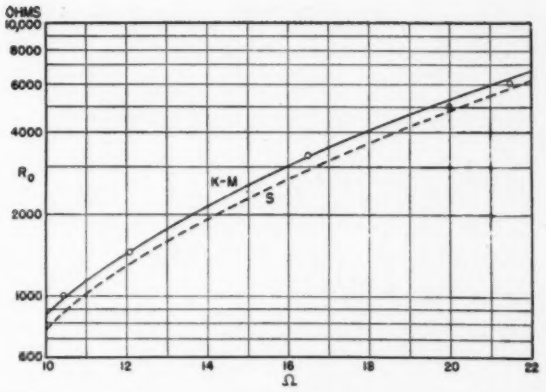


FIG. 14. Resistance at anti-resonance as a function of Ω. The solid-line curve marked K-M is according to the King-Middleton second-order theory; the broken-line curve is according to the transmission-line theory of S. A. Schelkunoff. The broken-line curve and the experimental points indicated by small circles are taken from S. A. Schelkunoff, Proc. I.R.E. **29**, 511, Fig. 26 (September, 1941).

## APPENDIX

With the help of the appendix to reference (10), it is seen that

$$\int_{-h}^{h}\frac{\cos\beta R_1}{R_1}dz'\doteq\Psi(z)_H-\text{Cin}\,\beta(h+z)-\text{Cin}\,\beta(h-z),\qquad h^2\gg a^2,\quad\text{(i)}$$

and

$$\int_{-h}^{h}\frac{\exp(-j\beta R_1)}{R_1}dz'\doteq\Psi_H(z)-\text{Cin}\,\beta(h+z)-\text{Cin}\,\beta(h-z)-j\,Si\,\beta(h+z)-j\,Si\,\beta(h-z),\quad h^2\gg a^2.\quad\text{(ii)}$$

From (i) and (ii) the following results, useful in the com-

TABLE II. Critical values related to the impedance characteristic of a cylindrical antenna for which $\Omega=2\ln(2h/a)=10$

| | Experimental data from Ph.D. Thesis of D. D. King | King-Middleton second-order theory | % | Modified Gray second-order theory | % | Hallén-Bouwkamp second-order theory | % | Unmodified Gray 1½ order theory | % | Schelkunoff transmission-line theory | % |
|---|---|---|---|---|---|---|---|---|---|---|---|
| $(R_0)_{\text{anti res.}}$ | 800 | 860 | 7.5 | 885 | 13.5 | 1150 | 47.5 | 740 | 7.5 | 740 | 7.5 |
| $\pi-\beta h_{\text{anti res.}}$ | 0.60 | 0.614 | 2.3 | 0.665 | 10.9 | 0.41 | 46.3 | 0.34 | 43.4 | 0.48 | 20 |
| $X_{\min}/X_{\max}$ | 1.95 | 1.8 | 7.7 | 1.84 | 5.7 | 1.06 | 46 | 1.54 | 21.0 | (1.4) | (28) |
| $(R_0)_{\text{res.}}$ | 71.5 | 71.0 | 0.7 | 67 | 6.3 | 60.6 | 15.2 | 77 | 7.7 | 61.4 | 14.1 |
| $(\pi/2)-\beta h_{\text{res.}}$ | 0.098 | 0.094 | 6.1 | 0.0895 | 8.2 | 0.0885 | 10.3 | 0.026 | 73.5 | 0.094 | 6.1 |
| $(R_0)_{\beta h=\pi/2}$ | 85 | 88 | 3.5 | 83.5 | 1.8 | 73.5 | 13.6 | 80 | 6.3 | 75 | 18 |
| $(X_0)_{\beta h=\pi/2}$ | 47 | 42.5 | 9.5 | 38 | 19.1 | 43.5 | 5.3 | 12 | 74.5 | 45 | 4.2 |

putation of the current distribution, may be obtained:

$$F_1(z)_g = F_1(z)_H + (\cos \beta z - \cos \beta h)[\Psi(z)_H - \Omega - \text{Cin } \beta(h+z) - \text{Cin } \beta(h-z)] + j \cos \beta h[Si\ \beta(h+z) + Si\ \beta(h-z)], \quad \text{(iii)}$$

and

$$G_1(z)_g = G_1(z)_H + (\sin \beta|z| - \sin \beta h)[\Psi(z)_H - \Omega - \text{Cin } \beta(h+z) - \text{Cin } \beta(h-z)] + j \sin \beta h[Si\ \beta(h+z) + Si\ \beta(h-z)]. \quad \text{(iv)}$$

Important special cases are

$$F_1(0)_g = F_1(0)_H + 2(\cos \beta h - 1)\ \text{Cin } \beta h + 2j \cos \beta h\ Si\ \beta h, \quad \text{(v)}$$

$$F_1(h)_g = F_1(h)_H + j \cos \beta h\ Si\ 2\beta h, \quad \text{(vi)}$$

and

$$G_1(0)_g = -Si\ 2\beta h + j\ \text{Cin } 2\beta h, \quad \text{(vii)}$$

$$G_1(h)_g = \sin \beta h[\Psi(h)_H - \text{Cin } 2\beta h] - S_1(h), \quad \text{(viii)}$$

where

$$\Psi(h)_H = \sinh^{-1} \frac{2h}{a}, \quad \Psi(0)_H = 2 \sinh^{-1} \frac{h}{a}, \quad \text{(ix)}$$

and

$$S_1(h) = \frac{\sin \beta h}{2}\{\text{Cin } 4\beta h - 2\ \text{Cin } 2\beta h\} + \frac{\cos \beta h}{2}\{Si\ 4\beta h - 2\ Si\ 2\beta h\} - j\frac{\cos \beta h}{2}\{\text{Cin } 4\beta h - 2\ \text{Cin } 2\beta h\} - j \sin \beta h \cdot Si\ 2\beta h + j\frac{\sin \beta h}{2} Si\ 4\beta h. \quad \text{(x)}$$

With the help of the above one may write

$$M_1(0)_g = M_1(0)_H + \sin \beta h\{j\ Si\ 2\beta h - 2\ \text{Cin } \beta h\}. \quad \text{(xi)}$$

$M_1(0)_H$, $F_1(0)_H$, $F_1(h)$ are tabulated in reference 4.

---

## Calendar of Meetings

| | |
|---|---|
| **April** | |
| 1– 4 | American Society of Mechanical Engineers, Chattanooga, Tennessee |
| 3– 5 | Society of Automotive Engineers, New York, New York |
| 8–12 | American Chemical Society, Atlantic City, New Jersey |
| 12–13 | American Physical Society, Southeastern Section, Atlanta, Georgia |
| 17–19 | American Society of Civil Engineers, Philadelphia, Pennsylvania |
| 18–20 | American Philosophical Society, Philadelphia, Pennsylvania |
| 22–24 | National Academy of Sciences, Washington, D. C. |
| 25–27 | American Physical Society, Cambridge, Massachusetts |
| 26–27 | American Mathematical Society, Chicago, Illinois |
| 26–27 | American Mathematical Society, New York, New York |
| 27 | American Mathematical Society, West Coast |
| 28–May 1 | American Ceramic Society, Inc., Buffalo, New York |
| **May** | |
| 6–10 | Society of Motion Picture Engineers, New York, New York |
| 10–11 | Acoustical Society of America, New York, New York |
| 27–29 | American Geophysical Union, Washington, D. C. |
| **June** | |
| 2– 5 | American Society of Refrigerating Engineers, St. Paul, Minnesota |
| 13–14 | Institute of Aeronautical Sciences, Detroit, Michigan |
| 17–20 | American Society of Mechanical Engineers, Detroit, Michigan |
| 20–23 | Society for the Promotion of Engineering Education, St Louis, Missouri |
| 24–28 | American Institute of Electrical Engineers, Detroit, Michigan |
| 24–28 | American Society for Testing Materials, Buffalo, New York |
| **July** | |
| 17–19 | American Society of Civil Engineers, Spokane, Washington |
| **August** | |
| 14–15 | Institute of Aeronautical Sciences, Los Angeles, California |
| 19–20 | Mathematical Association of America, Ithaca, New York |

# Correction of Diffraction Amplitudes for Lorentz and Polarization Factors

M. J. Buerger and Gilbert E. Klein
*Massachusetts Institute of Technology, Cambridge, Massachusetts*

(Received December 13, 1945)

The corrections for Lorentz and polarization factors for trial and error crystal structure computations are discussed, following the general method recently presented for correcting x-ray diffraction data used in Fourier syntheses. The Lorentz correction has the form $(1/S)\csc\Upsilon$, where $S$ is a scale constant characteristic of the reciprocal lattice level and whose form varies with the method of recording the data. The scale constant is eliminated by appropriate timing of the exposure. When many trial and error computations have to be made, there are advantages in using a scheme involving a correction factor $(\csc\Upsilon)^{\frac{1}{2}}$ instead of $\csc\Upsilon$. Tables are provided for these functions, for the polarization correction and for the combined Lorentz-polarization correction which is used in the special case of zero-level photographs. Tables are also provided for the functions $(h^2+k^2)^{\frac{1}{2}}$ and $(h^2+k^2+hk)^{\frac{1}{2}}$, which are useful for computing the argument for the zero-level corrections of tetragonal and hexagonal crystals.

## INTRODUCTION

In an earlier contribution,[1] the correction of x-ray diffraction intensities for Lorentz and polarization factors was discussed, and appropriate tables were presented for carrying out the correction. This procedure is important in deriving the $F$'s required for any of the several Fourier series methods of investigating crystal structures. In this paper we discuss the inverse problem, namely, the computation of expected x-ray diffraction intensities from a set of diffracted amplitudes, $F$. This computation is continually dealt with in fixing the parameters of atoms by the method of trial and error.

The theory of Lorentz and polarization corrections has already been discussed in detail.[1] We merely outline its essential features here. The relation between $F$ and the required intensity $I$ is

$$I \sim TLpF^2, \tag{1}$$

where $T$ is the time of the exposure, $L$ is the Lorentz factor, and $p$ is the polarization factor.

The polarization factor, $p$, is tabulated in Table I for the argument $\sin\theta$, and in Table II for the argument $\sigma$ (the distance of the reciprocal lattice point from the origin). For notes on the computation of $\sigma$, the reader is referred to the earlier paper.[1]

## THE LORENTZ FACTOR

For diffraction techniques which make use of a single crystal and which separate the diffraction record into layer lines, the Lorentz factor has the form

$$L = \frac{1}{S}\cdot\frac{1}{\sin\Upsilon}, \tag{2}$$

where $\Upsilon$ is an angular coordinate of the reflection,[2] and $S$ is a scale factor which is a function of the reciprocal lattice level coordinate and which varies in form[1] according to the recording method. For the equi-inclination Weissenberg method,

$$S = \cos^2\mu = (1-[\zeta/2]^2)^{\frac{1}{2}}. \tag{3}$$

If (1) and (2) are combined, and if the total time of exposure, $T$, is split into $T_0$ (the time of exposure chosen for the zero level) and $t$ (a numerical factor), there results

$$I \sim T_0\left[t\frac{1}{S}\right]\frac{1}{\sin\Upsilon}p|F|^2. \tag{4}$$

It is evident that the time of exposure, $T_0t$, can be selected for each level so that the product in brackets becomes unity. This merely requires that

$$t = S. \tag{5}$$

For the equi-inclination Weissenberg method, according to (3), the timing factor becomes

$$t = \cos^2\mu. \tag{6}$$

This procedure amounts to elimination of the scale part of the Lorentz factor by time cancella-

[1] M. J. Buerger and Gilbert E. Klein, "Correction of x-ray diffraction intensities for Lorentz and polarization factors," J. App. Phys. **16**, 408–418 (1945).

[2] M. J. Buerger, *X-Ray Crystallography* (John Wiley & Sons, Inc., New York, 1942), p. 222 *et seq.*

TABLE I. Polarization factor, $p\left(=\frac{1+\cos^2 2\theta}{2}\right)$, as a function of sin $\theta$.

| | .000 | .001 | .002 | .003 | .004 | .005 | .006 | .007 | .008 | .009 |
|---|---|---|---|---|---|---|---|---|---|---|
| .00 | 1.0000 | 1.0000 | 1.0000 | 1.0000 | 1.0000 | .9999 | .9999 | .9999 | .9999 | .9998 |
| .01 | .9998 | .9998 | .9997 | .9997 | .9996 | .9996 | .9995 | .9994 | .9994 | .9993 |
| .02 | .9992 | .9991 | .9990 | .9989 | .9989 | .9988 | .9987 | .9985 | .9984 | .9983 |
| .03 | .9982 | .9981 | .9980 | .9978 | .9977 | .9976 | .9974 | .9973 | .9971 | .9970 |
| .04 | .9968 | .9966 | .9965 | .9963 | .9961 | .9960 | .9958 | .9956 | .9954 | .9952 |
| .05 | .9950 | .9948 | .9946 | .9944 | .9942 | .9940 | .9937 | .9935 | .9933 | .9931 |
| .06 | .9928 | .9926 | .9923 | .9921 | .9918 | .9916 | .9913 | .9911 | .9908 | .9905 |
| .07 | .9902 | .9900 | .9897 | .9894 | .9891 | .9888 | .9885 | .9882 | .9879 | .9876 |
| .08 | .9873 | .9870 | .9866 | .9863 | .9860 | .9857 | .9853 | .9850 | .9846 | .9843 |
| .09 | .9839 | .9836 | .9832 | .9828 | .9825 | .9821 | .9817 | .9814 | .9810 | .9806 |
| .10 | .9802 | .9798 | .9794 | .9790 | .9786 | .9782 | .9778 | .9774 | .9769 | .9765 |
| .11 | .9761 | .9757 | .9752 | .9748 | .9743 | .9739 | .9735 | .9730 | .9725 | .9721 |
| .12 | .9716 | .9711 | .9707 | .9702 | .9697 | .9692 | .9688 | .9683 | .9678 | .9673 |
| .13 | .9668 | .9663 | .9658 | .9652 | .9647 | .9642 | .9637 | .9632 | .9626 | .9621 |
| .14 | .9616 | .9610 | .9605 | .9599 | .9594 | .9588 | .9583 | .9577 | .9571 | .9566 |
| .15 | .9560 | .9554 | .9549 | .9543 | .9537 | .9531 | .9525 | .9519 | .9513 | .9507 |
| .16 | .9501 | .9495 | .9489 | .9483 | .9477 | .9470 | .9464 | .9458 | .9451 | .9445 |
| .17 | .9439 | .9432 | .9426 | .9419 | .9413 | .9406 | .9400 | .9393 | .9386 | .9380 |
| .18 | .9373 | .9366 | .9360 | .9353 | .9346 | .9339 | .9332 | .9325 | .9318 | .9311 |
| .19 | .9304 | .9297 | .9290 | .9283 | .9276 | .9269 | .9261 | .9254 | .9247 | .9239 |
| .20 | .9232 | .9225 | .9217 | .9210 | .9202 | .9195 | .9187 | .9180 | .9172 | .9164 |
| .21 | .9157 | .9149 | .9142 | .9134 | .9126 | .9118 | .9110 | .9102 | .9095 | .9087 |
| .22 | .9079 | .9071 | .9063 | .9055 | .9047 | .9039 | .9031 | .9023 | .9014 | .9006 |
| .23 | .8998 | .8990 | .8981 | .8973 | .8965 | .8956 | .8948 | .8940 | .8931 | .8923 |
| .24 | .8914 | .8906 | .8897 | .8888 | .8880 | .8872 | .8863 | .8854 | .8846 | .8837 |
| .25 | .8828 | .8819 | .8811 | .8802 | .8793 | .8784 | .8775 | .8766 | .8757 | .8748 |
| .26 | .8739 | .8730 | .8721 | .8712 | .8703 | .8694 | .8685 | .8676 | .8667 | .8658 |
| .27 | .8648 | .8639 | .8630 | .8621 | .8611 | .8602 | .8593 | .8583 | .8574 | .8564 |
| .28 | .8555 | .8545 | .8536 | .8526 | .8517 | .8507 | .8498 | .8488 | .8479 | .8469 |
| .29 | .8459 | .8450 | .8440 | .8430 | .8420 | .8411 | .8401 | .8391 | .8382 | .8372 |
| .30 | .8362 | .8352 | .8342 | .8332 | .8323 | .8313 | .8303 | .8293 | .8283 | .8273 |
| .31 | .8263 | .8253 | .8243 | .8233 | .8223 | .8212 | .8202 | .8192 | .8182 | .8172 |
| .32 | .8162 | .8152 | .8141 | .8131 | .8121 | .8111 | .8100 | .8090 | .8080 | .8070 |
| .33 | .8059 | .8049 | .8039 | .8028 | .8018 | .8007 | .7997 | .7987 | .7976 | .7966 |
| .34 | .7955 | .7944 | .7934 | .7924 | .7913 | .7903 | .7892 | .7882 | .7871 | .7861 |
| .35 | .7850 | .7840 | .7829 | .7818 | .7808 | .7797 | .7787 | .7776 | .7765 | .7754 |
| .36 | .7744 | .7733 | .7723 | .7712 | .7701 | .7690 | .7680 | .7669 | .7658 | .7648 |
| .37 | .7637 | .7626 | .7615 | .7605 | .7594 | .7583 | .7572 | .7561 | .7551 | .7540 |
| .38 | .7529 | .7518 | .7507 | .7497 | .7486 | .7475 | .7464 | .7453 | .7442 | .7432 |
| .39 | .7421 | .7410 | .7399 | .7388 | .7377 | .7366 | .7356 | .7345 | .7334 | .7323 |
| .40 | .7312 | .7301 | .7290 | .7279 | .7268 | .7258 | .7247 | .7236 | .7225 | .7214 |
| .41 | .7203 | .7192 | .7182 | .7170 | .7160 | .7149 | .7138 | .7127 | .7116 | .7105 |
| .42 | .7094 | .7083 | .7073 | .7062 | .7051 | .7040 | .7029 | .7018 | .7007 | .6997 |
| .43 | .6986 | .6975 | .6964 | .6953 | .6942 | .6932 | .6921 | .6910 | .6899 | .6888 |
| .44 | .6878 | .6867 | .6856 | .6845 | .6835 | .6824 | .6813 | .6802 | .6792 | .6781 |
| .45 | .6770 | .6759 | .6749 | .6738 | .6727 | .6717 | .6706 | .6695 | .6685 | .6674 |
| .46 | .6663 | .6653 | .6642 | .6632 | .6621 | .6611 | .6600 | .6589 | .6579 | .6568 |
| .47 | .6558 | .6547 | .6537 | .6527 | .6516 | .6506 | .6495 | .6485 | .6474 | .6464 |
| .48 | .6454 | .6443 | .6433 | .6423 | .6412 | .6402 | .6392 | .6382 | .6371 | .6361 |
| .49 | .6351 | .6341 | .6331 | .6320 | .6310 | .6300 | .6290 | .6280 | .6270 | .6260 |
| .50 | .6250 | .6240 | .6230 | .6220 | .6210 | .6200 | .6190 | .6180 | .6170 | .6161 |
| .51 | .6151 | .6141 | .6132 | .6122 | .6112 | .6102 | .6093 | .6083 | .6073 | .6064 |
| .52 | .6054 | .6044 | .6035 | .6026 | .6016 | .6006 | .5997 | .5988 | .5979 | .5969 |
| .53 | .5960 | .5951 | .5942 | .5932 | .5923 | .5914 | .5905 | .5896 | .5887 | .5878 |
| .54 | .5869 | .5860 | .5851 | .5842 | .5833 | .5824 | .5815 | .5806 | .5798 | .5789 |
| .55 | .5780 | .5771 | .5763 | .5754 | .5746 | .5737 | .5729 | .5720 | .5712 | .5703 |
| .56 | .5695 | .5687 | .5678 | .5670 | .5662 | .5654 | .5645 | .5637 | .5629 | .5621 |
| .57 | .5613 | .5605 | .5597 | .5589 | .5582 | .5574 | .5566 | .5558 | .5551 | .5543 |
| .58 | .5535 | .5528 | .5520 | .5513 | .5505 | .5498 | .5490 | .5483 | .5476 | .5469 |
| .59 | .5461 | .5454 | .5447 | .5440 | .5433 | .5426 | .5419 | .5412 | .5406 | .5399 |
| .60 | .5392 | .5385 | .5379 | .5372 | .5365 | .5359 | .5353 | .5346 | .5340 | .5333 |
| .61 | .5327 | .5321 | .5315 | .5309 | .5303 | .5297 | .5291 | .5285 | .5279 | .5273 |
| .62 | .5267 | .5262 | .5256 | .5250 | .5245 | .5239 | .5234 | .5228 | .5223 | .5218 |
| .63 | .5213 | .5207 | .5202 | .5197 | .5192 | .5187 | .5182 | .5178 | .5173 | .5168 |
| .64 | .5163 | .5159 | .5154 | .5150 | .5145 | .5141 | .5137 | .5132 | .5128 | .5124 |
| .65 | .5120 | .5116 | .5112 | .5108 | .5105 | .5101 | .5097 | .5093 | .5090 | .5086 |
| .66 | .5083 | .5080 | .5076 | .5073 | .5070 | .5067 | .5064 | .5060 | .5058 | .5055 |
| .67 | .5052 | .5050 | .5047 | .5044 | .5042 | .5039 | .5037 | .5035 | .5033 | .5030 |

TABLE 1.—*Continued.*

| | .000 | .001 | .002 | .003 | .004 | .005 | .006 | .007 | .008 | .009 |
|---|---|---|---|---|---|---|---|---|---|---|
| .68 | .5028 | .5026 | .5024 | .5022 | .5021 | .5019 | .5017 | .5016 | .5014 | .5013 |
| .69 | .5011 | .5010 | .5009 | .5008 | .5007 | .5006 | .5005 | .5004 | .5003 | .5003 |
| .70 | .5002 | .5001 | .5001 | .5001 | .5000 | .5000 | .5000 | .5000 | .5000 | .5000 |
| .71 | .5000 | .5001 | .5001 | .5001 | .5002 | .5003 | .5003 | .5004 | .5005 | .5006 |
| .72 | .5007 | .5008 | .5009 | .5010 | .5012 | .5013 | .5014 | .5016 | .5018 | .5020 |
| .73 | .5022 | .5024 | .5026 | .5028 | .5030 | .5032 | .5035 | .5037 | .5040 | .5043 |
| .74 | .5045 | .5048 | .5051 | .5054 | .5057 | .5061 | .5064 | .5067 | .5071 | .5074 |
| .75 | .5078 | .5082 | .5086 | .5090 | .5094 | .5098 | .5102 | .5107 | .5111 | .5116 |
| .76 | .5120 | .5125 | .5130 | .5135 | .5140 | .5145 | .5150 | .5156 | .5161 | .5167 |
| .77 | .5173 | .5178 | .5184 | .5190 | .5196 | .5203 | .5209 | .5215 | .5222 | .5228 |
| .78 | .5235 | .5242 | .5249 | .5256 | .5263 | .5270 | .5278 | .5285 | .5293 | .5300 |
| .79 | .5308 | .5316 | .5324 | .5332 | .5340 | .5349 | .5357 | .5366 | .5374 | .5383 |
| .80 | .5392 | .5401 | .5410 | .5419 | .5429 | .5438 | .5448 | .5458 | .5468 | .5477 |
| .81 | .5487 | .5498 | .5508 | .5518 | .5529 | .5539 | .5550 | .5561 | .5572 | .5583 |
| .82 | .5594 | .5606 | .5617 | .5629 | .5641 | .5653 | .5664 | .5677 | .5689 | .5701 |
| .83 | .5714 | .5726 | .5739 | .5752 | .5765 | .5778 | .5791 | .5805 | .5818 | .5832 |
| .84 | .5845 | .5859 | .5873 | .5887 | .5902 | .5916 | .5931 | .5945 | .5960 | .5975 |
| .85 | .5990 | .6005 | .6021 | .6036 | .6052 | .6067 | .6083 | .6099 | .6115 | .6132 |
| .86 | .6148 | .6165 | .6181 | .6198 | .6215 | .6232 | .6250 | .6267 | .6284 | .6302 |
| .87 | .6320 | .6338 | .6356 | .6374 | .6393 | .6411 | .6430 | .6449 | .6468 | .6487 |
| .88 | .6506 | .6525 | .6545 | .6564 | .6584 | .6604 | .6624 | .6645 | .6665 | .6686 |
| .89 | .6706 | .6727 | .6748 | .6770 | .6791 | .6812 | .6834 | .6856 | .6878 | .6900 |
| .90 | .6922 | .6944 | .6967 | .6990 | .7013 | .7036 | .7059 | .7082 | .7106 | .7129 |
| .91 | .7153 | .7177 | .7201 | .7225 | .7250 | .7274 | .7299 | .7324 | .7349 | .7374 |
| .92 | .7400 | .7425 | .7451 | .7477 | .7503 | .7529 | .7556 | .7582 | .7609 | .7636 |
| .93 | .7663 | .7690 | .7718 | .7745 | .7773 | .7801 | .7829 | .7857 | .7886 | .7914 |
| .94 | .7943 | .7972 | .8001 | .8030 | .8060 | .8090 | .8119 | .8149 | .8179 | .8209 |
| .95 | .8240 | .8271 | .8302 | .8333 | .8364 | .8395 | .8427 | .8459 | .8490 | .8523 |
| .96 | .8555 | .8587 | .8620 | .8653 | .8686 | .8719 | .8752 | .8786 | .8819 | .8854 |
| .97 | .8888 | .8922 | .8957 | .8991 | .9026 | .9061 | .9096 | .9132 | .9168 | .9203 |
| .98 | .9239 | .9276 | .9312 | .9348 | .9385 | .9422 | .9459 | .9497 | .9534 | .9572 |
| .99 | .9610 | .9648 | .9686 | .9725 | .9764 | .9802 | .9842 | .9881 | .9920 | .9960 |

tion. Thus, if the original photographs are correctly timed according to (5), the apparent Lorentz corrections required for all levels are the same, and all computations take the form

$$I \sim p \csc \Upsilon |F|^2. \tag{7}$$

From this discussion, it is evident that provided time cancellation exposures are made, the Lorentz factor correction can be easily made with the aid of tables of csc $\Upsilon$ for the argument $\Upsilon$. The angle $\Upsilon$ is usually found by measuring the location of the diffraction spot on the film in millimeters. For standard diameter cameras this linear measurement is readily converted by inspection to degrees and tenths. The argument for csc $\Upsilon$ should thus be the angle $\Upsilon$ expressed in degrees and tenths. Such tables are already extant,[3] but for the sake of providing the reader with complete equipment for Lorentz and polarization correction, we include this information as Table III.

[3]Herbert Bristol Dwight, *Mathematical Tables* (McGraw-Hill Book Company, Inc., New York, 1941), pages 40–59.

For zero levels, both Lorentz and polarization factors can be given as functions of the same argument. We therefore provide the combined Lorentz-polarization factor, $L \cdot p$, for the arguments $\sin\theta$ and $\sigma$, in Tables IV and V, respectively. *These last two tables should be used for zero-level photographs only.*

## COMPUTATIONAL FORM AND FACTORS FOR TRIAL AND ERROR INVESTIGATIONS

The computation form given in (7) contains an operation which can often be eliminated with a consequent great saving of time and labor. This is especially desirable when more than one computation of the intensity of the same reflection must be made, particularly when it must be monotonously repeated as in the case of the location of atoms by the method of trial and error. This is the operation of squaring $|F|$. If the square roots of both sides of (7) are taken, there results

$$(I)^{\frac{1}{2}} \sim (p \csc \Upsilon)^{\frac{1}{2}} |F|. \tag{8}$$

TABLE II. Polarization factor, $\phi^{\circ}\left(=\frac{1+\cos^2 2\theta}{2}\right)$, as a function of $\sigma$.

| | .000 | .002 | .004 | .006 | .008 | | .000 | .002 | .004 | .006 | .008 |
|---|---|---|---|---|---|---|---|---|---|---|---|
| .00 | 1.0000 | 1.0000 | 1.0000 | 1.0000 | 1.0000 | .68 | .7955 | .7944 | .7934 | .7924 | .7913 |
| .01 | .9999 | .9999 | .9999 | .9999 | .9998 | .69 | .7903 | .7892 | .7882 | .7871 | .7861 |
| .02 | .9998 | .9998 | .9997 | .9997 | .9996 | .70 | .7850 | .7840 | .7829 | .7818 | .7808 |
| .03 | .9996 | .9995 | .9994 | .9994 | .9993 | .71 | .7797 | .7787 | .7776 | .7765 | .7754 |
| .04 | .9992 | .9991 | .9990 | .9989 | .9989 | .72 | .7744 | .7733 | .7723 | .7712 | .7701 |
| .05 | .9988 | .9987 | .9985 | .9984 | .9983 | .73 | .7690 | .7680 | .7669 | .7658 | .7648 |
| .06 | .9982 | .9981 | .9980 | .9978 | .9977 | .74 | .7637 | .7626 | .7615 | .7605 | .7594 |
| .07 | .9976 | .9974 | .9973 | .9971 | .9970 | .75 | .7583 | .7572 | .7561 | .7551 | .7540 |
| .08 | .9968 | .9966 | .9965 | .9963 | .9961 | .76 | .7529 | .7518 | .7507 | .7497 | .7486 |
| .09 | .9960 | .9958 | .9956 | .9954 | .9952 | .77 | .7475 | 7464 | .7453 | .7442 | .7432 |
| .10 | .9950 | .9948 | .9946 | .9944 | .9942 | .78 | .7421 | .7410 | .7399 | .7388 | .7377 |
| .11 | .9940 | .9937 | .9935 | .9933 | .9931 | .79 | .7366 | .7356 | .7345 | .7334 | .7323 |
| .12 | .9928 | .9926 | .9923 | .9921 | .9918 | .80 | .7312 | .7301 | .7290 | .7279 | .7268 |
| .13 | .9916 | .9913 | .9911 | .9908 | .9905 | .81 | .7258 | .7247 | .7236 | .7225 | .7214 |
| .14 | .9902 | .9900 | .9897 | .9894 | .9891 | .82 | .7203 | .7192 | .7182 | .7170 | .7160 |
| .15 | .9888 | .9885 | .9882 | .9879 | .9876 | .83 | .7149 | .7138 | .7127 | .7116 | .7105 |
| .16 | .9873 | .9870 | .9866 | .9863 | .9860 | .84 | .7094 | .7083 | .7073 | .7062 | .7051 |
| .17 | .9857 | .9853 | .9850 | .9846 | .9843 | .85 | .7040 | .7029 | .7018 | .7007 | .6997 |
| .18 | .9839 | .9836 | .9832 | .9828 | .9825 | .86 | .6986 | .6975 | .6964 | .6953 | .6942 |
| .19 | .9821 | .9817 | .9814 | .9810 | .9806 | .87 | .6932 | .6921 | .6910 | .6899 | .6888 |
| .20 | 9802 | .9798 | .9794 | .9790 | .9786 | .88 | .6878 | .6867 | .6856 | .6845 | .6835 |
| .21 | .9782 | .9778 | .9774 | .9769 | .9765 | .89 | .6824 | .6813 | .6802 | .6792 | .6781 |
| .22 | .9761 | .9757 | .9752 | .9748 | 9743 | .90 | .6770 | .6759 | .6749 | .6738 | .6727 |
| .23 | .9739 | .9735 | .9730 | .9725 | .9721 | .91 | .6717 | .6706 | .6695 | .6685 | .6674 |
| .24 | .9716 | .9711 | .9707 | .9702 | .9697 | .92 | .6663 | .6653 | .6642 | .6632 | .6621 |
| .25 | .9692 | .9688 | .9683 | .9678 | .9673 | .93 | .6611 | .6600 | .6589 | .6579 | .6568 |
| .26 | .9668 | .9663 | .9658 | .9652 | .9647 | .94 | .6558 | .6547 | .6537 | .6527 | .6516 |
| .27 | .9642 | .9637 | .9632 | .9626 | .9621 | .95 | .6506 | .6495 | .6485 | .6474 | .6464 |
| .28 | .9616 | .9610 | .9605 | .9599 | .9594 | .96 | .6454 | .6443 | .6433 | .6423 | .6412 |
| .29 | .9588 | .9583 | .9577 | .9571 | .9566 | .97 | .6402 | .6392 | .6382 | .6371 | .6361 |
| .30 | .9560 | .9554 | .9549 | .9543 | .9537 | .98 | .6351 | .6341 | .6331 | .6320 | .6310 |
| .31 | .9531 | .9525 | .9519 | .9513 | .9507 | .99 | .6300 | .6290 | .6280 | .6270 | .6260 |
| .32 | .9501 | .9495 | .9489 | .9483 | .9477 | 1 00 | .6250 | .6240 | .6230 | .6220 | .6210 |
| .33 | .9470 | .9464 | .9458 | .9451 | .9445 | 1.01 | .6200 | .6190 | .6180 | .6170 | .6161 |
| .34 | .9439 | .9432 | .9426 | .9419 | .9413 | 1.02 | .6151 | .6141 | .6132 | .6122 | .6112 |
| .35 | .9406 | .9400 | .9393 | .9386 | .9380 | 1.03 | .6102 | .6093 | .6083 | .6073 | .6064 |
| .36 | .9373 | .9366 | .9360 | .9353 | .9346 | 1.04 | .6054 | .6044 | .6035 | .6026 | .6016 |
| .37 | .9339 | .9332 | .9325 | .9318 | .9311 | 1.05 | .6006 | .5997 | .5988 | .5979 | .5969 |
| .38 | .9304 | .9297 | .9290 | .9283 | .9276 | 1.06 | .5960 | .5951 | .5942 | .5932 | .5923 |
| .39 | .9269 | .9261 | .9254 | .9247 | .9239 | 1.07 | .5914 | .5905 | .5896 | .5887 | .5878 |
| .40 | .9232 | .9225 | .9217 | .9210 | .9202 | 1.08 | .5869 | .5860 | .5851 | .5842 | .5833 |
| .41 | .9195 | .9187 | .9180 | .9172 | .9164 | 1.09 | 5824 | .5815 | .5806 | .5798 | .5789 |
| .42 | .9157 | .9149 | .9142 | .9134 | .9126 | 1.10 | .5780 | .5771 | .5763 | .5754 | .5746 |
| .43 | .9118 | .9110 | .9102 | .9095 | .9087 | 1.11 | .5737 | .5729 | .5720 | .5712 | .5703 |
| .44 | .9079 | .9071 | .9063 | .9055 | .9047 | 1.12 | .5695 | .5687 | .5678 | .5670 | .5662 |
| .45 | .9039 | .9031 | .9023 | .9014 | .9006 | 1.13 | .5654 | .5645 | .5637 | .5629 | .5621 |
| .46 | .8998 | .8990 | .8981 | .8973 | .8965 | 1.14 | .5613 | .5605 | .5597 | .5589 | .5582 |
| .47 | .8956 | .8948 | .8940 | .8931 | .8923 | 1.15 | .5574 | .5566 | .5558 | .5551 | .5543 |
| .48 | .8914 | .8906 | .8897 | .8888 | .8880 | 1.16 | .5535 | .5528 | .5520 | .5513 | .5505 |
| .49 | .8872 | .8863 | .8854 | .8846 | .8837 | 1.17 | .5498 | .5490 | .5483 | .5476 | .5469 |
| .50 | .8828 | .8819 | .8811 | .8802 | .8793 | 1.18 | .5461 | .5454 | .5447 | .5440 | .5433 |
| .51 | .8784 | .8775 | .8766 | .8757 | .8748 | 1.19 | .5426 | .5419 | .5412 | .5406 | .5399 |
| .52 | .8739 | .8730 | .8721 | .8712 | .8703 | 1.20 | .5392 | .5385 | .5379 | .5372 | .5365 |
| .53 | 8694 | .8685 | .8676 | .8667 | .8658 | 1.21 | .5359 | .5353 | .5346 | .5340 | .5333 |
| .54 | .8648 | .8639 | .8630 | .8621 | .8611 | 1.22 | .5327 | .5321 | .5315 | .5309 | .5303 |
| .55 | .8602 | .8593 | .8583 | .8574 | .8564 | 1.23 | .5297 | .5291 | .5285 | .5279 | .5273 |
| .56 | .8555 | .8545 | .8536 | .8526 | .8517 | 1.24 | .5267 | .5262 | .5256 | .5250 | .5245 |
| .57 | .8507 | .8498 | .8488 | .8479 | .8469 | 1.25 | .5239 | .5234 | .5228 | .5223 | .5218 |
| .58 | .8459 | .8450 | .8440 | .8430 | .8420 | 1.26 | .5213 | .5207 | .5202 | .5197 | .5192 |
| .59 | .8411 | .8401 | .8391 | .8382 | .8372 | 1.27 | .5187 | .5182 | .5178 | .5173 | .5168 |
| .60 | .8362 | .8352 | .8342 | .8332 | .8323 | 1.28 | .5163 | .5159 | .5154 | .5150 | .5145 |
| .61 | .8313 | 8303 | .8293 | .8283 | .8273 | 1.29 | .5141 | .5137 | .5132 | .5128 | .5124 |
| .62 | .8263 | .8253 | .8243 | .8233 | .8223 | 1.30 | .5120 | .5116 | .5112 | .5108 | .5105 |
| .63 | .8212 | .8202 | .8192 | .8182 | .8172 | 1.31 | .5101 | .5097 | .5093 | .5090 | .5086 |
| .64 | .8162 | .8152 | .8141 | .8131 | .8121 | 1.32 | .5083 | .5080 | .5076 | .5073 | .5070 |
| .65 | .8111 | .8100 | .8090 | .8080 | .8070 | 1.33 | .5067 | .5064 | .5060 | 5058 | .5055 |
| .66 | .8059 | .8049 | .8039 | .8028 | .8018 | 1.34 | .5052 | .5050 | .5047 | .5044 | .5042 |
| .67 | .8007 | .7997 | .7987 | .7976 | .7966 | 1.35 | .5039 | .5037 | .5035 | .5033 | .5030 |

TABLE II.—*Continued.*

| | .000 | .002 | .004 | .006 | .008 |
|---|---|---|---|---|---|
| 1.36 | .5028 | .5026 | .5024 | .5022 | .5021 |
| 1.37 | .5019 | .5017 | .5016 | .5014 | .5013 |
| 1.38 | .5011 | .5010 | .5009 | .5008 | .5007 |
| 1.39 | .5006 | .5005 | .5004 | .5003 | .5003 |
| 1.40 | .5002 | .5001 | .5001 | .5001 | .5000 |
| 1.41 | .5000 | .5000 | .5000 | .5000 | .5000 |
| 1.42 | .5000 | .5001 | .5001 | .5001 | .5002 |
| 1.43 | .5003 | .5003 | .5004 | .5005 | .5006 |
| 1.44 | .5007 | .5008 | .5009 | .5010 | .5012 |
| 1.45 | .5013 | .5014 | .5016 | .5018 | .5020 |
| 1.46 | .5022 | .5024 | .5026 | .5028 | .5030 |
| 1.47 | .5032 | .5035 | .5037 | .5040 | .5043 |
| 1.48 | .5045 | .5048 | .5051 | .5054 | .5057 |
| 1.49 | .5061 | .5064 | .5067 | .5071 | .5074 |
| 1.50 | .5078 | .5082 | .5086 | .5090 | .5094 |
| 1.51 | .5098 | .5102 | .5107 | .5111 | .5116 |
| 1.52 | .5120 | .5125 | .5130 | .5135 | .5140 |
| 1.53 | .5145 | .5150 | .5156 | .5161 | .5167 |
| 1.54 | .5173 | .5178 | .5184 | .5190 | .5196 |
| 1.55 | .5203 | .5209 | .5215 | .5222 | .5228 |
| 1.56 | .5235 | .5242 | .5249 | .5256 | .5263 |
| 1.57 | .5270 | .5278 | .5285 | .5293 | .5300 |
| 1.58 | .5308 | .5316 | .5324 | .5332 | .5340 |
| 1.59 | .5349 | .5357 | .5366 | .5374 | .5383 |
| 1.60 | .5392 | .5401 | .5410 | .5419 | .5429 |
| 1.61 | .5438 | .5448 | .5458 | .5468 | .5477 |
| 1.62 | .5487 | .5498 | .5508 | .5518 | .5529 |
| 1.63 | .5539 | .5550 | .5561 | .5572 | .5583 |
| 1.64 | .5594 | .5606 | .5617 | .5629 | .5641 |
| 1.65 | .5653 | .5664 | .5677 | .5689 | .5701 |
| 1.66 | .5714 | .5726 | 5739 | .5752 | .5765 |
| 1.67 | .5778 | .5791 | .5805 | .5818 | .5832 |
| 1.68 | .5845 | .5859 | .5873 | .5887 | .5902 |
| 1.69 | .5916 | .5931 | .5945 | .5960 | .5975 |
| 1.70 | .5990 | .6005 | .6021 | .6036 | .6052 |
| 1.71 | .6067 | .6083 | .6099 | .6115 | .6132 |
| 1.72 | .6148 | .6165 | .6181 | .6198 | .6215 |
| 1.73 | .6232 | .6250 | .6267 | .6284 | .6302 |
| 1.74 | .6320 | .6338 | .6356 | .6374 | .6393 |
| 1.75 | .6411 | .6430 | .6449 | .6468 | .6487 |
| 1.76 | .6506 | .6525 | .6545 | .6564 | .6584 |
| 1.77 | .6604 | .6624 | .6645 | .6665 | .6686 |
| 1.78 | .6706 | .6727 | .6748 | .6770 | .6791 |
| 1.79 | .6812 | .6834 | .6856 | .6878 | .6900 |
| 1.80 | .6922 | .6944 | .6967 | .6990 | .7013 |
| 1.81 | .7036 | .7059 | .7082 | .7106 | .7129 |
| 1.82 | .7153 | .7177 | .7201 | .7225 | .7250 |
| 1.83 | .7274 | .7299 | .7324 | .7349 | .7374 |
| 1.84 | .7400 | .7425 | .7451 | .7477 | .7503 |
| 1.85 | .7529 | .7556 | .7582 | .7609 | .7636 |
| 1.86 | .7663 | .7690 | .7718 | .7745 | .7773 |
| 1.87 | .7801 | .7829 | .7857 | .7886 | .7914 |
| 1.88 | .7943 | .7972 | .8001 | .8030 | .8060 |
| 1.89 | .8090 | .8119 | .8149 | .8179 | .8209 |
| 1.90 | .8240 | .8271 | .8302 | .8333 | .8364 |
| 1.91 | .8395 | .8427 | .8459 | .8490 | .8523 |
| 1.92 | .8555 | .8587 | .8620 | .8653 | .8686 |
| 1.93 | .8719 | .8752 | .8786 | .8819 | .8854 |
| 1.94 | .8888 | .8922 | .8957 | .8991 | .9026 |
| 1.95 | .9061 | .9096 | .9132 | .9168 | .9203 |
| 1.96 | .9239 | .9276 | .9312 | .9348 | .9385 |
| 1.97 | .9422 | .9459 | .9497 | .9534 | .9572 |
| 1.98 | .9610 | .9648 | .9686 | .9725 | .9764 |
| 1.99 | .9802 | .9842 | .9881 | .9920 | .9960 |

Advantage may be taken of this shortened computation in the event that the experimental intensities are not measured on a quantitative scale, but are merely compared by means of inequalities. If the several spectra *hkl* are arranged in order of decreasing intensity, $I$, then they are also arranged in order of decreasing $(I)^{\frac{1}{2}}$. Thus, if an arrangement of atoms can be found whose computed $(I)^{\frac{1}{2}}$'s are in the same order as the observed blackening on the x-ray photographs, the computed $I$'s are in the same order. In order to make use of this shortened form for trial and error computations, we present Tables VI–X, which are the square roots of the functions given in Tables I–V, respectively.

There are further advantages[4] to the use of square-root correction factors. This can be realized by arranging the computations in a certain form. This is derived as follows:

The amplitude, $F$, is complex, and, for computational purposes, is split into a real component and an imaginary component. Calling these components $A$ and $B$ for atoms of unit scattering power, the scattering power of a collection of actual atoms is given by

$$|F|^2=(f_1A_1+f_2A_2\cdots)^2+(f_1B_1+f_2B_2\cdots)^2, \quad (9)$$

where the subscripts 1, 2, $\cdots$ relate to the first, second, $\cdots$, etc., atoms in the cell, and $f$ is the scattering power of the particular atom for that reflection. Combining this with (7), the computation becomes

$$\begin{aligned} I\sim p\csc\Upsilon\{&(f_1A_1+f_2A_2+\cdots)^2 \\ &+(f_1B_1+f_2B_2+\cdots)^2\} \\ \sim\{&(p\csc\Upsilon)^{\frac{1}{2}}(f_1A_1+f_2A_2\cdots)\}^2 \\ &+\{(p\csc\Upsilon)^{\frac{1}{2}}(f_1B_1+f_2B_2+\cdots)\}^2. \end{aligned} \quad (10)$$

It is convenient and usual to lump together the $fA$ (and also the $fB$) terms for sets of identical atoms which are related by space group operations so that the terms in the parentheses of (9) are condensed to produce a "structure factor." This condensation can be symbolically represented by

$$f_1A_1+f_1A_2+f_1A_3+\cdots=f_1m_1\bar{A}_1. \quad (11)$$

Here, $m_1\bar{A}_1$ is the "structure factor" of the atom set I. It is composed of an integral part, $m_1$, which is the number of identical atoms in the set, and a trigonometric part $\bar{A}_1$. The form of the

[4] M. J. Buerger, "Numerical structure factor tables," Special Paper Number 33, Geological Society of America (1941), pages 7–11.

TABLE III. Unscaled part of Lorentz factor, $S \cdot L$ ($=\csc \tau$), as a function of $\tau$.

| | 0 | .1 | .2 | .3 | .4 | .5 | .6 | .7 | .8 | .9 |
|---|---|---|---|---|---|---|---|---|---|---|
| 0 | ∞ | 572.96 | 286.48 | 190.99 | 143.24 | 114.59 | 95.495 | 81.853 | 71.622 | 63.665 |
| 1 | 57.299 | 52.090 | 47.750 | 44.077 | 40.930 | 38.202 | 35.815 | 33.708 | 31.836 | 30.161 |
| 2 | 28.654 | 27.290 | 26.050 | 24.918 | 23.880 | 22.926 | 22.044 | 21.229 | 20.471 | 19.766 |
| 3 | 19.107 | 18.492 | 17.914 | 17.372 | 16.862 | 16.380 | 15.926 | 15.496 | 15.089 | 14.703 |
| 4 | 14.336 | 13.987 | 13.654 | 13.337 | 13.035 | 12.745 | 12.469 | 12.204 | 11.951 | 11.707 |
| 5 | 11.474 | 11.249 | 11.034 | 10.826 | 10.626 | 10.433 | 10.248 | 10.068 | 9.895 | 9.728 |
| 6 | 9.567 | 9.411 | 9.259 | 9.113 | 8.971 | 8.834 | 8.700 | 8.571 | 8.446 | 8.324 |
| 7 | 8.206 | 8.091 | 7.979 | 7.870 | 7.764 | 7.661 | 7.561 | 7.464 | 7.368 | 7.276 |
| 8 | 7.185 | 7.097 | 7.011 | 6.927 | 6.845 | 6.766 | 6.687 | 6.611 | 6.537 | 6.464 |
| 9 | 6.393 | 6.323 | 6.255 | 6.188 | 6.123 | 6.059 | 5.996 | 5.935 | 5.875 | 5.816 |
| 10 | 5.759 | 5.702 | 5.647 | 5.593 | 5.540 | 5.487 | 5.436 | 5.386 | 5.337 | 5.288 |
| 11 | 5.241 | 5.194 | 5.148 | 5.103 | 5.059 | 5.016 | 4.973 | 4.931 | 4.890 | 4.850 |
| 12 | 4.810 | 4.771 | 4.732 | 4.694 | 4.657 | 4.620 | 4.584 | 4.549 | 4.514 | 4.479 |
| 13 | 4.445 | 4.412 | 4.379 | 4.347 | 4.315 | 4.284 | 4.253 | 4.222 | 4.192 | 4.163 |
| 14 | 4.134 | 4.105 | 4.077 | 4.049 | 4.021 | 3.994 | 3.967 | 3.941 | 3.915 | 3.889 |
| 15 | 3.864 | 3.839 | 3.814 | 3.790 | 3.766 | 3.742 | 3.719 | 3.696 | 3.673 | 3.650 |
| 16 | 3.628 | 3.606 | 3.584 | 3.563 | 3.542 | 3.521 | 3.500 | 3.480 | 3.460 | 3.440 |
| 17 | 3.420 | 3.401 | 3.382 | 3.363 | 3.344 | 3.326 | 3.307 | 3.289 | 3.271 | 3.254 |
| 18 | 3.236 | 3.219 | 3.202 | 3.185 | 3.168 | 3.152 | 3.135 | 3.119 | 3.103 | 3.087 |
| 19 | 3.072 | 3.056 | 3.041 | 3.026 | 3.011 | 2.996 | 2.981 | 2.967 | 2.952 | 2.938 |
| 20 | 2.924 | 2.910 | 2.896 | 2.882 | 2.869 | 2.856 | 2.842 | 2.829 | 2.816 | 2.803 |
| 21 | 2.790 | 2.778 | 2.765 | 2.753 | 2.741 | 2.729 | 2.717 | 2.705 | 2.693 | 2.681 |
| 22 | 2.670 | 2.658 | 2.647 | 2.635 | 2.624 | 2.613 | 2.602 | 2.591 | 2.581 | 2.570 |
| 23 | 2.559 | 2.549 | 2.538 | 2.528 | 2.518 | 2.508 | 2.498 | 2.488 | 2.478 | 2.468 |
| 24 | 2.459 | 2.449 | 2.440 | 2.430 | 2.421 | 2.411 | 2.402 | 2.393 | 2.384 | 2.375 |
| 25 | 2.366 | 2.357 | 2.349 | 2.340 | 2.331 | 2.323 | 2.314 | 2.306 | 2.298 | 2.289 |
| 26 | 2.281 | 2.273 | 2.265 | 2.257 | 2.249 | 2.241 | 2.233 | 2.226 | 2.218 | 2.210 |
| 27 | 2.203 | 2.195 | 2.188 | 2.180 | 2.173 | 2.166 | 2.158 | 2.151 | 2.144 | 2.137 |
| 28 | 2.130 | 2.123 | 2.116 | 2.109 | 2.103 | 2.096 | 2.089 | 2.082 | 2.076 | 2.069 |
| 29 | 2.063 | 2.056 | 2.050 | 2.043 | 2.037 | 2.031 | 2.025 | 2.018 | 2.012 | 2.006 |
| 30 | 2.000 | 1.994 | 1.988 | 1.982 | 1.976 | 1.970 | 1.964 | 1.959 | 1.953 | 1.947 |
| 31 | 1.942 | 1.936 | 1.930 | 1.925 | 1.919 | 1.914 | 1.908 | 1.903 | 1.898 | 1.892 |
| 32 | 1.887 | 1.882 | 1.877 | 1.871 | 1.866 | 1.861 | 1.856 | 1.851 | 1.846 | 1.841 |
| 33 | 1.836 | 1.831 | 1.826 | 1.821 | 1.817 | 1.812 | 1.807 | 1.802 | 1.798 | 1.793 |
| 34 | 1.788 | 1.784 | 1.779 | 1.775 | 1.770 | 1.766 | 1.761 | 1.757 | 1.752 | 1.748 |
| 35 | 1.743 | 1.739 | 1.735 | 1.731 | 1.726 | 1.722 | 1.718 | 1.714 | 1.710 | 1.705 |
| 36 | 1.701 | 1.697 | 1.693 | 1.689 | 1.685 | 1.681 | 1.677 | 1.673 | 1.669 | 1.666 |
| 37 | 1.662 | 1.658 | 1.654 | 1.650 | 1.646 | 1.643 | 1.639 | 1.635 | 1.632 | 1.628 |
| 38 | 1.624 | 1.621 | 1.617 | 1.613 | 1.610 | 1.606 | 1.603 | 1.599 | 1.596 | 1.592 |
| 39 | 1.589 | 1.586 | 1.582 | 1.579 | 1.575 | 1.572 | 1.569 | 1.566 | 1.562 | 1.559 |
| 40 | 1.556 | 1.553 | 1.549 | 1.546 | 1.543 | 1.540 | 1.537 | 1.534 | 1.530 | 1.527 |
| 41 | 1.524 | 1.521 | 1.518 | 1.515 | 1.512 | 1.509 | 1.506 | 1.503 | 1.500 | 1.497 |
| 42 | 1.494 | 1.492 | 1.489 | 1.486 | 1.483 | 1.480 | 1.477 | 1.475 | 1.472 | 1.469 |
| 43 | 1.466 | 1.464 | 1.461 | 1.458 | 1.455 | 1.453 | 1.450 | 1.447 | 1.445 | 1.442 |
| 44 | 1.440 | 1.437 | 1.434 | 1.432 | 1.429 | 1.427 | 1.424 | 1.422 | 1.419 | 1.417 |
| 45 | 1.414 | 1.412 | 1.409 | 1.407 | 1.404 | 1.402 | 1.400 | 1.397 | 1.395 | 1.393 |
| 46 | 1.390 | 1.388 | 1.386 | 1.383 | 1.381 | 1.379 | 1.376 | 1.374 | 1.372 | 1.370 |
| 47 | 1.367 | 1.365 | 1.363 | 1.361 | 1.359 | 1.356 | 1.354 | 1.352 | 1.350 | 1.348 |
| 48 | 1.346 | 1.344 | 1.341 | 1.339 | 1.337 | 1.335 | 1.333 | 1.331 | 1.329 | 1.327 |
| 49 | 1.325 | 1.323 | 1.321 | 1.319 | 1.317 | 1.315 | 1.313 | 1.311 | 1.309 | 1.307 |
| 50 | 1.305 | 1.304 | 1.302 | 1.300 | 1.298 | 1.296 | 1.294 | 1.292 | 1.290 | 1.289 |
| 51 | 1.287 | 1.285 | 1.283 | 1.281 | 1.280 | 1.278 | 1.276 | 1.274 | 1.273 | 1.271 |
| 52 | 1.269 | 1.267 | 1.266 | 1.264 | 1.262 | 1.260 | 1.259 | 1.257 | 1.255 | 1.254 |
| 53 | 1.252 | 1.250 | 1.249 | 1.247 | 1.246 | 1.244 | 1.242 | 1.241 | 1.239 | 1.238 |
| 54 | 1.236 | 1.235 | 1.233 | 1.231 | 1.230 | 1.228 | 1.227 | 1.225 | 1.224 | 1.222 |
| 55 | 1.221 | 1.219 | 1.218 | 1.216 | 1.215 | 1.213 | 1.212 | 1.211 | 1.209 | 1.208 |
| 56 | 1.206 | 1.205 | 1.203 | 1.202 | 1.201 | 1.199 | 1.198 | 1.196 | 1.195 | 1.194 |
| 57 | 1.192 | 1.191 | 1.190 | 1.188 | 1.187 | 1.186 | 1.184 | 1.183 | 1.182 | 1.180 |
| 58 | 1.179 | 1.178 | 1.177 | 1.175 | 1.174 | 1.173 | 1.172 | 1.170 | 1.169 | 1.168 |
| 59 | 1.167 | 1.165 | 1.164 | 1.163 | 1.162 | 1.161 | 1.159 | 1.158 | 1.157 | 1.156 |
| 60 | 1.155 | 1.154 | 1.152 | 1.151 | 1.150 | 1.149 | 1.148 | 1.147 | 1.146 | 1.144 |
| 61 | 1.143 | 1.142 | 1.141 | 1.140 | 1.139 | 1.138 | 1.137 | 1.136 | 1.135 | 1.134 |
| 62 | 1.133 | 1.132 | 1.130 | 1.129 | 1.128 | 1.127 | 1.126 | 1.125 | 1.124 | 1.123 |
| 63 | 1.122 | 1.121 | 1.120 | 1.119 | 1.118 | 1.117 | 1.116 | 1.115 | 1.115 | 1.114 |
| 64 | 1.113 | 1.112 | 1.111 | 1.110 | 1.109 | 1.108 | 1.107 | 1.106 | 1.105 | 1.104 |
| 65 | 1.103 | 1.102 | 1.102 | 1.101 | 1.100 | 1.099 | 1.098 | 1.097 | 1.096 | 1.095 |
| 66 | 1.095 | 1.094 | 1.093 | 1.092 | 1.091 | 1.090 | 1.090 | 1.089 | 1.088 | 1.087 |
| 67 | 1.086 | 1.086 | 1.085 | 1.084 | 1.083 | 1.082 | 1.082 | 1.081 | 1.080 | 1.079 |
| 68 | 1.079 | 1.078 | 1.077 | 1.076 | 1.076 | 1.075 | 1.074 | 1.073 | 1.073 | 1.072 |
| 69 | 1.071 | 1.070 | 1.070 | 1.069 | 1.068 | 1.068 | 1.067 | 1.066 | 1.066 | 1.065 |

TABLE III.—*Continued.*

| | 0 | .1 | .2 | .3 | .4 | .5 | .6 | .7 | .8 | .9 |
|---|---|---|---|---|---|---|---|---|---|---|
| 70 | 1.064 | 1.064 | 1.063 | 1.062 | 1.062 | 1.061 | 1.060 | 1.060 | 1.059 | 1.058 |
| 71 | 1.058 | 1.057 | 1.056 | 1.056 | 1.055 | 1.054 | 1.054 | 1.053 | 1.053 | 1.052 |
| 72 | 1.051 | 1.051 | 1.050 | 1.050 | 1.049 | 1.049 | 1.048 | 1.047 | 1.047 | 1.046 |
| 73 | 1.046 | 1.045 | 1.045 | 1.044 | 1.043 | 1.043 | 1.042 | 1.042 | 1.041 | 1.041 |
| 74 | 1.040 | 1.040 | 1.039 | 1.039 | 1.038 | 1.038 | 1.037 | 1.037 | 1.036 | 1.036 |
| 75 | 1.035 | 1.035 | 1.034 | 1.034 | 1.033 | 1.033 | 1.032 | 1.032 | 1.032 | 1.031 |
| 76 | 1.031 | 1.030 | 1.030 | 1.029 | 1.029 | 1.028 | 1.028 | 1.028 | 1.027 | 1.027 |
| 77 | 1.026 | 1.026 | 1.025 | 1.025 | 1.025 | 1.024 | 1.024 | 1.023 | 1.023 | 1.023 |
| 78 | 1.022 | 1.022 | 1.022 | 1.021 | 1.021 | 1.020 | 1.020 | 1.020 | 1.019 | 1.019 |
| 79 | 1.019 | 1.018 | 1.018 | 1.018 | 1.017 | 1.017 | 1.017 | 1.016 | 1.016 | 1.016 |
| 80 | 1.015 | 1.015 | 1.015 | 1.015 | 1.014 | 1.014 | 1.014 | 1.013 | 1.013 | 1.013 |
| 81 | 1.012 | 1.012 | 1.012 | 1.012 | 1.011 | 1.011 | 1.011 | 1.011 | 1.010 | 1.010 |
| 82 | 1.010 | 1.010 | 1.009 | 1.009 | 1.009 | 1.009 | 1.008 | 1.008 | 1.008 | 1.008 |
| 83 | 1.008 | 1.007 | 1.007 | 1.007 | 1.007 | 1.006 | 1.006 | 1.006 | 1.006 | 1.006 |
| 84 | 1.006 | 1.005 | 1.005 | 1.005 | 1.005 | 1.005 | 1.004 | 1.004 | 1.004 | 1.004 |
| 85 | 1.004 | 1.004 | 1.004 | 1.003 | 1.003 | 1.003 | 1.003 | 1.003 | 1.003 | 1.003 |
| 86 | 1.002 | 1.002 | 1.002 | 1.002 | 1.002 | 1.002 | 1.002 | 1.002 | 1.002 | 1.001 |
| 87 | 1.001 | 1.001 | 1.001 | 1.001 | 1.001 | 1.001 | 1.001 | 1.001 | 1.001 | 1.001 |
| 88 | 1.001 | 1.001 | 1.000 | 1.000 | 1.000 | 1.000 | 1.000 | 1.000 | 1.000 | 1.000 |
| 89 | 1.000 | 1.000 | 1.000 | 1.000 | 1.000 | 1.000 | 1.000 | 1.000 | 1.000 | 1.000 |
| 90 | 1.000 | 1.000 | 1.000 | 1.000 | 1.000 | 1.000 | 1.000 | 1.000 | 1.000 | 1.000 |
| 91 | 1.000 | 1.000 | 1.000 | 1.000 | 1.000 | 1.000 | 1.000 | 1.000 | 1.001 | 1.001 |
| 92 | 1.001 | 1.001 | 1.001 | 1.001 | 1.001 | 1.001 | 1.001 | 1.001 | 1.001 | 1.001 |
| 93 | 1.001 | 1.002 | 1.002 | 1.002 | 1.002 | 1.002 | 1.002 | 1.002 | 1.002 | 1.002 |
| 94 | 1.003 | 1.003 | 1.003 | 1.003 | 1.003 | 1.003 | 1.003 | 1.004 | 1.004 | 1.004 |
| 95 | 1.004 | 1.004 | 1.004 | 1.004 | 1.005 | 1.005 | 1.005 | 1.005 | 1.005 | 1.006 |
| 96 | 1.006 | 1.006 | 1.006 | 1.006 | 1.006 | 1.007 | 1.007 | 1.007 | 1.007 | 1.008 |
| 97 | 1.008 | 1.008 | 1.008 | 1.008 | 1.009 | 1.009 | 1.009 | 1.009 | 1.010 | 1.010 |
| 98 | 1.010 | 1.010 | 1.011 | 1.011 | 1.011 | 1.011 | 1.012 | 1.012 | 1.012 | 1.012 |
| 99 | 1.013 | 1.013 | 1.013 | 1.014 | 1.014 | 1.014 | 1.015 | 1.015 | 1.015 | 1.015 |
| 100 | 1.016 | 1.016 | 1.016 | 1.017 | 1.017 | 1.017 | 1.018 | 1.018 | 1.018 | 1.019 |
| 101 | 1.019 | 1.019 | 1.020 | 1.020 | 1.020 | 1.021 | 1.021 | 1.022 | 1.022 | 1.022 |
| 102 | 1.023 | 1.023 | 1.023 | 1.024 | 1.024 | 1.025 | 1.025 | 1.025 | 1.026 | 1.026 |
| 103 | 1.027 | 1.027 | 1.028 | 1.028 | 1.028 | 1.029 | 1.029 | 1.030 | 1.030 | 1.031 |
| 104 | 1.031 | 1.032 | 1.032 | 1.032 | 1.033 | 1.033 | 1.034 | 1.034 | 1.035 | 1.035 |
| 105 | 1.036 | 1.036 | 1.037 | 1.037 | 1.038 | 1.038 | 1.039 | 1.039 | 1.040 | 1.040 |
| 106 | 1.041 | 1.041 | 1.042 | 1.042 | 1.043 | 1.043 | 1.044 | 1.045 | 1.045 | 1.046 |
| 107 | 1.046 | 1.047 | 1.047 | 1.048 | 1.049 | 1.049 | 1.050 | 1.050 | 1.051 | 1.051 |
| 108 | 1.052 | 1.053 | 1.053 | 1.054 | 1.054 | 1.055 | 1.056 | 1.056 | 1.057 | 1.058 |
| 109 | 1.058 | 1.059 | 1.060 | 1.060 | 1.061 | 1.062 | 1.062 | 1.063 | 1.064 | 1.064 |
| 110 | 1.065 | 1.066 | 1.066 | 1.067 | 1.068 | 1.068 | 1.069 | 1.070 | 1.070 | 1.071 |
| 111 | 1.072 | 1.073 | 1.073 | 1.074 | 1.075 | 1.076 | 1.076 | 1.077 | 1.078 | 1.079 |
| 112 | 1.079 | 1.080 | 1.081 | 1.082 | 1.082 | 1.083 | 1.084 | 1.085 | 1.086 | 1.086 |
| 113 | 1.087 | 1.088 | 1.089 | 1.090 | 1.090 | 1.091 | 1.092 | 1.093 | 1.094 | 1.095 |
| 114 | 1.095 | 1.096 | 1.097 | 1.098 | 1.099 | 1.100 | 1.101 | 1.102 | 1.102 | 1.103 |
| 115 | 1.104 | 1.105 | 1.106 | 1.107 | 1.108 | 1.109 | 1.110 | 1.111 | 1.112 | 1.113 |
| 116 | 1.114 | 1.115 | 1.115 | 1.116 | 1.117 | 1.118 | 1.119 | 1.120 | 1.121 | 1.122 |
| 117 | 1.123 | 1.124 | 1.125 | 1.126 | 1.127 | 1.128 | 1.129 | 1.130 | 1.132 | 1.133 |
| 118 | 1.134 | 1.135 | 1.136 | 1.137 | 1.138 | 1.139 | 1.140 | 1.141 | 1.142 | 1.143 |
| 119 | 1.144 | 1.146 | 1.147 | 1.148 | 1.149 | 1.150 | 1.151 | 1.152 | 1.154 | 1.155 |
| 120 | 1.156 | 1.157 | 1.158 | 1.159 | 1.161 | 1.162 | 1.163 | 1.164 | 1.165 | 1.167 |
| 121 | 1.168 | 1.169 | 1.170 | 1.172 | 1.173 | 1.174 | 1.175 | 1.177 | 1.178 | 1.179 |
| 122 | 1.180 | 1.182 | 1.183 | 1.184 | 1.186 | 1.187 | 1.188 | 1.190 | 1.191 | 1.192 |
| 123 | 1.194 | 1.195 | 1.196 | 1.198 | 1.199 | 1.201 | 1.202 | 1.203 | 1.205 | 1.206 |
| 124 | 1.208 | 1.209 | 1.211 | 1.212 | 1.213 | 1.215 | 1.216 | 1.218 | 1.219 | 1.221 |
| 125 | 1.222 | 1.224 | 1.225 | 1.227 | 1.228 | 1.230 | 1.231 | 1.233 | 1.235 | 1.236 |
| 126 | 1.238 | 1.239 | 1.241 | 1.242 | 1.244 | 1.246 | 1.247 | 1.249 | 1.250 | 1.252 |
| 127 | 1.254 | 1.255 | 1.257 | 1.259 | 1.260 | 1.262 | 1.264 | 1.266 | 1.267 | 1.269 |
| 128 | 1.271 | 1.273 | 1.274 | 1.276 | 1.278 | 1.280 | 1.281 | 1.283 | 1.285 | 1.287 |
| 129 | 1.289 | 1.290 | 1.292 | 1.294 | 1.296 | 1.298 | 1.300 | 1.302 | 1.304 | 1.305 |
| 130 | 1.307 | 1.309 | 1.311 | 1.313 | 1.315 | 1.317 | 1.319 | 1.321 | 1.323 | 1.325 |
| 131 | 1.327 | 1.329 | 1.331 | 1.333 | 1.335 | 1.337 | 1.339 | 1.341 | 1.344 | 1.346 |
| 132 | 1.348 | 1.350 | 1.352 | 1.354 | 1.356 | 1.359 | 1.361 | 1.363 | 1.365 | 1.367 |
| 133 | 1.370 | 1.372 | 1.374 | 1.376 | 1.379 | 1.381 | 1.383 | 1.386 | 1.388 | 1.390 |
| 134 | 1.393 | 1.395 | 1.397 | 1.400 | 1.402 | 1.404 | 1.407 | 1.409 | 1.412 | 1.414 |
| 135 | 1.417 | 1.419 | 1.422 | 1.424 | 1.427 | 1.429 | 1.432 | 1.434 | 1.437 | 1.440 |
| 136 | 1.442 | 1.445 | 1.447 | 1.450 | 1.453 | 1.455 | 1.458 | 1.461 | 1.464 | 1.466 |
| 137 | 1.469 | 1.472 | 1.475 | 1.477 | 1.480 | 1.483 | 1.486 | 1.489 | 1.492 | 1.494 |
| 138 | 1.497 | 1.500 | 1.503 | 1.506 | 1.509 | 1.512 | 1.515 | 1.518 | 1.521 | 1.524 |
| 139 | 1.527 | 1.530 | 1.534 | 1.537 | 1.540 | 1.543 | 1.546 | 1.549 | 1.553 | 1.556 |

TABLE III.—*Continued.*

| | 0 | .1 | .2 | .3 | .4 | .5 | .6 | .7 | .8 | .9 |
|---|---|---|---|---|---|---|---|---|---|---|
| 140 | 1.559 | 1.562 | 1.566 | 1.569 | 1.572 | 1.575 | 1.579 | 1.582 | 1.586 | 1.589 |
| 141 | 1.592 | 1.596 | 1.599 | 1.603 | 1.606 | 1.610 | 1.613 | 1.617 | 1.621 | 1.624 |
| 142 | 1.628 | 1.632 | 1.635 | 1.639 | 1.643 | 1.646 | 1.650 | 1.654 | 1.658 | 1.662 |
| 143 | 1.666 | 1.669 | 1.673 | 1.677 | 1.681 | 1.685 | 1.689 | 1.693 | 1.697 | 1.701 |
| 144 | 1.705 | 1.710 | 1.714 | 1.718 | 1.722 | 1.726 | 1.731 | 1.735 | 1.739 | 1.743 |
| 145 | 1.748 | 1.752 | 1.757 | 1.761 | 1.766 | 1.770 | 1.775 | 1.779 | 1.784 | 1.788 |
| 146 | 1.793 | 1.798 | 1.802 | 1.807 | 1.812 | 1.817 | 1.821 | 1.826 | 1.831 | 1.836 |
| 147 | 1.841 | 1.846 | 1.851 | 1.856 | 1.861 | 1.866 | 1.871 | 1.877 | 1.882 | 1.887 |
| 148 | 1.892 | 1.898 | 1.903 | 1.908 | 1.914 | 1.919 | 1.925 | 1.930 | 1.936 | 1.942 |
| 149 | 1.947 | 1.953 | 1.959 | 1.964 | 1.970 | 1.976 | 1.982 | 1.988 | 1.994 | 2.000 |
| 150 | 2.006 | 2.012 | 2.018 | 2.025 | 2.031 | 2.037 | 2.043 | 2.050 | 2.056 | 2.063 |
| 151 | 2.069 | 2.076 | 2.082 | 2.089 | 2.096 | 2.103 | 2.109 | 2.116 | 2.123 | 2.130 |
| 152 | 2.137 | 2.144 | 2.151 | 2.158 | 2.166 | 2.173 | 2.180 | 2.188 | 2.195 | 2.203 |
| 153 | 2.210 | 2.218 | 2.226 | 2.233 | 2.241 | 2.249 | 2.257 | 2.265 | 2.273 | 2.281 |
| 154 | 2.289 | 2.298 | 2.306 | 2.314 | 2.323 | 2.331 | 2.340 | 2.349 | 2.357 | 2.366 |
| 155 | 2.375 | 2.384 | 2.393 | 2.402 | 2.411 | 2.421 | 2.430 | 2.440 | 2.449 | 2.459 |
| 156 | 2.468 | 2.478 | 2.488 | 2.498 | 2.508 | 2.518 | 2.528 | 2.538 | 2.549 | 2.559 |
| 157 | 2.570 | 2.581 | 2.591 | 2.602 | 2.613 | 2.624 | 2.635 | 2.647 | 2.658 | 2.670 |
| 158 | 2.681 | 2.693 | 2.705 | 2.717 | 2.729 | 2.741 | 2.753 | 2.765 | 2.778 | 2.790 |
| 159 | 2.803 | 2.816 | 2.829 | 2.842 | 2.856 | 2.869 | 2.882 | 2.896 | 2.910 | 2.924 |
| 160 | 2.938 | 2.952 | 2.967 | 2.981 | 2.996 | 3.011 | 3.026 | 3.041 | 3.056 | 3.072 |
| 161 | 3.087 | 3.103 | 3.119 | 3.135 | 3.152 | 3.168 | 3.185 | 3.202 | 3.219 | 3.236 |
| 162 | 3.254 | 3.271 | 3.289 | 3.307 | 3.326 | 3.344 | 3.363 | 3.382 | 3.401 | 3.420 |
| 163 | 3.440 | 3.460 | 3.480 | 3.500 | 3.521 | 3.542 | 3.563 | 3.584 | 3.606 | 3.628 |
| 164 | 3.650 | 3.673 | 3.696 | 3.719 | 3.742 | 3.766 | 3.790 | 3.814 | 3.839 | 3.864 |
| 165 | 3.889 | 3.915 | 3.941 | 3.967 | 3.994 | 4.021 | 4.049 | 4.077 | 4.105 | 4.134 |
| 166 | 4.163 | 4.192 | 4.222 | 4.253 | 4.284 | 4.315 | 4.347 | 4.379 | 4.412 | 4.445 |
| 167 | 4.479 | 4.514 | 4.549 | 4.584 | 4.620 | 4.657 | 4.694 | 4.732 | 4.771 | 4.810 |
| 168 | 4.850 | 4.890 | 4.931 | 4.973 | 5.016 | 5.059 | 5.103 | 5.148 | 5.194 | 5.241 |
| 169 | 5.288 | 5.337 | 5.386 | 5.436 | 5.487 | 5.540 | 5.593 | 5.647 | 5.702 | 5.759 |
| 170 | 5.816 | 5.875 | 5.935 | 5.996 | 6.059 | 6.123 | 6.188 | 6.255 | 6.323 | 6.393 |
| 171 | 6.464 | 6.537 | 6.611 | 6.687 | 6.766 | 6.845 | 6.927 | 7.011 | 7.097 | 7.185 |
| 172 | 7.276 | 7.368 | 7.464 | 7.561 | 7.661 | 7.764 | 7.870 | 7.979 | 8.091 | 8.206 |
| 173 | 8.324 | 8.446 | 8.571 | 8.700 | 8.834 | 8.971 | 9.113 | 9.259 | 9.411 | 9.567 |
| 174 | 9.728 | 9.895 | 10.068 | 10.248 | 10.433 | 10.626 | 10.826 | 11.034 | 11.249 | 11.474 |
| 175 | 11.707 | 11.951 | 12.204 | 12.469 | 12.745 | 13.035 | 13.337 | 13.654 | 13.987 | 14.336 |
| 176 | 14.703 | 15.089 | 15.496 | 15.926 | 16.380 | 16.862 | 17.372 | 17.914 | 18.492 | 19.107 |
| 177 | 19.766 | 20.471 | 21.229 | 22.044 | 22.926 | 23.880 | 24.918 | 26.050 | 27.290 | 28.654 |
| 178 | 30.161 | 31.836 | 33.708 | 35.815 | 38.202 | 40.930 | 44.077 | 47.750 | 52.090 | 57.299 |
| 179 | 63.665 | 71.622 | 81.853 | 95.495 | 114.59 | 143.24 | 190.99 | 286.48 | 572.96 | ∞ |

entire structure factor is available in several places[5,6] and the variation of the trigonometric part with the location of a representative atom of the set is also available.[4,7] Substituting (11) in (10), it becomes

$$I\sim\{[(p\csc\Upsilon)^{\frac{1}{2}}f_{\mathrm{I}}m_{\mathrm{I}}]\bar{A}_{\mathrm{I}}+[(p\csc\Upsilon)^{\frac{1}{2}}f_{\mathrm{II}}m_{\mathrm{II}}]\bar{A}_{\mathrm{II}}+\cdots\}^2$$

The advantage in using the square roots of the corrections is that the computations represented by the several terms in square brackets need be made only once for each particular reflection for the entire trial and error computation process. It is applied as a coefficient to the only variable parts of the computation, namely $\bar{A}$ and $\bar{B}$. Designating this coefficient by

$$I\sim\{(p\csc\Upsilon)^{\frac{1}{2}}(f_{\mathrm{I}}m_{\mathrm{I}}\bar{A}_{\mathrm{I}}+f_{\mathrm{II}}m_{\mathrm{II}}\bar{A}_{\mathrm{II}}+\cdots)\}^2+\{(p\csc\Upsilon)^{\frac{1}{2}}(f_{\mathrm{I}}m_{\mathrm{I}}\bar{B}_{\mathrm{I}}+f_{\mathrm{II}}m_{\mathrm{II}}\bar{B}_{\mathrm{II}}+\cdots)\}^2. \quad (12)$$

For computational purposes, this is expanded and arranged in columns as follows:

$$+\{[(p\csc\Upsilon)^{\frac{1}{2}}f_{\mathrm{I}}m_{\mathrm{I}}]\bar{B}_{\mathrm{I}}+[(p\csc\Upsilon)^{\frac{1}{2}}f_{\mathrm{II}}m_{\mathrm{II}}]\bar{B}_{\mathrm{II}}+\cdots\}^2. \quad (13)$$

$$C=(p\csc\Upsilon)^{\frac{1}{2}}fm, \quad (14)$$

[5] *International Tables for the Determination of Crystal Structures* (Gebrüder Borntraeger, Berlin, 1935).

[6] Kathleen Lonsdale, *Simplified Structure Factor and Electron Density Formulae for the 230 Space Groups of Mathematical Crystallography* (G. Bell & Sons, Ltd., London, 1936).

[7] W. L. Bragg and H. Lipson, "The employment of contoured graphs of structure-factor in crystal analysis," Zeits. f. Krist. (A) **95**, 323–337 (1936).

TABLE IV. Lorentz-polarization factor, $L \cdot p \left( = \frac{1}{\sin 2\theta} \cdot \frac{1+\cos^2 2\theta}{2} \right)$, as a function of $\sin \theta$.

*Valid only for zero level when* $\mu = 0$.

| | .000 | .001 | .002 | .003 | .004 | .005 | .006 | .007 | .008 | .009 |
|---|---|---|---|---|---|---|---|---|---|---|
| .00 | ∞ | 502.51 | 249.37 | 166.66 | 125.62 | 100.19 | 83.327 | 71.268 | 62.531 | 55.516 |
| .01 | 49.990 | 45.464 | 41.637 | 38.448 | 35.713 | 33.340 | 31.234 | 29.403 | 27.775 | 26.297 |
| .02 | 24.986 | 23.800 | 22.705 | 21.721 | 20.818 | 19.975 | 19.208 | 18.501 | 17.842 | 17.218 |
| .03 | 16.645 | 16.111 | 15.598 | 15.127 | 14.682 | 14.257 | 13.862 | 13.489 | 13.128 | 12.786 |
| .04 | 12.472 | 12.163 | 11.874 | 11.598 | 11.330 | 11.078 | 10.833 | 10.602 | 10.382 | 10.165 |
| .05 | 9.9675 | 9.7664 | 9.5755 | 9.3944 | 9.2199 | 9.0492 | 8.8870 | 8.7312 | 8.5777 | 8.4315 |
| .06 | 8.2880 | 8.1513 | 8.0176 | 7.8894 | 7.7658 | 7.6434 | 7.5272 | 7.4120 | 7.3024 | 7.1938 |
| .07 | 7.0904 | 6.9898 | 6.8905 | 6.7953 | 6.7013 | 6.6110 | 6.5218 | 6.4362 | 6.3514 | 6.2704 |
| .08 | 6.1899 | 6.1123 | 6.0359 | 5.9621 | 5.8893 | 5.8192 | 5.7493 | 5.6823 | 5.6158 | 5.5518 |
| .09 | 5.4882 | 5.4274 | 5.3669 | 5.3072 | 5.2488 | 5.1928 | 5.1367 | 5.0821 | 5.0291 | 4.9766 |
| .10 | 4.9258 | 4.8751 | 4.8268 | 4.7777 | 4.7300 | 4.6841 | 4.6382 | 4.5937 | 4.5494 | 4.5061 |
| .11 | 4.4642 | 4.4222 | 4.3810 | 4.3413 | 4.3013 | 4.2623 | 4.2247 | 4.1869 | 4.1497 | 4.1137 |
| .12 | 4.0779 | 4.0425 | 4.0079 | 3.9743 | 3.9405 | 3.9074 | 3.8748 | 3.8434 | 3.8117 | 3.7806 |
| .13 | 3.7499 | 3.7203 | 3.6906 | 3.6612 | 3.6324 | 3.6040 | 3.5764 | 3.5487 | 3.5216 | 3.4947 |
| .14 | 3.4682 | 3.4422 | 3.4164 | 3.3915 | 3.3664 | 3.3417 | 3.3174 | 3.2934 | 3.2696 | 3.2488 |
| .15 | 3.2231 | 3.2003 | 3.1779 | 3.1556 | 3.1337 | 3.1120 | 3.0906 | 3.0696 | 3.0487 | 3.0281 |
| .16 | 3.0081 | 2.9877 | 2.9679 | 2.9482 | 2.9292 | 2.9097 | 2.8908 | 2.8721 | 2.8533 | 2.8350 |
| .17 | 2.8170 | 2.7992 | 2.7815 | 2.7641 | 2.7468 | 2.7295 | 2.7126 | 2.6960 | 2.6794 | 2.6629 |
| .18 | 2.6467 | 2.6308 | 2.6150 | 2.5991 | 2.5837 | 2.5684 | 2.5533 | 2.5380 | 2.5232 | 2.5086 |
| .19 | 2.4938 | 2.4794 | 2.4650 | 2.4509 | 2.4370 | 2.4230 | 2.4093 | 2.3956 | 2.3821 | 2.3689 |
| .20 | 2.3556 | 2.3426 | 2.3295 | 2.3167 | 2.3039 | 2.2914 | 2.2788 | 2.2663 | 2.2541 | 2.2419 |
| .21 | 2.2298 | 2.2180 | 2.2060 | 2.1944 | 2.1828 | 2.1712 | 2.1599 | 2.1485 | 2.1372 | 2.1262 |
| .22 | 2.1152 | 2.1042 | 2.0933 | 2.0827 | 2.0720 | 2.0614 | 2.0509 | 2.0405 | 2.0303 | 2.0201 |
| .23 | 2.0099 | 1.9999 | 1.9899 | 1.9800 | 1.9702 | 1.9605 | 1.9508 | 1.9412 | 1.9317 | 1.9223 |
| .24 | 1.9129 | 1.9037 | 1.8945 | 1.8854 | 1.8763 | 1.8674 | 1.8585 | 1.8497 | 1.8409 | 1.8322 |
| .25 | 1.8234 | 1.8149 | 1.8064 | 1.7980 | 1.7896 | 1.7812 | 1.7729 | 1.7648 | 1.7567 | 1.7485 |
| .26 | 1.7405 | 1.7325 | 1.7246 | 1.7167 | 1.7089 | 1.7012 | 1.6936 | 1.6859 | 1.6783 | 1.6707 |
| .27 | 1.6633 | 1.6559 | 1.6485 | 1.6412 | 1.6339 | 1.6267 | 1.6195 | 1.6124 | 1.6053 | 1.5982 |
| .28 | 1.5913 | 1.5843 | 1.5774 | 1.5707 | 1.5638 | 1.5571 | 1.5503 | 1.5438 | 1.5372 | 1.5306 |
| .29 | 1.5240 | 1.5175 | 1.5110 | 1.5046 | 1.4982 | 1.4919 | 1.4856 | 1.4794 | 1.4732 | 1.4670 |
| .30 | 1.4609 | 1.4548 | 1.4488 | 1.4428 | 1.4368 | 1.4309 | 1.4250 | 1.4191 | 1.4133 | 1.4075 |
| .31 | 1.4017 | 1.3960 | 1.3903 | 1.3847 | 1.3791 | 1.3734 | 1.3679 | 1.3624 | 1.3569 | 1.3515 |
| .32 | 1.3460 | 1.3407 | 1.3353 | 1.3300 | 1.3247 | 1.3193 | 1.3142 | 1.3089 | 1.3038 | 1.2986 |
| .33 | 1.2935 | 1.2885 | 1.2834 | 1.2784 | 1.2733 | 1.2684 | 1.2635 | 1.2586 | 1.2537 | 1.2488 |
| .34 | 1.2440 | 1.2392 | 1.2344 | 1.2296 | 1.2249 | 1.2202 | 1.2156 | 1.2109 | 1.2063 | 1.2017 |
| .35 | 1.1972 | 1.1926 | 1.1881 | 1.1836 | 1.1791 | 1.1747 | 1.1702 | 1.1659 | 1.1615 | 1.1571 |
| .36 | 1.1528 | 1.1485 | 1.1442 | 1.1399 | 1.1357 | 1.1315 | 1.1273 | 1.1232 | 1.1191 | 1.1149 |
| .37 | 1.1108 | 1.1067 | 1.1027 | 1.0986 | 1.0946 | 1.0907 | 1.0867 | 1.0827 | 1.0788 | 1.0748 |
| .38 | 1.0709 | 1.0671 | 1.0632 | 1.0594 | 1.0556 | 1.0518 | 1.0480 | 1.0443 | 1.0406 | 1.0369 |
| .39 | 1.0331 | 1.0295 | 1.0258 | 1.0222 | 1.0185 | 1.0150 | 1.0114 | 1.0078 | 1.0043 | 1.0007 |
| .40 | .9972 | .9937 | .9903 | .9868 | .9834 | .9800 | .9765 | .9731 | .9698 | .9664 |
| .41 | .9631 | .9597 | .9564 | .9532 | .9499 | .9467 | .9434 | .9402 | .9370 | .9338 |
| .42 | .9306 | .9274 | .9243 | .9212 | .9181 | .9149 | .9119 | .9088 | .9057 | .9027 |
| .43 | .8997 | .8967 | .8937 | .8907 | .8877 | .8848 | .8819 | .8789 | .8761 | .8732 |
| .44 | .8703 | .8674 | .8646 | .8618 | .8590 | .8561 | .8534 | .8506 | .8478 | .8450 |
| .45 | .8423 | .8396 | .8369 | .8342 | .8315 | .8288 | .8262 | .8235 | .8209 | .8183 |
| .46 | .8157 | .8131 | .8105 | .8080 | .8054 | .8029 | .8003 | .7978 | .7953 | .7929 |
| .47 | .7904 | .7879 | .7854 | .7830 | .7806 | .7782 | .7758 | .7734 | .7710 | .7687 |
| .48 | .7663 | .7639 | .7616 | .7593 | .7570 | .7547 | .7524 | .7501 | .7479 | .7456 |
| .49 | .7434 | .7412 | .7390 | .7368 | .7346 | .7324 | .7302 | .7281 | .7259 | .7238 |
| .50 | .7217 | .7195 | .7175 | .7153 | .7133 | .7112 | .7091 | .7071 | .7051 | .7031 |
| .51 | .7010 | .6991 | .6971 | .6951 | .6931 | .6912 | .6892 | .6873 | .6853 | .6834 |
| .52 | .6815 | .6796 | .6777 | .6758 | .6740 | .6722 | .6703 | .6685 | .6667 | .6648 |
| .53 | .6630 | .6612 | .6595 | .6577 | .6559 | .6542 | .6524 | .6507 | .6490 | .6473 |
| .54 | .6456 | .6439 | .6422 | .6406 | .6389 | .6372 | .6356 | .6340 | .6324 | .6308 |
| .55 | .6292 | .6276 | .6260 | .6249 | .6229 | .6213 | .6198 | .6182 | .6167 | .6152 |
| .56 | .6137 | .6122 | .6107 | .6092 | .6078 | .6064 | .6049 | .6035 | .6021 | .6006 |
| .57 | .5993 | .5978 | .5965 | .5951 | .5937 | .5924 | .5910 | .5897 | .5884 | .5871 |
| .58 | .5857 | .5844 | .5832 | .5819 | .5806 | .5794 | .5781 | .5769 | .5756 | .5744 |
| .59 | .5732 | .5720 | .5708 | .5696 | .5685 | .5673 | .5661 | .5650 | .5639 | .5628 |
| .60 | .5616 | .5605 | .5594 | .5583 | .5573 | .5562 | .5552 | .5541 | .5531 | .5520 |
| .61 | .5510 | .5500 | .5490 | .5480 | .5470 | .5461 | .5451 | .5442 | .5432 | .5423 |
| .62 | .5414 | .5405 | .5396 | .5387 | .5378 | .5369 | .5360 | .5352 | .5343 | .5335 |
| .63 | .5327 | .5319 | .5311 | .5303 | .5295 | .5287 | .5279 | .5272 | .5264 | .5257 |
| .64 | .5250 | .5243 | .5235 | .5229 | .5222 | .5215 | .5208 | .5202 | .5195 | .5189 |
| .65 | .5182 | .5176 | .5170 | .5164 | .5158 | .5153 | .5147 | .5141 | .5136 | .5131 |
| .66 | .5125 | .5120 | .5115 | .5110 | .5105 | .5101 | .5096 | .5091 | .5087 | .5083 |

TABLE IV.—*Continued.*

| | .000 | .001 | .002 | .003 | .004 | .005 | .006 | .007 | .008 | .009 |
|---|---|---|---|---|---|---|---|---|---|---|
| .67 | .5079 | .5075 | .5070 | .5067 | .5063 | .5059 | .5056 | .5052 | .5049 | .5045 |
| .68 | .5042 | .5039 | .5036 | .5034 | .5031 | .5028 | .5026 | .5023 | .5021 | .5019 |
| .69 | .5017 | .5015 | .5013 | .5011 | .5010 | .5008 | .5007 | .5006 | .5005 | .5004 |
| .70 | .5003 | .5002 | .5001 | .5001 | .5000 | .5000 | .5000 | .5000 | .5000 | .5000 |
| .71 | .5000 | .5001 | .5001 | .5002 | .5003 | .5004 | .5005 | .5006 | .5007 | .5008 |
| .72 | .5010 | .5012 | .5013 | .5015 | .5017 | .5019 | .5022 | .5024 | .5027 | .5030 |
| .73 | .5032 | .5035 | .5038 | .5042 | .5045 | .5048 | .5052 | .5056 | .5060 | .5064 |
| .74 | .5068 | .5072 | .5077 | .5081 | .5086 | .5091 | .5096 | .5101 | .5107 | .5112 |
| .75 | .5118 | .5124 | .5130 | .5136 | .5142 | .5148 | .5155 | .5162 | .5169 | .5176 |
| .76 | .5183 | .5190 | .5198 | .5205 | .5213 | .5221 | .5230 | .5238 | .5247 | .5255 |
| .77 | .5264 | .5273 | .5282 | .5292 | .5301 | .5311 | .5321 | .5331 | .5341 | .5352 |
| .78 | .5362 | .5373 | .5384 | .5396 | .5407 | .5418 | .5430 | .5442 | .5454 | .5467 |
| .79 | .5479 | .5492 | .5505 | .5518 | .5532 | .5545 | .5559 | .5573 | .5587 | .5602 |
| .80 | .5616 | .5631 | .5647 | .5662 | .5677 | .5693 | .5709 | .5726 | .5742 | .5759 |
| .81 | .5776 | .5793 | .5811 | .5828 | .5846 | .5864 | .5883 | .5902 | .5921 | .5940 |
| .82 | .5960 | .5980 | .6000 | .6020 | .6041 | .6061 | .6083 | .6104 | .6126 | .6148 |
| .83 | .6171 | .6194 | .6217 | .6240 | .6264 | .6288 | .6312 | .6337 | .6362 | .6387 |
| .84 | .6412 | .6438 | .6465 | .6491 | .6518 | .6546 | .6574 | .6602 | .6630 | .6659 |
| .85 | .6688 | .6718 | .6749 | .6779 | .6810 | .6841 | .6873 | .6905 | .6938 | .6971 |
| .86 | .7005 | .7039 | .7073 | .7108 | .7143 | .7179 | .7216 | .7253 | .7290 | .7328 |
| .87 | .7367 | .7405 | .7445 | .7485 | .7526 | .7567 | .7609 | .7652 | .7694 | .7738 |
| .88 | .7782 | .7827 | .7873 | .7919 | .7966 | .8014 | .8062 | .8111 | .8161 | .8212 |
| .89 | .8263 | .8315 | .8368 | .8422 | .8476 | .8531 | .8588 | .8645 | .8703 | .8762 |
| .90 | .8822 | .8883 | .8945 | .9008 | .9072 | .9137 | .9203 | .9270 | .9338 | .9409 |
| .91 | .9479 | .9551 | .9624 | .9699 | .9775 | .9852 | .9931 | 1.0011 | 1.0093 | 1.0176 |
| .92 | 1.0261 | 1.0348 | 1.0436 | 1.0526 | 1.0618 | 1.0711 | 1.0807 | 1.0904 | 1.1003 | 1.1105 |
| .93 | 1.1209 | 1.1314 | 1.1423 | 1.1533 | 1.1647 | 1.1762 | 1.1881 | 1.2002 | 1.2126 | 1.2253 |
| .94 | 1.2384 | 1.2517 | 1.2654 | 1.2794 | 1.2939 | 1.3086 | 1.3238 | 1.3393 | 1.3555 | 1.3720 |
| .95 | 1.3889 | 1.4064 | 1.4244 | 1.4430 | 1.4621 | 1.4819 | 1.5023 | 1.5235 | 1.5452 | 1.5678 |
| .96 | 1.5913 | 1.6156 | 1.6408 | 1.6670 | 1.6942 | 1.7226 | 1.7521 | 1.7831 | 1.8153 | 1.8491 |
| .97 | 1.8845 | 1.9217 | 1.9608 | 2.0019 | 2.0451 | 2.0911 | 2.1399 | 2.1917 | 2.2469 | 2.3056 |
| .98 | 2.3689 | 2.4367 | 2.5103 | 2.5898 | 2.6767 | 2.7719 | 2.8766 | 2.9932 | 3.1239 | 3.2717 |
| .99 | 3.4403 | 3.6364 | 3.8671 | 4.1458 | 4.4898 | 4.9321 | 5.5296 | 6.4024 | 7.8633 | 11.152 |

TABLE V. Lorentz-polarization factor, $L \cdot p \left(= \frac{1}{\sin 2\theta} \cdot \frac{1+\cos^2 2\theta}{2}\right)$, as a function of $\sigma$.

*Valid only for zero level when* $\mu = 0$.

| | .000 | .002 | .004 | .006 | .008 | | .000 | .002 | .004 | .006 | .008 |
|---|---|---|---|---|---|---|---|---|---|---|---|
| .00 | ∞ | 502.51 | 249.37 | 166.66 | 125.62 | .29 | 3.3417 | 3.3174 | 3.2934 | 3.2696 | 3.2488 |
| .01 | 100.19 | 83.327 | 71.268 | 62.531 | 55.516 | .30 | 3.2231 | 3.2003 | 3.1779 | 3.1556 | 3.1337 |
| .02 | 49.990 | 45.464 | 41.637 | 38.448 | 35.713 | .31 | 3.1120 | 3.0906 | 3.0696 | 3.0487 | 3.0281 |
| .03 | 33.340 | 31.234 | 29.403 | 27.775 | 26.297 | .32 | 3.0081 | 2.9877 | 2.9679 | 2.9482 | 2.9292 |
| .04 | 24.986 | 23.800 | 22.705 | 21.721 | 20.818 | .33 | 2.9097 | 2.8908 | 2.8721 | 2.8533 | 2.8350 |
| .05 | 19.975 | 19.208 | 18.501 | 17.842 | 17.218 | .34 | 2.8170 | 2.7992 | 2.7815 | 2.7641 | 2.7468 |
| .06 | 16.645 | 16.111 | 15.598 | 15.127 | 14.682 | .35 | 2.7295 | 2.7126 | 2.6960 | 2.6794 | 2.6629 |
| .07 | 14.257 | 13.862 | 13.489 | 13.128 | 12.786 | .36 | 2.6467 | 2.6308 | 2.6150 | 2.5991 | 2.5837 |
| .08 | 12.472 | 12.163 | 11.874 | 11.598 | 11.330 | .37 | 2.5684 | 2.5533 | 2.5380 | 2.5232 | 2.5086 |
| .09 | 11.078 | 10.833 | 10.602 | 10.382 | 10.165 | .38 | 2.4938 | 2.4794 | 2.4650 | 2.4509 | 2.4370 |
| .10 | 9.9675 | 9.7664 | 9.5755 | 9.3944 | 9.2199 | .39 | 2.4230 | 2.4093 | 2.3956 | 2.3821 | 2.3689 |
| .11 | 9.0492 | 8.8870 | 8.7312 | 8.5777 | 8.4315 | .40 | 2.3556 | 2.3426 | 2.3295 | 2.3167 | 2.3039 |
| .12 | 8.2880 | 8.1513 | 8.0176 | 7.8894 | 7.7658 | .41 | 2.2914 | 2.2788 | 2.2663 | 2.2541 | 2.2419 |
| .13 | 7.6434 | 7.5272 | 7.4120 | 7.3024 | 7.1938 | .42 | 2.2298 | 2.2180 | 2.2060 | 2.1944 | 2.1828 |
| .14 | 7.0904 | 6.9898 | 6.8905 | 6.7953 | 6.7013 | .43 | 2.1712 | 2.1599 | 2.1485 | 2.1372 | 2.1262 |
| .15 | 6.6110 | 6.5218 | 6.4362 | 6.3514 | 6.2704 | .44 | 2.1152 | 2.1042 | 2.0933 | 2.0827 | 2.0720 |
| .16 | 6.1899 | 6.1123 | 6.0359 | 5.9621 | 5.8893 | .45 | 2.0614 | 2.0509 | 2.0405 | 2.0303 | 2.0201 |
| .17 | 5.8192 | 5.7493 | 5.6823 | 5.6158 | 5.5518 | .46 | 2.0099 | 1.9999 | 1.9899 | 1.9800 | 1.9702 |
| .18 | 5.4882 | 5.4274 | 5.3669 | 5.3072 | 5.2488 | .47 | 1.9605 | 1.9508 | 1.9412 | 1.9317 | 1.9223 |
| .19 | 5.1928 | 5.1367 | 5.0821 | 5.0291 | 4.9766 | .48 | 1.9129 | 1.9037 | 1.8945 | 1.8854 | 1.8763 |
| .20 | 4.9258 | 4.8751 | 4.8268 | 4.7777 | 4.7300 | .49 | 1.8674 | 1.8585 | 1.8497 | 1.8409 | 1.8322 |
| .21 | 4.6841 | 4.6382 | 4.5937 | 4.5494 | 4.5061 | .50 | 1.8234 | 1.8149 | 1.8064 | 1.7980 | 1.7896 |
| .22 | 4.4642 | 4.4222 | 4.3810 | 4.3413 | 4.3013 | .51 | 1.7812 | 1.7729 | 1.7648 | 1.7567 | 1.7485 |
| .23 | 4.2623 | 4.2247 | 4.1869 | 4.1497 | 4.1137 | .52 | 1.7405 | 1.7325 | 1.7246 | 1.7167 | 1.7089 |
| .24 | 4.0779 | 4.0425 | 4.0079 | 3.9743 | 3.9405 | .53 | 1.7012 | 1.6936 | 1.6859 | 1.6783 | 1.6707 |
| .25 | 3.9074 | 3.8748 | 3.8434 | 3.8117 | 3.7806 | .54 | 1.6633 | 1.6559 | 1.6485 | 1.6412 | 1.6339 |
| .26 | 3.7499 | 3.7203 | 3.6906 | 3.6612 | 3.6324 | .55 | 1.6267 | 1.6195 | 1.6124 | 1.6053 | 1.5982 |
| .27 | 3.6040 | 3.5764 | 3.5487 | 3.5216 | 3.4947 | .56 | 1.5913 | 1.5843 | 1.5774 | 1.5707 | 1.5638 |
| .28 | 3.4682 | 3.4422 | 3.4164 | 3.3915 | 3.3664 | .57 | 1.5571 | 1.5503 | 1.5438 | 1.5372 | 1.5306 |

TABLE V.—*Continued.*

| | .000 | .002 | .004 | .006 | .008 | | .000 | .002 | .004 | .006 | .008 |
|---|---|---|---|---|---|---|---|---|---|---|---|
| .58 | 1.5240 | 1.5175 | 1.5110 | 1.5046 | 1.4982 | 1.29 | .5215 | .5208 | .5202 | .5195 | .5189 |
| .59 | 1.4919 | 1.4856 | 1.4794 | 1.4732 | 1.4670 | 1.30 | .5182 | .5176 | .5170 | .5164 | .5158 |
| .60 | 1.4609 | 1.4548 | 1.4488 | 1.4428 | 1.4368 | 1.31 | .5153 | .5147 | .5141 | .5136 | .5131 |
| .61 | 1.4309 | 1.4250 | 1.4191 | 1.4133 | 1.4075 | 1.32 | .5125 | .5120 | .5115 | .5110 | .5105 |
| .62 | 1.4017 | 1.3960 | 1.3903 | 1.3847 | 1.3791 | 1.33 | .5101 | .5096 | .5091 | .5087 | .5083 |
| .63 | 1.3734 | 1.3679 | 1.3624 | 1.3569 | 1.3515 | 1.34 | .5079 | .5075 | .5070 | .5067 | .5063 |
| .64 | 1.3460 | 1.3407 | 1.3353 | 1.3300 | 1.3247 | 1.35 | .5059 | .5056 | .5052 | .5049 | .5045 |
| .65 | 1.3193 | 1.3142 | 1.3089 | 1.3038 | 1.2986 | 1.36 | .5042 | .5039 | .5036 | .5034 | .5031 |
| .66 | 1.2935 | 1.2885 | 1.2834 | 1.2784 | 1.2733 | 1.37 | .5028 | .5026 | .5023 | .5021 | .5019 |
| .67 | 1.2684 | 1.2635 | 1.2586 | 1.2537 | 1.2488 | 1.38 | .5017 | .5015 | .5013 | .5011 | .5010 |
| .68 | 1.2440 | 1.2392 | 1.2344 | 1.2296 | 1.2249 | 1.39 | .5008 | .5007 | .5006 | .5005 | .5004 |
| .69 | 1.2202 | 1.2156 | 1.2109 | 1.2063 | 1.2017 | 1.40 | .5003 | .5002 | .5001 | .5001 | .5000 |
| .70 | 1.1972 | 1.1926 | 1.1881 | 1.1836 | 1.1791 | 1.41 | .5000 | .5000 | .5000 | .5000 | .5000 |
| .71 | 1.1747 | 1.1702 | 1.1659 | 1.1615 | 1.1571 | 1.42 | .5000 | .5001 | .5001 | .5002 | 5003 |
| .72 | 1.1528 | 1.1485 | 1.1442 | 1.1399 | 1.1357 | 1.43 | .5004 | .5005 | .5006 | .5007 | .5008 |
| .73 | 1.1315 | 1.1273 | 1.1232 | 1.1191 | 1.1149 | 1.44 | .5010 | .5012 | .5013 | .5015 | .5017 |
| .74 | 1.1108 | 1.1067 | 1.1027 | 1.0986 | 1.0946 | 1.45 | .5019 | .5022 | .5024 | .5027 | .5030 |
| .75 | 1.0907 | 1.0867 | 1.0827 | 1.0788 | 1.0748 | 1.46 | .5032 | .5035 | .5038 | .5042 | .5045 |
| .76 | 1.0709 | 1.0671 | 1.0632 | 1.0594 | 1.0556 | 1.47 | .5048 | .5052 | .5056 | .5060 | .5064 |
| .77 | 1.0518 | 1.0480 | 1.0443 | 1.0406 | 1.0369 | 1.48 | .5068 | .5072 | .5077 | .5081 | .5086 |
| .78 | 1.0331 | 1.0295 | 1.0258 | 1.0222 | 1.0185 | 1.49 | .5091 | .5096 | .5101 | .5107 | .5112 |
| .79 | 1.0150 | 1.0114 | 1.0078 | 1.0043 | 1.0007 | 1.50 | .5118 | .5124 | .5130 | .5136 | .5142 |
| .80 | .9972 | .9937 | .9903 | .9868 | .9834 | 1.51 | .5148 | .5155 | .5162 | .5169 | .5176 |
| .81 | .9800 | .9765 | .9731 | .9698 | .9664 | 1.52 | .5183 | .5190 | .5198 | .5205 | .5213 |
| .82 | .9631 | .9597 | .9564 | .9532 | .9499 | 1.53 | .5221 | .5230 | .5238 | .5247 | .5255 |
| .83 | .9467 | .9434 | .9402 | .9370 | .9338 | 1.54 | .5264 | .5273 | .5282 | .5292 | .5301 |
| .84 | .9306 | .9274 | .9243 | .9212 | .9181 | 1.55 | .5311 | .5321 | .5331 | .5341 | .5352 |
| .85 | .9149 | .9119 | .9088 | .9057 | .9027 | 1.56 | .5362 | .5373 | .5384 | .5396 | .5407 |
| .86 | .8997 | .8967 | .8937 | .8907 | .8877 | 1.57 | .5418 | .5430 | .5442 | .5454 | .5467 |
| .87 | .8848 | .8819 | .8789 | .8761 | .8732 | 1.58 | .5479 | .5492 | .5505 | .5518 | .5532 |
| .88 | .8703 | .8674 | .8646 | .8618 | .8590 | 1.59 | .5545 | .5559 | .5573 | .5587 | .5602 |
| .89 | .8561 | .8534 | .8506 | .8478 | .8450 | 1.60 | .5616 | .5631 | .5647 | .5662 | .5677 |
| .90 | .8423 | .8396 | .8369 | .8342 | .8315 | 1.61 | .5693 | .5709 | .5726 | .5742 | .5759 |
| .91 | .8288 | .8262 | .8235 | .8209 | .8183 | 1.62 | .5776 | .5793 | .5811 | .5828 | .5846 |
| .92 | .8157 | .8131 | .8105 | .8080 | .8054 | 1.63 | .5864 | .5883 | .5902 | .5921 | .5940 |
| .93 | .8029 | .8003 | .7978 | .7953 | .7929 | 1.64 | .5960 | .5980 | .6000 | .6020 | .6041 |
| .94 | .7904 | .7879 | .7854 | .7830 | .7806 | 1.65 | .6061 | .6083 | .6104 | .6126 | .6148 |
| .95 | .7782 | 7758 | .7734 | .7710 | .7687 | 1.66 | .6171 | .6194 | .6217 | .6240 | .6264 |
| 96 | .7663 | .7639 | .7616 | .7593 | .7570 | 1.67 | .6288 | .6312 | .6337 | .6362 | .6387 |
| .97 | .7547 | .7524 | .7501 | .7479 | .7456 | 1.68 | .6412 | .6438 | .6465 | .6491 | .6518 |
| 98 | .7434 | .7412 | .7390 | .7368 | .7346 | 1.69 | .6546 | .6574 | .6602 | .6630 | .6659 |
| .99 | .7324 | .7302 | .7281 | .7259 | .7238 | 1.70 | .6688 | .6718 | .6749 | .6779 | .6810 |
| 1.00 | .7217 | .7195 | .7175 | .7153 | .7133 | 1.71 | .6841 | .6873 | .6905 | .6938 | .6971 |
| 1.01 | .7112 | .7091 | .7071 | .7051 | .7031 | 1.72 | .7005 | .7039 | .7073 | .7108 | .7143 |
| 1.02 | .7010 | .6991 | .6971 | .6951 | .6931 | 1.73 | .7179 | .7216 | .7253 | .7290 | .7328 |
| 1.03 | .6912 | .6892 | .6873 | .6853 | .6834 | 1.74 | .7367 | .7405 | .7445 | .7485 | .7526 |
| 1.04 | .6815 | .6796 | .6777 | .6758 | .6740 | 1.75 | .7567 | .7609 | .7652 | .7694 | .7738 |
| 1.05 | .6722 | .6703 | .6685 | .6667 | .6648 | 1.76 | .7782 | .7827 | .7873 | .7919 | .7966 |
| 1.06 | .6630 | .6612 | .6595 | .6577 | .6559 | 1.77 | .8014 | .8062 | .8111 | .8161 | .8212 |
| 1.07 | 6542 | .6524 | .6507 | .6490 | .6473 | 1.78 | .8263 | .8315 | .8368 | .8422 | .8476 |
| 1.08 | .6456 | .6439 | .6422 | .6406 | .6389 | 1.79 | .8531 | .8588 | .8645 | .8703 | .8762 |
| 1.09 | .6372 | .6356 | .6340 | .6324 | .6308 | 1.80 | .8822 | .8883 | .8945 | .9008 | .9072 |
| 1.10 | .6292 | .6276 | .6260 | .6249 | .6229 | 1.81 | .9137 | .9203 | .9270 | .9338 | .9409 |
| 1.11 | .6213 | 6198 | .6182 | .6167 | .6152 | 1.82 | .9479 | .9551 | .9624 | .9699 | .9775 |
| 1.12 | .6137 | .6122 | .6107 | .6092 | .6078 | 1.83 | .9852 | .9931 | 1.0011 | 1.0093 | 1.0176 |
| 1.13 | .6064 | .6049 | .6035 | .6021 | .6006 | 1.84 | 1.0261 | 1.0348 | 1.0436 | 1.0526 | 1.0618 |
| 1.14 | .5993 | .5978 | .5965 | .5951 | .5937 | 1.85 | 1.0711 | 1.0807 | 1.0904 | 1.1003 | 1.1105 |
| 1.15 | .5924 | .5910 | .5897 | .5884 | .5871 | 1.86 | 1.1209 | 1.1314 | 1.1423 | 1.1533 | 1.1647 |
| 1.16 | .5857 | .5844 | .5832 | .5819 | .5806 | 1.87 | 1.1762 | 1.1881 | 1.2002 | 1.2126 | 1.2253 |
| 1.17 | .5794 | .5781 | .5769 | .5756 | .5744 | 1.88 | 1.2384 | 1.2517 | 1.2654 | 1.2794 | 1.2939 |
| 1.18 | .5732 | .5720 | .5708 | .5696 | .5685 | 1.89 | 1.3086 | 1.3238 | 1.3393 | 1.3555 | 1.3720 |
| 1.19 | .5673 | .5661 | .5650 | .5639 | .5628 | 1.90 | 1.3889 | 1.4064 | 1.4244 | 1.4430 | 1.4621 |
| 1.20 | .5616 | .5605 | .5594 | .5583 | .5573 | 1.91 | 1.4819 | 1.5023 | 1.5235 | 1.5452 | 1.5678 |
| 1.21 | .5562 | .5552 | .5541 | .5531 | .5520 | 1.92 | 1.5913 | 1.6156 | 1.6408 | 1.6670 | 1.6942 |
| 1.22 | .5510 | .5500 | .5490 | .5480 | .5470 | 1.93 | 1.7226 | 1.7521 | 1.7831 | 1.8153 | 1.8491 |
| 1.23 | .5461 | .5451 | .5442 | .5432 | .5423 | 1.94 | 1.8845 | 1.9217 | 1.9608 | 2.0019 | 2.0451 |
| 1.24 | .5414 | .5405 | .5396 | .5387 | .5378 | 1.95 | 2.0911 | 2.1399 | 2.1917 | 2.2469 | 2.3056 |
| 1.25 | .5369 | .5360 | .5352 | .5343 | 5335 | 1.96 | 2.3689 | 2.4367 | 2.5103 | 2.5898 | 2.6767 |
| 1.26 | .5327 | .5319 | .5311 | .5303 | .5295 | 1.97 | 2.7719 | 2.8766 | 2.9932 | 3.1239 | 3.2717 |
| 1.27 | .5287 | .5279 | .5272 | .5264 | .5257 | 1.98 | 3.4403 | 3.6364 | 3.8671 | 4.1458 | 4.4898 |
| 1.28 | .5250 | .5243 | .5235 | .5229 | .5222 | 1.99 | 4.9321 | 5.5296 | 6.4024 | 7.8633 | 11.152 |

TABLE VI. Polarization factor, $(p)^{\frac{1}{2}} \left[ = \left( \frac{1+\cos^2 2\theta}{2} \right)^{\frac{1}{2}} \right]$, as a function of sin $\theta$.

| | .000 | .001 | .002 | .003 | .004 | .005 | .006 | .007 | .008 | .009 |
|---|---|---|---|---|---|---|---|---|---|---|
| .00 | 1.000 | 1.000 | 1.000 | 1.000 | 1.000 | 1.000 | 1.000 | 1.000 | 1.000 | 1.000 |
| .01 | 1.000 | 1.000 | 1.000 | 1.000 | 1.000 | 1.000 | 1.000 | 1.000 | 1.000 | 1.000 |
| .02 | 1.000 | 1.000 | .999 | .999 | .999 | .999 | .999 | .999 | .999 | .999 |
| .03 | .999 | .999 | .999 | .999 | .999 | .999 | .999 | .999 | .999 | .998 |
| .04 | .998 | .998 | .998 | .998 | .998 | .998 | .998 | .998 | .998 | .998 |
| .05 | .997 | .997 | .997 | .997 | .997 | .997 | .997 | .997 | .997 | .997 |
| .06 | .996 | .996 | .996 | .996 | .996 | .996 | .996 | .996 | .995 | .995 |
| .07 | .995 | .995 | .995 | .995 | .995 | .994 | .994 | .994 | .994 | .994 |
| .08 | .994 | .993 | .993 | .993 | .993 | .993 | .993 | .992 | .992 | .992 |
| .09 | .992 | .992 | .992 | .991 | .991 | .991 | .991 | .991 | .990 | .990 |
| .10 | .990 | .990 | .990 | .989 | .989 | .989 | .989 | .989 | .988 | .988 |
| .11 | .988 | .988 | .988 | .987 | .987 | .987 | .987 | .986 | .986 | .986 |
| .12 | .986 | .985 | .985 | .985 | .985 | .984 | .984 | .984 | .984 | .984 |
| .13 | .983 | .983 | .983 | .982 | .982 | .982 | .982 | .981 | .981 | .981 |
| .14 | .981 | .980 | .980 | .980 | .979 | .979 | .979 | .979 | .978 | .978 |
| .15 | .978 | .977 | .977 | .977 | .977 | .976 | .976 | .976 | .975 | .975 |
| .16 | .975 | .974 | .974 | .974 | .973 | .973 | .973 | .973 | .972 | .972 |
| .17 | .972 | .971 | .971 | .971 | .970 | .970 | .970 | .969 | .969 | .969 |
| .18 | .968 | .968 | .967 | .967 | .967 | .966 | .966 | .966 | .965 | .965 |
| .19 | .965 | .964 | .964 | .963 | .963 | .963 | .962 | .962 | .962 | .961 |
| .20 | .961 | .960 | .960 | .960 | .959 | .959 | .958 | .958 | .958 | .957 |
| .21 | .957 | .957 | .956 | .956 | .955 | .955 | .954 | .954 | .954 | .953 |
| .22 | .953 | .952 | .952 | .952 | .951 | .951 | .950 | .950 | .949 | .949 |
| .23 | .949 | .948 | .948 | .947 | .947 | .946 | .946 | .946 | .945 | .945 |
| .24 | .944 | .944 | .943 | .943 | .942 | .942 | .941 | .941 | .941 | .940 |
| .25 | .940 | .939 | .939 | .938 | .938 | .937 | .937 | .936 | .936 | .935 |
| .26 | .935 | .934 | .934 | .933 | .933 | .932 | .932 | .931 | .931 | .930 |
| .27 | .930 | .929 | .929 | .928 | .928 | .927 | .927 | .926 | .926 | .925 |
| .28 | .925 | .924 | .924 | .923 | .923 | .922 | .922 | .921 | .921 | .920 |
| .29 | .920 | .919 | .919 | .918 | .918 | .917 | .917 | .916 | .916 | .915 |
| .30 | .914 | .914 | .913 | .913 | .912 | .912 | .911 | .911 | .910 | .910 |
| .31 | .909 | .908 | .908 | .907 | .907 | .906 | .906 | .905 | .905 | .904 |
| .32 | .903 | .903 | .902 | .902 | .901 | .901 | .900 | .899 | .899 | .898 |
| .33 | .898 | .897 | .897 | .896 | .895 | .895 | .894 | .894 | .893 | .893 |
| .34 | .892 | .891 | .891 | .890 | .890 | .889 | .888 | .888 | .887 | .887 |
| .35 | .886 | .885 | .885 | .884 | .884 | .883 | .882 | .882 | .881 | .881 |
| .36 | .880 | .879 | .879 | .878 | .878 | .877 | .876 | .876 | .875 | .875 |
| .37 | .874 | .873 | .873 | .872 | .871 | .871 | .870 | .870 | .869 | .868 |
| .38 | .868 | .867 | .866 | .866 | .865 | .865 | .864 | .863 | .863 | .862 |
| .39 | .861 | .861 | .860 | .860 | .859 | .858 | .858 | .857 | .856 | .856 |
| .40 | .855 | .854 | .854 | .853 | .853 | .852 | .851 | .851 | .850 | .849 |
| .41 | .849 | .848 | .847 | .847 | .846 | .846 | .845 | .844 | .844 | .843 |
| .42 | .842 | .842 | .841 | .840 | .840 | .839 | .838 | .838 | .837 | .836 |
| .43 | .836 | .835 | .835 | .834 | .833 | .833 | .832 | .831 | .831 | .830 |
| .44 | .829 | .829 | .828 | .827 | .827 | .826 | .825 | .825 | .824 | .823 |
| .45 | .823 | .822 | .822 | .821 | .820 | .820 | .819 | .818 | .818 | .817 |
| .46 | .816 | .816 | .815 | .814 | .814 | .813 | .812 | .812 | .811 | .810 |
| .47 | .810 | .809 | .809 | .808 | .807 | .807 | .806 | .805 | .805 | .804 |
| .48 | .803 | .803 | .802 | .801 | .801 | .800 | .800 | .799 | .798 | .798 |
| .49 | .797 | .796 | .796 | .795 | .794 | .794 | .793 | .792 | .792 | .791 |
| .50 | .791 | .790 | .789 | .789 | .788 | .787 | .787 | .786 | .785 | .785 |
| .51 | .784 | .784 | .783 | .782 | .782 | .781 | .781 | .780 | .779 | .779 |
| .52 | .778 | .777 | .777 | .776 | .776 | .775 | .774 | .774 | .773 | .773 |
| .53 | .772 | .771 | .771 | .770 | .770 | .769 | .768 | .768 | .767 | .767 |
| .54 | .766 | .766 | .765 | .764 | .764 | .763 | .763 | .762 | .761 | .761 |
| .55 | .760 | .760 | .759 | .759 | .758 | .757 | .757 | .756 | .756 | .755 |
| .56 | .755 | .754 | .754 | .753 | .752 | .752 | .751 | .751 | .750 | .750 |
| .57 | .749 | .749 | .748 | .748 | .747 | .747 | .746 | .746 | .745 | .745 |
| .58 | .744 | .744 | .743 | .742 | .742 | .741 | .741 | .740 | .740 | .740 |
| .59 | .739 | .739 | .738 | .738 | .737 | .737 | .736 | .736 | .735 | .735 |
| .60 | .734 | .734 | .733 | .733 | .732 | .732 | .732 | .731 | .731 | .730 |
| .61 | .730 | .729 | .729 | .729 | .728 | .728 | .727 | .727 | .727 | .726 |
| .62 | .726 | .725 | .725 | .725 | .724 | .724 | .723 | .723 | .723 | .722 |
| .63 | .722 | .722 | .721 | .721 | .721 | .720 | .720 | .720 | .719 | .719 |
| .64 | .719 | .718 | .718 | .718 | .717 | .717 | .717 | .716 | .716 | .716 |
| .65 | .716 | .715 | .715 | .715 | .714 | .714 | .714 | .714 | .713 | .713 |
| .66 | .713 | .713 | .712 | .712 | .712 | .712 | .712 | .711 | .711 | .711 |
| .67 | .711 | .710 | .710 | .710 | .710 | .710 | .710 | .710 | .709 | .709 |

TABLE VI.—*Continued.*

| | .000 | .001 | .002 | .003 | .004 | .005 | .006 | .007 | .008 | .009 |
|---|---|---|---|---|---|---|---|---|---|---|
| .68 | .709 | .709 | .709 | .709 | .709 | .708 | .708 | .708 | .708 | .708 |
| .69 | .708 | .708 | .708 | .708 | .708 | .708 | .707 | .707 | .707 | .707 |
| .70 | .707 | .707 | .707 | .707 | .707 | .707 | .707 | .707 | .707 | .707 |
| .71 | .707 | .707 | .707 | .707 | .707 | .707 | .707 | .707 | .707 | .708 |
| .72 | .708 | .708 | .708 | .708 | .708 | .708 | .708 | .708 | .708 | .709 |
| .73 | .709 | .709 | .709 | .709 | .709 | .709 | .710 | .710 | .710 | .710 |
| .74 | .710 | .710 | .711 | .711 | .711 | .711 | .712 | .712 | .712 | .712 |
| .75 | .713 | .713 | .713 | .713 | .714 | .714 | .714 | .715 | .715 | .715 |
| .76 | .716 | .716 | .716 | .717 | .717 | .717 | .718 | .718 | .718 | .719 |
| .77 | .719 | .720 | .720 | .720 | .721 | .721 | .722 | .722 | .723 | .723 |
| .78 | .724 | .724 | .724 | .725 | .725 | .726 | .726 | .727 | .728 | .728 |
| .79 | .729 | .729 | .730 | .730 | .731 | .731 | .732 | .733 | .733 | .734 |
| .80 | .734 | .735 | .736 | .736 | .737 | .737 | .738 | .739 | .739 | .740 |
| .81 | .741 | .741 | .742 | .743 | .744 | .744 | .745 | .746 | .746 | .747 |
| .82 | .748 | .749 | .749 | .750 | .751 | .752 | .753 | .753 | .754 | .755 |
| .83 | .756 | .757 | .758 | .758 | .759 | .760 | .761 | .762 | .763 | .764 |
| .84 | .765 | .765 | .766 | .767 | .768 | .769 | .770 | .771 | .772 | .773 |
| .85 | .774 | .775 | .776 | .777 | .778 | .779 | .780 | .781 | .782 | .783 |
| .86 | .784 | .785 | .786 | .787 | .788 | .789 | .791 | .792 | .793 | .794 |
| .87 | .795 | .796 | .797 | .798 | .800 | .801 | .802 | .803 | .804 | .805 |
| .88 | .807 | .808 | .809 | .810 | .811 | .813 | .814 | .815 | .816 | .818 |
| .89 | .819 | .820 | .821 | .823 | .824 | .825 | .827 | .828 | .829 | .831 |
| .90 | .832 | .833 | .835 | .836 | .837 | .839 | .840 | .842 | .843 | .844 |
| .91 | .846 | .847 | .849 | .850 | .851 | .853 | .854 | .856 | .857 | .859 |
| .92 | .860 | .862 | .863 | .865 | .866 | .868 | .869 | .871 | .872 | .874 |
| .93 | .875 | .877 | .879 | .880 | .882 | .883 | .885 | .886 | .888 | .890 |
| .94 | .891 | .893 | .894 | .896 | .898 | .899 | .901 | .903 | .904 | .906 |
| .95 | .908 | .909 | .911 | .913 | .915 | .916 | .918 | .920 | .921 | .923 |
| .96 | .925 | .927 | .928 | .930 | .932 | .934 | .936 | .937 | .939 | .941 |
| .97 | .943 | .945 | .946 | .948 | .950 | .952 | .954 | .956 | .957 | .959 |
| .98 | .961 | .963 | .965 | .967 | .969 | .971 | .973 | .975 | .976 | .978 |
| .99 | .980 | .982 | .984 | .986 | .988 | .990 | .992 | .994 | .996 | .998 |

TABLE VII. Polarization factor, $(p)^{\frac{1}{2}}\left[=\left(\frac{1+\cos^2 2\theta}{2}\right)^{\frac{1}{2}}\right]$, as a function of $\sigma$.

| | .000 | .002 | .004 | .006 | .008 | | .000 | .002 | .004 | .006 | .008 |
|---|---|---|---|---|---|---|---|---|---|---|---|
| .00 | 1.000 | 1.000 | 1.000 | 1.000 | 1.000 | .31 | .976 | .976 | .976 | .975 | .975 |
| .01 | 1.000 | 1.000 | 1.000 | 1.000 | 1.000 | .32 | .975 | .974 | .974 | .974 | .973 |
| .02 | 1.000 | 1.000 | 1.000 | 1.000 | 1.000 | .33 | .973 | .973 | .973 | .972 | .972 |
| .03 | 1.000 | 1.000 | 1.000 | 1.000 | 1.000 | .34 | .972 | .971 | .971 | .971 | .970 |
| .04 | 1.000 | 1.000 | .999 | .999 | .999 | .35 | .970 | .970 | .969 | .969 | .969 |
| .05 | .999 | .999 | .999 | .999 | .999 | .36 | .968 | .968 | .967 | .967 | .967 |
| .06 | .999 | .999 | .999 | .999 | .999 | .37 | .966 | .966 | .966 | .965 | .965 |
| .07 | .999 | .999 | .999 | .999 | .998 | .38 | .965 | .964 | .964 | .963 | .963 |
| .08 | .998 | .998 | .998 | .998 | .998 | .39 | .963 | .962 | .962 | .962 | .961 |
| .09 | .998 | .998 | .998 | .998 | .998 | .40 | .961 | .960 | .960 | .960 | .959 |
| .10 | .997 | .997 | .997 | .997 | .997 | .41 | .959 | .958 | .958 | .958 | .957 |
| .11 | .997 | .997 | .997 | .997 | .997 | .42 | .957 | .957 | .956 | .956 | .955 |
| .12 | .996 | .996 | .996 | .996 | .996 | .43 | .955 | .954 | .954 | .954 | .953 |
| .13 | .996 | .996 | .996 | .995 | .995 | .44 | .953 | .952 | .952 | .952 | .951 |
| .14 | .995 | .995 | .995 | .995 | .995 | .45 | .951 | .950 | .950 | .949 | .949 |
| .15 | .994 | .994 | .994 | .994 | .994 | .46 | .949 | .948 | .948 | .947 | .947 |
| .16 | .994 | .993 | .993 | .993 | .993 | .47 | .946 | .946 | .946 | .945 | .945 |
| .17 | .993 | .993 | .992 | .992 | .992 | .48 | .944 | .944 | .943 | .943 | .942 |
| .18 | .992 | .992 | .992 | .991 | .991 | .49 | .942 | .941 | .941 | .941 | .940 |
| .19 | .991 | .991 | .991 | .990 | .990 | .50 | .940 | .939 | .939 | .938 | .938 |
| .20 | .990 | .990 | .990 | .989 | .989 | .51 | .937 | .937 | .936 | .936 | .935 |
| .21 | .989 | .989 | .989 | .988 | .988 | .52 | .935 | .934 | .934 | .933 | .933 |
| .22 | .988 | .988 | .988 | .987 | .987 | .53 | .932 | .932 | .931 | .931 | .930 |
| .23 | .987 | .987 | .986 | .986 | .986 | .54 | .930 | .929 | .929 | .928 | .928 |
| .24 | .986 | .985 | .985 | .985 | .985 | .55 | .927 | .927 | .926 | .926 | .925 |
| .25 | .984 | .984 | .984 | .984 | .984 | .56 | .925 | .924 | .924 | .923 | .923 |
| .26 | .983 | .983 | .983 | .982 | .982 | .57 | .922 | .922 | .921 | .921 | .920 |
| .27 | .982 | .982 | .981 | .981 | .981 | .58 | .920 | .919 | .919 | .918 | .918 |
| .28 | .981 | .980 | .980 | .980 | .979 | .59 | .917 | .917 | .916 | .916 | .915 |
| .29 | .979 | .979 | .979 | .978 | .978 | .60 | .914 | .914 | .913 | .913 | .912 |
| .30 | .978 | .977 | .977 | .977 | .977 | .61 | .912 | .911 | .911 | .910 | .910 |

TABLE VII.—*Continued.*

| | .000 | .002 | .004 | .006 | .008 | | .000 | .002 | .004 | .006 | .008 |
|---|---|---|---|---|---|---|---|---|---|---|---|
| .62 | .909 | .908 | .908 | .907 | .907 | 1.31 | .714 | .714 | .714 | .713 | .713 |
| .63 | .906 | .906 | .905 | .905 | .904 | 1.32 | .713 | .713 | .712 | .712 | .712 |
| .64 | .903 | .903 | .902 | .902 | .901 | 1.33 | .712 | .712 | .711 | .711 | .711 |
| .65 | .901 | .900 | .899 | .899 | .898 | 1.34 | .711 | .710 | .710 | .710 | .710 |
| .66 | .898 | .897 | .897 | .896 | .895 | 1.35 | .710 | .710 | .710 | .709 | .709 |
| .67 | .895 | .894 | .894 | .893 | .893 | 1.36 | .709 | .709 | .709 | .709 | .709 |
| .68 | .892 | .891 | .891 | .890 | .890 | 1.37 | .708 | .708 | .708 | .708 | .708 |
| .69 | .889 | .888 | .888 | .887 | .887 | 1.38 | .708 | .708 | .708 | .708 | .708 |
| .70 | .886 | .885 | .885 | .884 | .884 | 1.39 | .708 | .707 | .707 | .707 | .707 |
| .71 | .883 | .882 | .882 | .881 | .881 | 1.40 | .707 | .707 | .707 | .707 | .707 |
| .72 | .880 | .879 | .879 | .878 | .878 | 1.41 | .707 | .707 | .707 | .707 | .707 |
| .73 | .877 | .876 | .876 | .875 | .875 | 1.42 | .707 | .707 | .707 | .707 | .707 |
| .74 | .874 | .873 | .873 | .872 | .871 | 1.43 | .707 | .707 | .707 | .707 | .708 |
| .75 | .871 | .870 | .870 | .869 | .868 | 1.44 | .708 | .708 | .708 | .708 | .708 |
| .76 | .868 | .867 | .866 | .866 | .865 | 1.45 | .708 | .708 | .708 | .708 | .709 |
| .77 | .865 | .864 | .863 | .863 | .862 | 1.46 | .709 | .709 | .709 | .709 | .709 |
| .78 | .861 | .861 | .860 | .860 | .859 | 1.47 | .709 | .710 | .710 | .710 | .710 |
| .79 | .858 | .858 | .857 | .856 | .856 | 1.48 | .710 | .710 | .711 | .711 | .711 |
| .80 | .855 | .854 | .854 | .853 | .853 | 1.49 | .711 | .712 | .712 | .712 | .712 |
| .81 | .852 | .851 | .851 | .850 | .849 | 1.50 | .713 | .713 | .713 | .713 | .714 |
| .82 | .849 | .848 | .847 | .847 | .846 | 1.51 | .714 | .714 | .715 | .715 | .715 |
| .83 | .846 | .845 | .844 | .844 | .843 | 1.52 | .716 | .716 | .716 | .717 | .717 |
| .84 | .842 | .842 | .841 | .840 | .840 | 1.53 | .717 | .718 | .718 | .718 | .719 |
| .85 | .839 | .838 | .838 | .837 | .836 | 1.54 | .719 | .720 | .720 | .720 | .721 |
| .86 | .836 | .835 | .835 | .834 | .833 | 1.55 | .721 | .722 | .722 | .723 | .723 |
| .87 | .833 | .832 | .831 | .831 | .830 | 1.56 | .724 | .724 | .724 | .725 | .725 |
| .88 | .829 | .829 | .828 | .827 | .827 | 1.57 | .726 | .726 | .727 | .728 | .728 |
| .89 | .826 | .825 | .825 | .824 | .823 | 1.58 | .729 | .729 | .730 | .730 | .731 |
| .90 | .823 | .822 | .822 | .821 | .820 | 1.59 | .731 | .732 | .733 | .733 | .734 |
| .91 | .820 | .819 | .818 | .818 | .817 | 1.60 | .734 | .735 | .736 | .736 | .737 |
| .92 | .816 | .816 | .815 | .814 | .814 | 1.61 | .737 | .738 | .739 | .739 | .740 |
| .93 | .813 | .812 | .812 | .811 | .810 | 1.62 | .741 | .741 | .742 | .743 | .744 |
| .94 | .810 | .809 | .809 | .808 | .807 | 1.63 | .744 | .745 | .746 | .746 | .747 |
| .95 | .807 | .806 | .805 | .805 | .804 | 1.64 | .748 | .749 | .749 | .750 | .751 |
| .96 | .803 | .803 | .802 | .801 | .801 | 1.65 | .752 | .753 | .753 | .754 | .755 |
| .97 | .800 | .800 | .799 | .798 | .798 | 1.66 | .756 | .757 | .758 | .758 | .759 |
| .98 | .797 | .796 | .796 | .795 | .794 | 1.67 | .760 | .761 | .762 | .763 | .764 |
| .99 | .794 | .793 | .792 | .792 | .791 | 1.68 | .765 | .765 | .766 | .767 | .768 |
| 1.00 | .791 | .790 | .789 | .789 | .788 | 1.69 | .769 | .770 | .771 | .772 | .773 |
| 1.01 | .787 | .787 | .786 | .785 | .785 | 1.70 | .774 | .775 | .776 | .777 | .778 |
| 1.02 | .784 | .784 | .783 | .782 | .782 | 1.71 | .779 | .780 | .781 | .782 | .783 |
| 1.03 | .781 | .781 | .780 | .779 | .779 | 1.72 | .784 | .785 | .786 | .787 | .788 |
| 1.04 | .778 | .777 | .777 | .776 | .776 | 1.73 | .789 | .791 | .792 | .793 | .794 |
| 1.05 | .775 | .774 | .774 | .773 | .773 | 1.74 | .795 | .796 | .797 | .798 | .800 |
| 1.06 | .772 | .771 | .771 | .770 | .770 | 1.75 | .801 | .802 | .803 | .804 | .805 |
| 1.07 | .769 | .768 | .768 | .767 | .767 | 1.76 | .807 | .808 | .809 | .810 | .811 |
| 1.08 | .766 | .766 | .765 | .764 | .764 | 1.77 | .813 | .814 | .815 | .816 | .818 |
| 1.09 | .763 | .763 | .762 | .761 | .761 | 1.78 | .819 | .820 | .821 | .823 | .824 |
| 1.10 | .760 | .760 | .759 | .759 | .758 | 1.79 | .825 | .827 | .828 | .829 | .831 |
| 1.11 | .757 | .757 | .756 | .756 | .755 | 1.80 | .832 | .833 | .835 | .836 | .837 |
| 1.12 | .755 | .754 | .754 | .753 | .752 | 1.81 | .839 | .840 | .842 | .843 | .844 |
| 1.13 | .752 | .751 | .751 | .750 | .750 | 1.82 | .846 | .847 | .849 | .850 | .851 |
| 1.14 | .749 | .749 | .748 | .748 | .747 | 1.83 | .853 | .854 | .856 | .857 | .859 |
| 1.15 | .747 | .746 | .746 | .745 | .745 | 1.84 | .860 | .862 | .863 | .865 | .866 |
| 1.16 | .744 | .744 | .743 | .742 | .742 | 1.85 | .868 | .869 | .871 | .872 | .874 |
| 1.17 | .741 | .741 | .740 | .740 | .740 | 1.86 | .875 | .877 | .879 | .880 | .882 |
| 1.18 | .739 | .739 | .738 | .738 | .737 | 1.87 | .883 | .885 | .886 | .888 | .890 |
| 1.19 | .737 | .736 | .736 | .735 | .735 | 1.88 | .891 | .893 | .894 | .896 | .898 |
| 1.20 | .734 | .734 | .733 | .733 | .732 | 1.89 | .899 | .901 | .903 | .904 | .906 |
| 1.21 | .732 | .732 | .731 | .731 | .730 | 1.90 | .908 | .909 | .911 | .913 | .915 |
| 1.22 | .730 | .729 | .729 | .729 | .728 | 1.91 | .916 | .918 | .920 | .921 | .923 |
| 1.23 | .728 | .727 | .727 | .727 | .726 | 1.92 | .925 | .927 | .928 | .930 | .932 |
| 1.24 | .726 | .725 | .725 | .725 | .724 | 1.93 | .934 | .936 | .937 | .939 | .941 |
| 1.25 | .724 | .723 | .723 | .723 | .722 | 1.94 | .943 | .945 | .946 | .948 | .950 |
| 1.26 | .722 | .722 | .721 | .721 | .721 | 1.95 | .952 | .954 | .956 | .957 | .959 |
| 1.27 | .720 | .720 | .720 | .719 | .719 | 1.96 | .961 | .963 | .965 | .967 | .969 |
| 1.28 | .719 | .718 | .718 | .718 | .717 | 1.97 | .971 | .973 | .975 | .976 | .978 |
| 1.29 | .717 | .717 | .716 | .716 | .716 | 1.98 | .980 | .982 | .984 | .986 | .988 |
| 1.30 | .716 | .715 | .715 | .715 | .714 | 1.99 | .990 | .992 | .994 | .996 | .998 |

TABLE VIII. Unscaled part of Lorentz factor, $(S \cdot L)^{\frac{1}{2}}$ $[=(\csc \Upsilon)^{\frac{1}{2}}]$, as a function of $\Upsilon$.

| | 0 | .1 | .2 | .3 | .4 | .5 | .6 | .7 | .8 | .9 |
|---|---|---|---|---|---|---|---|---|---|---|
| 0 | ∞ | 23.09 | 16.09 | 13.08 | 11.10 | 10.07 | 9.772 | 9.047 | 8.463 | 7.979 |
| 1 | 7.570 | 7.217 | 6.910 | 6.639 | 6.398 | 6.181 | 5.985 | 5.806 | 5.643 | 5.492 |
| 2 | 5.353 | 5.224 | 5.123 | 4.992 | 4.887 | 4.789 | 4.695 | 4.608 | 4.524 | 4.446 |
| 3 | 4.371 | 4.300 | 4.232 | 4.168 | 4.106 | 4.047 | 3.991 | 3.937 | 3.885 | 3.834 |
| 4 | 3.787 | 3.740 | 3.695 | 3.652 | 3.611 | 3.571 | 3.531 | 3.493 | 3.457 | 3.422 |
| 5 | 3.387 | 3.354 | 3.321 | 3.291 | 3.260 | 3.230 | 3.202 | 3.173 | 3.146 | 3.119 |
| 6 | 3.093 | 3.068 | 3.043 | 3.019 | 2.995 | 2.972 | 2.950 | 2.928 | 2.906 | 2.885 |
| 7 | 2.865 | 2.844 | 2.825 | 2.805 | 2.786 | 2.768 | 2.750 | 2.732 | 2.714 | 2.697 |
| 8 | 2.680 | 2.664 | 2.648 | 2.632 | 2.616 | 2.601 | 2.586 | 2.571 | 2.557 | 2.542 |
| 9 | 2.528 | 2.515 | 2.501 | 2.488 | 2.474 | 2.462 | 2.449 | 2.436 | 2.424 | 2.412 |
| 10 | 2.400 | 2.388 | 2.376 | 2.365 | 2.354 | 2.342 | 2.332 | 2.321 | 2.310 | 2.300 |
| 11 | 2.289 | 2.279 | 2.269 | 2.259 | 2.249 | 2.240 | 2.230 | 2.221 | 2.211 | 2.202 |
| 12 | 2.193 | 2.184 | 2.175 | 2.167 | 2.158 | 2.149 | 2.141 | 2.133 | 2.125 | 2.116 |
| 13 | 2.108 | 2.100 | 2.093 | 2.085 | 2.077 | 2.070 | 2.062 | 2.055 | 2.047 | 2.040 |
| 14 | 2.033 | 2.026 | 2.019 | 2.012 | 2.005 | 1.998 | 1.992 | 1.985 | 1.979 | 1.972 |
| 15 | 1.966 | 1.959 | 1.953 | 1.947 | 1.941 | 1.934 | 1.928 | 1.922 | 1.917 | 1.910 |
| 16 | 1.905 | 1.899 | 1.893 | 1.888 | 1.882 | 1.876 | 1.871 | 1.865 | 1.860 | 1.855 |
| 17 | 1.849 | 1.844 | 1.839 | 1.834 | 1.829 | 1.824 | 1.819 | 1.814 | 1.809 | 1.804 |
| 18 | 1.799 | 1.794 | 1.789 | 1.785 | 1.780 | 1.775 | 1.771 | 1.766 | 1.762 | 1.757 |
| 19 | 1.753 | 1.748 | 1.744 | 1.740 | 1.735 | 1.731 | 1.727 | 1.722 | 1.718 | 1.714 |
| 20 | 1.710 | 1.706 | 1.702 | 1.698 | 1.694 | 1.690 | 1.686 | 1.682 | 1.678 | 1.674 |
| 21 | 1.670 | 1.667 | 1.663 | 1.659 | 1.656 | 1.652 | 1.648 | 1.645 | 1.641 | 1.637 |
| 22 | 1.634 | 1.630 | 1.627 | 1.623 | 1.620 | 1.616 | 1.613 | 1.610 | 1.607 | 1.603 |
| 23 | 1.600 | 1.597 | 1.593 | 1.590 | 1.587 | 1.584 | 1.581 | 1.577 | 1.574 | 1.571 |
| 24 | 1.568 | 1.565 | 1.562 | 1.559 | 1.556 | 1.553 | 1.550 | 1.547 | 1.544 | 1.541 |
| 25 | 1.538 | 1.535 | 1.533 | 1.530 | 1.527 | 1.524 | 1.521 | 1.519 | 1.516 | 1.513 |
| 26 | 1.510 | 1.508 | 1.505 | 1.502 | 1.500 | 1.497 | 1.494 | 1.492 | 1.489 | 1.487 |
| 27 | 1.484 | 1.482 | 1.479 | 1.476 | 1.474 | 1.472 | 1.469 | 1.467 | 1.464 | 1.462 |
| 28 | 1.459 | 1.457 | 1.455 | 1.452 | 1.450 | 1.448 | 1.445 | 1.443 | 1.441 | 1.438 |
| 29 | 1.436 | 1.434 | 1.432 | 1.429 | 1.427 | 1.425 | 1.423 | 1.421 | 1.418 | 1.416 |
| 30 | 1.414 | 1.412 | 1.410 | 1.408 | 1.406 | 1.404 | 1.402 | 1.400 | 1.397 | 1.395 |
| 31 | 1.393 | 1.391 | 1.389 | 1.387 | 1.385 | 1.383 | 1.381 | 1.379 | 1.377 | 1.375 |
| 32 | 1.374 | 1.372 | 1.370 | 1.368 | 1.366 | 1.364 | 1.362 | 1.361 | 1.359 | 1.357 |
| 33 | 1.355 | 1.353 | 1.351 | 1.349 | 1.348 | 1.346 | 1.344 | 1.342 | 1.341 | 1.339 |
| 34 | 1.337 | 1.336 | 1.334 | 1.332 | 1.330 | 1.329 | 1.327 | 1.326 | 1.324 | 1.322 |
| 35 | 1.320 | 1.319 | 1.317 | 1.316 | 1.314 | 1.312 | 1.311 | 1.309 | 1.308 | 1.306 |
| 36 | 1.304 | 1.303 | 1.301 | 1.300 | 1.298 | 1.297 | 1.295 | 1.293 | 1.292 | 1.291 |
| 37 | 1.289 | 1.288 | 1.286 | 1.285 | 1.283 | 1.282 | 1.280 | 1.279 | 1.277 | 1.276 |
| 38 | 1.274 | 1.273 | 1.272 | 1.270 | 1.269 | 1.267 | 1.266 | 1.265 | 1.263 | 1.262 |
| 39 | 1.261 | 1.259 | 1.258 | 1.257 | 1.255 | 1.254 | 1.253 | 1.251 | 1.250 | 1.249 |
| 40 | 1.247 | 1.246 | 1.245 | 1.243 | 1.242 | 1.241 | 1.240 | 1.239 | 1.237 | 1.236 |
| 41 | 1.235 | 1.233 | 1.232 | 1.231 | 1.230 | 1.228 | 1.227 | 1.226 | 1.225 | 1.224 |
| 42 | 1.222 | 1.221 | 1.220 | 1.219 | 1.218 | 1.217 | 1.215 | 1.214 | 1.213 | 1.212 |
| 43 | 1.211 | 1.210 | 1.209 | 1.207 | 1.206 | 1.205 | 1.204 | 1.203 | 1.202 | 1.201 |
| 44 | 1.200 | 1.199 | 1.197 | 1.196 | 1.195 | 1.194 | 1.193 | 1.192 | 1.191 | 1.190 |
| 45 | 1.189 | 1.188 | 1.187 | 1.186 | 1.185 | 1.184 | 1.183 | 1.182 | 1.181 | 1.180 |
| 46 | 1.179 | 1.178 | 1.177 | 1.176 | 1.175 | 1.174 | 1.173 | 1.172 | 1.171 | 1.170 |
| 47 | 1.169 | 1.168 | 1.167 | 1.167 | 1.166 | 1.165 | 1.164 | 1.163 | 1.162 | 1.161 |
| 48 | 1.160 | 1.159 | 1.158 | 1.157 | 1.156 | 1.155 | 1.155 | 1.154 | 1.153 | 1.152 |
| 49 | 1.151 | 1.150 | 1.149 | 1.148 | 1.148 | 1.147 | 1.146 | 1.145 | 1.144 | 1.143 |
| 50 | 1.142 | 1.142 | 1.141 | 1.140 | 1.139 | 1.138 | 1.138 | 1.137 | 1.136 | 1.135 |
| 51 | 1.134 | 1.134 | 1.133 | 1.132 | 1.131 | 1.130 | 1.130 | 1.129 | 1.128 | 1.127 |
| 52 | 1.126 | 1.126 | 1.125 | 1.124 | 1.123 | 1.122 | 1.122 | 1.121 | 1.120 | 1.120 |
| 53 | 1.119 | 1.118 | 1.118 | 1.117 | 1.116 | 1.115 | 1.114 | 1.114 | 1.113 | 1.113 |
| 54 | 1.112 | 1.111 | 1.110 | 1.110 | 1.109 | 1.108 | 1.108 | 1.107 | 1.106 | 1.105 |
| 55 | 1.105 | 1.104 | 1.104 | 1.103 | 1.102 | 1.101 | 1.101 | 1.100 | 1.100 | 1.099 |
| 56 | 1.098 | 1.098 | 1.097 | 1.096 | 1.096 | 1.095 | 1.095 | 1.094 | 1.093 | 1.093 |
| 57 | 1.092 | 1.091 | 1.091 | 1.090 | 1.089 | 1.089 | 1.088 | 1.088 | 1.087 | 1.086 |
| 58 | 1.086 | 1.085 | 1.085 | 1.084 | 1.084 | 1.083 | 1.083 | 1.082 | 1.081 | 1.081 |
| 59 | 1.080 | 1.079 | 1.079 | 1.078 | 1.078 | 1.077 | 1.077 | 1.076 | 1.076 | 1.075 |
| 60 | 1.075 | 1.074 | 1.073 | 1.073 | 1.072 | 1.072 | 1.071 | 1.071 | 1.070 | 1.070 |
| 61 | 1.069 | 1.069 | 1.068 | 1.068 | 1.067 | 1.067 | 1.066 | 1.066 | 1.065 | 1.065 |
| 62 | 1.064 | 1.064 | 1.063 | 1.063 | 1.062 | 1.062 | 1.061 | 1.061 | 1.060 | 1.060 |
| 63 | 1.059 | 1.059 | 1.058 | 1.058 | 1.057 | 1.057 | 1.056 | 1.056 | 1.056 | 1.055 |
| 64 | 1.055 | 1.055 | 1.054 | 1.054 | 1.053 | 1.053 | 1.052 | 1.052 | 1.051 | 1.051 |
| 65 | 1.050 | 1.050 | 1.050 | 1.049 | 1.049 | 1.048 | 1.048 | 1.047 | 1.047 | 1.046 |
| 66 | 1.046 | 1.046 | 1.045 | 1.045 | 1.045 | 1.044 | 1.044 | 1.044 | 1.043 | 1.043 |
| 67 | 1.042 | 1.042 | 1.042 | 1.041 | 1.041 | 1.040 | 1.040 | 1.040 | 1.039 | 1.039 |
| 68 | 1.039 | 1.038 | 1.038 | 1.037 | 1.037 | 1.037 | 1.036 | 1.036 | 1.036 | 1.035 |

TABLE VIII.—*Continued.*

| | 0 | .1 | .2 | .3 | .4 | .5 | .6 | .7 | .8 | .9 |
|---|---|---|---|---|---|---|---|---|---|---|
| 69 | 1.035 | 1.034 | 1.034 | 1.034 | 1.033 | 1.033 | 1.033 | 1.032 | 1.032 | 1.032 |
| 70 | 1.031 | 1.031 | 1.031 | 1.031 | 1.031 | 1.030 | 1.030 | 1.030 | 1.029 | 1.029 |
| 71 | 1.029 | 1.028 | 1.028 | 1.028 | 1.027 | 1.027 | 1.027 | 1.026 | 1.026 | 1.026 |
| 72 | 1.025 | 1.025 | 1.025 | 1.025 | 1.024 | 1.024 | 1.024 | 1.023 | 1.023 | 1.023 |
| 73 | 1.023 | 1.022 | 1.022 | 1.022 | 1.021 | 1.021 | 1.021 | 1.021 | 1.020 | 1.020 |
| 74 | 1.020 | 1.020 | 1.019 | 1.019 | 1.019 | 1.019 | 1.018 | 1.018 | 1.018 | 1.018 |
| 75 | 1.017 | 1.017 | 1.017 | 1.017 | 1.016 | 1.016 | 1.016 | 1.016 | 1.016 | 1.015 |
| 76 | 1.015 | 1.015 | 1.015 | 1.014 | 1.014 | 1.014 | 1.014 | 1.014 | 1.013 | 1.013 |
| 77 | 1.013 | 1.013 | 1.012 | 1.012 | 1.012 | 1.012 | 1.012 | 1.011 | 1.011 | 1.011 |
| 78 | 1.011 | 1.011 | 1.011 | 1.010 | 1.010 | 1.010 | 1.010 | 1.010 | 1.009 | 1.009 |
| 79 | 1.009 | 1.009 | 1.009 | 1.009 | 1.008 | 1.008 | 1.008 | 1.008 | 1.008 | 1.008 |
| 80 | 1.007 | 1.007 | 1.007 | 1.007 | 1.007 | 1.007 | 1.007 | 1.006 | 1.006 | 1.006 |
| 81 | 1.006 | 1.006 | 1.006 | 1.006 | 1.005 | 1.005 | 1.005 | 1.005 | 1.005 | 1.005 |
| 82 | 1.005 | 1.005 | 1.004 | 1.004 | 1.004 | 1.004 | 1.004 | 1.004 | 1.004 | 1.004 |
| 83 | 1.004 | 1.003 | 1.003 | 1.003 | 1.003 | 1.003 | 1.003 | 1.003 | 1.003 | 1.003 |
| 84 | 1.003 | 1.002 | 1.002 | 1.002 | 1.002 | 1.002 | 1.002 | 1.002 | 1.002 | 1.002 |
| 85 | 1.002 | 1.002 | 1.002 | 1.001 | 1.001 | 1.001 | 1.001 | 1.001 | 1.001 | 1.001 |
| 86 | 1.001 | 1.001 | 1.001 | 1.001 | 1.001 | 1.001 | 1.001 | 1.001 | 1.001 | 1.000 |
| 87 | 1.000 | 1.000 | 1.000 | 1.000 | 1.000 | 1.000 | 1.000 | 1.000 | 1.000 | 1.000 |
| 88 | 1.000 | 1.000 | 1.000 | 1.000 | 1.000 | 1.000 | 1.000 | 1.000 | 1.000 | 1.000 |
| 89 | 1.000 | 1.000 | 1.000 | 1.000 | 1.000 | 1.000 | 1.000 | 1.000 | 1.000 | 1.000 |
| 90 | 1.000 | 1.000 | 1.000 | 1.000 | 1.000 | 1.000 | 1.000 | 1.000 | 1.000 | 1.000 |
| 91 | 1.000 | 1.000 | 1.000 | 1.000 | 1.000 | 1.000 | 1.000 | 1.000 | 1.000 | 1.000 |
| 92 | 1.000 | 1.000 | 1.000 | 1.000 | 1.000 | 1.000 | 1.000 | 1.000 | 1.000 | 1.000 |
| 93 | 1.000 | 1.001 | 1.001 | 1.001 | 1.001 | 1.001 | 1.001 | 1.001 | 1.001 | 1.001 |
| 94 | 1.001 | 1.001 | 1.001 | 1.001 | 1.001 | 1.001 | 1.001 | 1.002 | 1.002 | 1.002 |
| 95 | 1.002 | 1.002 | 1.002 | 1.002 | 1.002 | 1.002 | 1.002 | 1.002 | 1.002 | 1.003 |
| 96 | 1.003 | 1.003 | 1.003 | 1.003 | 1.003 | 1.003 | 1.003 | 1.003 | 1.003 | 1.004 |
| 97 | 1.004 | 1.004 | 1.004 | 1.004 | 1.004 | 1.004 | 1.004 | 1.004 | 1.005 | 1.005 |
| 98 | 1.005 | 1.005 | 1.005 | 1.005 | 1.005 | 1.005 | 1.006 | 1.006 | 1.006 | 1.006 |
| 99 | 1.006 | 1.006 | 1.006 | 1.007 | 1.007 | 1.007 | 1.007 | 1.007 | 1.007 | 1.007 |
| 100 | 1.008 | 1.008 | 1.008 | 1.008 | 1.008 | 1.008 | 1.009 | 1.009 | 1.009 | 1.009 |
| 101 | 1.009 | 1.009 | 1.010 | 1.010 | 1.010 | 1.010 | 1.010 | 1.011 | 1.011 | 1.011 |
| 102 | 1.011 | 1.011 | 1.011 | 1.012 | 1.012 | 1.012 | 1.012 | 1.012 | 1.013 | 1.013 |
| 103 | 1.013 | 1.013 | 1.014 | 1.014 | 1.014 | 1.014 | 1.014 | 1.015 | 1.015 | 1.015 |
| 104 | 1.015 | 1.016 | 1.016 | 1.016 | 1.016 | 1.016 | 1.017 | 1.017 | 1.017 | 1.017 |
| 105 | 1.018 | 1.018 | 1.018 | 1.018 | 1.019 | 1.019 | 1.019 | 1.019 | 1.020 | 1.020 |
| 106 | 1.020 | 1.020 | 1.021 | 1.021 | 1.021 | 1.021 | 1.022 | 1.022 | 1.022 | 1.023 |
| 107 | 1.023 | 1.023 | 1.023 | 1.024 | 1.024 | 1.024 | 1.025 | 1.025 | 1.025 | 1.025 |
| 108 | 1.026 | 1.026 | 1.026 | 1.027 | 1.027 | 1.027 | 1.028 | 1.028 | 1.028 | 1.029 |
| 109 | 1.029 | 1.029 | 1.030 | 1.030 | 1.030 | 1.031 | 1.031 | 1.031 | 1.031 | 1.031 |
| 110 | 1.032 | 1.032 | 1.032 | 1.033 | 1.033 | 1.033 | 1.034 | 1.034 | 1.034 | 1.035 |
| 111 | 1.035 | 1.036 | 1.036 | 1.036 | 1.037 | 1.037 | 1.037 | 1.038 | 1.038 | 1.039 |
| 112 | 1.039 | 1.039 | 1.040 | 1.040 | 1.040 | 1.041 | 1.041 | 1.042 | 1.042 | 1.042 |
| 113 | 1.043 | 1.043 | 1.044 | 1.044 | 1.044 | 1.045 | 1.045 | 1.045 | 1.046 | 1.046 |
| 114 | 1.046 | 1.047 | 1.047 | 1.048 | 1.048 | 1.049 | 1.049 | 1.050 | 1.050 | 1.050 |
| 115 | 1.051 | 1.051 | 1.052 | 1.052 | 1.053 | 1.053 | 1.054 | 1.054 | 1.055 | 1.055 |
| 116 | 1.055 | 1.056 | 1.056 | 1.056 | 1.057 | 1.057 | 1.058 | 1.058 | 1.059 | 1.059 |
| 117 | 1.060 | 1.060 | 1.061 | 1.061 | 1.062 | 1.062 | 1.063 | 1.063 | 1.064 | 1.064 |
| 118 | 1.065 | 1.065 | 1.066 | 1.066 | 1.067 | 1.067 | 1.068 | 1.068 | 1.069 | 1.069 |
| 119 | 1.070 | 1.070 | 1.071 | 1.071 | 1.072 | 1.072 | 1.073 | 1.073 | 1.074 | 1.075 |
| 120 | 1.075 | 1.076 | 1.076 | 1.077 | 1.077 | 1.078 | 1.078 | 1.079 | 1.079 | 1.080 |
| 121 | 1.081 | 1.081 | 1.082 | 1.083 | 1.083 | 1.084 | 1.084 | 1.085 | 1.085 | 1.086 |
| 122 | 1.086 | 1.087 | 1.088 | 1.088 | 1.089 | 1.089 | 1.090 | 1.091 | 1.091 | 1.092 |
| 123 | 1.093 | 1.093 | 1.094 | 1.095 | 1.095 | 1.096 | 1.096 | 1.097 | 1.098 | 1.098 |
| 124 | 1.099 | 1.100 | 1.100 | 1.101 | 1.101 | 1.102 | 1.103 | 1.104 | 1.104 | 1.105 |
| 125 | 1.105 | 1.106 | 1.107 | 1.108 | 1.108 | 1.109 | 1.110 | 1.110 | 1.111 | 1.112 |
| 126 | 1.113 | 1.113 | 1.114 | 1.114 | 1.115 | 1.116 | 1.117 | 1.118 | 1.118 | 1.119 |
| 127 | 1.120 | 1.120 | 1.121 | 1.122 | 1.122 | 1.123 | 1.124 | 1.125 | 1.126 | 1.126 |
| 128 | 1.127 | 1.128 | 1.129 | 1.130 | 1.130 | 1.131 | 1.132 | 1.133 | 1.134 | 1.134 |
| 129 | 1.135 | 1.136 | 1.137 | 1.138 | 1.138 | 1.139 | 1.140 | 1.141 | 1.142 | 1.142 |
| 130 | 1.143 | 1.144 | 1.145 | 1.146 | 1.147 | 1.148 | 1.148 | 1.149 | 1.150 | 1.151 |
| 131 | 1.152 | 1.153 | 1.154 | 1.155 | 1.155 | 1.156 | 1.157 | 1.158 | 1.159 | 1.160 |
| 132 | 1.161 | 1.162 | 1.163 | 1.164 | 1.165 | 1.166 | 1.167 | 1.167 | 1.168 | 1.169 |
| 133 | 1.170 | 1.171 | 1.172 | 1.173 | 1.174 | 1.175 | 1.176 | 1.177 | 1.178 | 1.179 |
| 134 | 1.180 | 1.181 | 1.182 | 1.183 | 1.184 | 1.185 | 1.186 | 1.187 | 1.188 | 1.189 |
| 135 | 1.190 | 1.191 | 1.192 | 1.193 | 1.194 | 1.195 | 1.196 | 1.197 | 1.199 | 1.200 |
| 136 | 1.201 | 1.202 | 1.203 | 1.204 | 1.205 | 1.206 | 1.207 | 1.209 | 1.210 | 1.211 |
| 137 | 1.212 | 1.213 | 1.214 | 1.215 | 1.217 | 1.218 | 1.219 | 1.220 | 1.221 | 1.222 |

TABLE VIII.—*Continued.*

| | 0 | .1 | .2 | .3 | .4 | .5 | .6 | .7 | .8 | .9 |
|---|---|---|---|---|---|---|---|---|---|---|
| 138 | 1.224 | 1.225 | 1.226 | 1.227 | 1.228 | 1.230 | 1.231 | 1.232 | 1.233 | 1.235 |
| 139 | 1.236 | 1.237 | 1.239 | 1.240 | 1.241 | 1.242 | 1.243 | 1.245 | 1.246 | 1.247 |
| 140 | 1.249 | 1.250 | 1.251 | 1.253 | 1.254 | 1.255 | 1.257 | 1.258 | 1.259 | 1.261 |
| 141 | 1.262 | 1.263 | 1.265 | 1.266 | 1.267 | 1.269 | 1.270 | 1.272 | 1.273 | 1.274 |
| 142 | 1.276 | 1.277 | 1.279 | 1.280 | 1.282 | 1.283 | 1.285 | 1.286 | 1.288 | 1.289 |
| 143 | 1.291 | 1.292 | 1.293 | 1.295 | 1.297 | 1.298 | 1.300 | 1.301 | 1.303 | 1.304 |
| 144 | 1.306 | 1.308 | 1.309 | 1.311 | 1.312 | 1.314 | 1.316 | 1.317 | 1.319 | 1.320 |
| 145 | 1.322 | 1.324 | 1.326 | 1.327 | 1.329 | 1.330 | 1.332 | 1.334 | 1.336 | 1.337 |
| 146 | 1.339 | 1.341 | 1.342 | 1.344 | 1.346 | 1.348 | 1.349 | 1.351 | 1.353 | 1.355 |
| 147 | 1.357 | 1.359 | 1.361 | 1.362 | 1.364 | 1.366 | 1.368 | 1.370 | 1.372 | 1.374 |
| 148 | 1.375 | 1.377 | 1.379 | 1.381 | 1.383 | 1.385 | 1.387 | 1.389 | 1.391 | 1.393 |
| 149 | 1.395 | 1.397 | 1.400 | 1.402 | 1.404 | 1.406 | 1.408 | 1.410 | 1.412 | 1.414 |
| 150 | 1.416 | 1.418 | 1.421 | 1.423 | 1.425 | 1.427 | 1.429 | 1.432 | 1.434 | 1.436 |
| 151 | 1.438 | 1.441 | 1.443 | 1.445 | 1.448 | 1.450 | 1.452 | 1.455 | 1.457 | 1.459 |
| 152 | 1.462 | 1.464 | 1.467 | 1.469 | 1.472 | 1.474 | 1.476 | 1.479 | 1.482 | 1.484 |
| 153 | 1.487 | 1.489 | 1.492 | 1.494 | 1.497 | 1.500 | 1.502 | 1.505 | 1.508 | 1.510 |
| 154 | 1.513 | 1.516 | 1.519 | 1.521 | 1.524 | 1.527 | 1.530 | 1.533 | 1.535 | 1.538 |
| 155 | 1.541 | 1.544 | 1.547 | 1.550 | 1.553 | 1.556 | 1.559 | 1.562 | 1.565 | 1.568 |
| 156 | 1.571 | 1.574 | 1.577 | 1.581 | 1.584 | 1.587 | 1.590 | 1.593 | 1.597 | 1.600 |
| 157 | 1.603 | 1.607 | 1.610 | 1.613 | 1.616 | 1.620 | 1.623 | 1.627 | 1.630 | 1.634 |
| 158 | 1.637 | 1.641 | 1.645 | 1.648 | 1.652 | 1.656 | 1.659 | 1.663 | 1.667 | 1.670 |
| 159 | 1.674 | 1.678 | 1.682 | 1.686 | 1.690 | 1.694 | 1.698 | 1.702 | 1.706 | 1.710 |
| 160 | 1.714 | 1.718 | 1.722 | 1.727 | 1.731 | 1.735 | 1.740 | 1.744 | 1.748 | 1.753 |
| 161 | 1.757 | 1.762 | 1.766 | 1.771 | 1.775 | 1.780 | 1.785 | 1.789 | 1.794 | 1.799 |
| 162 | 1.804 | 1.809 | 1.814 | 1.819 | 1.824 | 1.829 | 1.834 | 1.839 | 1.844 | 1.849 |
| 163 | 1.855 | 1.860 | 1.865 | 1.871 | 1.876 | 1.882 | 1.888 | 1.893 | 1.899 | 1.905 |
| 164 | 1.910 | 1.917 | 1.922 | 1.928 | 1.934 | 1.941 | 1.947 | 1.953 | 1.959 | 1.966 |
| 165 | 1.972 | 1.979 | 1.985 | 1.992 | 1.998 | 2.005 | 2.012 | 2.019 | 2.026 | 2.033 |
| 166 | 2.040 | 2.047 | 2.055 | 2.062 | 2.070 | 2.077 | 2.085 | 2.093 | 2.100 | 2.108 |
| 167 | 2.116 | 2.125 | 2.133 | 2.141 | 2.149 | 2.158 | 2.167 | 2.175 | 2.184 | 2.193 |
| 168 | 2.202 | 2.211 | 2.221 | 2.230 | 2.240 | 2.249 | 2.259 | 2.269 | 2.279 | 2.289 |
| 169 | 2.300 | 2.310 | 2.321 | 2.332 | 2.342 | 2.354 | 2.365 | 2.376 | 2.388 | 2.400 |
| 170 | 2.412 | 2.424 | 2.436 | 2.449 | 2.462 | 2.474 | 2.488 | 2.501 | 2.515 | 2.528 |
| 171 | 2.542 | 2.557 | 2.571 | 2.586 | 2.601 | 2.616 | 2.632 | 2.648 | 2.664 | 2.680 |
| 172 | 2.697 | 2.714 | 2.732 | 2.750 | 2.768 | 2.786 | 2.805 | 2.825 | 2.844 | 2.865 |
| 173 | 2.885 | 2.906 | 2.928 | 2.950 | 2.972 | 2.995 | 3.019 | 3.043 | 3.068 | 3.093 |
| 174 | 3.119 | 3.146 | 3.173 | 3.202 | 3.230 | 3.260 | 3.291 | 3.321 | 3.354 | 3.387 |
| 175 | 3.422 | 3.457 | 3.493 | 3.531 | 3.571 | 3.611 | 3.652 | 3.695 | 3.740 | 3.787 |
| 176 | 3.834 | 3.885 | 3.937 | 3.991 | 4.047 | 4.106 | 4.168 | 4.232 | 4.300 | 4.371 |
| 177 | 4.446 | 4.524 | 4.608 | 4.695 | 4.789 | 4.887 | 4.992 | 5.123 | 5.224 | 5.353 |
| 178 | 5.492 | 5.643 | 5.806 | 5.985 | 6.181 | 6.398 | 6.639 | 6.910 | 7.217 | 7.570 |
| 179 | 7.979 | 8.463 | 9.047 | 9.772 | 10.07 | 11.10 | 13.08 | 16.09 | 23.09 | ∞ |

the computation reduces to the following comparatively simple form

$$\begin{aligned} I\sim\{&C_{\mathrm{I}}\bar{A}_{\mathrm{I}} && +\{C_{\mathrm{I}}\bar{B}_{\mathrm{I}}\\ &+C_{\mathrm{II}}\bar{A}_{\mathrm{II}} && +C_{\mathrm{II}}\bar{B}_{\mathrm{II}}\\ &+C_{\mathrm{III}}\bar{A}_{\mathrm{III}} && +C_{\mathrm{III}}\bar{B}_{\mathrm{III}}\}^2\\ &+\cdots\}^2. && \end{aligned} \tag{15}$$

In the fortunate case that the crystal has inversion centers and that the origin is chosen at one of these, the right-hand column of (15), which represents the imaginary component, vanishes, and the computation can be further simplified to

$$\begin{aligned} (I)^{\frac{1}{2}}\sim &C_1\bar{A}_1\\ &+C_2\bar{A}_2\\ &+C_3\bar{A}_3\\ &\cdot\\ &\cdot\\ &\cdot \end{aligned} \tag{16}$$

The above computing scheme is discussed in greater detail elsewhere.[4]

## APPENDIX

In an earlier paper we presented tables which simplified the computation of $\sigma$, which is the argument required when looking up the polarization factor of a reflection. We take this opportunity to present two other tables which simplify this computation further for the particular case of zero level reflections of tetragonal and hexagonal crystals. For these cases,

$$\text{Tetragonal: } \sigma_0=\xi=a^*(h^2+k^2)^{\frac{1}{2}}, \tag{17}$$

$$\text{Hexagonal: } \sigma_0=\xi=a^*(h^2+k^2+hk)^{\frac{1}{2}}. \tag{18}$$

The functions $(h^2+k^2)^{\frac{1}{2}}$ and $(h^2+k^2+hk)^{\frac{1}{2}}$ are given in Tables XI and XII.

TABLE IX. Lorentz-polarization factor, $(L\cdot p)^{\frac{1}{2}}\left[=\left(\frac{1}{\sin 2\theta}\cdot\frac{1+\cos^2 2\theta}{2}\right)^{\frac{1}{2}}\right]$, as a function of $\sin\theta$.

*Valid only for zero level when $\mu=0$.*

| | .000 | .001 | .002 | .003 | .004 | .005 | .006 | .007 | .008 | .009 |
|---|---|---|---|---|---|---|---|---|---|---|
| .00 | ∞ | 22.42 | 15.79 | 12.91 | 11.21 | 10.01 | 9.129 | 8.442 | 7.908 | 7.451 |
| .01 | 7.070 | 6.742 | 6.453 | 6.201 | 5.976 | 5.774 | 5.588 | 5.422 | 5.271 | 5.128 |
| .02 | 5.000 | 4.879 | 4.766 | 4.660 | 4.563 | 4.470 | 4.383 | 4.301 | 4.224 | 4.150 |
| .03 | 4.080 | 4.014 | 3.950 | 3.890 | 3.831 | 3.776 | 3.723 | 3.673 | 3.624 | 3.576 |
| .04 | 3.531 | 3.487 | 3.445 | 3.406 | 3.366 | 3.329 | 3.291 | 3.256 | 3.222 | 3.189 |
| .05 | 3.157 | 3.125 | 3.095 | 3.065 | 3.036 | 3.008 | 2.981 | 2.955 | 2.939 | 2.904 |
| .06 | 2.889 | 2.855 | 2.832 | 2.809 | 2.787 | 2.765 | 2.744 | 2.722 | 2.702 | 2.682 |
| .07 | 2.663 | 2.644 | 2.623 | 2.607 | 2.589 | 2.571 | 2.554 | 2.537 | 2.520 | 2.504 |
| .08 | 2.488 | 2.472 | 2.457 | 2.442 | 2.427 | 2.412 | 2.398 | 2.384 | 2.370 | 2.356 |
| .09 | 2.343 | 2.330 | 2.317 | 2.304 | 2.291 | 2.279 | 2.266 | 2.254 | 2.243 | 2.231 |
| .10 | 2.219 | 2.208 | 2.197 | 2.186 | 2.175 | 2.164 | 2.154 | 2.143 | 2.133 | 2.123 |
| .11 | 2.113 | 2.103 | 2.093 | 2.084 | 2.074 | 2.064 | 2.055 | 2.046 | 2.037 | 2.028 |
| .12 | 2.019 | 2.011 | 2.002 | 1.993 | 1.985 | 1.977 | 1.969 | 1.960 | 1.952 | 1.944 |
| .13 | 1.936 | 1.929 | 1.921 | 1.913 | 1.906 | 1.898 | 1.891 | 1.884 | 1.877 | 1.869 |
| .14 | 1.862 | 1.855 | 1.848 | 1.842 | 1.835 | 1.828 | 1.821 | 1.815 | 1.808 | 1.802 |
| .15 | 1.795 | 1.789 | 1.783 | 1.777 | 1.770 | 1.764 | 1.758 | 1.752 | 1.746 | 1.740 |
| .16 | 1.734 | 1.729 | 1.723 | 1.717 | 1.711 | 1.706 | 1.700 | 1.695 | 1.689 | 1.684 |
| .17 | 1.678 | 1.673 | 1.668 | 1.663 | 1.657 | 1.652 | 1.647 | 1.642 | 1.637 | 1.632 |
| .18 | 1.627 | 1.622 | 1.617 | 1.612 | 1.607 | 1.602 | 1.598 | 1.593 | 1.588 | 1.584 |
| .19 | 1.579 | 1.574 | 1.570 | 1.566 | 1.561 | 1.557 | 1.552 | 1.548 | 1.543 | 1.539 |
| .20 | 1.535 | 1.531 | 1.526 | 1.522 | 1.518 | 1.514 | 1.510 | 1.505 | 1.501 | 1.497 |
| .21 | 1.493 | 1.489 | 1.485 | 1.481 | 1.477 | 1.473 | 1.470 | 1.466 | 1.462 | 1.458 |
| .22 | 1.454 | 1.451 | 1.447 | 1.443 | 1.439 | 1.436 | 1.432 | 1.429 | 1.425 | 1.421 |
| .23 | 1.418 | 1.414 | 1.411 | 1.407 | 1.404 | 1.400 | 1.397 | 1.393 | 1.390 | 1.386 |
| .24 | 1.383 | 1.380 | 1.377 | 1.373 | 1.370 | 1.366 | 1.363 | 1.360 | 1.357 | 1.354 |
| .25 | 1.350 | 1.347 | 1.344 | 1.341 | 1.338 | 1.335 | 1.332 | 1.329 | 1.326 | 1.322 |
| .26 | 1.319 | 1.316 | 1.313 | 1.310 | 1.307 | 1.304 | 1.301 | 1.298 | 1.295 | 1.293 |
| .27 | 1.290 | 1.287 | 1.284 | 1.281 | 1.278 | 1.276 | 1.273 | 1.270 | 1.267 | 1.264 |
| .28 | 1.261 | 1.259 | 1.256 | 1.253 | 1.251 | 1.248 | 1.245 | 1.243 | 1.240 | 1.237 |
| .29 | 1.235 | 1.232 | 1.229 | 1.227 | 1.224 | 1.221 | 1.219 | 1.216 | 1.214 | 1.211 |
| .30 | 1.209 | 1.206 | 1.204 | 1.201 | 1.199 | 1.196 | 1.194 | 1.191 | 1.189 | 1.187 |
| .31 | 1.184 | 1.182 | 1.179 | 1.177 | 1.174 | 1.172 | 1.170 | 1.167 | 1.165 | 1.163 |
| .32 | 1.160 | 1.158 | 1.155 | 1.153 | 1.151 | 1.148 | 1.146 | 1.144 | 1.142 | 1.140 |
| .33 | 1.138 | 1.135 | 1.133 | 1.130 | 1.128 | 1.126 | 1.124 | 1.122 | 1.120 | 1.118 |
| .34 | 1.115 | 1.113 | 1.111 | 1.109 | 1.107 | 1.105 | 1.103 | 1.100 | 1.098 | 1.096 |
| .35 | 1.094 | 1.092 | 1.090 | 1.088 | 1.086 | 1.084 | 1.082 | 1.080 | 1.078 | 1.076 |
| .36 | 1.074 | 1.072 | 1.070 | 1.068 | 1.066 | 1.064 | 1.062 | 1.060 | 1.058 | 1.056 |
| .37 | 1.054 | 1.052 | 1.050 | 1.048 | 1.046 | 1.045 | 1.043 | 1.041 | 1.039 | 1.037 |
| .38 | 1.035 | 1.033 | 1.031 | 1.029 | 1.028 | 1.026 | 1.024 | 1.022 | 1.020 | 1.018 |
| .39 | 1.016 | 1.015 | 1.013 | 1.011 | 1.009 | 1.007 | 1.005 | 1.004 | 1.002 | 1.000 |
| .40 | .999 | .997 | .995 | .993 | .992 | .990 | .988 | .986 | .985 | .983 |
| .41 | .981 | .980 | .978 | .976 | .975 | .973 | .971 | .970 | .968 | .966 |
| .42 | .965 | .963 | .961 | .960 | .958 | .957 | .955 | .953 | .952 | .950 |
| .43 | .949 | .947 | .945 | .944 | .942 | .941 | .939 | .937 | .936 | .934 |
| .44 | .933 | .931 | .930 | .928 | .927 | .925 | .924 | .922 | .921 | .919 |
| .45 | .918 | .916 | .915 | .913 | .912 | .910 | .909 | .907 | .906 | .905 |
| .46 | .903 | .902 | .900 | .899 | .897 | .896 | .895 | .893 | .892 | .890 |
| .47 | .889 | .888 | .886 | .885 | .884 | .882 | .881 | .879 | .878 | .877 |
| .48 | .875 | .874 | .873 | .871 | .870 | .869 | .867 | .866 | .865 | .863 |
| .49 | .862 | .861 | .860 | .858 | .857 | .856 | .855 | .853 | .852 | .851 |
| .50 | .850 | .848 | .847 | .846 | .845 | .843 | .842 | .841 | .840 | .839 |
| .51 | .837 | .836 | .835 | .834 | .833 | .831 | .830 | .829 | .828 | .827 |
| .52 | .826 | .824 | .823 | .822 | .821 | .820 | .819 | .818 | .817 | .815 |
| .53 | .814 | .813 | .812 | .811 | .810 | .809 | .808 | .807 | .806 | .805 |
| .54 | .803 | .802 | .801 | .800 | .799 | .798 | .797 | .796 | .795 | .794 |
| .55 | .793 | .792 | .791 | .790 | .789 | .788 | .787 | .786 | .785 | .784 |
| .56 | .783 | .782 | .781 | .781 | .780 | .779 | .778 | .777 | .776 | .775 |
| .57 | .774 | .773 | .772 | .771 | .771 | .770 | .769 | .768 | .767 | .766 |
| .58 | .765 | .764 | .764 | .763 | .762 | .761 | .760 | .760 | .759 | .758 |
| .59 | .757 | .756 | .756 | .755 | .754 | .753 | .752 | .752 | .751 | .750 |
| .60 | .749 | .749 | .748 | .747 | .747 | .746 | .745 | .744 | .744 | .743 |
| .61 | .742 | .742 | .741 | .740 | .740 | .739 | .738 | .738 | .737 | .736 |
| .62 | .736 | .735 | .735 | .734 | .733 | .733 | .732 | .732 | .731 | .730 |
| .63 | .730 | .729 | .729 | .728 | .728 | .727 | .727 | .726 | .726 | .725 |
| .64 | .725 | .724 | .724 | .723 | .723 | .722 | .722 | .721 | .721 | .720 |
| .65 | .720 | .719 | .719 | .719 | .718 | .718 | .717 | .717 | .717 | .716 |
| .66 | .716 | .716 | .715 | .715 | .714 | .714 | .714 | .714 | .713 | .713 |

TABLE IX.—*Continued.*

| | .000 | .001 | .002 | .003 | .004 | .005 | .006 | .007 | .008 | .009 |
|---|---|---|---|---|---|---|---|---|---|---|
| .67 | .713 | .712 | .712 | .712 | .712 | .711 | .711 | .711 | .711 | .710 |
| .68 | .710 | .710 | .710 | .710 | .709 | .709 | .709 | .709 | .709 | .708 |
| .69 | .708 | .708 | .708 | .708 | .708 | .708 | .708 | .708 | .707 | .707 |
| .70 | .707 | .707 | .707 | .707 | .707 | .707 | .707 | .707 | .707 | .707 |
| .71 | .707 | .707 | .707 | .707 | .707 | .707 | .707 | .708 | .708 | .708 |
| .72 | .708 | .708 | .708 | .708 | .708 | .708 | .709 | .709 | .709 | .709 |
| .73 | .709 | .710 | .710 | .710 | .710 | .710 | .711 | .711 | .711 | .712 |
| .74 | .712 | .712 | .713 | .713 | .713 | .714 | .714 | .714 | .715 | .715 |
| .75 | .715 | .716 | .716 | .717 | .717 | .717 | .718 | .718 | .719 | .719 |
| .76 | .720 | .720 | .721 | .721 | .722 | .723 | .723 | .724 | .724 | .725 |
| .77 | .726 | .726 | .727 | .727 | .728 | .729 | .729 | .730 | .731 | .732 |
| .78 | .732 | .733 | .734 | .735 | .735 | .736 | .737 | .738 | .739 | .739 |
| .79 | .740 | .741 | .742 | .743 | .744 | .745 | .746 | .747 | .747 | .748 |
| .80 | .749 | .750 | .751 | .752 | .753 | .755 | .756 | .757 | .758 | .759 |
| .81 | .760 | .761 | .762 | .763 | .765 | .766 | .767 | .768 | .769 | .771 |
| .82 | .772 | .773 | .775 | .776 | .777 | .779 | .780 | .781 | .783 | .784 |
| .83 | .786 | .787 | .788 | .790 | .791 | .793 | .794 | .796 | .798 | .799 |
| .84 | .801 | .802 | .804 | .806 | .807 | .809 | .811 | .813 | .814 | .816 |
| .85 | .818 | .820 | .822 | .823 | .825 | .827 | .829 | .831 | .833 | .835 |
| .86 | .837 | .839 | .841 | .843 | .845 | .847 | .849 | .852 | .854 | .856 |
| .87 | .858 | .861 | .863 | .865 | .868 | .870 | .872 | .875 | .877 | .880 |
| .88 | .882 | .885 | .887 | .890 | .893 | .895 | .898 | .901 | .903 | .906 |
| .89 | .909 | .912 | .915 | .918 | .921 | .924 | .927 | .930 | .933 | .936 |
| .90 | .939 | .942 | .946 | .949 | .952 | .956 | .959 | .963 | .966 | .970 |
| .91 | .974 | .977 | .981 | .985 | .989 | .993 | .997 | 1.000 | 1.004 | 1.009 |
| .92 | 1.013 | 1.017 | 1.022 | 1.026 | 1.031 | 1.035 | 1.040 | 1.044 | 1.049 | 1.054 |
| .93 | 1.059 | 1.063 | 1.069 | 1.074 | 1.079 | 1.084 | 1.090 | 1.095 | 1.100 | 1.107 |
| .94 | 1.113 | 1.119 | 1.125 | 1.131 | 1.138 | 1.144 | 1.151 | 1.157 | 1.164 | 1.171 |
| .95 | 1.179 | 1.186 | 1.193 | 1.201 | 1.209 | 1.217 | 1.226 | 1.235 | 1.243 | 1.252 |
| .96 | 1.261 | 1.271 | 1.281 | 1.291 | 1.301 | 1.313 | 1.324 | 1.335 | 1.347 | 1.360 |
| .97 | 1.373 | 1.386 | 1.400 | 1.415 | 1.430 | 1.446 | 1.463 | 1.481 | 1.499 | 1.519 |
| .98 | 1.539 | 1.561 | 1.584 | 1.609 | 1.636 | 1.665 | 1.696 | 1.730 | 1.767 | 1.809 |
| .99 | 1.855 | 1.907 | 1.966 | 2.036 | 2.119 | 2.221 | 2.352 | 2.520 | 2.804 | 3.339 |

TABLE X. Lorentz-polarization factor, $(L\cdot p)^{\frac{1}{2}}\left[=\left(\frac{1}{\sin 2\theta}\cdot\frac{1+\cos^2 2\theta}{2}\right)^{\frac{1}{2}}\right]$, as a function of $\sigma$.

*Valid only for zero level when* $\mu=0$.

| | .000 | .002 | .004 | .006 | .008 | | .000 | .002 | .004 | .006 | .008 |
|---|---|---|---|---|---|---|---|---|---|---|---|
| .00 | ∞ | 22.42 | 15.79 | 12.91 | 11.21 | .30 | 1.795 | 1.789 | 1.783 | 1.777 | 1.770 |
| .01 | 10.01 | 9.129 | 8.442 | 7.908 | 7.451 | .31 | 1.764 | 1.758 | 1.752 | 1.746 | 1.740 |
| .02 | 7.070 | 6.742 | 6.453 | 6.201 | 5.976 | .32 | 1.734 | 1.729 | 1.723 | 1.717 | 1.711 |
| .03 | 5.774 | 5.588 | 5.422 | 5.271 | 5.128 | .33 | 1.706 | 1.700 | 1.695 | 1.689 | 1.684 |
| .04 | 5.000 | 4.879 | 4.766 | 4.660 | 4.563 | .34 | 1.678 | 1.673 | 1.668 | 1.663 | 1.657 |
| .05 | 4.470 | 4.383 | 4.301 | 4.224 | 4.150 | .35 | 1.652 | 1.647 | 1.642 | 1.637 | 1.632 |
| .06 | 4.080 | 4.014 | 3.950 | 3.890 | 3.831 | .36 | 1.627 | 1.622 | 1.617 | 1.612 | 1.607 |
| .07 | 3.776 | 3.723 | 3.673 | 3.624 | 3.576 | .37 | 1.602 | 1.598 | 1.593 | 1.588 | 1.584 |
| .08 | 3.531 | 3.487 | 3.445 | 3.406 | 3.366 | .38 | 1.579 | 1.574 | 1.570 | 1.566 | 1.561 |
| .09 | 3.329 | 3.291 | 3.256 | 3.222 | 3.189 | .39 | 1.557 | 1.552 | 1.548 | 1.543 | 1.539 |
| .10 | 3.157 | 3.125 | 3.095 | 3.065 | 3.036 | .40 | 1.535 | 1.531 | 1.526 | 1.522 | 1.518 |
| .11 | 3.008 | 2.981 | 2.955 | 2.939 | 2.904 | .41 | 1.514 | 1.510 | 1.505 | 1.501 | 1.497 |
| .12 | 2.889 | 2.855 | 2.832 | 2.809 | 2.787 | .42 | 1.493 | 1.489 | 1.485 | 1.481 | 1.477 |
| .13 | 2.765 | 2.744 | 2.722 | 2.702 | 2.682 | .43 | 1.473 | 1.470 | 1.466 | 1.462 | 1.458 |
| .14 | 2.663 | 2.644 | 2.623 | 2.607 | 2.589 | .44 | 1.454 | 1.451 | 1.447 | 1.443 | 1.439 |
| .15 | 2.571 | 2.554 | 2.537 | 2.520 | 2.504 | .45 | 1.436 | 1.432 | 1.429 | 1.425 | 1.421 |
| .16 | 2.488 | 2.472 | 2.457 | 2.442 | 2.427 | .46 | 1.418 | 1.414 | 1.411 | 1.407 | 1.404 |
| .17 | 2.412 | 2.398 | 2.384 | 2.370 | 2.356 | .47 | 1.400 | 1.397 | 1.393 | 1.390 | 1.386 |
| .18 | 2.343 | 2.330 | 2.317 | 2.304 | 2.291 | .48 | 1.383 | 1.380 | 1.377 | 1.373 | 1.370 |
| .19 | 2.279 | 2.266 | 2.254 | 2.243 | 2.231 | .49 | 1.366 | 1.363 | 1.360 | 1.357 | 1.354 |
| .20 | 2.219 | 2.208 | 2.197 | 2.186 | 2.175 | .50 | 1.350 | 1.347 | 1.344 | 1.341 | 1.338 |
| .21 | 2.164 | 2.154 | 2.143 | 2.133 | 2.123 | .51 | 1.335 | 1.332 | 1.329 | 1.326 | 1.322 |
| .22 | 2.113 | 2.103 | 2.093 | 2.084 | 2.074 | .52 | 1.319 | 1.316 | 1.313 | 1.310 | 1.307 |
| .23 | 2.064 | 2.055 | 2.046 | 2.037 | 2.028 | .53 | 1.304 | 1.301 | 1.298 | 1.295 | 1.293 |
| .24 | 2.019 | 2.011 | 2.002 | 1.993 | 1.985 | .54 | 1.290 | 1.287 | 1.284 | 1.281 | 1.278 |
| .25 | 1.977 | 1.969 | 1.960 | 1.952 | 1.944 | .55 | 1.276 | 1.273 | 1.270 | 1.267 | 1.264 |
| .26 | 1.936 | 1.929 | 1.921 | 1.913 | 1.906 | .56 | 1.261 | 1.259 | 1.256 | 1.253 | 1.251 |
| .27 | 1.898 | 1.891 | 1.884 | 1.877 | 1.869 | .57 | 1.248 | 1.245 | 1.243 | 1.240 | 1.237 |
| .28 | 1.862 | 1.855 | 1.848 | 1.842 | 1.835 | .58 | 1.235 | 1.232 | 1.229 | 1.227 | 1.224 |
| .29 | 1.828 | 1.821 | 1.815 | 1.808 | 1.802 | .59 | 1.221 | 1.219 | 1.216 | 1.214 | 1.211 |

TABLE X.—*Continued.*

| | .000 | .002 | .004 | .006 | .008 | | .000 | .002 | .004 | .006 | .008 |
|---|---|---|---|---|---|---|---|---|---|---|---|
| .60 | 1.209 | 1.206 | 1.204 | 1.201 | 1.199 | 1.30 | .720 | .719 | .719 | .719 | .718 |
| .61 | 1.196 | 1.194 | 1.191 | 1.189 | 1.187 | 1.31 | .718 | .717 | .717 | .717 | .716 |
| .62 | 1.184 | 1.182 | 1.179 | 1.177 | 1.174 | 1.32 | .716 | .716 | .715 | .715 | .714 |
| .63 | 1.172 | 1.170 | 1.167 | 1.165 | 1.163 | 1.33 | .714 | .714 | .714 | .713 | .713 |
| .64 | 1.160 | 1.158 | 1.155 | 1.153 | 1.151 | 1.34 | .713 | .712 | .712 | .712 | .712 |
| .65 | 1.148 | 1.146 | 1.144 | 1.142 | 1.140 | 1.35 | .711 | .711 | .711 | .711 | .710 |
| .66 | 1.138 | 1.135 | 1.133 | 1.130 | 1.128 | 1.36 | .710 | .710 | .710 | .710 | .709 |
| .67 | 1.126 | 1.124 | 1.122 | 1.120 | 1.118 | 1.37 | .709 | .709 | .709 | .709 | .708 |
| .68 | 1.115 | 1.113 | 1.111 | 1.109 | 1.107 | 1.38 | .708 | .708 | .708 | .708 | .708 |
| .69 | 1.105 | 1.103 | 1.100 | 1.098 | 1.096 | 1.39 | .708 | .708 | .708 | .707 | .707 |
| .70 | 1.094 | 1.092 | 1.090 | 1.088 | 1.086 | 1.40 | .707 | .707 | .707 | .707 | .707 |
| .71 | 1.084 | 1.082 | 1.080 | 1.078 | 1.076 | 1.41 | .707 | .707 | .707 | .707 | .707 |
| .72 | 1.074 | 1.072 | 1.070 | 1.068 | 1.066 | 1.42 | .707 | .707 | .707 | .707 | .707 |
| .73 | 1.064 | 1.062 | 1.060 | 1.058 | 1.056 | 1.43 | .707 | .707 | .708 | .708 | .708 |
| .74 | 1.054 | 1.052 | 1.050 | 1.048 | 1.046 | 1.44 | .708 | .708 | .708 | .708 | .708 |
| .75 | 1.045 | 1.043 | 1.041 | 1.039 | 1.037 | 1.45 | .708 | .709 | .709 | .709 | .709 |
| .76 | 1.035 | 1.033 | 1.031 | 1.029 | 1.028 | 1.46 | .709 | .710 | .710 | .710 | .710 |
| .77 | 1.026 | 1.024 | 1.022 | 1.020 | 1.018 | 1.47 | .710 | .711 | .711 | .711 | .712 |
| .78 | 1.016 | 1.015 | 1.013 | 1.011 | 1.009 | 1.48 | .712 | .712 | .713 | .713 | .713 |
| .79 | 1.007 | 1.005 | 1.004 | 1.002 | 1.000 | 1.49 | .714 | .714 | .714 | .715 | .715 |
| .80 | .999 | .997 | .995 | .993 | .992 | 1.50 | .715 | .716 | .716 | .717 | .717 |
| .81 | .990 | .988 | .986 | .985 | .983 | 1.51 | .717 | .718 | .718 | .719 | .719 |
| .82 | .981 | .980 | .978 | .976 | .975 | 1.52 | .720 | .720 | .721 | .721 | .722 |
| .83 | .973 | .971 | .970 | .968 | .966 | 1.53 | .723 | .723 | .724 | .724 | .725 |
| .84 | .965 | .963 | .961 | .960 | .958 | 1.54 | .726 | .726 | .727 | .727 | .728 |
| .85 | .957 | .955 | .953 | .952 | .950 | 1.55 | .729 | .729 | .730 | .731 | .732 |
| .86 | .949 | .947 | .945 | .944 | .942 | 1.56 | .732 | .733 | .734 | .735 | .735 |
| .87 | .941 | .939 | .937 | .936 | .934 | 1.57 | .736 | .737 | .738 | .739 | .739 |
| .88 | .933 | .931 | .930 | .928 | .927 | 1.58 | .740 | .741 | .742 | .743 | .744 |
| .89 | .925 | .924 | .922 | .921 | .919 | 1.59 | .745 | .746 | .747 | .747 | .748 |
| .90 | .918 | .916 | .915 | .913 | .912 | 1.60 | .749 | .750 | .751 | .752 | .753 |
| .91 | .910 | .909 | .907 | .906 | .905 | 1.61 | .755 | .756 | .757 | .758 | .759 |
| .92 | .903 | .902 | .900 | .899 | .897 | 1.62 | .760 | .761 | .762 | .763 | .765 |
| .93 | .896 | .895 | .893 | .892 | .890 | 1.63 | .766 | .767 | .768 | .769 | .771 |
| .94 | .889 | .888 | .886 | .885 | .884 | 1.64 | .772 | .773 | .775 | .776 | .777 |
| .95 | .882 | .881 | .879 | .878 | .877 | 1.65 | .779 | .780 | .781 | .783 | .784 |
| .96 | .875 | .874 | .873 | .871 | .870 | 1.66 | .786 | .787 | .788 | .790 | .791 |
| .97 | .869 | .867 | .866 | .865 | .863 | 1.67 | .793 | .794 | .796 | .798 | .799 |
| .98 | .862 | .861 | .860 | .858 | .857 | 1.68 | .801 | .802 | .804 | .806 | .807 |
| .99 | .856 | .855 | .853 | .852 | .851 | 1.69 | .809 | .811 | .813 | .814 | .816 |
| 1.00 | .850 | .848 | .847 | .846 | .845 | 1.70 | .818 | .820 | .822 | .823 | .825 |
| 1.01 | .843 | .842 | .841 | .840 | .839 | 1.71 | .827 | .829 | .831 | .833 | .835 |
| 1.02 | .837 | .836 | .835 | .834 | .833 | 1.72 | .837 | .839 | .841 | .843 | .845 |
| 1.03 | .831 | .830 | .829 | .828 | .827 | 1.73 | .847 | .849 | .852 | .854 | .856 |
| 1.04 | .826 | .824 | .823 | .822 | .821 | 1.74 | .858 | .861 | .863 | .865 | .868 |
| 1.05 | .820 | .819 | .818 | .817 | .815 | 1.75 | .870 | .872 | .875 | .877 | .880 |
| 1.06 | .814 | .813 | .812 | .811 | .810 | 1.76 | .882 | .885 | .887 | .890 | .893 |
| 1.07 | .809 | .808 | .807 | .806 | .805 | 1.77 | .895 | .898 | .901 | .903 | .906 |
| 1.08 | .803 | .802 | .801 | .800 | .799 | 1.78 | .909 | .912 | .915 | .918 | .921 |
| 1.09 | .798 | .797 | .796 | .795 | .794 | 1.79 | .924 | .927 | .930 | .933 | .936 |
| 1.10 | .793 | .792 | .791 | .790 | .789 | 1.80 | .939 | .942 | .946 | .949 | .952 |
| 1.11 | .788 | .787 | .786 | .785 | .784 | 1.81 | .956 | .959 | .963 | .966 | .970 |
| 1.12 | .783 | .782 | .781 | .781 | .780 | 1.82 | .974 | .977 | .981 | .985 | .989 |
| 1.13 | .779 | .778 | .777 | .776 | .775 | 1.83 | .993 | .997 | 1.000 | 1.004 | 1.009 |
| 1.14 | .774 | .773 | .772 | .771 | .771 | 1.84 | 1.013 | 1.017 | 1.022 | 1.026 | 1.031 |
| 1.15 | .770 | .769 | .768 | .767 | .766 | 1.85 | 1.035 | 1.040 | 1.044 | 1.049 | 1.054 |
| 1.16 | .765 | .764 | .764 | .763 | .762 | 1.86 | 1.059 | 1.063 | 1.069 | 1.074 | 1.079 |
| 1.17 | .761 | .760 | .760 | .759 | .758 | 1.87 | 1.084 | 1.090 | 1.095 | 1.100 | 1.107 |
| 1.18 | .757 | .756 | .756 | .755 | .754 | 1.88 | 1.113 | 1.119 | 1.125 | 1.131 | 1.138 |
| 1.19 | .753 | .752 | .752 | .751 | .750 | 1.89 | 1.144 | 1.151 | 1.157 | 1.164 | 1.171 |
| 1.20 | .749 | .749 | .748 | .747 | .747 | 1.90 | 1.179 | 1.186 | 1.193 | 1.201 | 1.209 |
| 1.21 | .746 | .745 | .744 | .744 | .743 | 1.91 | 1.217 | 1.226 | 1.235 | 1.243 | 1.252 |
| 1.22 | .742 | .742 | .741 | .740 | .740 | 1.92 | 1.261 | 1.271 | 1.281 | 1.291 | 1.301 |
| 1.23 | .739 | .738 | .738 | .737 | .736 | 1.93 | 1.313 | 1.324 | 1.335 | 1.347 | 1.360 |
| 1.24 | .736 | .735 | .735 | .734 | .733 | 1.94 | 1.373 | 1.386 | 1.400 | 1.415 | 1.430 |
| 1.25 | .733 | .732 | .732 | .731 | .730 | 1.95 | 1.446 | 1.463 | 1.481 | 1.499 | 1.519 |
| 1.26 | .730 | .729 | .729 | .728 | .728 | 1.96 | 1.539 | 1.561 | 1.584 | 1.609 | 1.636 |
| 1.27 | .727 | .727 | .726 | .726 | .725 | 1.97 | 1.665 | 1.696 | 1.730 | 1.767 | 1.809 |
| 1.28 | .725 | .724 | .724 | .723 | .723 | 1.98 | 1.855 | 1.907 | 1.966 | 2.036 | 2.199 |
| 1.29 | .722 | .722 | .721 | .721 | .720 | 1.99 | 2.221 | 2.352 | 2.520 | 2.804 | 3.339 |

TABLE XI. $(h^2+k^2)^{\frac{1}{2}}$.

| h \ k | 0 | 1 | 2 | 3 | 4 | 5 | 6 | 7 | 8 | 9 | 10 | 11 | 12 | 13 | 14 | 15 | h \ k |
|---|---|---|---|---|---|---|---|---|---|---|---|---|---|---|---|---|---|
| 0 | 0 | 1.000 | 2.000 | 3.000 | 4.000 | 5.000 | 6.000 | 7.000 | 8.000 | 9.000 | 10.00 | 11.00 | 12.00 | 13.00 | 14.00 | 15.00 | 0 |
| 1 | 1.000 | 1.414 | 2.236 | 3.162 | 4.123 | 5.099 | 6.083 | 7.071 | 8.062 | 9.055 | 10.05 | 11.05 | 12.04 | 13.04 | 14.04 | 15.03 | 1 |
| 2 | 2.000 | 2.236 | 2.828 | 3.606 | 4.472 | 5.385 | 6.325 | 7.280 | 8.246 | 9.220 | 10.20 | 11.18 | 12.17 | 13.15 | 14.14 | 15.13 | 2 |
| 3 | 3.000 | 3.162 | 3.606 | 4.243 | 5.000 | 5.831 | 6.708 | 7.616 | 8.544 | 9.487 | 10.44 | 11.40 | 12.37 | 13.34 | 14.32 | 15.30 | 3 |
| 4 | 4.000 | 4.123 | 4.472 | 5.000 | 5.657 | 6.403 | 7.211 | 8.062 | 8.944 | 9.849 | 10.77 | 11.70 | 12.65 | 13.60 | 14.56 | 15.52 | 4 |
| 5 | 5.000 | 5.099 | 5.385 | 5.831 | 6.403 | 7.071 | 7.810 | 8.602 | 9.434 | 10.30 | 11.18 | 12.08 | 13.00 | 13.93 | 14.87 | 15.81 | 5 |
| 6 | 6.000 | 6.083 | 6.325 | 6.708 | 7.211 | 7.810 | 8.485 | 9.220 | 10.00 | 10.82 | 11.66 | 12.53 | 13.42 | 14.32 | 15.23 | 16.16 | 6 |
| 7 | 7.000 | 7.071 | 7.280 | 7.616 | 8.062 | 8.602 | 9.220 | 9.899 | 10.63 | 11.40 | 12.21 | 13.04 | 13.89 | 14.76 | 15.65 | 16.55 | 7 |
| 8 | 8.000 | 8.062 | 8.246 | 8.544 | 8.944 | 9.434 | 10.00 | 10.63 | 11.31 | 12.04 | 12.81 | 13.60 | 14.42 | 15.26 | 16.12 | 17.00 | 8 |
| 9 | 9.000 | 9.055 | 9.220 | 9.487 | 9.849 | 10.30 | 10.82 | 11.40 | 12.04 | 12.73 | 13.45 | 14.21 | 15.00 | 15.81 | 16.64 | 17.49 | 9 |
| 10 | 10.00 | 10.05 | 10.20 | 10.44 | 10.77 | 11.18 | 11.66 | 12.21 | 12.81 | 13.45 | 14.14 | 14.87 | 15.62 | 16.40 | 17.20 | 18.03 | 10 |
| 11 | 11.00 | 11.05 | 11.18 | 11.40 | 11.70 | 12.08 | 12.53 | 13.04 | 13.60 | 14.21 | 14.87 | 15.56 | 16.28 | 17.03 | 17.80 | 18.60 | 11 |
| 12 | 12.00 | 12.04 | 12.17 | 12.37 | 12.65 | 13.00 | 13.42 | 13.89 | 14.42 | 15.00 | 15.62 | 16.28 | 16.97 | 17.69 | 18.44 | 19.21 | 12 |
| 13 | 13.00 | 13.04 | 13.15 | 13.34 | 13.60 | 13.93 | 14.32 | 14.76 | 15.26 | 15.81 | 16.40 | 17.03 | 17.69 | 18.38 | 19.10 | 19.85 | 13 |
| 14 | 14.00 | 14.04 | 14.14 | 14.32 | 14.56 | 14.87 | 15.23 | 15.65 | 16.12 | 16.64 | 17.20 | 17.80 | 18.44 | 19.10 | 19.80 | 20.52 | 14 |
| 15 | 15.00 | 15.03 | 15.13 | 15.30 | 15.52 | 15.81 | 16.16 | 16.55 | 17.00 | 17.49 | 18.03 | 18.60 | 19.21 | 19.85 | 20.52 | 21.21 | 15 |
| 16 | 16.00 | 16.03 | 16.12 | 16.28 | 16.49 | 16.76 | 17.09 | 17.46 | 17.89 | 18.36 | 18.87 | 19.42 | 20.00 | 20.62 | 21.26 | 21.93 | 16 |
| 17 | 17.00 | 17.03 | 17.12 | 17.26 | 17.46 | 17.72 | 18.03 | 18.38 | 18.79 | 19.24 | 19.72 | 20.25 | 20.81 | 21.40 | 22.02 | 22.67 | 17 |
| 18 | 18.00 | 18.03 | 18.11 | 18.25 | 18.44 | 18.68 | 18.97 | 19.31 | 19.70 | 20.12 | 20.59 | 21.10 | 21.63 | 22.20 | 22.80 | 23.43 | 18 |
| 19 | 19.00 | 19.03 | 19.10 | 19.24 | 19.42 | 19.65 | 19.92 | 20.25 | 20.62 | 21.02 | 21.47 | 21.95 | 22.47 | 23.02 | 23.60 | 24.21 | 19 |
| 20 | 20.00 | 20.02 | 20.10 | 20.22 | 20.40 | 20.62 | 20.88 | 21.19 | 21.54 | 21.93 | 22.36 | 22.83 | 23.32 | 23.85 | 24.41 | 25.00 | 20 |
| 21 | 21.00 | 21.02 | 21.10 | 21.21 | 21.38 | 21.59 | 21.84 | 22.14 | 22.47 | 22.85 | 23.26 | 23.71 | 24.19 | 24.70 | 25.24 | 25.81 | 21 |
| 22 | 22.00 | 22.02 | 22.09 | 22.20 | 22.36 | 22.56 | 22.80 | 23.09 | 23.41 | 23.77 | 24.17 | 24.60 | 25.06 | 25.55 | 26.08 | 26.63 | 22 |
| 23 | 23.00 | 23.02 | 23.09 | 23.19 | 23.35 | 23.54 | 23.77 | 24.04 | 24.35 | 24.70 | 25.08 | 25.50 | 25.94 | 26.42 | 26.93 | 27.46 | 23 |
| 24 | 24.00 | 24.02 | 24.08 | 24.19 | 24.33 | 24.52 | 24.74 | 25.00 | 25.30 | 25.63 | 26.00 | 26.40 | 26.83 | 27.29 | 27.78 | 28.30 | 24 |
| 25 | 25.00 | 25.02 | 25.08 | 25.18 | 25.32 | 25.50 | 25.71 | 25.96 | 26.25 | 26.57 | 26.93 | 27.31 | 27.73 | 28.18 | 28.65 | 29.15 | 25 |
| 26 | 26.00 | 26.02 | 26.08 | 26.17 | 26.31 | 26.48 | 26.68 | 26.93 | 27.20 | 27.51 | 27.86 | 28.23 | 28.64 | 29.07 | 29.53 | 30.02 | 26 |
| 27 | 27.00 | 27.02 | 27.07 | 27.17 | 27.29 | 27.46 | 27.66 | 27.89 | 28.16 | 28.46 | 28.79 | 29.15 | 29.55 | 29.97 | 30.41 | 30.89 | 27 |
| 28 | 28.00 | 28.02 | 28.07 | 28.16 | 28.28 | 28.44 | 28.64 | 28.86 | 29.12 | 29.41 | 29.73 | 30.08 | 30.46 | 30.87 | 31.30 | 31.76 | 28 |
| 29 | 29.00 | 29.02 | 29.07 | 29.15 | 29.27 | 29.43 | 29.61 | 29.83 | 30.08 | 30.36 | 30.68 | 31.02 | 31.38 | 31.78 | 32.20 | 32.65 | 29 |
| 30 | 30.00 | 30.02 | 30.07 | 30.15 | 30.27 | 30.41 | 30.59 | 30.81 | 31.05 | 31.32 | 31.62 | 31.95 | 32.31 | 32.70 | 33.11 | 33.54 | 30 |

TABLE XI.—*Continued.*

| h \ k | 16 | 17 | 18 | 19 | 20 | 21 | 22 | 23 | 24 | 25 | 26 | 27 | 28 | 29 | 30 | h \ k |
|---|---|---|---|---|---|---|---|---|---|---|---|---|---|---|---|---|
| 0 | 16.00 | 17.00 | 18.00 | 19.00 | 20.00 | 21.00 | 22.00 | 23.00 | 24.00 | 25.00 | 26.00 | 27.00 | 28.00 | 29.00 | 30.00 | 0 |
| 1 | 16.03 | 17.03 | 18.03 | 19.03 | 20.02 | 21.02 | 22.02 | 23.02 | 24.02 | 25.02 | 26.02 | 27.02 | 28.02 | 29.02 | 30.02 | 1 |
| 2 | 16.12 | 17.12 | 18.11 | 19.10 | 20.10 | 21.10 | 22.09 | 23.09 | 24.08 | 25.08 | 26.08 | 27.07 | 28.07 | 29.07 | 30.07 | 2 |
| 3 | 16.28 | 17.26 | 18.25 | 19.24 | 20.22 | 21.21 | 22.20 | 23.19 | 24.19 | 25.18 | 26.17 | 27.17 | 28.16 | 29.15 | 30.15 | 3 |
| 4 | 16.49 | 17.46 | 18.44 | 19.42 | 20.40 | 21.38 | 22.36 | 23.35 | 24.33 | 25.32 | 26.31 | 27.29 | 28.28 | 29.27 | 30.27 | 4 |
| 5 | 16.76 | 17.72 | 18.68 | 19.65 | 20.62 | 21.59 | 22.56 | 23.54 | 24.52 | 25.50 | 26.48 | 27.46 | 28.44 | 29.43 | 30.41 | 5 |
| 6 | 17.09 | 18.03 | 18.97 | 19.92 | 20.88 | 21.84 | 22.80 | 23.77 | 24.74 | 25.71 | 26.68 | 27.66 | 28.64 | 29.61 | 30.59 | 6 |
| 7 | 17.46 | 18.38 | 19.31 | 20.25 | 21.19 | 22.14 | 23.09 | 24.04 | 25.00 | 25.96 | 26.93 | 27.89 | 28.86 | 29.83 | 30.81 | 7 |
| 8 | 17.89 | 18.79 | 19.70 | 20.62 | 21.54 | 22.47 | 23.41 | 24.35 | 25.30 | 26.25 | 27.20 | 28.16 | 29.12 | 30.08 | 31.05 | 8 |
| 9 | 18.36 | 19.24 | 20.12 | 21.02 | 21.93 | 22.85 | 23.77 | 24.70 | 25.63 | 26.57 | 27.51 | 28.46 | 29.41 | 30.36 | 31.32 | 9 |
| 10 | 18.87 | 19.72 | 20.59 | 21.47 | 22.36 | 23.26 | 24.17 | 25.08 | 26.00 | 26.93 | 27.86 | 28.79 | 29.73 | 30.68 | 31.62 | 10 |
| 11 | 19.42 | 20.25 | 21.10 | 21.95 | 22.83 | 23.71 | 24.60 | 25.50 | 26.40 | 27.31 | 28.23 | 29.15 | 30.08 | 31.02 | 31.95 | 11 |
| 12 | 20.00 | 20.81 | 21.63 | 22.47 | 23.32 | 24.19 | 25.06 | 25.94 | 26.83 | 27.73 | 28.64 | 29.55 | 30.46 | 31.38 | 32.31 | 12 |
| 13 | 20.62 | 21.40 | 22.20 | 23.02 | 23.85 | 24.70 | 25.55 | 26.42 | 27.29 | 28.18 | 29.07 | 29.97 | 30.87 | 31.78 | 32.70 | 13 |
| 14 | 21.26 | 22.02 | 22.80 | 23.60 | 24.41 | 25.24 | 26.08 | 26.93 | 27.78 | 28.65 | 29.53 | 30.41 | 31.30 | 32.20 | 33.11 | 14 |
| 15 | 21.93 | 22.67 | 23.43 | 24.21 | 25.00 | 25.81 | 26.63 | 27.46 | 28.30 | 29.15 | 30.02 | 30.89 | 31.76 | 32.65 | 33.54 | 15 |
| 16 | 22.63 | 23.35 | 24.08 | 24.84 | 25.61 | 26.40 | 27.20 | 28.02 | 28.84 | 29.68 | 30.53 | 31.38 | 32.25 | 33.12 | 34.00 | 16 |
| 17 | 23.35 | 24.04 | 24.76 | 25.50 | 26.25 | 27.02 | 27.80 | 28.60 | 29.41 | 30.23 | 31.06 | 31.91 | 32.76 | 33.62 | 34.48 | 17 |
| 18 | 24.08 | 24.76 | 25.46 | 26.17 | 26.91 | 27.66 | 28.43 | 29.21 | 30.00 | 30.81 | 31.62 | 32.45 | 33.29 | 34.13 | 34.99 | 18 |
| 19 | 24.84 | 25.50 | 26.17 | 26.87 | 27.59 | 28.32 | 29.07 | 29.83 | 30.61 | 31.40 | 32.20 | 33.02 | 33.84 | 34.67 | 35.51 | 19 |
| 20 | 25.61 | 26.25 | 26.91 | 27.59 | 28.28 | 29.00 | 29.73 | 30.48 | 31.24 | 32.02 | 32.80 | 33.60 | 34.41 | 35.23 | 36.06 | 20 |
| 21 | 26.40 | 27.02 | 27.66 | 28.32 | 29.00 | 29.70 | 30.41 | 31.14 | 31.89 | 32.65 | 33.42 | 34.21 | 35.00 | 35.81 | 36.62 | 21 |
| 22 | 27.20 | 27.80 | 28.43 | 29.07 | 29.73 | 30.41 | 31.11 | 31.83 | 32.56 | 33.30 | 34.06 | 34.83 | 35.61 | 36.40 | 37.20 | 22 |
| 23 | 28.02 | 28.60 | 29.21 | 29.83 | 30.48 | 31.14 | 31.83 | 32.53 | 33.24 | 33.97 | 34.71 | 35.47 | 36.24 | 37.01 | 37.80 | 23 |
| 24 | 28.84 | 29.41 | 30.00 | 30.61 | 31.24 | 31.89 | 32.56 | 33.24 | 33.94 | 34.66 | 35.38 | 36.12 | 36.88 | 37.64 | 38.42 | 24 |
| 25 | 29.68 | 30.23 | 30.81 | 31.40 | 32.02 | 32.65 | 33.30 | 33.97 | 34.66 | 35.36 | 36.07 | 36.80 | 37.54 | 38.29 | 39.05 | 25 |
| 26 | 30.53 | 31.06 | 31.62 | 32.20 | 32.80 | 33.42 | 34.06 | 34.71 | 35.38 | 36.07 | 36.77 | 37.48 | 38.21 | 38.95 | 39.70 | 26 |
| 27 | 31.38 | 31.91 | 32.45 | 33.02 | 33.60 | 34.21 | 34.83 | 35.47 | 36.12 | 36.80 | 37.48 | 38.18 | 38.90 | 39.62 | 40.36 | 27 |
| 28 | 32.25 | 32.76 | 33.29 | 33.84 | 34.41 | 35.00 | 35.61 | 36.24 | 36.88 | 37.54 | 38.21 | 38.90 | 39.60 | 40.31 | 41.04 | 28 |
| 29 | 33.12 | 33.62 | 34.13 | 34.67 | 35.23 | 35.81 | 36.40 | 37.01 | 37.64 | 38.29 | 38.95 | 39.62 | 40.31 | 41.01 | 41.73 | 29 |
| 30 | 34.00 | 34.48 | 34.99 | 35.51 | 36.06 | 36.62 | 37.20 | 37.80 | 38.42 | 39.05 | 39.70 | 40.36 | 41.04 | 41.73 | 42.43 | 30 |

TABLE XII. $(h^2+k^2+hk)^{\frac{1}{2}}$.

| h \ k | 0 | 1 | 2 | 3 | 4 | 5 | 6 | 7 | 8 | 9 | 10 | 11 | 12 | 13 | 14 | 15 | h \ k |
|---|---|---|---|---|---|---|---|---|---|---|---|---|---|---|---|---|---|
| 0 | 0 | 1.000 | 2.000 | 3.000 | 4.000 | 5.000 | 6.000 | 7.000 | 8.000 | 9.000 | 10.00 | 11.00 | 12.00 | 13.00 | 14.00 | 15.00 | 0 |
| 1 | 1.000 | 1.732 | 2.646 | 3.606 | 4.583 | 5.568 | 6.557 | 7.550 | 8.544 | 9.539 | 10.54 | 11.53 | 12.53 | 13.53 | 14.53 | 15.52 | 1 |
| 2 | 2.000 | 2.646 | 3.464 | 4.359 | 5.292 | 6.245 | 7.211 | 8.185 | 9.165 | 10.15 | 11.14 | 12.12 | 13.11 | 14.11 | 15.10 | 16.09 | 2 |
| 3 | 3.000 | 3.606 | 4.359 | 5.196 | 6.083 | 7.000 | 7.937 | 8.888 | 9.849 | 10.82 | 11.79 | 12.77 | 13.75 | 14.73 | 15.72 | 16.70 | 3 |
| 4 | 4.000 | 4.583 | 5.292 | 6.083 | 6.928 | 7.810 | 8.718 | 9.644 | 10.58 | 11.53 | 12.49 | 13.45 | 14.42 | 15.39 | 16.37 | 17.35 | 4 |
| 5 | 5.000 | 5.568 | 6.245 | 7.000 | 7.810 | 8.660 | 9.539 | 10.44 | 11.36 | 12.29 | 13.23 | 14.18 | 15.13 | 16.09 | 17.06 | 18.03 | 5 |
| 6 | 6.000 | 6.557 | 7.211 | 7.937 | 8.718 | 9.539 | 10.39 | 11.27 | 12.17 | 13.08 | 14.00 | 14.93 | 15.87 | 16.82 | 17.78 | 18.73 | 6 |
| 7 | 7.000 | 7.550 | 8.185 | 8.888 | 9.644 | 10.44 | 11.27 | 12.12 | 13.00 | 13.89 | 14.80 | 15.72 | 16.64 | 17.58 | 18.52 | 19.47 | 7 |
| 8 | 8.000 | 8.544 | 9.165 | 9.849 | 10.58 | 11.36 | 12.17 | 13.00 | 13.86 | 14.73 | 15.62 | 16.52 | 17.44 | 18.36 | 19.29 | 20.22 | 8 |
| 9 | 9.000 | 9.539 | 10.15 | 10.82 | 11.53 | 12.29 | 13.08 | 13.89 | 14.73 | 15.59 | 16.46 | 17.35 | 18.25 | 19.16 | 20.07 | 21.00 | 9 |
| 10 | 10.00 | 10.54 | 11.14 | 11.79 | 12.49 | 13.23 | 14.00 | 14.80 | 15.62 | 16.46 | 17.32 | 18.19 | 19.08 | 19.97 | 20.88 | 21.79 | 10 |
| 11 | 11.00 | 11.53 | 12.12 | 12.77 | 13.45 | 14.18 | 14.93 | 15.72 | 16.52 | 17.35 | 18.19 | 19.05 | 19.92 | 20.81 | 21.70 | 22.61 | 11 |
| 12 | 12.00 | 12.53 | 13.11 | 13.75 | 14.42 | 15.13 | 15.87 | 16.64 | 17.44 | 18.25 | 19.08 | 19.92 | 20.78 | 21.66 | 22.54 | 23.43 | 12 |
| 13 | 13.00 | 13.53 | 14.11 | 14.73 | 15.39 | 16.09 | 16.82 | 17.58 | 18.36 | 19.16 | 19.97 | 20.81 | 21.66 | 22.52 | 23.39 | 24.27 | 13 |
| 14 | 14.00 | 14.53 | 15.10 | 15.72 | 16.37 | 17.06 | 17.78 | 18.52 | 19.29 | 20.07 | 20.88 | 21.70 | 22.54 | 23.39 | 24.25 | 25.12 | 14 |
| 15 | 15.00 | 15.52 | 16.09 | 16.70 | 17.35 | 18.03 | 18.73 | 19.47 | 20.22 | 21.00 | 21.79 | 22.61 | 23.43 | 24.27 | 25.12 | 25.98 | 15 |
| 16 | 16.00 | 16.52 | 17.09 | 17.69 | 18.33 | 19.00 | 19.70 | 20.42 | 21.17 | 21.93 | 22.72 | 23.52 | 24.33 | 25.16 | 26.00 | 26.85 | 16 |
| 17 | 17.00 | 17.52 | 18.08 | 18.68 | 19.31 | 19.97 | 20.66 | 21.38 | 22.11 | 22.87 | 23.64 | 24.43 | 25.24 | 26.06 | 26.89 | 27.73 | 17 |
| 18 | 18.00 | 18.52 | 19.08 | 19.67 | 20.30 | 20.95 | 21.63 | 22.34 | 23.07 | 23.81 | 24.58 | 25.36 | 26.15 | 26.96 | 27.78 | 28.62 | 18 |
| 19 | 19.00 | 19.52 | 20.07 | 20.66 | 21.28 | 21.93 | 22.61 | 23.30 | 24.02 | 24.76 | 25.51 | 26.29 | 27.07 | 27.87 | 28.69 | 29.51 | 19 |
| 20 | 20.00 | 20.52 | 21.07 | 21.66 | 22.27 | 22.91 | 23.58 | 24.27 | 24.98 | 25.71 | 26.46 | 27.22 | 28.00 | 28.79 | 29.60 | 30.41 | 20 |
| 21 | 21.00 | 21.52 | 22.07 | 22.65 | 23.26 | 23.90 | 24.56 | 25.24 | 25.94 | 26.66 | 27.40 | 28.16 | 28.93 | 29.72 | 30.51 | 31.32 | 21 |
| 22 | 22.00 | 22.52 | 23.07 | 23.64 | 24.25 | 24.88 | 25.53 | 26.21 | 26.91 | 27.62 | 28.35 | 29.10 | 29.87 | 30.64 | 31.43 | 32.23 | 22 |
| 23 | 23.00 | 23.52 | 24.06 | 24.64 | 25.24 | 25.87 | 26.51 | 27.18 | 27.87 | 28.58 | 29.31 | 30.05 | 30.81 | 31.58 | 32.36 | 33.15 | 23 |
| 24 | 24.00 | 24.52 | 25.06 | 25.63 | 26.23 | 26.85 | 27.50 | 28.16 | 28.84 | 29.55 | 30.27 | 31.00 | 31.75 | 32.51 | 33.29 | 34.07 | 24 |
| 25 | 25.00 | 25.51 | 26.06 | 26.63 | 27.22 | 27.84 | 28.48 | 29.14 | 29.82 | 30.51 | 31.22 | 31.95 | 32.70 | 33.45 | 34.22 | 35.00 | 25 |
| 26 | 26.00 | 26.51 | 27.06 | 27.62 | 28.21 | 28.83 | 29.46 | 30.12 | 30.79 | 31.48 | 32.19 | 32.91 | 33.65 | 34.39 | 35.16 | 35.93 | 26 |
| 27 | 27.00 | 27.51 | 28.05 | 28.62 | 29.21 | 29.82 | 30.45 | 31.10 | 31.76 | 32.45 | 33.15 | 33.87 | 34.60 | 35.34 | 36.10 | 36.86 | 27 |
| 28 | 28.00 | 28.51 | 29.05 | 29.61 | 30.20 | 30.81 | 31.43 | 32.08 | 32.74 | 33.42 | 34.12 | 34.83 | 35.55 | 36.29 | 37.04 | 37.80 | 28 |
| 29 | 29.00 | 29.51 | 30.05 | 30.61 | 31.19 | 31.80 | 32.42 | 33.06 | 33.72 | 34.39 | 35.09 | 35.79 | 36.51 | 37.24 | 37.99 | 38.74 | 29 |
| 30 | 30.00 | 30.51 | 31.05 | 31.61 | 32.19 | 32.79 | 33.41 | 34.04 | 34.70 | 35.37 | 36.06 | 36.76 | 37.47 | 38.20 | 38.94 | 39.69 | 30 |

TABLE XII.—*Continued.*

| h \ k | 16 | 17 | 18 | 19 | 20 | 21 | 22 | 23 | 24 | 25 | 26 | 27 | 28 | 29 | 30 | h \ k |
|---|---|---|---|---|---|---|---|---|---|---|---|---|---|---|---|---|
| 0 | 16.00 | 17.00 | 18.00 | 19.00 | 20.00 | 21.00 | 22.00 | 23.00 | 24.00 | 25.00 | 26.00 | 27.00 | 28.00 | 29.00 | 30.00 | 0 |
| 1 | 16.52 | 17.52 | 18.52 | 19.52 | 20.52 | 21.52 | 22.52 | 23.52 | 24.52 | 25.51 | 26.51 | 27.51 | 28.51 | 29.51 | 30.51 | 1 |
| 2 | 17.09 | 18.08 | 19.08 | 20.07 | 21.07 | 22.07 | 23.07 | 24.06 | 25.06 | 26.06 | 27.06 | 28.05 | 29.05 | 30.05 | 31.05 | 2 |
| 3 | 17.69 | 18.68 | 19.67 | 20.66 | 21.66 | 22.65 | 23.64 | 24.64 | 25.63 | 26.63 | 27.62 | 28.62 | 29.61 | 30.61 | 31.61 | 3 |
| 4 | 18.33 | 19.31 | 20.30 | 21.28 | 22.27 | 23.26 | 24.25 | 25.24 | 26.23 | 27.22 | 28.21 | 29.21 | 30.20 | 31.19 | 32.19 | 4 |
| 5 | 19.00 | 19.97 | 20.95 | 21.93 | 22.91 | 23.90 | 24.88 | 25.87 | 26.85 | 27.84 | 28.83 | 29.82 | 30.81 | 31.80 | 32.79 | 5 |
| 6 | 19.70 | 20.66 | 21.63 | 22.61 | 23.58 | 24.56 | 25.53 | 26.51 | 27.50 | 28.48 | 29.46 | 30.45 | 31.43 | 32.42 | 33.41 | 6 |
| 7 | 20.42 | 21.38 | 22.34 | 23.30 | 24.27 | 25.24 | 26.21 | 27.18 | 28.16 | 29.14 | 30.12 | 31.10 | 32.08 | 33.06 | 34.04 | 7 |
| 8 | 21.17 | 22.11 | 23.07 | 24.02 | 24.98 | 25.94 | 26.91 | 27.87 | 28.84 | 29.82 | 30.79 | 31.76 | 32.74 | 33.72 | 34.70 | 8 |
| 9 | 21.93 | 22.87 | 23.81 | 24.76 | 25.71 | 26.66 | 27.62 | 28.58 | 29.55 | 30.51 | 31.48 | 32.45 | 33.42 | 34.39 | 35.37 | 9 |
| 10 | 22.72 | 23.64 | 24.58 | 25.51 | 26.46 | 27.40 | 28.35 | 29.31 | 30.27 | 31.22 | 32.19 | 33.15 | 34.12 | 35.09 | 36.06 | 10 |
| 11 | 23.52 | 24.43 | 25.36 | 26.29 | 27.22 | 28.16 | 29.10 | 30.05 | 31.00 | 31.95 | 32.91 | 33.87 | 34.83 | 35.79 | 36.76 | 11 |
| 12 | 24.33 | 25.24 | 26.15 | 27.07 | 28.00 | 28.93 | 29.87 | 30.81 | 31.75 | 32.70 | 33.65 | 34.60 | 35.55 | 36.51 | 37.47 | 12 |
| 13 | 25.16 | 26.06 | 26.96 | 27.87 | 28.79 | 29.72 | 30.64 | 31.58 | 32.51 | 33.45 | 34.39 | 35.34 | 36.29 | 37.24 | 38.20 | 13 |
| 14 | 26.00 | 26.89 | 27.78 | 28.69 | 29.60 | 30.51 | 31.43 | 32.36 | 33.29 | 34.22 | 35.16 | 36.10 | 37.04 | 37.99 | 38.94 | 14 |
| 15 | 26.85 | 27.73 | 28.62 | 29.51 | 30.41 | 31.32 | 32.23 | 33.15 | 34.07 | 35.00 | 35.93 | 36.86 | 37.80 | 38.74 | 39.69 | 15 |
| 16 | 27.71 | 28.58 | 29.46 | 30.35 | 31.24 | 32.14 | 33.05 | 33.96 | 34.87 | 35.79 | 36.72 | 37.64 | 38.57 | 39.51 | 40.45 | 16 |
| 17 | 28.58 | 29.44 | 30.32 | 31.19 | 32.08 | 32.97 | 33.87 | 34.77 | 35.68 | 36.59 | 37.51 | 38.43 | 39.36 | 40.29 | 41.22 | 17 |
| 18 | 29.46 | 30.32 | 31.18 | 32.05 | 32.92 | 33.81 | 34.70 | 35.59 | 36.50 | 37.40 | 38.31 | 39.23 | 40.15 | 41.07 | 42.00 | 18 |
| 19 | 30.35 | 31.19 | 32.05 | 32.91 | 33.78 | 34.66 | 35.54 | 36.43 | 37.32 | 38.22 | 39.13 | 40.04 | 40.95 | 41.87 | 42.79 | 19 |
| 20 | 31.24 | 32.08 | 32.92 | 33.78 | 34.64 | 35.51 | 36.39 | 37.27 | 38.16 | 39.05 | 39.95 | 40.85 | 41.76 | 42.67 | 43.59 | 20 |
| 21 | 32.14 | 32.97 | 33.81 | 34.66 | 35.51 | 36.37 | 37.24 | 38.12 | 39.00 | 39.89 | 40.78 | 41.68 | 42.58 | 43.49 | 44.40 | 21 |
| 22 | 33.05 | 33.87 | 34.70 | 35.54 | 36.39 | 37.24 | 38.11 | 38.97 | 39.85 | 40.73 | 41.62 | 42.51 | 43.41 | 44.31 | 45.21 | 22 |
| 23 | 33.96 | 34.77 | 35.59 | 36.43 | 37.27 | 38.12 | 38.97 | 39.84 | 40.71 | 41.58 | 42.46 | 43.35 | 44.24 | 45.13 | 46.03 | 23 |
| 24 | 34.87 | 35.68 | 36.50 | 37.32 | 38.16 | 39.00 | 39.85 | 40.71 | 41.57 | 42.44 | 43.31 | 44.19 | 45.08 | 45.97 | 46.86 | 24 |
| 25 | 35.79 | 36.59 | 37.40 | 38.22 | 39.05 | 39.89 | 40.73 | 41.58 | 42.44 | 43.30 | 44.17 | 45.04 | 45.92 | 46.81 | 47.70 | 25 |
| 26 | 36.72 | 37.51 | 38.31 | 39.13 | 39.95 | 40.78 | 41.62 | 42.46 | 43.31 | 44.17 | 45.03 | 45.90 | 46.78 | 47.66 | 48.54 | 26 |
| 27 | 37.64 | 38.43 | 39.23 | 40.04 | 40.85 | 41.68 | 42.51 | 43.35 | 44.19 | 45.04 | 45.90 | 46.77 | 47.63 | 48.51 | 49.39 | 27 |
| 28 | 38.57 | 39.36 | 40.15 | 40.95 | 41.76 | 42.58 | 43.41 | 44.24 | 45.08 | 45.92 | 46.78 | 47.63 | 48.50 | 49.37 | 50.24 | 28 |
| 29 | 39.51 | 40.29 | 41.07 | 41.87 | 42.67 | 43.49 | 44.31 | 45.13 | 45.97 | 46.81 | 47.66 | 48.51 | 49.37 | 50.23 | 51.10 | 29 |
| 30 | 40.45 | 41.22 | 42.00 | 42.79 | 43.59 | 44.40 | 45.21 | 46.03 | 46.86 | 47.70 | 48.54 | 49.39 | 50.24 | 51.10 | 51.96 | 30 |

# Further Improvement in the Resolving Power of the Electron Microscope

JAMES HILLIER
*RCA Laboratories, Princeton, New Jersey*
(Received February 2, 1946)

THERE are a number of independent possible methods of determining experimentally the electron optical properties of the magnetic electron microscope objectives in use at the present time.[1] From these determinations it has been possible to obtain corresponding independent calculated values for the maximum resolving power which should be attainable with the magnetic electron microscope. All such values have been found to lie in the range 5A to 10A. On the other hand, direct experimental determinations of the resolving powers of existing instruments have given no values below 20A. Furthermore, publications reporting systematic investigations of the reasons for this discrepancy have been singularly lacking.

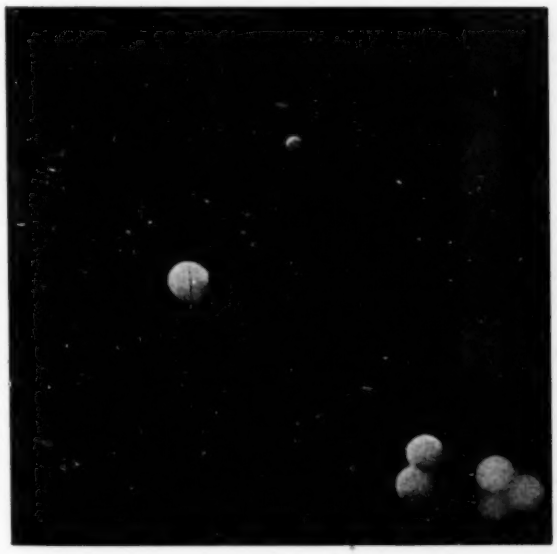

FIG. 1a. An electron micrograph of polystyrene latex on a collodion plus silica substrate and shadowed with approximately 10A of chromium. Additional information: Electronic magnification, 14,600×. Focal length of the objective 2.5 mm. No limiting aperture. Angular aperture of illumination $10^{-4}$ rad., approximately. Accelerating potential 50 kv. Recorded on medium lantern slide; 5-second exposure. Developed 3 minutes in D-72. Micrograph obtained by R. F. Baker. Specimen prepared by N. R. Davidson and R. F. Baker.

[1] V. K. Zworykin, G. A. Morton, E. G. Ramberg, J. Hillier, and A. W. Vance, *Electron Optics and the Electron Microscope* (John Wiley and Sons, New York, 1945).

Research workers interested in the problem of improving the ultimate performance of the electron microscope have been well aware of the absence of serious work on this important problem. They have also realized, however, the futility of attempting to carry out a systematic study when significant results are obtainable in only an extremely small percentage of the experiments. For instance, in the author's own laboratory, only 10–15 exposures definitely showing a resolving power of 20A had been obtained from over 25,000 exposures made during the five-year period 1940–1945.

During this time, the efforts of electron microscope designers and engineers had been concentrated on the elimination of all those defects which provided accidental disturbances of the images. Recently, this work was greatly accelerated in this laboratory by the development of a new gun providing a twenty-fold increase in the intensity of the image and considerable

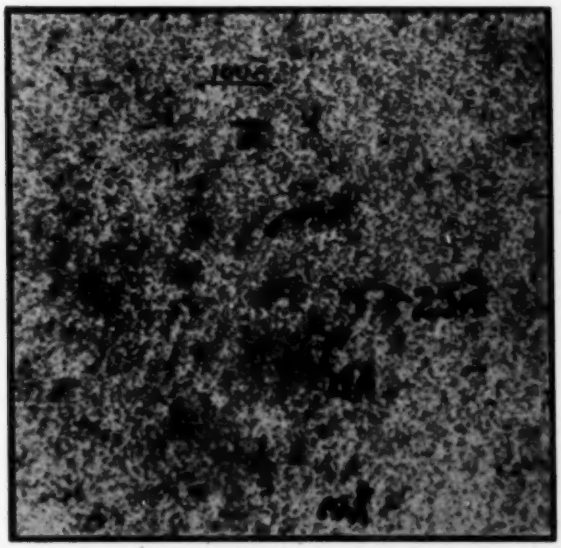

FIG. 1b. A 16× enlargement of a portion of Fig. 1a. An attempt has been made to eliminate some of the effects of photographic grain by slightly defocusing the enlarger. Chromium particles can be distinguished from photographic grain by the fact that they are elongated as a result of a slight astigmatism of the objective.

FIG. 2. A photometric trace of the sharp edge of one of the particles of polystyrene latex shown in Fig. 1a.

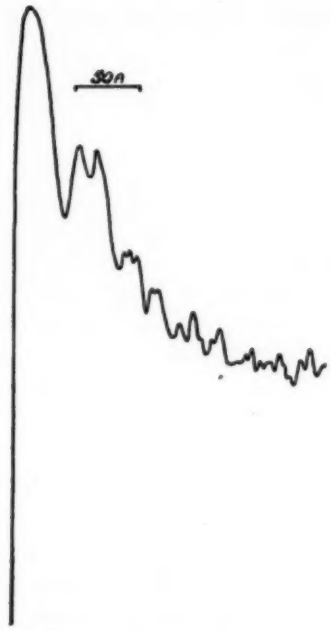


FIG. 3. A photometric trace of the Fresnel fringes obtained at an edge in a very slightly out of focus image of MgO.

improvement in the electron optical properties of the specimen illumination.[2,3] This improvement has made practical the use of a telescopic viewing device (10×) similar to that described by von Ardenne,[4] which enables the operator to examine the final image visually at magnifications as high as 300,000× at satisfactory intensities and under the best conditions for making the final photographic exposures.

The accumulation of electron microscope engineering knowledge and the above mentioned developments have resulted in an instrument in this laboratory (a modified RCA Model EMU) which when operated by the author or his associates seldom fails to provide images showing resolutions of the order of 20A (measured center to center on definitely resolved particles).

With this degree of performance available it was soon very obvious that it has been a *lack of axial symmetry* in the magnetic fields of the lenses that has limited their resolving power. The author has since undertaken to produce a lens possessing a greater degree of symmetry and at the time of writing has obtained at least one lens which shows considerable improvement. Since the techniques used are exploratory in nature and the accuracy achieved is not yet susceptible to measurement, neither will be discussed here. The purpose of this note is rather to report that a few images have been obtained with this lens which show a resolving power better than 13A and possibly as low as 8.5A corresponding to a useful magnification of over 200,000!

In order to obtain a representative value for the limiting resolving power, three different measurements were used in its evaluation: (1) The distance between centers of just resolved particles—13A (see Fig. 1). (2) Half the width of the contour in the image of a sharp edge, taken from external maximum to the internal minimum—8.5A (see Fig. 2). (3) The estimated minimum possible separation, consistent with resolution, between Fresnel fringes in the image of a sharp edge—10A (see Fig. 3). These measurements give a mean value of 10.5A for the resolving power of the present lens.

This work indicates that the calculated limiting resolving power of the present magnetic lenses is obtainable in practice. On the other hand, it has revealed an imposing list of technical problems which must be solved before such

[2] J. Hillier and R. F. Baker, "A discussion of the illuminating system of the electron microscope," J. App. Phys. **16**, 469–483 (1945).
[3] J. Hillier, and R. F. Baker, "On the improvement of resolution in the electron diffraction cameras," J. App. Phys. **17**, 12 (1946).
[4] M. von Ardenne, *Elektronen Übermikroskopie* (Verlagsbuchhandlung Julius Springer, Berlin, 1940).

high resolving power will be consistently obtainable or before it will be available for general scientific research.

Through suggestions and discussions a number of workers have contributed to this development. It is with pleasure that the author acknowledges the part played in the work by his co-workers in the RCA Laboratories in Princeton and by Mr. Perry C. Smith and his associates of the RCA Victor Division in Camden.

---

## Preparation of Electron Microscope Specimens for Determination of Particle Size Distribution in Aqueous Suspensions

A. M. Cravath, A. E. Smith, J. R. Vinograd, and J. N. Wilson
*Shell Development Company, Emeryville, California*

(Received December 17, 1945)

Small droplets of the suspension to be examined are deposited from a mist upon a specimen film whose surface has been treated to promote wetting by the droplets. This procedure makes the entire residue left by a whole droplet available for examination and promotes uniform dispersion of the deposit.

In order to overcome difficulties experienced in measuring the size distribution of particles in polystyrene latices the following procedures for mounting specimens for electron microscope examination were developed. It is believed they may be of general utility.

When diluted latex (*ca.* 0.01 percent polystyrene) was applied with a medicine dropper to untreated cellulose ester specimen films and allowed to dry, there appeared on the films some areas in which the particles were well dispersed, but these areas were adjacent to dense streaks and ridges of particles which could not be measured. It was not certain that the two types of deposit had identical compositions. When the diluted latex was applied as a fine mist, the whole deposit of some droplets was well dispersed but other droplets gave deposits having a dense ring of unmeasurable particles. With certain samples good deposits were rare. It seemed probable that the rings were caused by poor wetting, the liquid surface meeting the film at a large contact angle and pushing the particles ahead as it receded until such a high concentration was reached that a ridge was deposited. This supposition was supported by the observation that droplets of visible size maintained large contact angles when they were made to shrink by blotting with the edge of a filter paper. A few experiments with Aerosol OT indicated that an effective concentration of wetting agent would contaminate the samples excessively.

The above difficulties were overcome by (*a*) hydrolyzing the surface of the cellulose ester film enough to promote good wetting and uniform deposition of droplets and (*b*) applying the latex in the form of extremely fine droplets.

A convenient procedure is to place a drop of ten percent sodium hydroxide solution on a cellulose

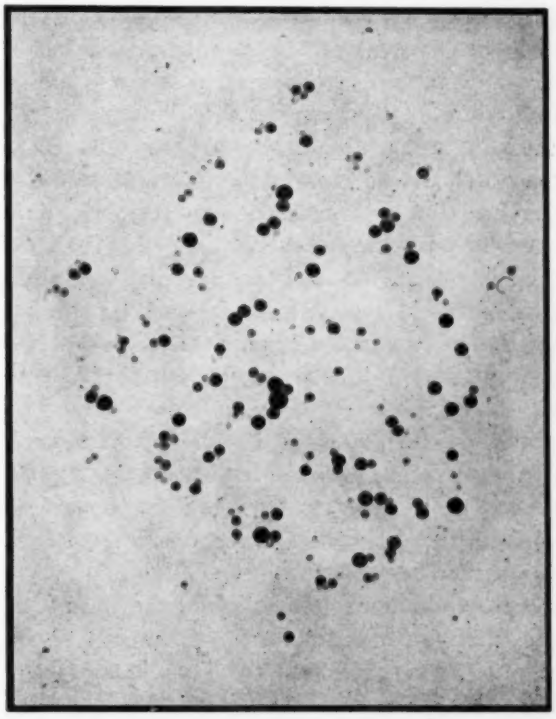

Fig. 1. Polystyrene latex. Good dispersion from mist droplet on untreated film. 21,000×.

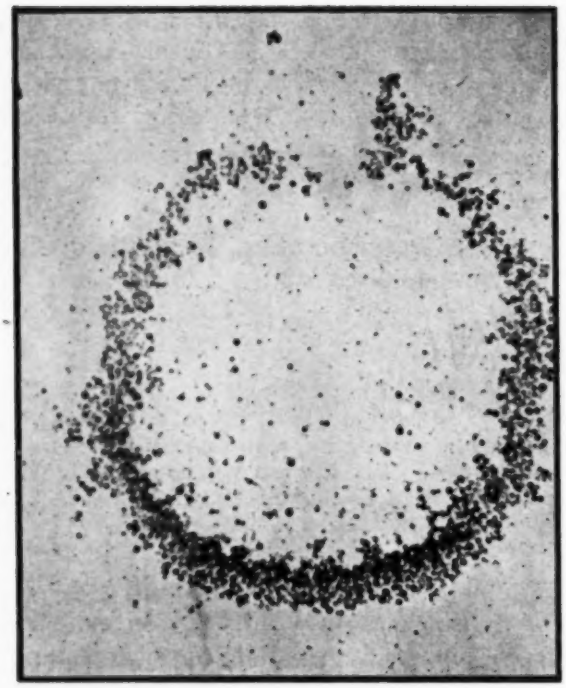

FIG. 2. Polystyrene latex. Poor dispersion from mist droplet on untreated film. 11,000×.

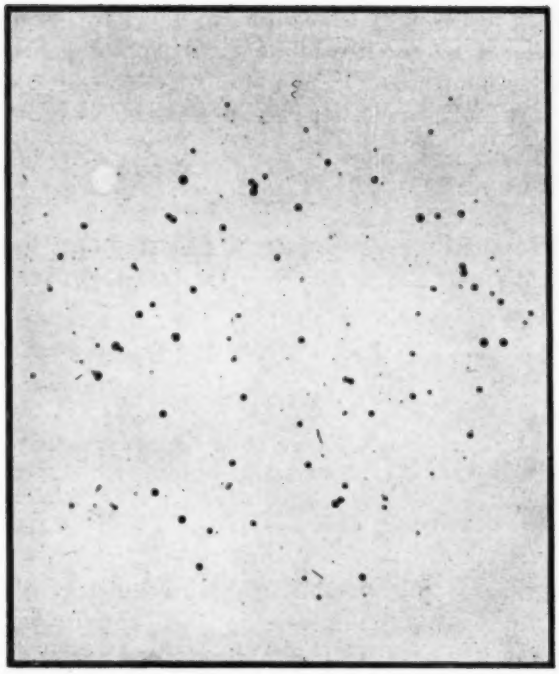

FIG. 3. Polystyrene latex. Good dispersion from mist droplet on treated film. 13,000×.

acetate-butyrate film after the film is attached to the specimen screen. The drop should not reach quite to the edge of the film. The screen is held up to the light and watched. After a few seconds a hole sometimes appears in the film, usually near the edge, and gradually grows. If the hole reaches the center before the treatment has proceeded for the time that experience shows necessary to make the film wettable (about 20 seconds), the specimen is discarded. Satisfactory films are rinsed with distilled water from a wash bottle and dried. The film is placed on a microscope slide in a horizontal test tube (*ca.* 3×10 cm), and the aqueous sample is sprayed from an atomizer which gives a fine mist (e.g., DeVilbis No. 14), the spray being directed against the end of the tube so that the larger droplets deposit there and only the finer droplets travel back toward the mouth and settle on the film. (The diameter of the droplet which left the deposit shown in Fig. 1 has been calculated from the solid content, the number of particles and the size distribution to have been 7.4 microns. Since the diameter of the deposit is about 3 microns, considerable evaporation and shrinkage must have occurred before the particles were deposited.)

The surface hydrolysis procedure was found to reduce the contact angle between the film and a visible water droplet to approximately zero.

An alternative procedure for surface hydrolysis has been tried in which the cellulose ester films are cast on sodium hydroxide solution instead of on water. Solutions of cellulose acetate-butyrate or nitrate in amyl acetate were found not to spread on the surface of ten percent sodium hydroxide, but spreading did occur on a three percent hydroxide solution. Nitrocellulose films were attacked so rapidly that they could not be transferred to the specimen screens. Cellulose acetate-butyrate films rapidly grew brittle and weak and soon took on a dull appearance, although they were still strong enough to be transferred to the specimen screen several minutes after forming. In the electron microscope, specimens prepared with these films were indistinguishable from those prepared by the more convenient method described first.

Figures 1–3 show examples of deposits on treated and untreated film.

# Here and There

### New Appointments

Dr. John D. Strong joined the Johns Hopkins University staff in February as professor of physics.

Dr. William V. Houston, formerly professor of physics at California Institute of Technology, began his new work as president of Rice Institute on March 1.

Dr. Frank G. Dunnington, who has been at the Radiation Laboratory, Massachusetts Institute of Technology, during the war, has returned to active duty at Rutgers University and has been promoted to associate professor. He will become chairman of the Physics Department on the retirement this year of Dr. George Winchester, present department head.

Dr. Raymond G. Spencer, formerly chairman of the metals and minerals research division of the Armour Research Foundation, Chicago, is now director of the Washington University Foundation, St. Louis.

The following persons were recently added to the staff of Philips Laboratories, Inc., Irvington, New York: Dr. James G. Black, Carol M. Veronda, Frank Grace, and George A. Espersen. Dr. Victor Wouk has joined the Engineering Laboratories staff of North American Philips Company, Inc., at Dobbs Ferry, New York.

Dr. George E. Ziegler, Executive Scientist of the Midwest Research Institute, Kansas City, Missouri, has been elected chairman and editor of the recently established Technical Societies Council of the Kansas City Area. He was formerly chairman of physics research at Armour Research Foundation in Chicago.

### Westinghouse Science Writing Award Fund

The American Association for the Advancement of Science has announced the establishment of the George Westinghouse Science Writing Award Fund to give national recognition to newspaper writers and newspapers contributing most to better popular understanding of the achievements of science and technology. The fund has been provided by the Westinghouse Educational Foundation in commemoration of the 100th anniversary of the birth of George Westinghouse. It provides an annual cash award of $1000 to a newspaper writer for outstanding science reporting of the year, and a citation to the newspaper whose science news coverage in the preceding year is adjudged most complete and authoritative and most interestingly presented. The first annual awards, covering the year 1946, will be made at the winter meeting of the A.A.A.S. in December 1946.

### American Chemical Society Fellowships

The American Chemical Society will award fellowships aggregating $210,000 in 1946 and 1947 to aid in the training of chemists and chemical engineers. Predoctoral students whose work was interrupted by the war will receive $100,000. Grants of $110,000 will be made to holders of the doctor's degree who desire to devote one or two years to research and teaching. The predoctoral fellowships will carry an annual stipend of $1200 for single candidates and $1800 for married candidates, plus a maximum of $500 a year for tuition and laboratory charges. In the selection of recipients, great weight will be given to each applicant's sacrifices and contributions to the war effort, with special consideration for those who had begun their graduate work before they entered war service.

"The granting of these predoctoral fellowships is an immediate post-war measure," the Society announced. "While successful candidates may reasonably expect continuation of support until their postgraduate work is complete (for a maximum period of three years), continued aid will be contingent upon satisfactory progress by the fellow."

Postdoctoral fellowships will carry a stipend of $2500 a year, with the understanding that the institutions at which the recipients study will provide an additional sum for teaching. Awards will be for one year, and will be renewable for a second year upon proof of satisfactory performance. Chemists and chemical engineers who received the doctor's degree since January 1, 1940, and have been engaged in war work, or persons who will have obtained the doctorate during the twelve-month period prior to November 1 of the year in which the award is made, are eligible for postdoctoral fellowships. Applications should be sent to Dr. W. Albert Noyes, Jr., head of the Chemistry Department, University of Rochester, and must be submitted prior to February 1, 1947, by those who intend to begin work by November 1, 1947. Application blanks may be obtained from Dr. Noyes or from the Society's headquarters, 1155—16th Street, N.W., Washington 6, D. C.

### Officers for Division of High Polymer Physics

New officers for the Division of High Polymer Physics of the American Physical Society for 1946 are as follows:

*Chairman:* Howard A. Robinson, Armstrong Cork Company
*Vice Chairman:* S. L. Gerhard, U. S. Rubber Company
*Secretary:* W. James Lyons, Firestone Tire and Rubber Company
*Treasurer;* Lawrence A. Wood, National Bureau of Standards

### Adolph Lomb Medal Notice

The Adolph Lomb Medal Committee of the Optical Society of America is engaged in helping to name a recipient for its award which should be made "to a person under thirty (30) years of age who shall have made a noteworthy contribution to optics" (J. Opt. Soc. Am., June, 1940). The choice this year is made more difficult by the wartime restrictions and lack of publications on optical developments of the last several years. To help the committee avoid making a glaring omission, if you know of a possible candidate for this award, would you please communicate your suggestion together with a brief presentation of his or her achievements to some member of the Committee, preferably the chairman, *BEFORE JUNE 1, 1946*? Members of the Committee are:

Dr. Selig Hecht, Columbia University, New York, New York
Dr. Elmer Hutchisson, Case School of Applied Science, Cleveland, Ohio
Dr. W. F. Meggers, National Bureau of Standards, Washington, D. C.
Dr. George S. Monk, University of Chicago, Chicago, Illinois
Dr. Brian O'Brien, University of Rochester, Rochester, New York
*Chairman:* Dr. Mary E. Warga, University of Pittsburgh, Pittsburgh 13, Pennsylvania

# New Books

## Sequential Analysis of Statistical Data: Applications

Prepared by the STATISTICAL RESEARCH GROUP OF COLUMBIA UNIVERSITY for The Applied Mathematics Panel, National Defense Research Committee, Office of Scientific Research and Development. Columbia University Press, New York, 1945. Price $6.25

One of the developments fostered by wartime shortages of time and man-power is the sequential method of testing a statistical hypothesis. It differs from standard sampling plans in that the sample size is a random variable, testing being stopped whenever a decision is indicated at a pre-set level of assurance. As each unit is inspected, the data accumulated are analyzed and one of three alternatives is indicated: accept hypothesis, reject hypothesis, or continue testing. This plan results in termination of testing at the earliest possible time, reductions in the amount of data required for the same risks of wrong decisions frequently running as high as 50 percent compared with constant-sample-size plans.

Against this advantage must be weighed the disadvantages in industrial inspection of increased responsibility on the inspector and difficulty of guarding against inspector bias as a decision is approached. Nevertheless, the method has been used successfully in many plants for acceptance of war material, and the disadvantages mentioned are usually not serious in applications to experimentation.

The book reviewed here is a manual in which the design of a sequential plan is reduced to the solution of simple algebraic equations followed by a graphical or tabular scoring of results. It is a revised edition of the restricted report originally prepared by H. A. Freeman from the theory developed by A. Wald in 1943, and includes more recent theoretical developments. The form of the original report is retained—six self-contained sections and two appendices, all in pamphlet form and gathered in a loose-leaf ring binder. Each of the sections (except the first, which is a general introduction) takes up a particular type of problem, presents the equations necessary for setting up a test plan, and works a typical example. Thus sequential analysis is applied to data from inspection by attributes (binomial distribution); to inspection by variables (normal distribution), where either the mean or the variability is questioned; and to comparison of data with a standard value, or with data from an alternative method or process. The appendices discuss the nature and theory of sequential analysis, although, for greater mathematical rigor, the reader is referred to the works of A. Wald.

In order to capitalize on the ease with which it may be removed from the binder, each section is made independent of the others by repetition of an adequate explanation of terms and ideas. The book should prove of considerable value to those concerned with analysis of statistical data in experimentation or acceptance sampling.

D. K. WRIGHT, JR.
*Case School of Applied Science*

## Basic Mathematics for War and Industry

BY PAUL H. DAUS, JOHN M. GLEASON, AND WILLIAM H. WHYBURN. Pp. 11+277, The Macmillan Company, New York, 1944. Price $2.00.

This book consists of five chapters treating, in that order, arithmetic, algebra, geometry, plane trigonometry, and solid geometry and spherical trigonometry. Three tables are appended—of powers and roots, of four place common logarithms, and of four place trigonometric functions (both natural and logarithmic values). Answers are provided for every problem. A protractor, graduated both in degrees and mils, is inserted in the back cover.

The chapter on arithmetic treats the elementary operations, on integers and fractions, common and decimal, approximation and significant figures, percentage and extraction of square roots. Under algebra, the book deals with the fundamental operations on polynomials and fractions (for some reason, division of polynomials is omitted), factoring, ratio and proportion, radicals (square root only), linear equations and systems of linear equations, quadratic equations (one misses systems of quadratic equations), and graphical solutions of equations. The geometry of the triangle, polygon, and circle is taken up in the third chapter. Here the authors deftly dispose of the difficulties that greet the student in the conventional text by frankly presenting as axioms such theorems as those on the congruence of triangles under various conditions or the proportionality of sides for triangles with equal angles. The chapter is enriched by sections treating the triangle of velocity in air navigation, the wind star, radius of action, interception, angular and rim speeds. In the work on trigonometry, the authors make efficient use of the line values of the trigonometric functions, manage to depart from the conventional texts by presenting what they call the cotangent law and the altitude law for the triangle, treat thoroughly the solution of the triangles, including the aid of logarithms, and enliven it all by presenting, both in the text and in the exercises, genuinely practical and stimulating problems. The last chapter presents the rudiments of solid geometry in fifteen brief, but well done, pages (the various theorems dealing with mensuration, in solid as well as plane geometry, are disposed of as formulas, stated in the chapter on algebra, and given without proof), the rest of the chapter being given over to a good treatment of spherical trigonometry, including the celestial sphere, and once again, such a beguiling topic as "mounting of parts on a tilting table for machining."

Throughout, the exposition is fresh and in many places original, the applications to shop and technical problems numerous, natural, and attractive, and the figures are well drawn. In all, the authors have succeeded in packing a surprisingly large amount of material, and organizing that material well, in the brief space of this book. The authors' purpose, stated in the preface, to provide a useful compendium of elementary mathematics for technical and shop workers, has been achieved here with substantial adequacy.

M. MORRIS
*Case School of Applied Science*